frontiers | Research Topics

Current challenges in inflammation and pain biology: The role of natural and synthetic compounds

Edited by
Emer S. Ferro, Jack Arbiser, Elizabeth S. Fernandes and Soraia K. P. Costa

Published in
Frontiers in Pharmacology
Frontiers in Physiology

FRONTIERS EBOOK COPYRIGHT STATEMENT

The copyright in the text of individual articles in this ebook is the property of their respective authors or their respective institutions or funders. The copyright in graphics and images within each article may be subject to copyright of other parties. In both cases this is subject to a license granted to Frontiers.

The compilation of articles constituting this ebook is the property of Frontiers.

Each article within this ebook, and the ebook itself, are published under the most recent version of the Creative Commons CC-BY licence. The version current at the date of publication of this ebook is CC-BY 4.0. If the CC-BY licence is updated, the licence granted by Frontiers is automatically updated to the new version.

When exercising any right under the CC-BY licence, Frontiers must be attributed as the original publisher of the article or ebook, as applicable.

Authors have the responsibility of ensuring that any graphics or other materials which are the property of others may be included in the CC-BY licence, but this should be checked before relying on the CC-BY licence to reproduce those materials. Any copyright notices relating to those materials must be complied with.

Copyright and source acknowledgement notices may not be removed and must be displayed in any copy, derivative work or partial copy which includes the elements in question.

All copyright, and all rights therein, are protected by national and international copyright laws. The above represents a summary only. For further information please read Frontiers' Conditions for Website Use and Copyright Statement, and the applicable CC-BY licence.

ISSN 1664-8714
ISBN 978-2-8325-2816-7
DOI 10.3389/978-2-8325-2816-7

About Frontiers

Frontiers is more than just an open access publisher of scholarly articles: it is a pioneering approach to the world of academia, radically improving the way scholarly research is managed. The grand vision of Frontiers is a world where all people have an equal opportunity to seek, share and generate knowledge. Frontiers provides immediate and permanent online open access to all its publications, but this alone is not enough to realize our grand goals.

Frontiers journal series

The Frontiers journal series is a multi-tier and interdisciplinary set of open-access, online journals, promising a paradigm shift from the current review, selection and dissemination processes in academic publishing. All Frontiers journals are driven by researchers for researchers; therefore, they constitute a service to the scholarly community. At the same time, the *Frontiers journal series* operates on a revolutionary invention, the tiered publishing system, initially addressing specific communities of scholars, and gradually climbing up to broader public understanding, thus serving the interests of the lay society, too.

Dedication to quality

Each Frontiers article is a landmark of the highest quality, thanks to genuinely collaborative interactions between authors and review editors, who include some of the world's best academicians. Research must be certified by peers before entering a stream of knowledge that may eventually reach the public - and shape society; therefore, Frontiers only applies the most rigorous and unbiased reviews. Frontiers revolutionizes research publishing by freely delivering the most outstanding research, evaluated with no bias from both the academic and social point of view. By applying the most advanced information technologies, Frontiers is catapulting scholarly publishing into a new generation.

What are Frontiers Research Topics?

Frontiers Research Topics are very popular trademarks of the *Frontiers journals series*: they are collections of at least ten articles, all centered on a particular subject. With their unique mix of varied contributions from Original Research to Review Articles, Frontiers Research Topics unify the most influential researchers, the latest key findings and historical advances in a hot research area.

Find out more on how to host your own Frontiers Research Topic or contribute to one as an author by contacting the Frontiers editorial office: frontiersin.org/about/contact

Current challenges in inflammation and pain biology: The role of natural and synthetic compounds

Topic editors

Emer S. Ferro — University of São Paulo, Brazil
Jack Arbiser — Emory University, United States
Elizabeth S. Fernandes — Pelé Pequeno Príncipe Research Institute, Brazil
Soraia K. P. Costa — University of São Paulo, Brazil

Citation

Ferro, E. S., Arbiser, J., Fernandes, E. S., Costa, S. K. P., eds. (2023). *Current challenges in inflammation and pain biology: The role of natural and synthetic compounds*. Lausanne: Frontiers Media SA. doi: 10.3389/978-2-8325-2816-7

Table of contents

frontiers | Frontiers in Physiology

TYPE Editorial
PUBLISHED 07 September 2022
DOI 10.3389/fphys.2022.1008538

Check for updates

OPEN ACCESS

EDITED AND REVIEWED BY
Geoffrey A. Head,
Baker Heart and Diabetes Institute, Australia

*CORRESPONDENCE
Elizabeth Soares Fernandes,
elizabeth.fernandes@pelepequenoprincipe.org.br

SPECIALTY SECTION
This article was submitted to Integrative Physiology, a section of the journal Frontiers in Physiology

RECEIVED 31 July 2022
ACCEPTED 12 August 2022
PUBLISHED 07 September 2022

CITATION
Fernandes ES, Ferro ES, Simão G, Alves de Góis G, Arbiser J and Pereira Costa SK (2022), Editorial: Current challenges in inflammation and pain biology: The role of natural and synthetic compounds.
Front. Physiol. 13:1008538.
doi: 10.3389/fphys.2022.1008538

COPYRIGHT
© 2022 Fernandes, Ferro, Simão, Alves de Góis, Arbiser and Pereira Costa. This is an open-access article distributed under the terms of the Creative Commons Attribution License (CC BY). The use, distribution or reproduction in other forums is permitted, provided the original author(s) and the copyright owner(s) are credited and that the original publication in this journal is cited, in accordance with accepted academic practice. No use, distribution or reproduction is permitted which does not comply with these terms.

Editorial: Current challenges in inflammation and pain biology: The role of natural and synthetic compounds

Elizabeth Soares Fernandes[1,2]*, Emer Suavinho Ferro[3], Gisele Simão[1,2], Guilherme Alves de Góis[3], Jack Arbiser[4] and Soraia Kátia Pereira Costa[3]

[1]Programa de Pós-graduação em Biotecnologia Aplicada à Saúde da Criança e do Adolescente, Faculdades Pequeno Príncipe, Curitiba, Brazil, [2]Instituto de Pesquisa Pelé Pequeno Príncipe, Curitiba, Brazil, [3]Departamento de Farmacologia, Universidade de São Paulo, São Paulo, Brazil, [4]Veterans Administration Medical Center, School of Medicine, Emory University, Atlanta, NY, United States

KEYWORDS

pain, inflammation, mechanisms of disease, natural compounds, synthetic therapies

Editorial on the Research Topic
Current challenges in inflammation and pain biology: The role of natural and synthetic compounds

Inflammation and pain are complex physiological responses which can evolve to chronic disorders. They involve an intricate network of molecules and receptors (Chen et al., 2018; Yam et al., 2018), often making their management, a clinical challenge. The discovery and development of natural and synthetic compounds with analgesic and/or anti-inflammatory activities have highly contributed to halt or attenuate different types of painful and inflammatory diseases (Atanasov et al., 2021; Beck et al., 2022). Their side effects, of special concern in chronic pathologies, prompted an increasing number of non-clinical and clinical studies aiming at evaluating the effectiveness and safety of novel natural and synthetic products for treating inflammation and pain. However, the costs involved in developing and implementing new therapies and the several challenges encountered including low selectivity, high incidence of adverse effects and/or unfavourable pharmacokinetics properties of drug candidates have been major setbacks in the field (Tautermann, 2020). These, highlight the need for novel studies focused on the discovery and development of analgesic and anti-inflammatory drugs. This Research Topic brings together senior researchers, clinicians, and researchers, to share science and hopes to treat inflammatory and painful disorders.

Eight articles were published in the Current Challenges in Inflammation and Pain Biology: The Role of Natural and Synthetic Compounds Research Topic; these have been viewed more than 12,000 times. The articles published in this collection provided new information on diverse pathologies, including nephropathy, dermatitis, rheumatoid

arthritis (RA), cerebral ischemia, diabetes, osteogenesis, and neuropathic and abdominal pain. They also explored novel therapeutic strategies for these diseases such as synthetic and natural compounds, as well as the effects of laser photobiomodulation.

Two of the articles were reviews, and one, a mini-review. The review by Campos et al. discussed the importance of the endocannabinoid system in chronic neuropathic pain and the evidence for the use of cannabinoids to treat this disorder. Shang et al. revised the different inflammatory pathways involved in cerebral ischemia and highlighted the potential of major classes of natural compounds in containing damage caused by inflammation in this pathology. The mini-review by Decraecker et al. focused on the physiological roles of proteases and on the emerging use of protease inhibitors as therapies for visceral hypersensitivity and inflammatory bowel disease.

Five original articles were also published in this Research Topic. By using *in vivo* and *in vitro* models, Liu et al. demonstrated that inhibition of NLRP3 inflammasome activation by the natural compound methyl gallate ameliorates hyperuricemia nephropathy. Methyl gallate diminished uric acid production, promoted uric acid excretion, and reduced mouse renal injury. These effects were associated with the ability of the compound to inhibit NLRP3 oligomerization and assembly by impairing reactive oxygen species production by mouse bone marrow-derived macrophages and peripheral blood mononuclear cells (PBMCs) from healthy subjects and patients with gout.

In another very interesting study, Ramirez-Perez et al. demonstrated the effects of ST2825, a synthetic inhibitor of MyD88 dimerization, on PBMCs from RA patients who were naive for therapy with disease-modifying anti-rheumatic drugs. Analysis of RNA-sequencing data indicated that the *in vitro* incubation of ST2825 down-regulates different genes such as those involved in the complement and matrix metalloproteinases pathways, and chemokine signalling in RA PBMCs. They also suggested ST2825 can potentially modulate these genes in synovial cells of arthritic patients, and highlighted the compound as an emerging therapeutic strategy for RA.

In a report by Li et al., the role of CB2R was investigated in an *in vivo* model of psoriatic dermatitis induced by imiquimod. The authors found increased CB2R protein expression in the epidermis of human psoriatic skin lesions. Then, they used the synthetic CB2R agonist JWH-133 and CB2R knockout and wild type mice to demonstrate that CB2R is an important target for the management of psoriasis-associated itch and inflammation. Proliferation and prolongation of nerve fibres paralleled to high expression of nerve growth factor were observed in psoriatic skin lesions. CB2R deficiency resulted in exacerbated pruritus due to increased expression of pro-inflammatory cytokines and accumulation of $CD4^+$ T cells in the inflamed skin. Also, a higher proportion of splenic Th17/Treg cells were noted in mice lacking of CB2R. In contrast, treatment with JWH-133 protected against the disorder, an effect largely prevented by the CBR2 antagonist AM-630.

Ding et al. assessed the anti-diabetic actions of astilbin, a natural occurring flavonoid. It was found that this compound ameliorates type-1 diabetes in NOD mice, reducing hyperglycemia and preventing weight loss. This effect was associated with less infiltration of $CD4^+$ T cells in the pancreas. TNFα and IFNγ release by $CD4^+$ T cells was markedly impaired by astilbin. At molecular level, the effects of this flavonoid on $CD4^+$ T cells were due to PPARγ activation and downstream down-regulation of STAT3, NF-κB, Akt, p38 MAPK, and mTOR, in addition to increased expression of SOCS3 and PTEN.

Finally, *in vitro* irradiation of laser photobiomodulation at 808 nm was found to affect the proliferation, growth and differentiation factors, mineralization, and extracellular matrix remodeling genes in human dental pulp stem cells stimulated with lipopolysaccharide (da Rocha et al.). PAR2-PAR4 genes were up-regulated whilst PAR-1 was down-regulated by the laser therapy. The laser irradiation also markedly attenuated the gene expression of the matrix metalloproteinases 8 and 9, in addition to those of TNFα, bone morphogenetic proteins 1, 4 and 7, and growth factors including FGF1, GDF10, IGF2, TGFβ1 and VEGFB. Furthermore, genes for receptors (vitamin D receptor, FGF receptor) and proteins such as those from the Smad family (Smad 1 and 4) were down-regulated by the therapy. These findings indicate the potential of the laser therapy at infrared wavelength to prevent bone resorption and inflammation, and therefore, protect dental structures.

Despite the need for continuing searching for new therapeutic options, the studies published in this Research Topic present novel therapeutic approaches which might represent future forms of control/cure of inflammation and pain. Therefore, we would like to thank all the authors for their efforts to elucidate mechanisms of action of such therapies, as well as the reviewers who provided important contributions to the published manuscripts.

Author contributions

The editorial board members contributed equally to editing this collection. GS and GAdeG equally contributed to the interpretation and summarization of the Research Topic information.

Funding

This work was supported by the Conselho Nacional de Desenvolvimento Científico e Tecnológico (CNPq; grant

numbers 305676/2019-9 and 408053/2018-6, to ESF; and 312514/2019-0 to SKPC), PIBIT-CNPq, Coordenação de Aperfeiçoamento de Pessoal de Nível Superior (Finance Code 001), Fundação de Amparo à Pesquisa do Estado de São Paulo (FAPESP; 2016/06146-5, to SKPC), Instituto de Pesquisa Pelé Pequeno Príncipe, and INCT-INOVAMED.

Acknowledgments

The invited editorial committee would like to thank all the contributors to this collection, authors, and reviewers for their availability and dedicated time in the editorial process.

Conflict of interest

The authors declare that the research was conducted in the absence of any commercial or financial relationships that could be construed as a potential conflict of interest.

Publisher's note

All claims expressed in this article are solely those of the authors and do not necessarily represent those of their affiliated organizations, or those of the publisher, the editors and the reviewers. Any product that may be evaluated in this article, or claim that may be made by its manufacturer, is not guaranteed or endorsed by the publisher.

References

Atanasov, A. G., Zotchev, S. B., Dirsch, V. M., and Supuran, C. T.International Natural Product Sciences Taskforce (2021). Natural products in drug discovery: Advances and opportunities. *Nat. Rev. Drug. Discov.* 20 (3), 200–216. doi:10.1038/s41573-020-00114-z

Beck, H., Härter, M., Haß, B., Schmeck, C., and Baerfacker, L. (2022). Small molecules and their impact in drug discovery: A perspective on the occasion of the 125th anniversary of the bayer chemical research laboratory. *Drug Discov. Today* 27 (6), 1560–1574. doi:10.1016/j.drudis.2022.02.015

Chen, L., Deng, H., Cui, H., Fang, J., Zuo, Z., Deng, J., et al. (2018). Inflammatory responses and inflammation-associated diseases in organs. *Oncotarget* 9 (6), 7204–7218. doi:10.18632/oncotarget.23208

Tautermann, C. S. (2020). "Current and future challenges in modern drug discovery," in *Quantum mechanics in drug discovery*. Editor A. Heifetz (New York, NY: Humana), 2114. Methods in Molecular Biology. doi:10.1007/978-1-0716-0282-9_1

Yam, M. F., Loh, Y. C., Tan, C. S., Khadijah Adam, S., Abdul Manan, N., and Basir, R. (2018). General pathways of pain sensation and the major neurotransmitters involved in pain regulation. *Int. J. Mol. Sci.* 19, 2164. doi:10.3390/ijms19082164

frontiers in Physiology

REVIEW
published: 30 November 2021
doi: 10.3389/fphys.2021.785176

Cannabinoid Therapeutics in Chronic Neuropathic Pain: From Animal Research to Human Treatment

Raquel Maria P. Campos, Andrey F. L. Aguiar, Yolanda Paes-Colli, Priscila Martins Pinheiro Trindade, Bruna K. Ferreira, Ricardo A. de Melo Reis and Luzia S. Sampaio**

Laboratório de Neuroquímica, Instituto de Biofísica Carlos Chagas Filho (IBCCF), Centro de Ciências da Saúde, Universidade Federal do Rio de Janeiro, Rio de Janeiro, Brazil

OPEN ACCESS

Edited by:
Emer S. Ferro, University of São Paulo, Brazil

Reviewed by:
Patrícia Reckziegel, Universidade Federal de São Paulo, Brazil
Chi Him Eddie Ma, City University of Hong Kong, Hong Kong SAR, China
Alexandra Latini, Federal University of Santa Catarina, Brazil

***Correspondence:**
Luzia S. Sampaio
sampaio.lu@biof.ufrj.br
Raquel Maria P. Campos
camposrp@biof.ufrj.br

Specialty section:
This article was submitted to Integrative Physiology, a section of the journal Frontiers in Physiology

Received: *28 September 2021*
Accepted: *10 November 2021*
Published: *30 November 2021*

Citation:
Campos RMP, Aguiar AFL, Paes-Colli Y, Trindade PMP, Ferreira BK, de Melo Reis RA and Sampaio LS (2021) Cannabinoid Therapeutics in Chronic Neuropathic Pain: From Animal Research to Human Treatment. Front. Physiol. 12:785176. doi: 10.3389/fphys.2021.785176

Despite the importance of pain as a warning physiological system, chronic neuropathic pain is frequently caused by damage in the nervous system, followed by persistence over a long period, even in the absence of dangerous stimuli or after healing of injuries. Chronic neuropathic pain affects hundreds of millions of adults worldwide, creating a direct impact on quality of life. This pathology has been extensively characterized concerning its cellular and molecular mechanisms, and the endocannabinoid system (eCS) is widely recognized as pivotal in the development of chronic neuropathic pain. Scientific evidence has supported that phyto-, synthetic and endocannabinoids are efficient for pain management, while strong data arise from the therapeutic use of Cannabis-derived products. The use of medicinal Cannabis products is directed toward not only relieving symptoms of chronic pain, but also improving several aspects of patients' welfare. Here, we review the involvement of eCS, along with other cellular and molecular elements, in chronic neuropathic pain pathology and how this system can be targeted for pain management.

Keywords: neuropathic pain, endocannabinoid, cannabidiol, THC, cannabis

CHRONIC NEUROPATHIC PAIN

Chronic pain is classified by the International Association for the Study of Pain (IASP) as a pain that lasts more than 3 months, even after its primary cause is cured (Raja et al., 2020). One of the main types of chronic ache is neuropathic pain, that occurs when pain is caused by a lesion or disease of the somatosensory nervous system (Raja et al., 2020). Chronic neuropathic pain

Abbreviations: 2-AG, 2-arachidonoylglycerol; AEA, anandamide; ASR-9, aggregated 9-factor symptom relief; ATP, adenosine triphosphate; cAMP, cyclic adenosine monophosphate; CB1R, cannabinoid receptor type 1; CB2R, cannabinoid receptor type 2; CBC, cannabichromene; CBD, cannabidiol; CBDV, cannabidivarin; CBN, cannabinol; CNS, central nervous system; COX-2, cyclooxygenase-2; CYP, cytochrome p450; DRG, dorsal root ganglia; EAAT2, excitatory amino acid transporter 2; eCBs, endocannabinoids; eCS, endocannabinoid system; eEPSC, evoked excitatory postsynaptic currents; FAAH, fatty acid amino hydrolase; GABA, γ-aminobutyric acid; IASP, International Association for the Study of Pain; IL-17, interleukin 17; IL-1β, interleukin 1β; IL-6, interleukin 6; MAGL, monoacylglycerol lipase; NF-κb, nuclear factor κ B; P2X4 - P2X purinoceptor 4; p38 MAPK, p38 mitogen-activated protein kinase; PDQ7, Pain Detect Questionnaire 7; PEA, palmitoylethanolamide; PNS, peripheral nervous system; THCV, Δ^9-tetrahydrocannabivarin; TNF-α, tumor necrosis factor-α; TRP, transient receptor potential; TRPA1, transient receptor potential subfamily A member 1; TRPM8, transient receptor potential subfamily M member 8; TRPV1, transient receptor potential subfamily V member 1; Δ^9-THC, Δ^9-tetrahydrocannabinol.

has several causes, such as the use of medicines (chemotherapy drugs, for example), metabolic diseases (such as diabetic neuropathy), demyelinating diseases (for instance, multiple sclerosis) and mechanical injuries (Meacham et al., 2017; Alles and Smith, 2018). The epidemiology of this disease varies across the globe, but it is estimated that 7–10% of all adults worldwide suffer from chronic neuropathic pain (van Hecke et al., 2014; Mücke et al., 2018). The main symptoms consist of spontaneous burning pain, numbness, and hyperalgesia (increased pain perception of noxious stimuli) and allodynia (pain hypersensitivity to normally innocuous stimuli) (Rani Sagar et al., 2012; Meacham et al., 2017; Alles and Smith, 2018). Patients may also experience social and economic consequences, since it is highly uncomfortable to conduct routine tasks while feeling pain. The physical and social impairment, along with the daily pain, can occasionally lead to depression (Knaster et al., 2012; Radat et al., 2013; Pitcher et al., 2019).

Physiological pain pathways include the peripheral and central nervous system (PNS and CNS, respectively), and the pain matrix revealed by neuroimaging in the last two decades is formed by central areas responsible for the process of pain (Legrain et al., 2011; **Figure 1**). Here, we focus on the plasticity in the spinal cord, particularly in the dorsal horn, due to its key role as a central integrator of afferent sensory information, besides being a region where significant part of pain processing occurs (Rani Sagar et al., 2012; West et al., 2015; Alles and Smith, 2018).

ANATOMICAL, CELLULAR, AND MOLECULAR ELEMENTS OF PAIN PROCESSING IN THE SPINAL CORD

The spinal cord is protected by the vertebral column and it is involved in motor and sensory processing, in addition to integrating the body with the brain through different pathways. Anatomically, the spinal cord is divided into an external white matter and an internal gray matter. The latter is subdivided in 10 laminae going from dorsal to ventral spinal cord, which differ from each other based on inputs received and neuron types (Rexed, 1952).

The dorsal horn consists of laminae I to VI, and receives information mostly from sensory neurons located in the dorsal root ganglia (DRG). The DRG neurons transduce mechanical, thermal or nociceptive information and can be classified as Aδ, C, or Aβ fibers (Rexed, 1952; Le Pichon and Chesler, 2014; Alles and Smith, 2018). Lamina I receives noxious, mechanical and thermal inputs from Aδ and C fibers. Lamina II consists of two zones: the outer zone, which receives inputs from C fibers, and the inner zone, receiving information from Aδ and C fibers. Aδ and Aβ fibers connect with other neurons in Laminae III to V carrying tactile and pressure information. Lamina VI receives sensory information from muscle spindles, consisting mostly of propriospinal neurons (**Figure 1**). All laminae have a high number of inhibitory GABAergic and glycinergic interneurons that help modulate sensory inputs. Also, it is important to highlight that most of the laminae in the dorsal horn make connections with neurons from different brain regions through ascendant and descendant pathways (West et al., 2015; Alles and Smith, 2018; **Figure 1**).

The synapses between Aδ, Aβ, and C fibers and spinal cord neurons are excitatory, having glutamate as neurotransmitter (West et al., 2015; Alles and Smith, 2018). Glutamate release from sensory fibres is regulated by inhibitory interneurons present in all laminae of the dorsal horn through γ-aminobutyric acid (GABA) or glycine release, modulating noxious transmission (West et al., 2015). The sensory information travels through different pathways, such as the spinothalamic tract, to different brain areas known as pain matrix, which includes the thalamus, the anterior cingulate cortex, the periaqueductal gray matter, the amygdala and others (D'Mello and Dickenson, 2008; Cohen and Mao, 2014; Colloca et al., 2017; **Figure 1**). Pain modulation is a top-down process: after information processing in higher brain centers, neurons that form the descendant pathways make synapses in the dorsal horn, releasing serotonin, GABA and glycine (D'Mello and Dickenson, 2008; Ossipov et al., 2010; West et al., 2015; Colloca et al., 2017; **Figure 1**).

ENDOCANNABINOID SYSTEM IN PHYSIOLOGICAL PAIN PROCESSING

The endocannabinoid system (eCS) main components are the G protein-coupled cannabinoid receptors CB1 (CB1R) and CB2 (CB2R), the endocannabinoids (eCBs) for example anandamide (AEA) and 2-arachidonoylglycerol (2-AG), and the enzymes involved in their metabolism, such as fatty acid amino hydrolase (FAAH) and monoacylglycerol lipase (MAGL), responsible for the degradation of AEA and 2-AG, respectively (Howlett et al., 2002; **Figure 2**). The eCS is an on-demand system and heterogeneously present in different structures of the CNS and PNS, including important regions of pain processing, such as the DRGs, spinal cord, thalamus, amygdala and others (Tsou et al., 1998; Farquhar-Smith et al., 2000; Katona et al., 2001; Starowicz and Finn, 2017; Finn et al., 2021; **Figure 1**).

In relation to pain modulation in the dorsal spinal cord, the eCS acts as a regulator of the synaptic transmission in the DRGs. CB1R is expressed in the presynaptic sensory fibers of trigeminal ganglion and dorsal root ganglion, besides the nerve endings of primary sensory neurons in dermis, whose afferent fibers conduct nociception (Salio et al., 2002; Price et al., 2003; Veress et al., 2013; Zou and Kumar, 2018). Following the release of neurotransmitters, glutamatergic receptors are activated in the postsynaptic terminal, inducing Ca^{2+} influx and its increased concentration inside the cell. Therefore, higher levels of intracellular Ca^{2+} promotes activation of enzymes responsible for eCBs synthesis, mostly AEA and 2-AG, which are then released into the synaptic cleft and bind to CBRs in the presynaptic terminal. CBR activity induces blockade of voltage-gated Ca^{2+} channels presynaptically and inhibits adenylate cyclase, decreasing levels of cAMP and triggering the signaling cascade involved in synaptic plasticity, besides modulating sensory transmission through this feedback mechanism in the dorsal horn (Shen et al., 1996; Mecha et al., 2015; **Figure 2A**). This was demonstrated by the development

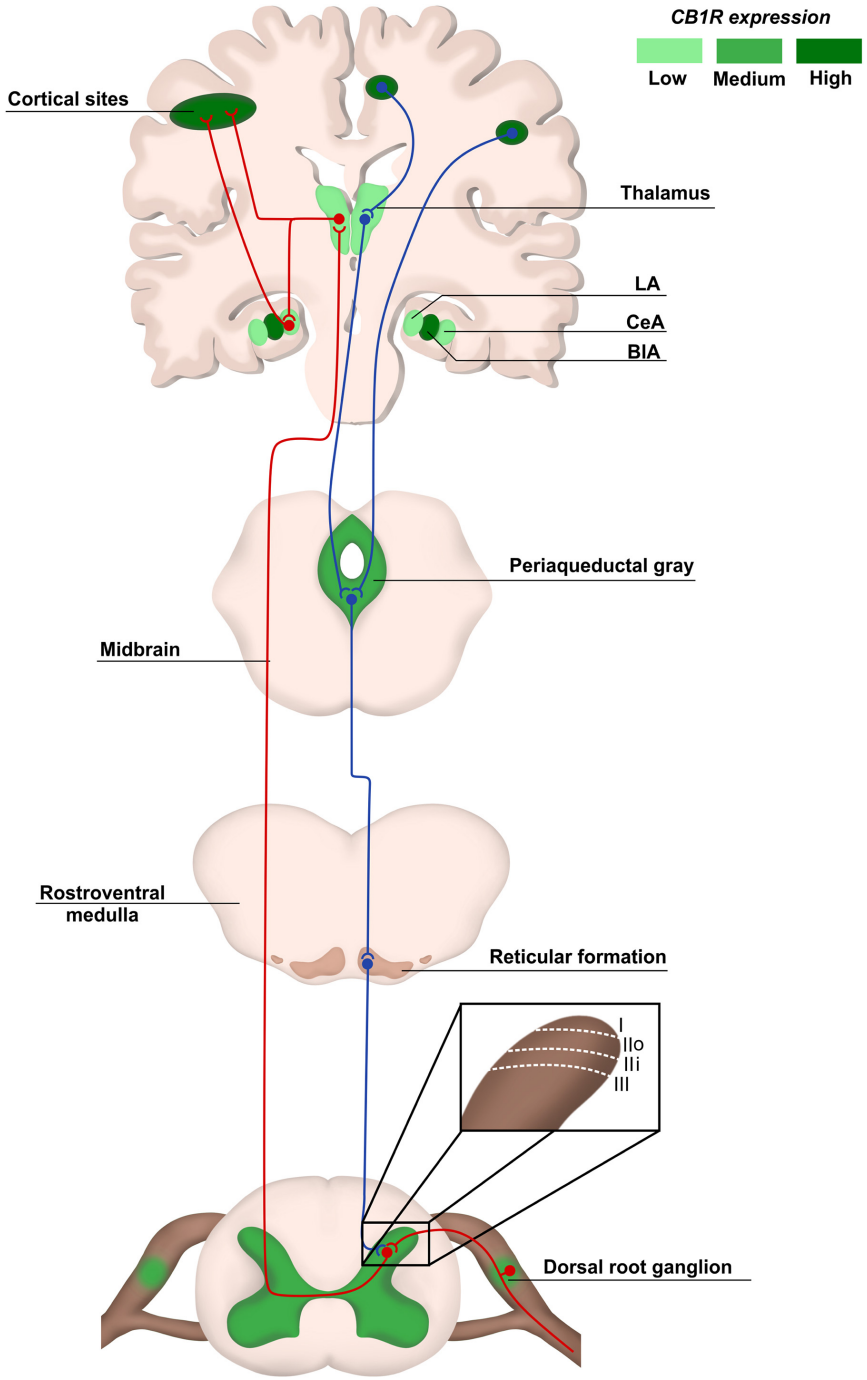

FIGURE 1 | Pain anatomical pathways and CB1R expression. Ascending pain pathways (in red) are carried from the body periphery through sensory neurons of dorsal root ganglia (DRG) that synapse mainly with laminaes I to III in the dorsal spinal cord. Projection neurons make connections with brain areas such as thalamus and cortex. The descending pathways (in blue), responsible for pain modulation, involve areas such as the periaqueductal gray matter and amygdala, ending in the dorsal spinal cord. The CB1R distribution is heterogeneous in pain pathway areas, being more concentrated in regions such as cortex and Central Amygdala (CeA). LA, lateral amygdala; CeA, central amygdala; BIA, basolateral amigdala.

of thermal hyperalgesia and blockage of inhibition of evoked excitatory postsynaptic currents (eEPSC) in laminae II neurons in mice after administration of CB1R antagonists (Richardson et al., 1997; Yang et al., 2016).

Another important component associated with the eCS is the transient receptor potential family (TRP). The TRP cation channel subfamily V member 1 (TRPV1) has a relevant role in nociceptive transduction in the PNS since it is activated, opening

a Ca^{2+} channel and increasing this ion concentration inside the neurons, by heat, acidic substances and capsaicin, besides being expressed in the soma and nerve terminals of sensory neurons from DRG (Caterina et al., 1999; Immke and Gavva, 2006; Lauria et al., 2006). The TRP cation channel subfamily M member 8 (TRPM8) and subfamily A member 1 (TRPA1) also act as nociceptors and they are activated by menthol/cold temperatures and noxious cold/pungent compounds, respectively (Storozhuk and Zholos, 2018). Although TRPV1 and TRPM8 were not initially considered eCS-related receptors, they are directly influenced by different endocannabinoids, such as AEA, since this molecule is an agonist for the former and antagonist for the latter (Zygmunt et al., 1999; De Petrocellis et al., 2007; **Figure 2A**).

Clinical evidence for the role of the eCS in pain management was reported based on a serendipitous case of a Scottish patient (Habib et al., 2019). Authors described the clinical data from a woman submitted to orthopedic surgery, a procedure recognized for being associated with severe pain, with no need for analgesics. The same patient also had a long clinical history of cuts and burns without any sensation of pain. Genetic investigation revealed a deletion in the gene responsible for FAAH transcription, which led to reduced degradation and higher levels of AEA in peripheral blood and probably other organs.

The major eCS components are also present in glial cells, such as astrocytes and microglia, even though CB2R is more expressed than CB1R in microglia, as also shown in other immunological cells, such as lymphocytes and neutrophils (Hegyi et al., 2009; Greineisen and Turner, 2010; Maccarrone et al., 2015). In astrocytes, CB1R-mediated signaling promotes increase of intracellular Ca^{2+} levels, while activation of microglial CB2R maintains the resting state or anti-inflammatory polarity of this cell type (Greineisen and Turner, 2010; Mecha et al., 2015; **Figure 2A**).

CELLULAR AND MOLECULAR CHANGES IN THE SPINAL CORD ASSOCIATED WITH CHRONIC NEUROPATHIC PAIN

The nervous system is plastic, with the ability to change and readapt in response to environmental stimuli. In this context, maladaptive plasticity processes can result in malfunction of the nervous system physiology (Kuner and Flor, 2017; Meacham et al., 2017). For instance, hyperalgesia is related to neuronal hyperexcitability triggered by cytokines and inflammatory mediators released in the periphery or in the spinal cord (Colloca et al., 2017; Kuner and Flor, 2017; Meacham et al., 2017). This is followed by a decrease of GABA- and glycine-mediated neurotransmission, caused not only by the reduction of their release, but also because of inhibitory interneurons apoptosis (Moore et al., 2002; Janssen et al., 2011; Foster et al., 2015). The decrease of GABA-mediated signaling reduces presynaptic inhibition, especially in Lamina II, which allows Aβ fibers to communicate with neurons in Lamina I, therefore contributing for allodynia (Alles and Smith, 2018).

The central sensitization of the spinal cord, which is the increased responsiveness of nociceptive neurons in the CNS when compared to normal threshold, may occur for several reasons, one of them being the dysfunction of glutamate signaling (Meacham et al., 2017). The expression of glutamate transporters is downregulated after PNS injury, increasing the availability of glutamate to their receptors and decreasing neuron-firing threshold (Sung et al., 2003). Changes in the expression of voltage-gated calcium channels, such as the upregulation of α2δ-1 subunit, also contribute to neuron hyperexcitability by increasing Ca^{2+} permeability to the intracellular medium (Li et al., 2004; D'Arco et al., 2015).

The unbalanced synaptic communication in the dorsal horn of the spinal cord is one of the main causes for chronic neuropathic pain consolidation. However, synapses not only contain pre- and postsynaptic elements, but also the participation of glial cells, such as astrocytes and microglia, which have their physiological state shifted and contribute to this pathology, similarly to neurons. After PNS injury, it is well-known that astrocytes and microglial cells in the spinal cord show increased reactivity, identifiable by changes in their morphology and secreted molecules (Burgos et al., 2012; Alles and Smith, 2018). After an aversive stimulus, these cells produce pro-inflammatory mediators, such as interleukins -17, -1β, -6 (IL-17, IL-1β, and IL-6), and Tumor Necrosis Factor-α (TNF-α), which establish an inflammatory environment involved in the maintenance of chronic neuropathic pain (Wieseler-Frank et al., 2005; Stemkowski et al., 2017). Part of these molecules are chemoattractant for immune cells, which explains the infiltration of T cells (Choi et al., 2015; Sun et al., 2017). Indeed, several studies describe the correlation between lymphocyte invasion in the spinal cord and the development of chronic pain, also by the production and release of cytokines as IL-17 by this cell type (Kleinschnitz et al., 2006; Davoli-Ferreira et al., 2020).

Glial cells are also involved in hyperalgesia and allodynia generation. Astrocytes potentiate glutamatergic signaling by reducing the expression of excitatory amino acid transporter 2 (EAAT2) in these cells, which promotes increased glutamate concentration externally to the neuron (Cata et al., 2006). In addition, the contents of purinergic receptors are increased in the microglial cytoplasmic membrane. The continuous adenosine triphosphate (ATP) release from injured and stressed cells in the microenvironment induces constant stimulation of microglia reactivity, proliferation and pro-inflammatory polarity (Tsuda et al., 2013; Peng et al., 2016; Alles and Smith, 2018). In fact, P2X purinoceptor 4 (P2X4) stimulation in the spinal cord of non-injured adult rats is sufficient to induce allodynia (Tsuda et al., 2003; Niu et al., 2017).

ENDOCANNABINOID SYSTEM AS TARGET FOR CHRONIC NEUROPATHIC PAIN TREATMENT

As previously mentioned, the unbalance of eCS physiological signaling can induce chronic neuropathic pain symptoms (Richardson et al., 1997; Yang et al., 2016). The eCS components

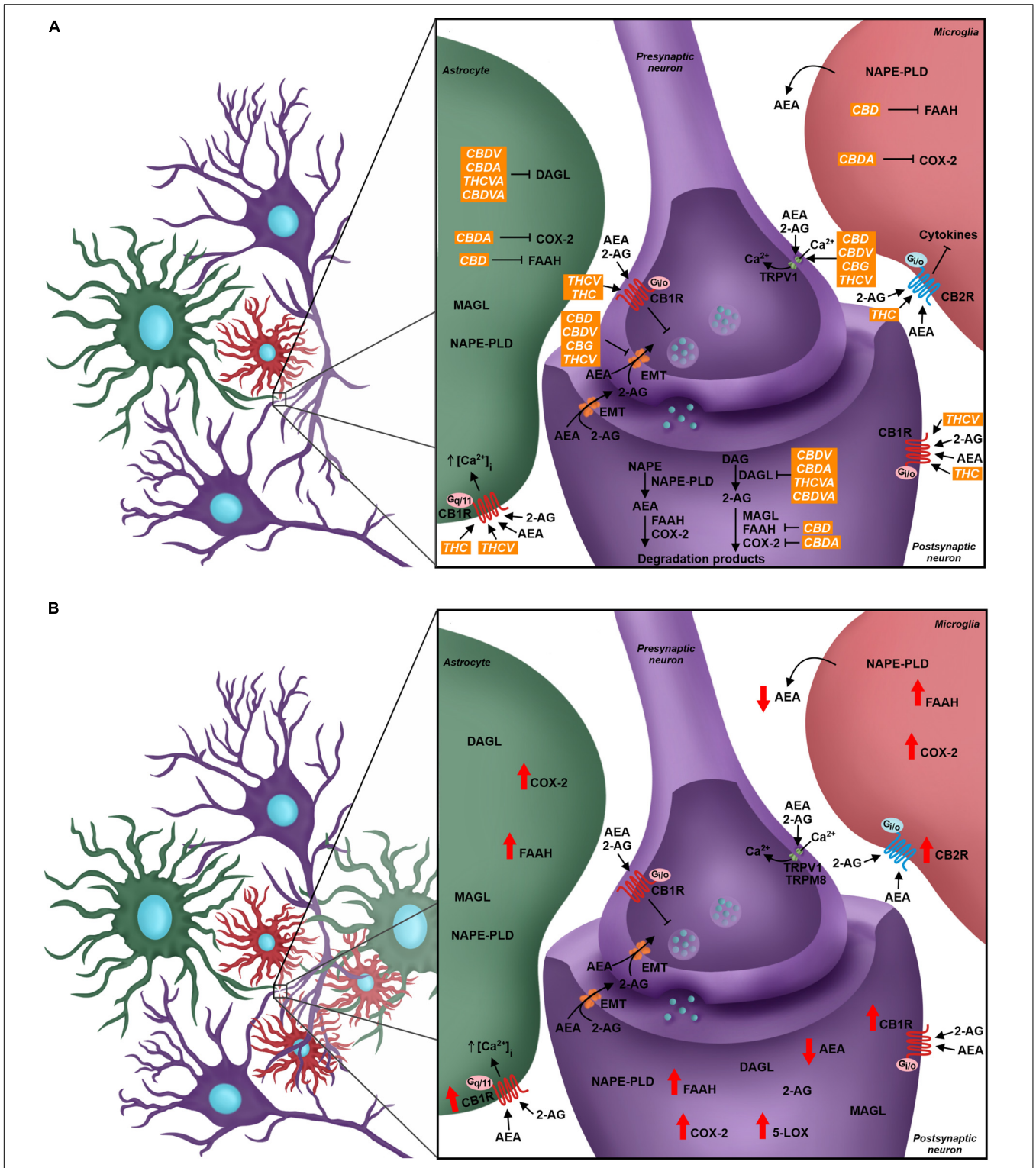

FIGURE 2 | The role of the endocannabinoid system (eCS) in the quadripartite synapse, its modulation by phytocannabinoids and alterations due to Neuropathic Pain. **(A)** Neurons, astrocytes, and microglial cells have the eCS components, and the endocannabinoid signaling through CB1R and CB2R leads to different outcomes in each cell. The presynaptic neuron expresses CB1R, TRPV1, TRPM8, and the endocannabinoid membrane transporter (EMT). Receptors are targeted by endocannabinoids (AEA and 2-AG). CB1R modulation activates signaling cascades that inhibit Ca^{2+} intracellular influx, which decreases the fusion of intracellular vesicles with the neuron membrane, changing the neurotransmitter release flow. The postsynaptic neuron also presents, besides the receptors, all the elements of the ECS, such as the AEA and 2-AG synthesis enzymes, respectively NAPE-PLD and DAGL, and the degradation enzymes, FAAH, MAGL, and other enzymes such

(Continued)

FIGURE 2 | as COX2. In green: Astrocyte takes part in the synapse and expresses different elements of the eCS such as endocannabinoids' synthesis and degradation enzymes and cannabinoid receptors, where the activation of CB1R may favor the influx of Ca^{2+} ions. Microglia expresses components of the eCS; the CB2R expression is higher than CB1R, and its modulation is linked to the production and secretion of different cytokines. Phytocannabinoids modulate the eCS through many targets. THC and THCV are CB1R agonists, while CBD, CBDV, CBG, and THCV are TRPV1 agonists. The EMT transporter is the pharmacological target of the phytocannabinoids CBD, CBDV, CBG, and THCV. The phytocannabinoids also act over enzyme activity - CBD inhibits FAAH, CBDA inhibits COX-2 and CBDV, CBDA, THCVA and CBDVA inhibit DAGL. **(B)** In the Neuropathic Pain scenario, there is glial reactivity, leading to the increase of astrocyte and microglia next to neurons, especially in the dorsal spinal cord. The eCS is modulated and the levels of expression of your components change. There is a higher expression of CB1R and CB2R in neurons and glial cells. Enzymes such as FAAH, COX-2, and 5-LOX also increase their expression, and in result, there is a decrease of AEA levels and increase of pro-inflammatory mediators. CBD, cannabidiol; THC, tetrahydrocannabinol; CBDV; cannabidivarin; CBDA, cannabidiolic acid; THCVA, tetrahydrocannabivarinic acid; CBDVA, cannabidivarinic acid; THCV, tetrahydrocannabivarin; CBG, cannabigerol.

are highly susceptible to molecular alterations, and such events are observed in chronic neuropathic pain pathogenesis, both in the CNS and PNS (Rani Sagar et al., 2012; Starowicz and Finn, 2017). Indeed, it has been described that the expression of CB1R and CB2R, the eCB synthesis machinery and the expression of FAAH are increased in the spinal cord of animals submitted to murine models of chronic neuropathic pain (Zhang et al., 2003, 2010; Guindon et al., 2013; Davis, 2014; Malek et al., 2014). Although there is elevation in eCBs synthesis, activation of FAAH and alternative catabolic pathways, involving cytochrome p450 (CYP), cyclooxygenase-2 (COX-2) and lipoxygenases, increase AEA degradation and generates inflammatory mediators, such as prostaglandins, which influence neuron excitability (Kozak et al., 2002; Snider et al., 2009; Chouinard et al., 2011; Rani Sagar et al., 2012; Mecca et al., 2021). The reduction of AEA and CB1R-mediated negative feedback in excitatory synapses contribute to the hyperalgesia mechanism (**Figure 2B**).

The fact that the eCS is involved in the pathophysiological state of pain makes this system a valid target for chronic neuropathic pain treatment. Nowadays, treatments for chronic neuropathic pain consist of four lines of therapies that are chosen according to the patient's condition (**Table 1**), with opioids being the most used (Attal et al., 2010; Rani Sagar et al., 2012; Moulin et al., 2014; Finnerup et al., 2015).

Despite the variety of treatments, there are no effective pharmacotherapeutic strategies for mitigating chronic neuropathic pain, in addition to patients that do not respond properly to treatments and are resistant to current medicines available (Dworkin et al., 2010; Yekkirala et al., 2017). Moreover, there is a huge opioid crisis with severe consequences centered on drug addiction, respiratory depression and death by overdose (Moore and McQuay, 2005; Fornasari, 2017; CDC, 2021; WHO, 2021). The lack of a solid treatment with few or no side effects makes the pharmaceutical industry avid to pursue new alternatives for these patients, and the modulation of eCS has been considered a promising tool.

CB1R/CB2R agonists and antagonists have been described as a valuable option to successfully modulate the eCS in chronic neuropathic pain animal models, bringing an alternative of treatment for patients that do not respond well to other pharmacological therapies. In addition, an indicative that modulating cannabinoid receptors could be a good alternative instead of opioids is the increased density of cannabinoids receptors in the spinal cord, compared to opioid receptors (Hohmann et al., 1999), and high/moderate expression of cannabinoid receptors in brain areas responsible for pain modulation, such as cortex, amygdala and periaqueductal gray matter, at least in rodents (Befort, 2015; **Figure 1**).

In animal models of chronic neuropathic pain, the administration of the synthetic cannabinoid CP 55,940, a CB1R agonist, terminated thermal hyperalgesia and decreased mechanical allodynia, evaluated by hot plate test and von Frey test, respectively (De Vry et al., 2004; Scott et al., 2004; Romero-Sandoval and Eisenach, 2007). A single administration of WIN55, 212-2, a mixed CB1R/CB2R-receptor agonist, 7 days after nerve ligation (a murine model of chronic neuropathic pain), reduced cold allodynia and thermal hyperalgesia symptoms, evaluated by acetone and hot plate test, respectively (Bridges et al., 2001; Rahn et al., 2007). The use of WIN55, 212-2 also improved mechanical allodynia at von Frey test in chemotherapy-induced chronic neuropathic pain, when animals presented behavior similar to those treated with opioids (Rahn et al., 2007; Burgos et al., 2012). At the cellular level, this agonist reduced glial reactivity and expression of inflammatory mediators, such as IL-6 and TNF-α (Burgos et al., 2012). It is important to notice that the combination of WIN55, 212-2 with selective CB1R and CB2R antagonists, SR141716 and SR144528, respectively, reversed the allodynia improvement, evaluated by von Frey test, demonstrating that both cannabinoid receptors are directly involved in these mechanisms and can be targeted for treatment purposes (Rahn et al., 2007). In addition, injection of JWH133 or JWH015, CB2R agonists, decreases mechanical allodynia after partial nerve ligation (Romero-Sandoval and Eisenach, 2007; Romero-Sandoval et al., 2008; Yamamoto et al., 2008). As described, CB2R is mostly expressed by microglial cells, which have their migration, proliferation and polarity modulated by cannabinoid receptor activation (Hegyi et al., 2009; Stella, 2009; Greineisen and Turner, 2010). Alternatively, CB2R activation by AM1241 decreases the expression of purinergic receptors P2Y, which is upregulated in microglia of chronic neuropathic animals, and decreases nuclear factor κ B (NF-κB) and p38 mitogen-activated protein kinase (p38 MAPK) phosphorylation, both involved in microglial activation and inflammatory response (Niu et al., 2017). The addition of 2-AG and AEA in primary microglial cell cultures increased the expression of both cannabinoid receptors and arginase-1, a marker for M2 microglia polarity, which is associated with pro-healing and anti-inflammatory responses (Mecha et al., 2015). The direct administration of AEA also led to better sensorial behavior in neuropathic murine animals, increasing mechanical and thermal threshold, evaluated by von Frey and hot plate tests (Guindon and Beaulieu, 2006; Desroches et al., 2008).

TABLE 1 | The four lines of treatment for chronic neuropathic pain.

Treatment	Mechanism of action	Line of treatment	References
Gabapentinoids	α2δ2-1 subunit of voltage-gated Ca^{2+} channels ligant	First-line treatment	Attal et al., 2010; Moulin et al., 2014; Hennemann-Krause and Sredni, 2016; Colloca et al., 2017
Tricyclic antidepressants	Inhibitors of Noradrenaline/Serotonin uptake systems	First-line treatment	Attal et al., 2010; Moulin et al., 2014; Hennemann-Krause and Sredni, 2016; Colloca et al., 2017
Noradrenaline/serotonin reuptake inhibitors	Inhibitors of noradrenaline/serotonin reuptake systems	First-line treatment	Attal et al., 2010; Moulin et al., 2014; Hennemann-Krause and Sredni, 2016; Colloca et al., 2017
Weak opioids	Opioid receptors agonists	Second-line treatment	Attal et al., 2010; Moulin et al., 2014; Hennemann-Krause and Sredni, 2016; Colloca et al., 2017
Strong opioids	Opioid receptors agonists	Second-line treatment	Attal et al., 2010; Moulin et al., 2014; Hennemann-Krause and Sredni, 2016; Colloca et al., 2017
Cannabinoids	Endocannabinoid system modulators	Third-line treatment	Attal et al., 2010; Moulin et al., 2014; Colloca et al., 2017
Selective serotonin reuptake inhibitors (SSRI)	Inhibitors of selective serotonin reuptake system	Fourth-line treatment	Moulin et al., 2014
Botulinum toxin	Inhibitors of acetylcholine release	Fourth-line treatment	Moulin et al., 2014
Methadone	Opioid and NMDA receptors	Fourth-line treatment	Moulin et al., 2014
Lamotrigine	Inhibitors of voltage-gated Na^{+} and Ca^{2+} channels	Fourth-line treatment	Moulin et al., 2014
Lacosamide	Slow inactivation of voltage-gated Na^{+} channels	Fourth-line treatment	Moulin et al., 2014
Tapentadol	Opioid receptors agonist and inhibitor of noradrenaline uptake system	Fourth-line treatment	Moulin et al., 2014
Topical lidocaine	Sodium channel blocker	Fourth-line treatment	Moulin et al., 2014
Topical capsaicin	TRPV1 receptor desensitization	Fourth-line treatment	Moulin et al., 2014

Moreover, some studies referred to the catabolic enzyme FAAH as an alternative target to modulate eCB levels. Intraperitoneal administration of the FAAH blocker URB597 and MAGL blocker JZL184 led to an increase in the mechanical threshold and a reduction of cold allodynia, in von Frey and acetone tests, in chronic neuropathic rats, respectively (Clapper et al., 2010; Guindon et al., 2013). The oral administration of another FAAH blocker, ST4070, also produced the same improvement in several animal models of chronic neuropathic pain, such as those induced by chemotherapy drugs and diabetes (Caprioli et al., 2012). Changes in animal behavior due to pain is probably correlated to the increased availability of eCB and other bioactive lipids, for instance AEA and palmitoylethanolamide (PEA), respectively (Caprioli et al., 2012).

After the enlightenment of eCS participation in pain modulation in physiological and pathological states, researchers started to investigate if classical analgesics mechanisms could involve the eCS. Regarding the effects of dipyrone, a common non-steroidal anti-inflammatory drug widely used primarily as an analgesic and antipyretic, the exact action mechanisms remain controversial. Studies on mice suggest that dipyrone-induced suppression of thermal antinociceptive, hypothermic and locomotor activity is mediated by a CB1R/CB2R-independent mechanism (Schlosburg et al., 2012). On the other hand, AM251, a CB1 antagonist, reversed the effects of dipyrone on locomotor activity, cataleptic response and thermal analgesia (Crunfli et al., 2015). Both AM251 and capsazepine, a TRPV1 antagonist, favored the decrease in body temperature caused by dipyrone. However, the CB2 receptor antagonist AM630 did not alter the hypothermic response to dipyrone (Crunfli et al., 2015). These results suggest that the eCS role, especially CB1R-mediated, in the analgesic effect of dipyrone is still a matter of debate.

Although the evidence in animal models is promising and suggests that inhibitors of catabolic enzymes might be a way of treating chronic neuropathic pain, clinical trials did not show the same outcome. In January 2016, it came to public attention that a drug named BIA10-2474, a FAAH inhibitor, led to severe adverse events in some volunteers in the clinical trial, in which five people had to be hospitalized, two had brain damage and one died (Mallet et al., 2016). Nowadays, in clinical practice, the synthetic cannabinoids used to treat neuropathic chronic pain are Dronabinol (Marinol® – Solvay Pharmaceuticals) and Nabilone (Cesamet® – Meda Pharmaceuticals), both having a chemical formula based on Δ^9-tetrahydrocannabinol (Δ^9-THC) (Stasiulewicz et al., 2020). Although these compounds may improve symptoms related to chronic neuropathic pain, some side effects such as euphoria, dysphoria, sleep disturbance and disorientation may occur. Diversely, the use of medicinal cannabis shows better results and less adverse events (Cannabis-In-Cachexia-Study-Group et al., 2006; Frank et al., 2008; Narang et al., 2008; Aviram and Samuelly-Leichtag, 2017).

MEDICINAL CANNABIS IN ANIMAL MODELS AND CLINICAL EVIDENCE

Cannabis sp. has been used to treat several pathologies, including pain episodes, since ancient China (Bonini et al., 2018). The main components in *Cannabis* sp. are the phytocannabinoids, and more than 100 of these compounds have been described

thus far. Even though the most investigated phytocannabinoids are cannabidiol (CBD) and Δ^9-THC, the latter known for its psychoactive effect, several other phytocannabinoids such as cannabidivarin (CBDV), Δ^9-tetrahydrocannabivarin (THCV) and their acidic forms are also being considered for therapeutic purposes (Di Marzo and Piscitelli, 2015; Cristino et al., 2020).

Phytocannabinoids act over several targets to modulate the eCS. For instance, while THC acts as CB1R and CB2R agonist, and THCV is a CB1R antagonist and TRPV1 agonist, CBD and CBDV inhibit eCB-degradation enzymes FAAH and MAGL (Di Marzo and Piscitelli, 2015; Cristino et al., 2020). Some phytocannabinoids also act in other neurochemical systems. For example, CBD can act over the serotoninergic and glycinergic receptors present in neurons, which are involved in pain processing, besides acting as TRPV1 and TRPM8 antagonist (Russo et al., 2005; De Petrocellis et al., 2008; Ahrens et al., 2009; García-Gutiérrez et al., 2020; **Figure 2A**).

Despite the recent statement from the IASP not encouraging the use of cannabinoids for pain treatment based on lack of quality researches reinforcing its safety and efficacy (IASP Presidential Task Force on Cannabis and Cannabinoid Analgesia, 2021), the positive outcomes and advantages over other pharmacological tools are compelling in animal research and clinical trials. For instance, Abraham et al. (2020) demonstrated in animals a phenomenon similar to what happens with patients. Neuropathic rats had a good response to morphine treatment, but the effect did not last up to 22 days after induction of pain, followed by drug-resistance. However, this effect was not observed in THC- and CBD-treated rats.

Tetrahydrocannabinol is known as the main analgesic compound from *Cannabis* sp. (Russo, 2008; Maayah et al., 2020). Several studies described a reduction of allodynic and hypersensitive behavior in animals, based on von Frey and hot plate tests results, after THC administration (Harris et al., 2016, 2019; Abraham et al., 2020). In addition to the fact that THC is a CB1R and CB2R agonist, reducing neurotransmitters release by neurons, especially glutamate, it also acts as TRPM8 antagonist and TRPA1 agonist (De Petrocellis et al., 2008; Storozhuk and Zholos, 2018). Another mechanism of action is inhibiting COX-2, which leads to increased levels of AEA and decreased levels of prostaglandins, whose therapeutic properties in chronic neuropathic pain pathology are the reduction of pro-inflammatory signaling, and probably, the decrease in glial and immunological cells response (Burstein et al., 1973; Ruhaak et al., 2011; **Figure 2A**).

CBD also contributes to decreased chronic neuropathic pain symptoms. Studies that investigated acute and chronic treatments of chronic neuropathic pain-induced rats with isolated CBD showed significantly increased mechanical and thermal threshold when compared to animals that received vehicle, evaluated by von Frey and hot plate tests (Xiong et al., 2012; Harris et al., 2016; King et al., 2017; Abraham et al., 2020; Silva-Cardoso et al., 2021). A plausible hypothesis that might explain how CBD improves the pathologic pain sensation is related to an increase in AEA levels due to FAAH inhibition and their agonist activity on TRPV1 agonist (Bisogno et al., 2001; Massi et al., 2008; Silva-Cardoso et al., 2021; **Figure 2A**). Silva-Cardoso et al. (2021) also demonstrated that CBD treatment decreased CB1R expression in pain matrix regions, which was up-regulated in animals submitted to chronic neuropathic pain models.

Furthermore, the combination of CBD and THC synergizes their positive effects and reduces THC side effects (Carlini et al., 1974; McPartland and Russo, 2001). In fact, the co-administration of CBD and THC decreases dysphoria, anxiety, panic attacks, and other psychoactive effects that THC may cause (Grinspoon and Bakalar, 1993; King et al., 2017). Authors also described that CBD competes with THC for the binding site of CYP2C19 enzyme in the liver and inhibits THC hydroxylation, which prolongs THC bioavailability, and therefore its effects (Jones and Pertwee, 1972; Benowitz et al., 1980).

The involvement of other compounds from *Cannabis* sp. in pain improvement have also been reported, for example, cannabinol (CBN) and cannabichromene (CBC), acting as CB2R agonist and inhibitor of cyclooxygenase, respectively (Burstein et al., 1973; Showalter et al., 1996; **Figure 2A**). Terpenes are another class of secondary metabolites present in *Cannabis* sp. with biological relevance and they may play a role in pain treatment, such as the terpenoid β-caryophyllene, which directly modulates the eCS as a CB2R agonist (Gertsch et al., 2008). In the chronic neuropathic pain animal model, the daily gavage of β-caryophyllene decreased nociceptive hyperalgesia and mechanical allodynia in a dose-dependent manner, as demonstrated by hot plate and von Frey tests. The treatment also reduced microglial reactivity and inflammatory response at spinal dorsal horn, probably due to β-caryophyllene-mediated increased expression of CB2R (Klauke et al., 2014; Segat et al., 2017). Other terpenoids participate in pain modulation through anti-inflammatory response. For instance, administration of β-myrcene increased thermal and nociceptive threshold either in healthy mice (Rao et al., 1990) or under inflammatory pain (Lorenzetti et al., 1991). Additionally, α-pinene also seems to control pain through anti-inflammatory pathways, decreasing cyclooxygenase-2 expression in an animal model of inflammatory pain (Li et al., 2016). Lastly, flavonoids, a group of chemical compounds present not only in *Cannabis* sp., but also in other plants, have anti-inflammatory properties and can decrease the release of pro-inflammatory cytokines from astrocytes and microglia (Gui et al., 2018; Nadipelly et al., 2018).

Several compounds present in the *Cannabis* sp. extract synergize with each other and might modulate their effects when compared to isolated phytocannabinoids (Carlini et al., 1974; Russo, 2008). The synergistic action of phytocannabinoids producing a potentiated pharmacological effect is called entourage effect (King et al., 2017). This property was described in several studies that reported higher efficacy of *Cannabis* sp. extract compared to administration of isolated CBD and THC in decreasing allodynia and hyperalgesia in rats, evaluated by hot plate and von Frey tests (Comelli et al., 2008; Casey et al., 2017; Harris et al., 2019). Indeed, Comelli et al. (2008) described that the improvement in hyperalgesia through the use of *Cannabis* sp. extract was not affected by the use of cannabinoid receptor antagonists, reinforcing the fact that phytocannabinoids and other compounds in

the extract act synergistically modulating several receptors and pathways. Additionally, the administration of a 1:1 CBD:THC extract has been described to positively modulate CD4+ lymphocytes in the spleen and thymus of female rats submitted to a nerve cuffed model for chronic neuropathic pain, which suggests that *Cannabis* sp. extract may also modulate immune response in the CNS related to chronic neuropathic pain development (Linher-Melville et al., 2020).

Patients consume medical *Cannabis sp.* products through different administration routes, such as smoked, vaporized, oromucosal aerosol, oily extract and capsules, although some studies describe that inhaling procedures can present health risks for patients (Aviram and Samuelly-Leichtag, 2017; Maayah et al., 2020). As described in animal studies, tests showed that *Cannabis* sp. full extract, such as Sativex®, an oromucosal spray of 1:1 CBD:THC, was more effective for treating chronic neuropathic pain than synthetic THC, such as Dronabinol (Cannabis-In-Cachexia-Study-Group et al., 2006; Langford et al., 2013; Ferrè et al., 2016; Schimrigk et al., 2017). Nurmikko et al. (2007) coordinated a randomized, double-blind, placebo-controlled study to evaluate the analgesic properties of a THC:CBD (1:1) extract in 125 patients that had peripheral neuropathic pain symptoms. During the treatment with the extract, individuals continued with other analgesic medication previously prescribed. Sixty-three patients were in the placebo group, while 62 made use of the extract and were able to determine their own dose, although none of them had more than 48 spray doses per day. The group that was treated with the extract showed better results in pain scores, dynamic allodynia, punctual allodynia when compared to patients from the other group. An appendix of the study evaluated the same patients for 52 weeks and continued to observe the analgesic effect of the extract without dose adjustment or toxicity symptoms.

A more complete and recent study from the Germain Pain e-registry digital platform collected anonymous information related to the therapeutic approaches used for pain management (Ueberall et al., 2019). Using the answers from a Pain Detect Questionnaire 7 (PDQ7), patients were grouped with nociceptive, mixed and chronic neuropathic pain. Individuals used 1:1 CBD:THC Sativex® oromucosal spray, 8–12 times/day, for 12 weeks. After 3 months of *Cannabis* sp. spray use, the pain intensity decreased at least half in 67.5% of the patients, having a better effect in neuropathic and mixed pain patients. Another important information from this study consists in improved patient's welfare after *Cannabis sp.* treatment. This was measured by the Aggregated 9-Factor Symptom Relief (ASR-9) questionnaire. Fifteen percent of the individuals in the study improved at least 50% of all 9 factors and 56% of the patients improved at least 5 factors, such as stress, depression, well-being and anxiety, and again, the improvement was higher in neuropathic and mixed pain patients.

Another advantage to the use of Cannabis-derived products is the significant decrease or even elimination of other drugs, such as opioids, from the therapy scheme, known for having severe adverse effects. As described by Ueberall et al. (2019), a significant number of patients stopped using strong opioids as analgesic strategy 12 weeks after using *Cannabis sp.* extracts. Other clinical and animal researches describe similar results in opioid-based therapies after the use of *Cannabis* sp. extracts (Williams et al., 2008; Okusanya et al., 2020; Takakuwa and Sulak, 2020).

Together with the relief of symptoms, adverse effects are often described by patients under use of medicinal cannabis. The most common are gastrointestinal disorders, metabolism and nutrition disorders, increased appetite, sedation, fatigue, dry mouth, dizziness, and nausea (Nurmikko et al., 2007; Lynch et al., 2014; Ueberall et al., 2019). Few patients described adverse effects related to the psychoactive properties of THC. One patient described anxiety, panic attack, and confusion in the Lynch study (Lynch et al., 2014) and only 3.6% of patients described anxiety, confusion, and disorientation in the Germain Pain e-registry based study (Ueberall et al., 2019), while, in Nurmikko et al. (2007), no psychoactive symptoms were listed by the participants. In general, most of the adverse effects are mild to moderate and are directly related to the dosage of THC in the product used in these researchers, besides the modulation of eCS in other organs and systems. However, it is important to highlight that in all clinical studies cited, patients with a history of psychotic disorder were excluded from the study.

DISCUSSION

Chronic neuropathic pain is a pathology that affects not only many individuals worldwide, but also their caregivers (Ojeda et al., 2014). Even though opioids are the main pharmacotherapeutic approach to reduce symptoms associated with chronic neuropathic pain, several reports describe its potential of inducing addiction and, as consequence, increasing mortality (Hser et al., 2015). In order to avoid side effects similar to those induced by opioids and have increased success in managing pain, new molecular targets are being continuously investigated for treatment of neuropathic chronic pain.

In this review, we describe how the eCS modulates the pathophysiological processing of pain, focusing mostly on animal models of chronic neuropathic pain and clinical trials. Several strategies have been developed to assess eCS role in chronic neuropathic pain management, such as the use of synthetic cannabinoid receptors agonists and degradation enzyme inhibitors, which have shown promising results in animal models. Unfortunately, it is not always possible to translate pre-clinical data into successful clinical application. As an example, the use of FAAH inhibitors, which showed positive results in many animal models, led to severe adverse effects and even death of a volunteer in a clinical trial (Mallet et al., 2016).

The use of Cannabis-based products is recommended as extracts, for instance Sativex®. Although some synthetic cannabinoids may also be indicated for pain treatment, such as Dronabinol and Nabilone, the use of medicinal *Cannabis* sp. has recently increased substantially, improving pain management and inducing fewer side effects (Mücke et al., 2018). Despite this evidence, the IASP states that it lacks reliable clinical studies about the use of phytocannabinoids and medicinal *Cannabis* sp.

to treat chronic pain (IASP Presidential Task Force on Cannabis and Cannabinoid Analgesia, 2021). Besides, there is little preclinical research that investigates the effect of *Cannabis* sp. extracts, the latter more commonly used by patients.

The role of eCS as a pharmacological target and the advantages of using medicinal *Cannabis sp.* to treat pain is remarkable, as described in this review. However, further investigation must be performed using animal models and in clinical practice to understand more efficient ways to modulate the eCS in humans and to identify how the entourage effect may contribute to the potential of Cannabis-based treatments in pain management.

AUTHOR CONTRIBUTIONS

RC, AA, YP-C, and PT wrote different sections of the review. BF also designed the original figures from this manuscript. RM and LS also provided the intellectual assistance, reviewed, and corrected the manuscript. All authors performed the literature revision need for this review and approved the submitted version.

FUNDING

This study was supported by the Coordenação de Aperfeiçoamento de Pessoal de Nível Superior (CAPES), Fundação Carlos Chagas Filho de Amparo à Pesquisa do Estado do Rio de Janeiro (FAPERJ), and Conselho Nacional de Desenvolvimento Científico e Tecnológico (CNPq), LS was supported by FAPERJ, grant number E-26/202.997/2019; RM was supported by FAPERJ, grant numbers E-26/202.668/2018 and E-26/010.002215/2019; grant numbers 426342/2018-6 and 312157/2016-9; INCT-INNT (National Institute for Translational Neuroscience); and RC was supported by CAPES, grant number 88887.360870/2019-00.

REFERENCES

Abraham, A. D., Leung, E. J. Y., Wong, B. A., Rivera, Z. M. G., Kruse, L. C., Clark, J. J., et al. (2020). Orally consumed cannabinoids provide long-lasting relief of allodynia in a mouse model of chronic neuropathic pain. *Neuropsychopharmacology* 45, 1105–1114. doi: 10.1038/s41386-019-0585-3

Ahrens, J., Demir, R., Leuwer, M., de la Roche, J., Krampfl, K., Foadi, N., et al. (2009). The nonpsychotropic cannabinoid cannabidiol modulates and directly activates alpha-1 and alpha-1-beta glycine receptor function. *Pharmacology* 83, 217–222. doi: 10.1159/000201556

Alles, S. R. A., and Smith, P. A. (2018). Etiology and pharmacology of neuropathic pain. *Pharmacol. Rev.* 70, 315–347. doi: 10.1124/pr.117.014399

Attal, N., Cruccu, G., Baron, R., Haanpää, M., Hansson, P., Jensen, T. S., et al. (2010). EFNS guidelines on the pharmacological treatment of neuropathic pain: 2010 revision. *Eur. J. Neurol.* 17, 1113–e88. doi: 10.1111/j.1468-1331.2010.02999.x

Aviram, J., and Samuelly-Leichtag, G. (2017). Efficacy of Cannabis-based medicines for pain management: a systematic review and meta-analysis of randomized controlled trials. *Pain Physician* 20, E755–E796.

Befort, K. (2015). Interactions of the opioid and cannabinoid systems in reward: insights from knockout studies. *Front. Pharmacol.* 6:6. doi: 10.3389/fphar.2015.00006

Benowitz, N. L., Nguyen, T. L., Jones, R. T., Herning, R. I., and Bachman, J. (1980). Metabolic and psychophysiologic studies of cannabidiol-hexobarbital interaction. *Clin. Pharmacol. Ther.* 28, 115–120. doi: 10.1038/clpt.1980.139

Bisogno, T., Hanus, L., De Petrocellis, L., Tchilibon, S., Ponde, D. E., Brandi, I., et al. (2001). Molecular targets for cannabidiol and its synthetic analogues: effect on vanilloid VR1 receptors and on the cellular uptake and enzymatic hydrolysis of anandamide. *Br. J. Pharmacol.* 134, 845–852. doi: 10.1038/sj.bjp.0704327

Bonini, S. A., Premoli, M., Tambaro, S., Kumar, A., Maccarinelli, G., Memo, M., et al. (2018). *Cannabis sativa*: a comprehensive ethnopharmacological review of a medicinal plant with a long history. *J. Ethnopharmacol.* 227, 300–315. doi: 10.1016/j.jep.2018.09.004

Bridges, D., Ahmad, K., and Rice, A. S. (2001). The synthetic cannabinoid WIN55,212-2 attenuates hyperalgesia and allodynia in a rat model of neuropathic pain. *Br. J. Pharmacol.* 133, 586–594. doi: 10.1038/sj.bjp.0704110

Burgos, E., Gómez-Nicola, D., Pascual, D., Martín, M. I., Nieto-Sampedro, M., and Goicoechea, C. (2012). Cannabinoid agonist WIN 55,212-2 prevents the development of paclitaxel-induced peripheral neuropathy in rats. Possible involvement of spinal glial cells. *Eur. J. Pharmacol.* 682, 62–72. doi: 10.1016/j.ejphar.2012.02.008

Burstein, S., Levin, E., and Varanelli, C. (1973). Prostaglandins and cannabis. II. Inhibition of biosynthesis by the naturally occurring cannabinoids. *Biochem. Pharmacol.* 22, 2905–2910. doi: 10.1016/0006-2952(73)90158-5

Cannabis-In-Cachexia-Study-Group, Strasser, F., Luftner, D., Possinger, K., Ernst, G., Ruhstaller, T., et al. (2006). Comparison of orally administered cannabis extract and delta-9-tetrahydrocannabinol in treating patients with cancer-related anorexia-cachexia syndrome: a multicenter, phase III, randomized, double-blind, placebo-controlled clinical trial from the Cannabis-In-Cachexia-Study-Group. *J. Clin. Oncol.* 24, 3394–3400. doi: 10.1200/JCO.2005.05.1847

Caprioli, A., Coccurello, R., Rapino, C., Di Serio, S., Di Tommaso, M., Vertechy, M., et al. (2012). The novel reversible fatty acid amide hydrolase inhibitor ST4070 increases endocannabinoid brain levels and counteracts neuropathic pain in different animal models. *J. Pharmacol. Exp. Ther.* 342, 188–195. doi: 10.1124/jpet.111.191403

Carlini, E. A., Karniol, I. G., Renault, P. F., and Schuster, C. R. (1974). Effects of marihuana in laboratory animals and in man. *Br. J. Pharmacol.* 50, 299–309. doi: 10.1111/j.1476-5381.1974.tb08576.x

Casey, S. L., Atwal, N., and Vaughan, C. W. (2017). Cannabis constituent synergy in a mouse neuropathic pain model. *Pain* 158, 2452–2460. doi: 10.1097/j.pain.0000000000001051

Cata, J. P., Weng, H. R., Chen, J. H., and Dougherty, P. M. (2006). Altered discharges of spinal wide dynamic range neurons and down-regulation of glutamate transporter expression in rats with paclitaxel-induced hyperalgesia. *Neuroscience* 138, 329–338. doi: 10.1016/j.neuroscience.2005.11.009

Caterina, M. J., Rosen, T. A., Tominaga, M., Brake, A. J., and Julius, D. (1999). A capsaicin-receptor homologue with a high threshold for noxious heat. *Nature* 398, 436–441. doi: 10.1038/18906

CDC (2021). *Understanding the Epidemic*. Available online at: https://www.cdc.gov/opioids/basics/epidemic.html (accessed October 30, 2021).

Choi, B. M., Lee, S. H., An, S. M., Park, D. Y., Lee, G. W., and Noh, G. J. (2015). Corrigendum: the time-course and RNA interference of TNF-α, IL-6, and IL-1β expression on neuropathic pain induced by L5 spinal nerve transection in rats (Korean J Anesthesiol 2015 April 68(2): 159-169). *Korean J. Anesthesiol.* 68:311. doi: 10.4097/kjae.2015.68.3.311

Chouinard, F., Lefebvre, J. S., Navarro, P., Bouchard, L., Ferland, C., Lalancette-Hébert, M., et al. (2011). The endocannabinoid 2-arachidonoyl-glycerol activates human neutrophils: critical role of its hydrolysis and de novo leukotriene B4 biosynthesis. *J. Immunol.* 186, 3188–3196. doi: 10.4049/jimmunol.1002853

Clapper, J. R., Moreno-Sanz, G., Russo, R., Guijarro, A., Vacondio, F., Duranti, A., et al. (2010). Anandamide suppresses pain initiation through a peripheral endocannabinoid mechanism. *Nat. Neurosci.* 13, 1265–1270. doi: 10.1038/nn.2632

Cohen, S. P., and Mao, J. (2014). Neuropathic pain: mechanisms and their clinical implications. *BMJ* 348:f7656. doi: 10.1136/bmj.f7656

Colloca, L., Ludman, T., Bouhassira, D., Baron, R., Dickenson, A. H., Yarnitsky, D., et al. (2017). Neuropathic pain. *Nat. Rev. Dis. Primers* 3:17002. doi: 10.1038/nrdp.2017.2

Comelli, F., Giagnoni, G., Bettoni, I., Colleoni, M., and Costa, B. (2008). Antihyperalgesic effect of a *Cannabis sativa* extract in a rat model of neuropathic pain: mechanisms involved. *Phytother. Res.* 22, 1017–1024. doi: 10.1002/ptr.2401

Cristino, L., Bisogno, T., and Di Marzo, V. (2020). Cannabinoids and the expanded endocannabinoid system in neurological disorders. *Nat. Rev. Neurol.* 16, 9–29. doi: 10.1038/s41582-019-0284-z

Crunfli, F., Vilela, F. C., and Giusti-Paiva, A. (2015). Cannabinoid CB1 receptors mediate the effects of dipyrone. *Clin. Exp. Pharmacol. Physiol.* 42, 246–255. doi: 10.1111/1440-1681.12347

D'Arco, M., Margas, W., Cassidy, J. S., and Dolphin, A. C. (2015). The upregulation of α2δ-1 subunit modulates activity-dependent Ca^{2+} signals in sensory neurons. *J. Neurosci.* 35, 5891–5903. doi: 10.1523/jneurosci.3997-14.2015

Davis, M. P. (2014). Cannabinoids in pain management: CB1, CB2 and non-classic receptor ligands. *Expert Opin. Investig. Drugs* 23, 1123–1140. doi: 10.1517/13543784.2014.918603

Davoli-Ferreira, M., de Lima, K. A., Fonseca, M. M., Guimarães, R. M., Gomes, F. I., Cavallini, M. C., et al. (2020). Regulatory T cells counteract neuropathic pain through inhibition of the Th1 response at the site of peripheral nerve injury. *Pain* 161, 1730–1743. doi: 10.1097/j.pain.0000000000001879

De Petrocellis, L., Starowicz, K., Moriello, A. S., Vivese, M., Orlando, P., and Di Marzo, V. (2007). Regulation of transient receptor potential channels of melastatin type 8 (TRPM8): effect of cAMP, cannabinoid CB(1) receptors and endovanilloids. *Exp. Cell Res.* 313, 1911–1920. doi: 10.1016/j.yexcr.2007.01.008

De Petrocellis, L., Vellani, V., Schiano-Moriello, A., Marini, P., Magherini, P. C., Orlando, P., et al. (2008). Plant-derived cannabinoids modulate the activity of transient receptor potential channels of ankyrin type-1 and melastatin type-8. *J. Pharmacol. Exp. Ther.* 325, 1007–1015. doi: 10.1124/jpet.107.134809

De Vry, J., Kuhl, E., Franken-Kunkel, P., and Eckel, G. (2004). Pharmacological characterization of the chronic constriction injury model of neuropathic pain. *Eur. J. Pharmacol.* 491, 137–148. doi: 10.1016/j.ejphar.2004.03.051

Desroches, J., Guindon, J., Lambert, C., and Beaulieu, P. (2008). Modulation of the anti-nociceptive effects of 2-arachidonoyl glycerol by peripherally administered FAAH and MGL inhibitors in a neuropathic pain model. *Br. J. Pharmacol.* 155, 913–924. doi: 10.1038/bjp.2008.322

Di Marzo, V., and Piscitelli, F. (2015). The endocannabinoid system and its modulation by phytocannabinoids. *Neurotherapeutics* 12, 692–698. doi: 10.1007/s13311-015-0374-6

D'Mello, R., and Dickenson, A. H. (2008). Spinal cord mechanisms of pain. *Br. J. Anaesth.* 101, 8–16. doi: 10.1093/bja/aen088

Dworkin, R. H., O'Connor, A. B., Audette, J., Baron, R., Gourlay, G. K., Haanpää, M. L., et al. (2010). Recommendations for the pharmacological management of neuropathic pain: an overview and literature update. *Mayo Clin. Proc.* 85(Suppl. 3), S3–S14. doi: 10.4065/mcp.2009.0649

Farquhar-Smith, W. P., Egertová, M., Bradbury, E. J., McMahon, S. B., Rice, A. S., and Elphick, M. R. (2000). Cannabinoid CB(1) receptor expression in rat spinal cord. *Mol. Cell. Neurosci.* 15, 510–521. doi: 10.1006/mcne.2000.0844

Ferrè, L., Nuara, A., Pavan, G., Radaelli, M., Moiola, L., Rodegher, M., et al. (2016). Efficacy and safety of nabiximols (Sativex(®)) on multiple sclerosis spasticity in a real-life Italian monocentric study. *Neurol. Sci.* 37, 235–242. doi: 10.1007/s10072-015-2392-x

Finn, D. P., Haroutounian, S., Hohmann, A. G., Krane, E., Soliman, N., and Rice, A. S. C. (2021). Cannabinoids, the endocannabinoid system, and pain: a review of preclinical studies. *Pain* 162(Suppl. 1), S5–S25. doi: 10.1097/j.pain.0000000000002268

Finnerup, N. B., Attal, N., Haroutounian, S., McNicol, E., Baron, R., Dworkin, R. H., et al. (2015). Pharmacotherapy for neuropathic pain in adults: a systematic review and meta-analysis. *Lancet Neurol.* 14, 162–173. doi: 10.1016/s1474-4422(14)70251-0

Fornasari, D. (2017). Pharmacotherapy for neuropathic pain: a review. *Pain Ther.* 6(Suppl. 1), 25–33. doi: 10.1007/s40122-017-0091-4

Foster, E., Wildner, H., Tudeau, L., Haueter, S., Ralvenius, W. T., Jegen, M., et al. (2015). Targeted ablation, silencing, and activation establish glycinergic dorsal horn neurons as key components of a spinal gate for pain and itch. *Neuron* 85, 1289–1304. doi: 10.1016/j.neuron.2015.02.028

Frank, B., Serpell, M. G., Hughes, J., Matthews, J. N., and Kapur, D. (2008). Comparison of analgesic effects and patient tolerability of nabilone and dihydrocodeine for chronic neuropathic pain: randomised, crossover, double blind study. *BMJ* 336, 199–201. doi: 10.1136/bmj.39429.619653.80

García-Gutiérrez, M. S., Navarrete, F., Gasparyan, A., Austrich-Olivares, A., Sala, F., and Manzanares, J. (2020). Cannabidiol: a potential new alternative for the treatment of anxiety, depression, and psychotic disorders. *Biomolecules* 10:1575. doi: 10.3390/biom10111575

Gertsch, J., Leonti, M., Raduner, S., Racz, I., Chen, J. Z., Xie, X. Q., et al. (2008). Beta-caryophyllene is a dietary cannabinoid. *Proc. Natl. Acad. Sci. U.S.A.* 105, 9099–9104. doi: 10.1073/pnas.0803601105

Greineisen, W. E., and Turner, H. (2010). Immunoactive effects of cannabinoids: considerations for the therapeutic use of cannabinoid receptor agonists and antagonists. *Int. Immunopharmacol.* 10, 547–555. doi: 10.1016/j.intimp.2010.02.012

Grinspoon, L., and Bakalar, J. B. (1993). *Marihuana, the Forbidden Medicine*. New Haven, CT: Yale University Press.

Gui, Y., Zhang, J., Chen, L., Duan, S., Tang, J., Xu, W., et al. (2018). Icariin, a flavonoid with anti-cancer effects, alleviated paclitaxel-induced neuropathic pain in a SIRT1-dependent manner. *Mol. Pain* 14:1744806918768970. doi: 10.1177/1744806918768970

Guindon, J., and Beaulieu, P. (2006). Antihyperalgesic effects of local injections of anandamide, ibuprofen, rofecoxib and their combinations in a model of neuropathic pain. *Neuropharmacology* 50, 814–823. doi: 10.1016/j.neuropharm.2005.12.002

Guindon, J., Lai, Y., Takacs, S. M., Bradshaw, H. B., and Hohmann, A. G. (2013). Alterations in endocannabinoid tone following chemotherapy-induced peripheral neuropathy: effects of endocannabinoid deactivation inhibitors targeting fatty-acid amide hydrolase and monoacylglycerol lipase in comparison to reference analgesics following cisplatin treatment. *Pharmacol. Res.* 67, 94–109. doi: 10.1016/j.phrs.2012.10.013

Habib, A. M., Okorokov, A. L., Hill, M. N., Bras, J. T., Lee, M. C., Li, S., et al. (2019). Microdeletion in a FAAH pseudogene identified in a patient with high anandamide concentrations and pain insensitivity. *Br. J. Anaesth.* 123, e249–e253. doi: 10.1016/j.bja.2019.02.019

Harris, H. M., Rousseau, M. A., Wanas, A. S., Radwan, M. M., Caldwell, S., Sufka, K. J., et al. (2019). Role of cannabinoids and terpenes in cannabis-mediated analgesia in rats. *Cannabis Cannabinoid Res.* 4, 177–182. doi: 10.1089/can.2018.0054

Harris, H. M., Sufka, K. J., Gul, W., and ElSohly, M. A. (2016). Effects of delta-9-tetrahydrocannabinol and cannabidiol on cisplatin-induced neuropathy in mice. *Planta Med.* 82, 1169–1172. doi: 10.1055/s-0042-106303

Hegyi, Z., Kis, G., Holló, K., Ledent, C., and Antal, M. (2009). Neuronal and glial localization of the cannabinoid-1 receptor in the superficial spinal dorsal horn of the rodent spinal cord. *Eur. J. Neurosci.* 30, 251–262. doi: 10.1111/j.1460-9568.2009.06816.x

Hennemann-Krause, L., and Sredni, S. (2016). Systemic drug therapy for neuropathic pain. *Revista Dor* 17(Suppl. 1), 91–94. doi: 10.5935/1806-0013.20160057

Hohmann, A. G., Briley, E. M., and Herkenham, M. (1999). Pre- and postsynaptic distribution of cannabinoid and mu opioid receptors in rat spinal cord. *Brain Res.* 822, 17–25. doi: 10.1016/s0006-8993(98)01321-3

Howlett, A. C., Barth, F., Bonner, T. I., Cabral, G., Casellas, P., Devane, W. A., et al. (2002). International Union of Pharmacology. XXVII. Classification of cannabinoid receptors. *Pharmacol. Rev.* 54, 161–202. doi: 10.1124/pr.54.2.161

Hser, Y. I., Evans, E., Grella, C., Ling, W., and Anglin, D. (2015). Long-term course of opioid addiction. *Harv. Rev. Psychiatry* 23, 76–89. doi: 10.1097/HRP.0000000000000052

IASP Presidential Task Force on Cannabis and Cannabinoid Analgesia (2021). International Association for the Study of Pain presidential task force on cannabis and cannabinoid Analgesia position statement. *Pain* 162(Suppl. 1), S1–S2. doi: 10.1097/j.pain.0000000000002265

Immke, D. C., and Gavva, N. R. (2006). The TRPV1 receptor and nociception. *Semin. Cell. Dev. Biol.* 17, 582–591. doi: 10.1016/j.semcdb.2006.09.004

Janssen, S. P., Truin, M., Van Kleef, M., and Joosten, E. A. (2011). Differential GABAergic disinhibition during the development of painful peripheral neuropathy. *Neuroscience* 184, 183–194. doi: 10.1016/j.neuroscience.2011.03.060

Jones, G., and Pertwee, R. G. (1972). A metabolic interaction in vivo between cannabidiol and 1 -tetrahydrocannabinol. *Br. J. Pharmacol.* 45, 375–377. doi: 10.1111/j.1476-5381.1972.tb08092.x

Katona, I., Rancz, E. A., Acsady, L., Ledent, C., Mackie, K., Hajos, N., et al. (2001). Distribution of CB1 cannabinoid receptors in the amygdala and their role in the control of GABAergic transmission. *J. Neurosci.* 21, 9506–9518. doi: 10.1523/JNEUROSCI.21-23-09506.2001

King, K. M., Myers, A. M., Soroka-Monzo, A. J., Tuma, R. F., Tallarida, R. J., Walker, E. A., et al. (2017). Single and combined effects of Δ(9) -tetrahydrocannabinol and cannabidiol in a mouse model of chemotherapy-induced neuropathic pain. *Br. J. Pharmacol.* 174, 2832–2841. doi: 10.1111/bph.13887

Klauke, A. L., Racz, I., Pradier, B., Markert, A., Zimmer, A. M., Gertsch, J., et al. (2014). The cannabinoid CB2 receptor-selective phytocannabinoid beta-caryophyllene exerts analgesic effects in mouse models of inflammatory and neuropathic pain. *Eur. Neuropsychopharmacol.* 24, 608–620. doi: 10.1016/j.euroneuro.2013.10.008

Kleinschnitz, C., Hofstetter, H. H., Meuth, S. G., Braeuninger, S., Sommer, C., and Stoll, G. (2006). T cell infiltration after chronic constriction injury of mouse sciatic nerve is associated with interleukin-17 expression. *Exp. Neurol.* 200, 480–485. doi: 10.1016/j.expneurol.2006.03.014

Knaster, P., Karlsson, H., Estlander, A. M., and Kalso, E. (2012). Psychiatric disorders as assessed with SCID in chronic pain patients: the anxiety disorders precede the onset of pain. *Gen. Hosp. Psychiatry* 34, 46–52. doi: 10.1016/j.genhosppsych.2011.09.004

Kozak, K. R., Gupta, R. A., Moody, J. S., Ji, C., Boeglin, W. E., DuBois, R. N., et al. (2002). 15-Lipoxygenase metabolism of 2-arachidonylglycerol. Generation of a peroxisome proliferator-activated receptor alpha agonist. *J. Biol. Chem.* 277, 23278–23286. doi: 10.1074/jbc.M201084200

Kuner, R., and Flor, H. (2017). Structural plasticity and reorganisation in chronic pain. *Nat. Rev. Neurosci.* 18:113. doi: 10.1038/nrn.2017.5

Langford, R. M., Mares, J., Novotna, A., Vachova, M., Novakova, I., Notcutt, W., et al. (2013). A double-blind, randomized, placebo-controlled, parallel-group study of THC/CBD oromucosal spray in combination with the existing treatment regimen, in the relief of central neuropathic pain in patients with multiple sclerosis. *J. Neurol.* 260, 984–997. doi: 10.1007/s00415-012-6739-4

Lauria, G., Morbin, M., Lombardi, R., Capobianco, R., Camozzi, F., Pareyson, D., et al. (2006). Expression of capsaicin receptor immunoreactivity in human peripheral nervous system and in painful neuropathies. *J. Peripher. Nerv Syst.* 11, 262–271. doi: 10.1111/j.1529-8027.2006.0097.x

Le Pichon, C. E., and Chesler, A. T. (2014). The functional and anatomical dissection of somatosensory subpopulations using mouse genetics. *Front. Neuroanat.* 8:21. doi: 10.3389/fnana.2014.00021

Legrain, V., Iannetti, G. D., Plaghki, L., and Mouraux, A. (2011). The pain matrix reloaded: a salience detection system for the body. *Prog. Neurobiol.* 93, 111–124. doi: 10.1016/j.pneurobio.2010.10.005

Li, C. Y., Song, Y. H., Higuera, E. S., and Luo, Z. D. (2004). Spinal dorsal horn calcium channel alpha2delta-1 subunit upregulation contributes to peripheral nerve injury-induced tactile allodynia. *J. Neurosci.* 24, 8494–8499. doi: 10.1523/jneurosci.2982-04.2004

Li, X. J., Yang, Y. J., Li, Y. S., Zhang, W. K., and Tang, H. B. (2016). α-Pinene, linalool, and 1-octanol contribute to the topical anti-inflammatory and analgesic activities of frankincense by inhibiting COX-2. *J. Ethnopharmacol.* 179, 22–26. doi: 10.1016/j.jep.2015.12.039

Linher-Melville, K., Zhu, Y. F., Sidhu, J., Parzei, N., Shahid, A., Seesankar, G., et al. (2020). Evaluation of the preclinical analgesic efficacy of naturally derived, orally administered oil forms of Δ9-tetrahydrocannabinol (THC), cannabidiol (CBD), and their 1:1 combination. *PLoS One* 15:e0234176. doi: 10.1371/journal.pone.0234176

Lorenzetti, B. B., Souza, G. E., Sarti, S. J., Santos Filho, D., and Ferreira, S. H. (1991). Myrcene mimics the peripheral analgesic activity of lemongrass tea. *J. Ethnopharmacol.* 34, 43–48. doi: 10.1016/0378-8741(91)90187-i

Lynch, M. E., Cesar-Rittenberg, P., and Hohmann, A. G. (2014). A double-blind, placebo-controlled, crossover pilot trial with extension using an oral mucosal cannabinoid extract for treatment of chemotherapy-induced neuropathic pain. *J. Pain Symptom Manage.* 47, 166–173. doi: 10.1016/j.jpainsymman.2013.02.018

Maayah, Z. H., Takahara, S., Ferdaoussi, M., and Dyck, J. R. B. (2020). The molecular mechanisms that underpin the biological benefits of full-spectrum cannabis extract in the treatment of neuropathic pain and inflammation. *Biochim. Biophys. Acta Mol. Basis Dis.* 1866:165771. doi: 10.1016/j.bbadis.2020.165771

Maccarrone, M., Bab, I., Bíró, T., Cabral, G. A., Dey, S. K., Di Marzo, V., et al. (2015). Endocannabinoid signaling at the periphery: 50 years after THC. *Trends Pharmacol. Sci.* 36, 277–296. doi: 10.1016/j.tips.2015.02.008

Malek, N., Kucharczyk, M., and Starowicz, K. (2014). Alterations in the anandamide metabolism in the development of neuropathic pain. *Biomed. Res. Int.* 2014:686908. doi: 10.1155/2014/686908

Mallet, C., Dubray, C., and Dualé, C. (2016). FAAH inhibitors in the limelight, but regrettably. *Int. J. Clin. Pharmacol. Ther.* 54, 498–501. doi: 10.5414/cp202687

Massi, P., Valenti, M., Vaccani, A., Gasperi, V., Perletti, G., Marras, E., et al. (2008). 5-Lipoxygenase and anandamide hydrolase (FAAH) mediate the antitumor activity of cannabidiol, a non-psychoactive cannabinoid. *J. Neurochem.* 104, 1091–1100. doi: 10.1111/j.1471-4159.2007.05073.x

McPartland, J., and Russo, E. (2001). Cannabis and cannabis extracts: greater than the sum of their parts? *J. Cannabis Ther.* 1, 103–132. doi: 10.1300/J175v01n03_08

Meacham, K., Shepherd, A., Mohapatra, D. P., and Haroutounian, S. (2017). Neuropathic pain: central vs. Peripheral mechanisms. *Curr. Pain Headache Rep.* 21:28. doi: 10.1007/s11916-017-0629-5

Mecca, C. M., Chao, D., Yu, G., Feng, Y., Segel, I., Zhang, Z., et al. (2021). Dynamic change of endocannabinoid signaling in the medial prefrontal cortex controls the development of depression after neuropathic pain. *J. Neurosci.* 41, 7492–7508. doi: 10.1523/JNEUROSCI.3135-20.2021

Mecha, M., Feliú, A., Carrillo-Salinas, F. J., Rueda-Zubiaurre, A., Ortega-Gutiérrez, S., de Sola, R. G., et al. (2015). Endocannabinoids drive the acquisition of an alternative phenotype in microglia. *Brain Behav. Immun.* 49, 233–245. doi: 10.1016/j.bbi.2015.06.002

Moore, K. A., Kohno, T., Karchewski, L. A., Scholz, J., Baba, H., and Woolf, C. J. (2002). Partial peripheral nerve injury promotes a selective loss of GABAergic inhibition in the superficial dorsal horn of the spinal cord. *J. Neurosci.* 22, 6724–6731. doi: 10.1523/jneurosci.22-15-06724.2002

Moore, R. A., and McQuay, H. J. (2005). Prevalence of opioid adverse events in chronic non-malignant pain: systematic review of randomised trials of oral opioids. *Arthritis Res. Ther.* 7, R1046–R1051. doi: 10.1186/ar1782

Moulin, D., Boulanger, A., Clark, A. J., Clarke, H., Dao, T., Finley, G. A., et al. (2014). Pharmacological management of chronic neuropathic pain: revised consensus statement from the Canadian Pain Society. *Pain Res. Manag.* 19, 328–335. doi: 10.1155/2014/754693

Mücke, M., Phillips, T., Radbruch, L., Petzke, F., and Häuser, W. (2018). Cannabis-based medicines for chronic neuropathic pain in adults. *Cochrane Database Syst. Rev.* 3:Cd012182. doi: 10.1002/14651858.CD012182.pub2

Nadipelly, J., Sayeli, V., Kadhirvelu, P., Shanmugasundaram, J., Cheriyan, B. V., and Subramanian, V. (2018). Effect of certain trimethoxy flavones on paclitaxel - induced peripheral neuropathy in mice. *Integr. Med. Res.* 7, 159–167. doi: 10.1016/j.imr.2018.03.006

Narang, S., Gibson, D., Wasan, A. D., Ross, E. L., Michna, E., Nedeljkovic, S. S., et al. (2008). Efficacy of dronabinol as an adjuvant treatment for chronic pain patients on opioid therapy. *J. Pain* 9, 254–264. doi: 10.1016/j.jpain.2007.10.018

Niu, J., Huang, D., Zhou, R., Yue, M., Xu, T., Yang, J., et al. (2017). Activation of dorsal horn cannabinoid CB2 receptor suppresses the expression of P2Y(12) and P2Y(13) receptors in neuropathic pain rats. *J. Neuroinflammation* 14:185. doi: 10.1186/s12974-017-0960-0

Nurmikko, T. J., Serpell, M. G., Hoggart, B., Toomey, P. J., Morlion, B. J., and Haines, D. (2007). Sativex successfully treats neuropathic pain characterised by allodynia: a randomised, double-blind, placebo-controlled clinical trial. *Pain* 133, 210–220. doi: 10.1016/j.pain.2007.08.028

Ojeda, B., Salazar, A., Dueñas, M., Torres, L. M., Micó, J. A., and Failde, I. (2014). The impact of chronic pain: the perspective of patients, relatives, and caregivers. *Fam. Syst. Health* 32, 399–407. doi: 10.1037/fsh0000069

Okusanya, B. O., Asaolu, I. O., Ehiri, J. E., Kimaru, L. J., Okechukwu, A., and Rosales, C. (2020). Medical cannabis for the reduction of opioid dosage in the treatment of non-cancer chronic pain: a systematic review. *Syst. Rev.* 9:167. doi: 10.1186/s13643-020-01425-3

Ossipov, M. H., Dussor, G. O., and Porreca, F. (2010). Central modulation of pain. *J. Clin. Invest.* 120, 3779–3787. doi: 10.1172/jci43766

Peng, J., Gu, N., Zhou, L., B Eyo, U., Murugan, M., Gan, W. B., et al. (2016). Microglia and monocytes synergistically promote the transition from acute to chronic pain after nerve injury. *Nat. Commun.* 7:12029. doi: 10.1038/ncomms12029

Pitcher, M. H., Von Korff, M., Bushnell, M. C., and Porter, L. (2019). Prevalence and profile of high-impact chronic pain in the United States. *J. Pain.* 20, 146–160. doi: 10.1016/j.jpain.2018.07.006

Price, T. J., Helesic, G., Parghi, D., Hargreaves, K. M., and Flores, C. M. (2003). The neuronal distribution of cannabinoid receptor type 1 in the trigeminal ganglion of the rat. *Neuroscience* 120, 155–162. doi: 10.1016/s0306-4522(03)00333-6

Radat, F., Margot-Duclot, A., and Attal, N. (2013). Psychiatric co-morbidities in patients with chronic peripheral neuropathic pain: a multicentre cohort study. *Eur. J. Pain* 17, 1547–1557. doi: 10.1002/j.1532-2149.2013.00334.x

Rahn, E. J., Makriyannis, A., and Hohmann, A. G. (2007). Activation of cannabinoid CB1 and CB2 receptors suppresses neuropathic nociception evoked by the chemotherapeutic agent vincristine in rats. *Br. J. Pharmacol.* 152, 765–777. doi: 10.1038/sj.bjp.0707333

Raja, S. N., Carr, D. B., Cohen, M., Finnerup, N. B., Flor, H., Gibson, S., et al. (2020). The revised International Association for the Study of Pain definition of pain: concepts, challenges, and compromises. *Pain* 161, 1976–1982. doi: 10.1097/j.pain.0000000000001939

Rani Sagar, D., Burston, J. J., Woodhams, S. G., and Chapman, V. (2012). Dynamic changes to the endocannabinoid system in models of chronic pain. *Philos. Trans. R. Soc. Lond. B Biol. Sci.* 367, 3300–3311. doi: 10.1098/rstb.2011.0390

Rao, V. S., Menezes, A. M., and Viana, G. S. (1990). Effect of myrcene on nociception in mice. *J. Pharm. Pharmacol.* 42, 877–878. doi: 10.1111/j.2042-7158.1990.tb07046.x

Rexed, B. (1952). The cytoarchitectonic organization of the spinal cord in the cat. *J. Comp. Neurol.* 96, 414–495. doi: 10.1002/cne.900960303

Richardson, J. D., Aanonsen, L., and Hargreaves, K. M. (1997). SR 141716A, a cannabinoid receptor antagonist, produces hyperalgesia in untreated mice. *Eur. J. Pharmacol.* 319, R3–R4. doi: 10.1016/s0014-2999(96)00952-1

Romero-Sandoval, A., and Eisenach, J. C. (2007). Spinal cannabinoid receptor type 2 activation reduces hypersensitivity and spinal cord glial activation after paw incision. *Anesthesiology* 106, 787–794. doi: 10.1097/01.anes.0000264765.33673.6c

Romero-Sandoval, A., Nutile-McMenemy, N., and DeLeo, J. A. (2008). Spinal microglial and perivascular cell cannabinoid receptor type 2 activation reduces behavioral hypersensitivity without tolerance after peripheral nerve injury. *Anesthesiology* 108, 722–734. doi: 10.1097/ALN.0b013e318167af74

Ruhaak, L. R., Felth, J., Karlsson, P. C., Rafter, J. J., Verpoorte, R., and Bohlin, L. (2011). Evaluation of the cyclooxygenase inhibiting effects of six major cannabinoids isolated from *Cannabis sativa*. *Biol. Pharm. Bull.* 34, 774–778. doi: 10.1248/bpb.34.774

Russo, E. B. (2008). Cannabinoids in the management of difficult to treat pain. *Ther. Clin. Risk Manag.* 4, 245–259. doi: 10.2147/tcrm.s1928

Russo, E. B., Burnett, A., Hall, B., and Parker, K. K. (2005). Agonistic properties of cannabidiol at 5-HT1a receptors. *Neurochem. Res.* 30, 1037–1043. doi: 10.1007/s11064-005-6978-1

Salio, C., Fischer, J., Franzoni, M. F., and Conrath, M. (2002). Pre- and postsynaptic localizations of the CB1 cannabinoid receptor in the dorsal horn of the rat spinal cord. *Neuroscience* 110, 755–764. doi: 10.1016/s0306-4522(01)00584-x

Schimrigk, S., Marziniak, M., Neubauer, C., Kugler, E. M., Werner, G., and Abramov-Sommariva, D. (2017). Dronabinol is a safe long-term treatment option for neuropathic pain patients. *Eur. Neurol.* 78, 320–329. doi: 10.1159/000481089

Schlosburg, J. E., Radanova, L., Di Marzo, V., Imming, P., and Lichtman, A. H. (2012). Evaluation of the endogenous cannabinoid system in mediating the behavioral effects of dipyrone (metamizol) in mice. *Behav. Pharmacol.* 23, 722–726. doi: 10.1097/FBP.0b013e3283584794

Scott, D. A., Wright, C. E., and Angus, J. A. (2004). Evidence that CB-1 and CB-2 cannabinoid receptors mediate antinociception in neuropathic pain in the rat. *Pain* 109, 124–131. doi: 10.1016/j.pain.2004.01.020

Segat, G. C., Manjavachi, M. N., Matias, D. O., Passos, G. F., Freitas, C. S., Costa, R., et al. (2017). Antiallodynic effect of β-caryophyllene on paclitaxel-induced peripheral neuropathy in mice. *Neuropharmacology* 125, 207–219. doi: 10.1016/j.neuropharm.2017.07.015

Shen, M., Piser, T. M., Seybold, V. S., and Thayer, S. A. (1996). Cannabinoid receptor agonists inhibit glutamatergic synaptic transmission in rat hippocampal cultures. *J. Neurosci.* 16, 4322–4334. doi: 10.1523/jneurosci.16-14-04322.1996

Showalter, V. M., Compton, D. R., Martin, B. R., and Abood, M. E. (1996). Evaluation of binding in a transfected cell line expressing a peripheral cannabinoid receptor (CB2): identification of cannabinoid receptor subtype selective ligands. *J. Pharmacol. Exp. Ther.* 278, 989–999.

Silva-Cardoso, G. K., Lazarini-Lopes, W., Hallak, J. E., Crippa, J. A., Zuardi, A. W., Garcia-Cairasco, N., et al. (2021). Cannabidiol effectively reverses mechanical and thermal allodynia, hyperalgesia, and anxious behaviors in a neuropathic pain model: possible role of CB1 and TRPV1 receptors. *Neuropharmacology* 197:108712. doi: 10.1016/j.neuropharm.2021.108712

Snider, N. T., Nast, J. A., Tesmer, L. A., and Hollenberg, P. F. (2009). A cytochrome P450-derived epoxygenated metabolite of anandamide is a potent cannabinoid receptor 2-selective agonist. *Mol. Pharmacol.* 75, 965–972. doi: 10.1124/mol.108.053439

Starowicz, K., and Finn, D. P. (2017). Cannabinoids and pain: sites and mechanisms of action. *Adv. Pharmacol.* 80, 437–475. doi: 10.1016/bs.apha.2017.05.003

Stasiulewicz, A., Znajdek, K., Grudzień, M., Pawiński, T., and Sulkowska, A. (2020). A guide to targeting the endocannabinoid system in drug design. *Int. J. Mol. Sci.* 21:2778. doi: 10.3390/ijms21082778

Stella, N. (2009). Endocannabinoid signaling in microglial cells. *Neuropharmacology* 56(Suppl. 1), 244–253. doi: 10.1016/j.neuropharm.2008.07.037

Stemkowski, P. L., Garcia-Caballero, A., Gadotti, V. M., M'Dahoma, S., Chen, L., Souza, I. A., et al. (2017). Identification of interleukin-1 beta as a key mediator in the upregulation of Cav3.2-USP5 interactions in the pain pathway. *Mol. Pain* 13:1744806917724698. doi: 10.1177/1744806917724698

Storozhuk, M. V., and Zholos, A. V. (2018). TRP channels as novel targets for endogenous ligands: focus on endocannabinoids and nociceptive signalling. *Curr. Neuropharmacol.* 16, 137–150. doi: 10.2174/1570159X15666170424120802

Sun, C., Zhang, J., Chen, L., Liu, T., Xu, G., Li, C., et al. (2017). IL-17 contributed to the neuropathic pain following peripheral nerve injury by promoting astrocyte proliferation and secretion of proinflammatory cytokines. *Mol. Med. Rep.* 15, 89–96. doi: 10.3892/mmr.2016.6018

Sung, B., Lim, G., and Mao, J. (2003). Altered expression and uptake activity of spinal glutamate transporters after nerve injury contribute to the pathogenesis of neuropathic pain in rats. *J. Neurosci.* 23, 2899–2910. doi: 10.1523/jneurosci.23-07-02899.2003

Takakuwa, K. M., and Sulak, D. (2020). A survey on the effect that medical cannabis has on prescription opioid medication usage for the treatment of chronic pain at three medical cannabis practice sites. *Cureus* 12:e11848. doi: 10.7759/cureus.11848

Tsou, K., Brown, S., Sañudo-Peña, M. C., Mackie, K., and Walker, J. M. (1998). Immunohistochemical distribution of cannabinoid CB1 receptors in the rat central nervous system. *Neuroscience* 83, 393–411. doi: 10.1016/s0306-4522(97)00436-3

Tsuda, M., Masuda, T., Tozaki-Saitoh, H., and Inoue, K. (2013). P2X4 receptors and neuropathic pain. *Front. Cell. Neurosci.* 7:191. doi: 10.3389/fncel.2013.00191

Tsuda, M., Shigemoto-Mogami, Y., Koizumi, S., Mizokoshi, A., Kohsaka, S., Salter, M. W., et al. (2003). P2X4 receptors induced in spinal microglia gate tactile allodynia after nerve injury. *Nature* 424, 778–783. doi: 10.1038/nature01786

Ueberall, M. A., Essner, U., and Mueller-Schwefe, G. H. (2019). Effectiveness and tolerability of THC:CBD oromucosal spray as add-on measure in patients with severe chronic pain: analysis of 12-week open-label real-world data provided by the German Pain e-Registry. *J. Pain Res.* 12, 1577–1604. doi: 10.2147/jpr.S192174

van Hecke, O., Austin, S. K., Khan, R. A., Smith, B. H., and Torrance, N. (2014). Neuropathic pain in the general population: a systematic review of epidemiological studies. *Pain* 155, 654–662. doi: 10.1016/j.pain.2013.11.013

Veress, G., Meszar, Z., Muszil, D., Avelino, A., Matesz, K., Mackie, K., et al. (2013). Characterisation of cannabinoid 1 receptor expression in the perikarya, and

peripheral and spinal processes of primary sensory neurons. *Brain Struct. Funct.* 218, 733–750. doi: 10.1007/s00429-012-0425-2

West, S. J., Bannister, K., Dickenson, A. H., and Bennett, D. L. (2015). Circuitry and plasticity of the dorsal horn–toward a better understanding of neuropathic pain. *Neuroscience* 300, 254–275. doi: 10.1016/j.neuroscience.2015.05.020

Wieseler-Frank, J., Maier, S. F., and Watkins, L. R. (2005). Central proinflammatory cytokines and pain enhancement. *Neurosignals* 14, 166–174. doi: 10.1159/000087655

Williams, J., Haller, V. L., Stevens, D. L., and Welch, S. P. (2008). Decreased basal endogenous opioid levels in diabetic rodents: effects on morphine and delta-9-tetrahydrocannabinoid-induced antinociception. *Eur. J. Pharmacol.* 584, 78–86. doi: 10.1016/j.ejphar.2007.12.035

WHO (2021). *Opioid Overdose*. Available online at: https://www.who.int/news-room/fact-sheets/detail/opioid-overdose (accessed October 30, 2021).

Xiong, W., Cui, T., Cheng, K., Yang, F., Chen, S. R., Willenbring, D., et al. (2012). Cannabinoids suppress inflammatory and neuropathic pain by targeting α3 glycine receptors. *J. Exp. Med.* 209, 1121–1134. doi: 10.1084/jem.20120242

Yamamoto, W., Mikami, T., and Iwamura, H. (2008). Involvement of central cannabinoid CB2 receptor in reducing mechanical allodynia in a mouse model of neuropathic pain. *Eur. J Pharmacol.* 583, 56–61. doi: 10.1016/j.ejphar.2008.01.010

Yang, F., Xu, Q., Shu, B., Tiwari, V., He, S. Q., Vera-Portocarrero, L. P., et al. (2016). Activation of cannabinoid CB1 receptor contributes to suppression of spinal nociceptive transmission and inhibition of mechanical hypersensitivity by Aβ-fiber stimulation. *Pain* 157, 2582–2593. doi: 10.1097/j.pain.0000000000000680

Yekkirala, A. S., Roberson, D. P., Bean, B. P., and Woolf, C. J. (2017). Breaking barriers to novel analgesic drug development. *Nat. Rev. Drug Discov.* 16, 545–564. doi: 10.1038/nrd.2017.87

Zhang, G., Chen, W., Lao, L., and Marvizón, J. C. (2010). Cannabinoid CB1 receptor facilitation of substance P release in the rat spinal cord, measured as neurokinin 1 receptor internalization. *Eur. J. Neurosci.* 31, 225–237. doi: 10.1111/j.1460-9568.2009.07075.x

Zhang, J., Hoffert, C., Vu, H. K., Groblewski, T., Ahmad, S., and O'Donnell, D. (2003). Induction of CB2 receptor expression in the rat spinal cord of neuropathic but not inflammatory chronic pain models. *Eur. J. Neurosci.* 17, 2750–2754. doi: 10.1046/j.1460-9568.2003.02704.x

Zou, S., and Kumar, U. (2018). Cannabinoid receptors and the endocannabinoid system: signaling and function in the central nervous system. *Int. J. Mol. Sci.* 19:833. doi: 10.3390/ijms19030833

Zygmunt, P. M., Petersson, J., Andersson, D. A., Chuang, H., Sørgård, M., Di Marzo, V., et al. (1999). Vanilloid receptors on sensory nerves mediate the vasodilator action of anandamide. *Nature* 400, 452–457. doi: 10.1038/22761

Conflict of Interest: The authors declare that the research was conducted in the absence of any commercial or financial relationships that could be construed as a potential conflict of interest.

Publisher's Note: All claims expressed in this article are solely those of the authors and do not necessarily represent those of their affiliated organizations, or those of the publisher, the editors and the reviewers. Any product that may be evaluated in this article, or claim that may be made by its manufacturer, is not guaranteed or endorsed by the publisher.

Copyright © 2021 Campos, Aguiar, Paes-Colli, Trindade, Ferreira, de Melo Reis and Sampaio. This is an open-access article distributed under the terms of the Creative Commons Attribution License (CC BY). The use, distribution or reproduction in other forums is permitted, provided the original author(s) and the copyright owner(s) are credited and that the original publication in this journal is cited, in accordance with accepted academic practice. No use, distribution or reproduction is permitted which does not comply with these terms.

frontiers in Pharmacology

ORIGINAL RESEARCH
published: 20 December 2021
doi: 10.3389/fphar.2021.759040

Methyl Gallate Improves Hyperuricemia Nephropathy Mice Through Inhibiting NLRP3 Pathway

Peng Liu[1†], Wen Wang[1†], Qiang Li[1], Xin Hu[1], Bingyong Xu[2], Chen Wu[1], Lijie Bai[1], Li Ping[3], Zhou Lan[4] and Lvyi Chen[1]**

[1]School of Pharmaceutical Sciences, South-Central University for Nationalities, Wuhan, China, [2]Zhejiang Heze Pharmaceutical Technology Co., Ltd., Hangzhou, China, [3]Center for Drug Safety Evaluation and Research, College of Pharmaceutical Sciences, Zhejiang University, Hangzhou, China, [4]School of Pharmacy, Hubei University of Chinese Medicine, Wuhan, China

OPEN ACCESS

Edited by:
Elizabeth S. Fernandes, Pelé Pequeno Príncipe Research Institute, Brazil

Reviewed by:
Claudio Ferrante, University of Studies G. d'Annunzio Chieti and Pescara, Italy
José Roberto Santin, Universidade do Vale do Itajaí, Brazil

***Correspondence:**
Lvyi Chen
clyhappy05@163.com
Bingyong Xu
xubingyong@hezepharm.com

†These authors have contributed equally to this work

Specialty section:
This article was submitted to Inflammation Pharmacology, a section of the journal Frontiers in Pharmacology

Received: 15 August 2021
Accepted: 22 November 2021
Published: 20 December 2021

Citation:
Liu P, Wang W, Li Q, Hu X, Xu B, Wu C, Bai L, Ping L, Lan Z and Chen L (2021) Methyl Gallate Improves Hyperuricemia Nephropathy Mice Through Inhibiting NLRP3 Pathway. Front. Pharmacol. 12:759040. doi: 10.3389/fphar.2021.759040

Hyperuricemia nephropathy (HN) is a form of chronic tubulointerstitial inflammation, caused by the deposition of monosodium urate crystals (MSU) in the distal collecting duct and medullary interstitium, associated with a secondary inflammatory reaction. Numerous published reports indicated that NLRP3 inflammasome pathway play crucial roles in HN symptoms. The present study aims to investigate the protective effects of methyl gallate on HN mice and the underlying mechanisms. An HN model was established by intraperitoneal injection of potassium oxide (PO) to assess the effect of methyl gallate on renal histopathological changes, renal function, cytokine levels and expressions of NLRP3-related protein in HN mice. Moreover, *in vitro* models of lipopolysaccharide (LPS)-stimulated bone marrow-derived macrophages (BMDMs) and human peripheral blood mononuclear cells (PBMCs) were established to explore the mechanism of methyl gallate on NLRP3 inflammasome activation. The results showed that methyl gallate significantly ameliorated HN by inhibiting uric acid production and promoting uric acid excretion as well as ameliorating renal injury induced by NLRP3 activation. Mechanistically, methyl gallate is a direct NLRP3 inhibitor that inhibits NLRP3 inflammasome activation but has no effect on the activation of AIM2 or NLRC4 inflammasomes in macrophages. Furthermore, methyl gallate inhibited the assembly of NLRP3 inflammasomes by blocking the ROS over-generation and oligomerization of NLRP3. Methyl gallate was also active *ex vivo* against ATP-treated PBMCs and synovial fluid mononuclear cells from patients with gout. In conclusion, methyl gallate has a nephroprotective effect against PO-induced HN through blocking the oligomerization of NLRP3 and then exerting anti-inflammatory activity in the NLRP3-driven diseases.

Keywords: methyl gallate, NLRP3, uric acid, nephropathy, ROS

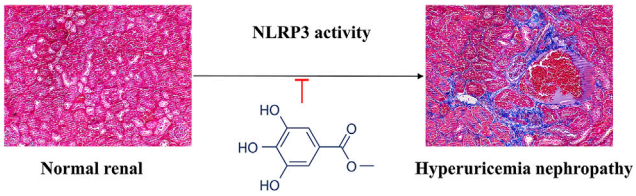

Graphical Abstract |

INTRODUCTION

Hyperuricemia is a metabolic disease caused by an imbalance in the synthesis or excretion of uric acid in the body. According to the consensus of Chinese experts on the treatment of hyperuricemia and gout, the incidence of hyperuricemia in China has increased year by year as the improvement of people's living standard, especially in developed cities and coastal areas, reaching 5–23.5% (Lu et al., 2020). Traditionally, hyperuricemia is thought to induce renal disease through the deposition of urate crystals in the glomerular collecting ducts in a manner similar to that of gouty arthritis (Mazzali et al., 2001; Lu et al., 2019). At present, drugs that have been listed for the treatment of hyperuricemia nephropathy (HN) are mainly including xanthine oxidase (XOD) inhibitors, uricosuric drugs, recombinant uricase supplements and other major classes. However, the widespread clinical use of these drugs are large limited due to the adverse effects and hepatotoxicity (Sattui and Gaffo, 2016). Therefore, it is urgent to explore a drug which has effects on both reducing the circulating uric acid synthesis and increasing renal uric acid excretion in the treatment of HN, so as to ameliorate the renal inflammation, renal fibrosis, oxidative stress or other injuries.

Polyphenols have a wide range of therapeutic effects because of their powerful antioxidant, anti-inflammatory, and immunomodulatory actions, with potential roles on different complications caused by oxidative stress, such as cardiovascular and neurodegenerative diseases (Yahfoufi et al., 2018). Recently, polyphenols have received considerable attention for their potential in modulating immune signaling pathways, inhibiting inflammatory mediators, and regulating various pathological states, including ischemia/reperfusion injury, neurodegenerative diseases, neuropathic pain, and arthritis (Chen et al., 2011; Chen and Lan, 2017; Rahimifard et al., 2017; Yahfoufi et al., 2018; Azam et al., 2019).

Methyl gallate is a gallotannin, widely distributed in edible plants such as *Rosa rugosa, Terminalia chebula* Retz., *Smilax china* Linnaeus, *Schinus terebinthifolius* Raddi, *Givotia rottleriformis* Griff., *Bergenia ligulata* (Wall), and *Paeonia sufruticosa* Andr. (Cho et al., 2004; Acharyya et al., 2015; Kamatham et al., 2015; Rosas et al., 2015; Sharanya et al., 2018; Park et al., 2019). Several studies have demonstrate that methyl gallate is associated with significant biological effects of antioxidant (Whang et al., 2005; Crispo et al., 2010), anti-tumor (Lee et al., 2010; Lee et al., 2013), antimicrobial activities (Choi et al., 2009), and anti-inflammatory effect on experimental colitis and arthritis (Kang et al., 2009; Correa et al., 2016). However, the effect of methyl gallate on HN, a condition associated with the development and progression of renal disease due to elevated uric acid levels, is unclear. The present study was aimed to explore the role of methyl gallate on HN and the underlying molecular mechanisms of its anti-inflammatory activity in the activation of NLRP3 inflammasome.

MATERIALS AND METHODS

Materials

Detail of materials are described in the online supplemental file.

Experimental Animal

Male C57BL/6 mice (No. SCXK (E) 2015-0018) were purchased from Hubei experimental animal research center (Wuhan, China), and *Nlrp3*$^{-/-}$ mice were purchased from Shanghai Model Organisms Center, Inc. The animals were housed in a temperature-controlled, regular 12-h light/dark cycle and provided with standard chow and water *ad libitum*. All experimental procedures were performed in accordance with the regulations of the Animal Ethics Committee of South-Central University for Nationalities (SCUN) (approval number: 2020-scuec-025), all procedures involving animals were performed in accordance with the SCUN Animal Experimentation Guidelines.

Cell Culture and Stimulation

Bone marrow-derived macrophages (BMDMs) were isolated from bone marrow of 6-8 weeks old mice and cultured in Dulbecco's modified Eagle medium (DMEM) supplemented with 10% FBS and 1% MCSF for 6–7 days. Human Lymphocyte Separation Medium (catalog no. P8610-200, Solarbio) was used to obtain human peripheral blood mononuclear cells (PBMCs). Prior to stimulation, PBMCs were cultured overnight in RPMI 1640 medium. To activate NLRP3 inflammasome, BMDMs or PBMCs were primed or un-primed with LPS (100 ng/ml, for 3 h) before being stimulated with nigericin (10 μM, for 1 h), or monosodium urate crystals (MSU) (200 μg/ml, for 6 h). To activate the other inflammasomes, salmonella typhimurium or poly A:T was added to the LPS-primed BMDMs.

Animals and Modeling

Healthy adult male mice fed in clean-grade animal houses with free food and water. After 1 week of adaptive feeding, mice were randomly divided into five groups (n = 10 in each group). 1) control group, injected intraperitoneally or given orally with equal volumes of saline; 2) vehicle group, injected intraperitoneally with PO (300 mg/kg) and given orally equal

amounts of saline, 3) and 4) methyl gallate groups, injected intraperitoneally with PO (300 mg/kg) and orally given methyl gallate 20 or 40 mg/kg, respectively; 5) allopurinol group, injected intraperitoneally with PO (300 mg/kg) and given orally allopurinol 5 mg/kg. Mice were given saline, methyl gallate or allopurinol by gavage 30 min before PO injection for 28 constitutive days.

Measurement of Uric Acid, Creatinine and BUN

Serum urate (Sur), urinary urate (Uur), serum creatinine (Scr), urinary creatinine (Ucr) and blood urea nitrogen (BUN) levels were measured using standard diagnostic kits. Protein concentrations were measured by the Bradford method using bovine serum albumin as a standard. Each test was performed in triplicate. The fraction excretion of uric acid (FEUA) was then calculated to assess the uric acid excretion-promoting effect of methyl gallate: FEUA = [(Uur) × (Scr)]/[(Ucr) × (Sur)] × 100, expressed as a percentage (Chen et al., 2011).

Enzyme-Linked Immunosorbent Assay

IL-6, IL-1β, TNF-a and IL-18 were detected by ELISA kits. The specific method and steps of the experiment were tested according to the experimental guidance given by R&D.

XOD Activity Detected

The liver tissue was removed from −80°C, 900 μL of pre-cooled physiological saline was added per 100 mg of tissue, homogenized in a grinder, and centrifuged at 8,000 r/min (4°C) for 10 min, the supernatant was obtained, and continue to centrifuge at 15,000 r/min for 30 min, remove the uppermost turbid material, and absorb the supernatant. The protein concentration was measured by BCA method, and the activity of XOD in liver and serum was detected by referring to the kit instructions.

Reactive Oxygen Species Staining

BMDMs at 2×10^5/ml were placed overnight on coverslips (Thermo Fisher Scientific) in 12-well plates. 12–18 h later, the medium was replaced with Opti-MEM containing 1% FBS. After that, methyl gallate was added for another 0.5 h as described, and then stimulated with MSU. Finally, BMDMs were stained with 2′,7′-dichlorofluorescin diacetate (DCFDA), and then washed with ice-cold PBS for three times and fixed with 4% PFA in PBS for 15 min.

ROS Assay

BMDMs were cultured in 96-well plates (1×10^6 cells/well) using phenol red-free RPMI medium (Gibco) for 24 h at 37°C in a humidified incubator with 5% CO_2. Cells were then loaded with the ROS-specific fluorescent probe H2DCFDA (20 μM final concentration; Sigma-Aldrich) for 30 min, washed twice with preheated medium, and exposed to MSU (200 μg/ml). In the treatment group, cells were incubated with 10 μM CP105,696 for 40 min prior to the addition of the MSU. Fluorescence was assessed at 10-min intervals over 1 h using a spectrofluorometer (Synergy 2; BioTek) with a fluorescein isothiocyanate filter (excitation 485 nm, emission 538 nm).

Hematoxylin and Eosin Staining

The left kidney of the mouse was fixed in 4% paraformaldehyde. After paraffin embedding, 4 μm serial sections were taken and H&E staining was performed by conventional methods.

Protein Extracts and Western Blotting

The kidney tissue obtained from the experimental mice in each group was first rinsed gently with pre-chilled 1 × PBS buffer twice, then the kidney tissue was placed in 2 ml EP, 500 μL of protein lysis solution was added, and homogenized with a tissue homogenizer. It was then centrifuged at 4°C and 12,000 rpm for 10 min using a low-temperature high-speed centrifuge. After centrifugation, the supernatant was sucked out and placed in a 1.5 ml EP tube and marked on ice. Then the total protein content was detected by BCA kit.

The above protein samples were denatured in Laemmle buffer and then boiled at 95°C for 10 min, separated by SDS-PAGE and transferred to PVDF membranes. Membranes were incubated overnight with primary antibodies (caspase 1, IL-1β and GSDMD lysed forms) and proteins were detected by enhanced chemiluminescence with anti-rabbit secondary antibody or anti-mouse secondary antibody.

Statistical Analysis

All experiments were performed at least three times. Values are presented as mean ± S.D. When means of two groups were compared, a 2-tailed Student's t-test was used to determine significance. When multiple treatment groups were compared, one-way ANOVA and Tukey's post hoc test were used to calculate significance between means. * p value < 0.05 was considered statistically significant. Data handling and statistical processing were performed using GraphPad Prism 8.0 (GraphPad Software, San Diego, CA, United States).

RESULTS

Effect of Methyl Gallate on Hyperuricemia and Renal Dysfunction

We first investigated whether methyl gallate had the effect on improving renal function and suppressing high uric acid levels in PO-treated mice. According to our previous study, 4 weeks of intraperitoneal injection of PO can lead to HN in mice. **Table 1** summarized the anti-hyperuricemia and renal protection effect of methyl gallate. Sur, Scr and BUN levels were significantly increased in the vehicle (PO-treated) mice compared to that of control mice. Methyl gallate at doses of 20 and 40 mg/kg and allopurinol at 5 mg/kg significantly reversed the levels of SUA, SCr and BUN in hyperuricemia mice to the normal value. Moreover, PO treatment could induce an obvious reduction in UUA and UCr levels compared with that of saline-treated mice. Methyl gallate at 20 and 40 mg/kg could significantly elevate UUA and UCr levels in hyperuricemia mice. As previously reported (Hu et al., 2009), FEUA, an important parameter of renal uric acid handling, was significantly reduced in hyperuricemia mice. In the present study, 20 and 40 mg/kg of methyl gallate and allopurinol significantly reversed FEUA in PO-treated HN mice.

TABLE 1 | The effects of methyl gallate on serum and urinary levels of uric acid and creatinine, as well as FEUA and BUN in PO-induced HN mice.

Group	Dose (mg/kg)	SUA (mg/dl)	SCr (mg/dl)	UUA (mg/dl)	UCr (mg/dl)	BUN (mg/dl)	FEUA
Control	PBS	2.45 ± 0.51	0.87 ± 0.08	43.56 ± 4.93	29.45 ± 3.51	30.20 ± 2.83	54.27 ± 11.25
Vehicle	PBS	5.89 ± 0.77$^{\#\#}$	2.35 ± 0.48$^{\#\#}$	30.68 ± 4.26$^{\#\#}$	30.83 ± 2.66	51.07 ± 6.87$^{\#\#\#}$	40.74 ± 12.22$^{\#\#}$
AL	5	3.36 ± 0.12**	1.68 ± 0.12**	34.26 ± 3.55	30.43 ± 3.88	42.35 ± 3.22*	57.38 ± 11.09**
MG	20	4.26 ± 0.53*	1.78 ± 0.21*	36.84 ± 4.83*	27.08 ± 3.04	40.02 ± 4.06**	57.57 ± 11.03**
—	40	3.18 ± 0.58**	1.44 ± 0.13***	40.55 ± 5.12**	26.44 ± 4.29*	36.82 ± 4.47***	72.22 ± 17.81***

Uric acid, creatinine and urea nitrogen in serum and urine were detected by kits. Al: allopurinol. MG: methyl gallate. Values are expressed as means ± S.D. (n = 10). Statistical differences were calculated by single-factor ANOVA with Tukey HSD test. Compared with control: $^{\#}p < 0.05$, $^{\#\#}p < 0.01$, $^{\#\#\#}p < 0.001$; Compared with vehicle: $^{*}p < 0.05$, $^{**}p < 0.01$, $^{***}p < 0.001$.

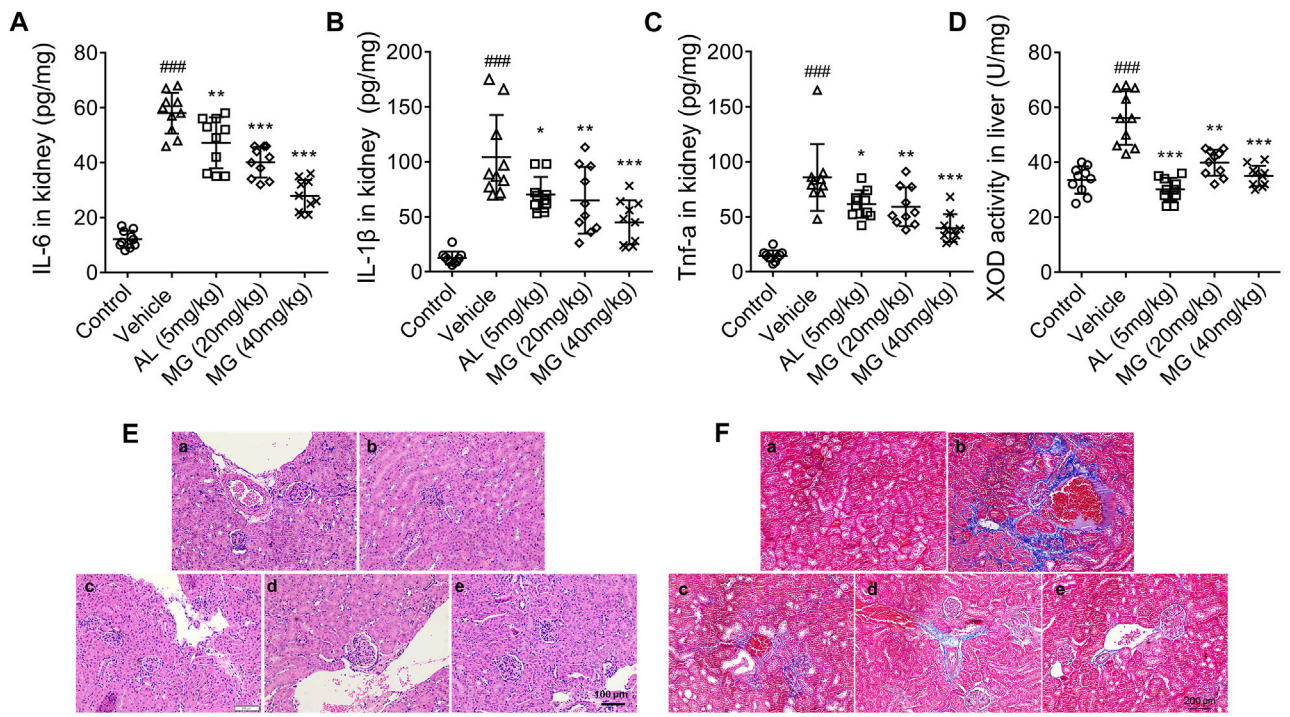

FIGURE 1 | Effect of methyl gallate on PO-induced HN. **(A–C)** Cytokines such as IL-6 **(A)**, IL-1β **(B)** and TNF-α **(C)** in kidney were detected by ELISA kits. **(D)** The activity of XOD in liver was detected by referring to the kit instructions. **(E,F)** HE-staining **(E)** or Masson staining **(F)** of kidney from mice in different groups. Scale bar, 100 μm. a: control; b: vehicle; c: allopurinol (5 mg/kg); d: MG (20 mg/kg); e: MG (40 mg/kg). Values are expressed as means ± S.D. (*n* = 10). Data were analyzed by single-factor ANOVA with Tukey HSD test. Compared with control group: $^{\#\#\#}p < 0.001$; Compared with vehicle group: $^{*}p < 0.05$, $^{**}p < 0.01$, $^{***}p < 0.001$. MG: methyl gallate.

HN is a form of chronic tubulointerstitial inflammation caused by the deposition of MSU in the distal collecting duct. Therefore, we further investigated whether methyl gallate could inhibit the chronic inflammation. The results showed that the levels of TNF-α, IL-6 and IL-1β were significantly increased in serum and renal tissues of PO-treated mice. However, correspondingly the production of TNF-α, IL-6 and IL-1β was effectively inhibited by methyl gallate and allopurinol (**Figures 1A–C**). It was speculated that this anti-inflammatory effect derived from their uric acid-lowering effect, especially allopurinol.

In the present study, the effect of methyl gallate on uric acid production was also investigated. XOD is a key enzyme that catalyzes uric acid production. XOD activity in the liver of HN mice was markedly attenuated by methyl gallate (**Figure 1D**), indicating that methyl gallate reduces uric acid production through inhibiting XOD activity *in vivo*.

HN is a chronic renal tubulointerstitial inflammation with histological changes including arteriosclerosis, glomerulosclerosis and tubulointerstitial fibrosis. As aforementioned results, compared to the control mice, the renal tubules of HN mice were significantly damaged, with severe dilatation of the proximal tubules, formation of casts, and massive detachment and necrosis of the tubular epithelium. All these tubulointerstitial lesions were improved to some extent after treatment with allopurinol and different doses of methyl gallate (**Figure 1E**). In addition, compared to the control mice, there were significant interstitial fibrous-like changes in the renal tissue of HN mice. However, methyl gallate were effective in alleviating these pathological damages, with only mild fibrous-like changes (**Figure 1F**).

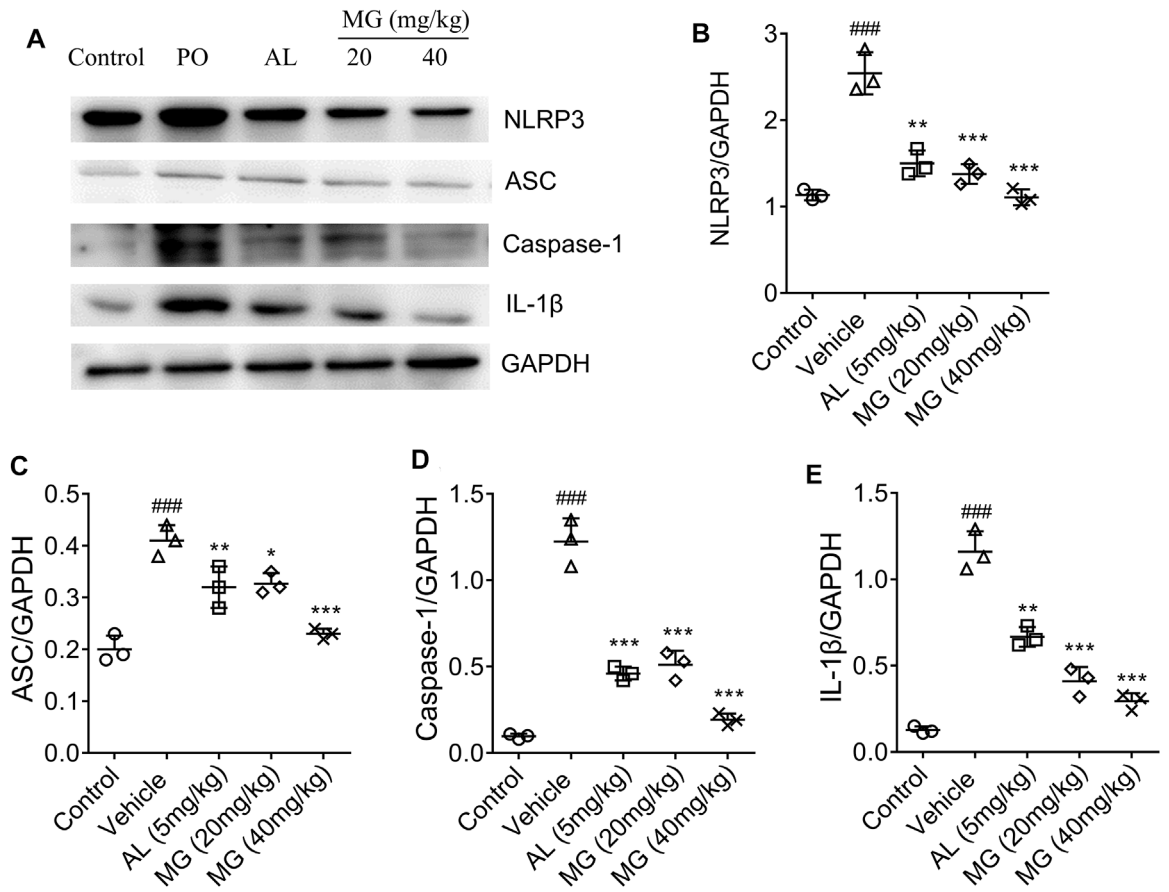

FIGURE 2 | Effect of methyl gallate on NLRP3 pathway in renal tissues. **(A)** Representative western blot analysis of NLRP3, ASC, caspase-1 and IL-1β in renal tissues of mice in different groups. **(B–E)** Western blotting analysis of NLRP3, ASC, caspase-1 and IL-1β in renal tissues of mice in different groups. Values are expressed as means ± S.D. ($n = 3$). Data were analyzed by single-factor ANOVA with Tukey HSD test. Compared with control group: $^{###}p < 0.001$; Compared with vehicle group: $^{*}p < 0.05$, $^{**}p < 0.01$., $^{***}p < 0.001$. MG: methyl gallate.

Effect of Methyl Gallate on NLRP3 Pathway in Kidney

NLRP3 has been reported to sense a variety of stimuli, ranging from bacterial toxins, ATP, crystalline structures such as MSU, silica, and alum (Ghaemi-Oskouie and Shi, 2011; Franklin et al., 2016). The up-regulated expression of NLRP3, ASC, caspase-1 and IL-1β proteins were observed in HN mice, while methyl gallate significantly reversed the levels of NLRP3, ASC, IL-1β and caspase-1 proteins to normal level (**Figure 2**). These results suggested that methyl gallate had a definite inhibitory effect on NLRP3 inflammasome activity in HN.

Methyl Gallate Inhibits NLRP3 Inflammasome Activation in BMDMs by ROS Pathway

To confirm the mechanism of methyl gallate on inhibiting NLRP3 inflammasome activation, the present study was first investigated whether methyl gallate inhibited caspase-1 cleavage and IL-1β secretion in MSU-stimulated BMDMs. It was observed that methyl gallate treatment blocked MSU-induced caspase-1 cleavage, secretion of IL-1β and IL-18, and pyroptosis in BMDMs (**Figures 3A–E**). Moreover, methyl gallate was reported to inhibit cytokine-induced activation of NF-κB (Ding et al., 2021; Zhang et al., 2021). In consistent with these studies, methyl gallate significantly inhibits the production of TNF-a in MSU-treated BMDMs (**Figure 3F**). These results indicated that methyl gallate suppressed both NLRP3 inflammasome activation and related gene expression in MSU-treated BMDMs. It is known that ROS provides the upstream signaling for MSU activation of NLRP3 (Gross et al., 2011), it could be inferred that methyl gallate had an inhibitory effect on ROS overproduction in MSU-treated BMDMs. Indeed, methyl gallate decreased the production of ROS by MSU (**Figures 3G,H**). This result suggested that methyl gallate was a blocker of the upstream pathway of NLRP3 inflammasome activation.

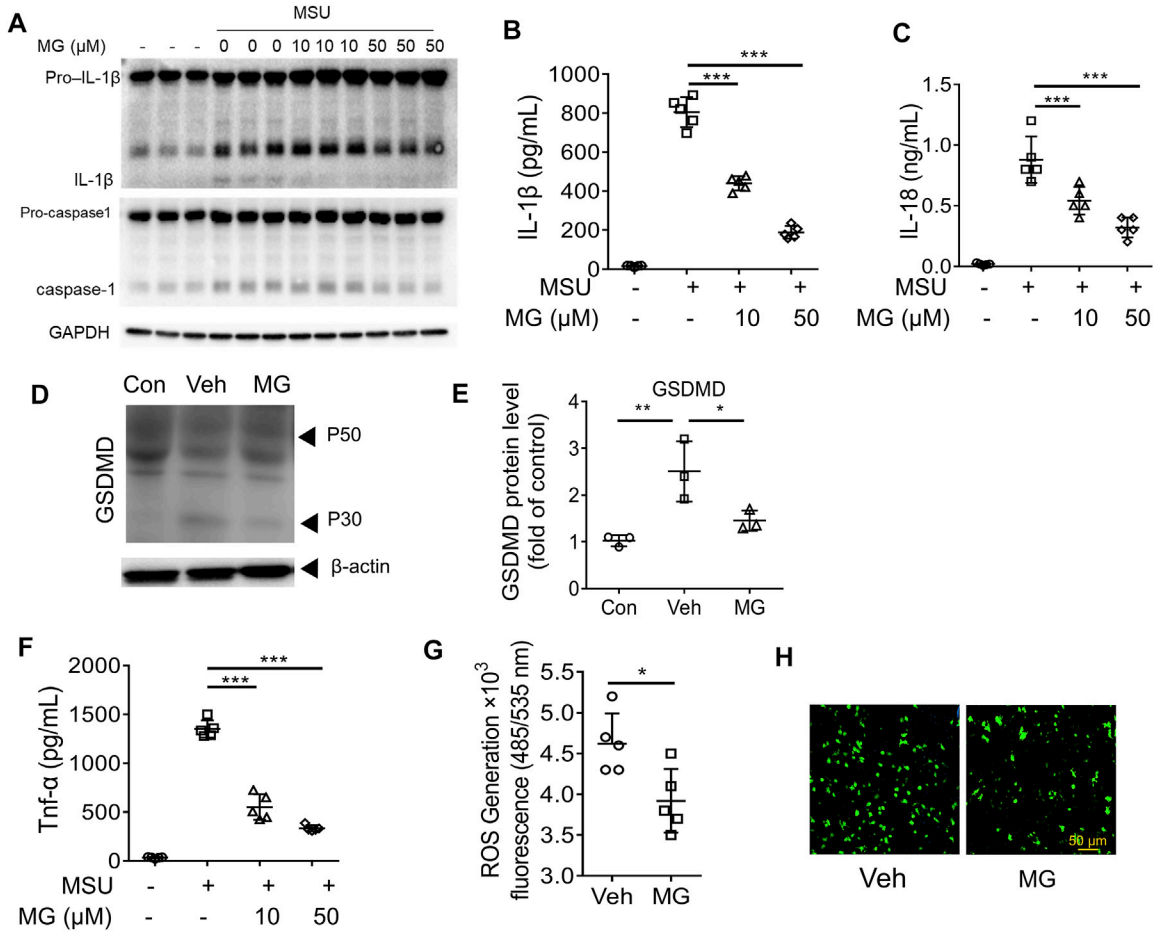

FIGURE 3 | Methyl gallate inhibits NLRP3 inflammasome activation in BMDMs by ROS pathway **(A)** Western blot analysis of the inhibitory effects of MG (10 and 50 μM) on cleaved IL-1β, activated caspase-1 (P20) in culture supernatants (SN) and pro-IL-1β, pro-caspase-1 in lysates (Input) of MSU stimulated BMDMs. **(B,C)** The inhibitory effects of MG (10 and 50 μM) on IL-1β secretion and LDH release in MSU stimulated BMDMs. **(D,E)** Western blot analysis of the inhibitory effects of MG (50 μM) on GSDMD express in MSU stimulated BMDMs. **(F)** The inhibitory effects of MG (10 and 50 μM) on TNF-α secretion in MSU stimulated LPS-primed BMDMs. **(G,H)** The inhibitory effects of MG (50 μM) on ROS production in MSU stimulated BMDMs by ROS assay **(G)** and ROS staining **(H)**. MG: methyl gallate, Veh: Vehicle, Con: Control. Data are expressed as mean ± S.D. (n = 6) and are representative of two independent experiments. Statistical differences were calculated by single-factor ANOVA with Tukey HSD test **(B,C,E,F)**, and unpaired Student's t-test **(G)**: $^{*}p < 0.05$, $^{**}p < 0.01$, $^{***}p < 0.001$.

Methyl Gallate Specifically Inhibits Activation of NLRP3 by Blocking the Oligomerization of NLRP3 Inflammasome in BMDMs

To further confirm the inhibitory effect of methyl gallate on the activation of inflammasomes, whether methyl gallate could inhibit the secretion of IL-1β in LPS-primed BMDMs treated with nigericin was explored. It was found that methyl gallate treatment blocked nigericin-induced IL-1β secretion but had no effect on the production of TNF-α (**Figures 4A,B**). In contrast, when BMDMs were incubated with methyl gallate for 30 min before 3-h LPS treatment, methyl gallate inhibited the production of TNF-α (**Figures 4C,D**). These results further suggested that methyl gallate could suppress the two signaling events of NLRP3 inflammasome activation.

The noncanonical activation of NLRP3 inflammasome by intracellular LPS leads to an alternative inflammasome pathway. We tested the release of interleukin-1β in BMDMs stimulated with the TLR2/4 agonist Pam3CSK4, and then transfected wild type and NLRP3 effective cells with LPS. Treatment with methyl gallate reduced the release of IL-1β in BMDMs cells. Cells lacking NLRP3 showed low or no IL-1β production, confirming the requirement of NLRP3 for IL-1β release (**Figure 4E**).

In addition to nigericin, we also studied the effects of other NLRP3 agonists (including MSU, Alum, and ATP) to understand whether methyl gallate is a co-inhibitor of NLPR3 inflammasome (**Figure 4F**). Similar to nigericin, methyl gallate significantly blocked these agonists-induced IL-1β secretion. These results indicated that methyl gallate was a potent and broad inhibitor for NLRP3 inflammasome activation. Additionally, methyl gallate had no effect on the activation of NLRC4 or AIM2 inflammasomes, which were triggered by salmonella typhimurium infection or poly A:T transfection, respectively (**Figure 4F**). Taken together, these results demonstrated that methyl gallate could specifically inhibit

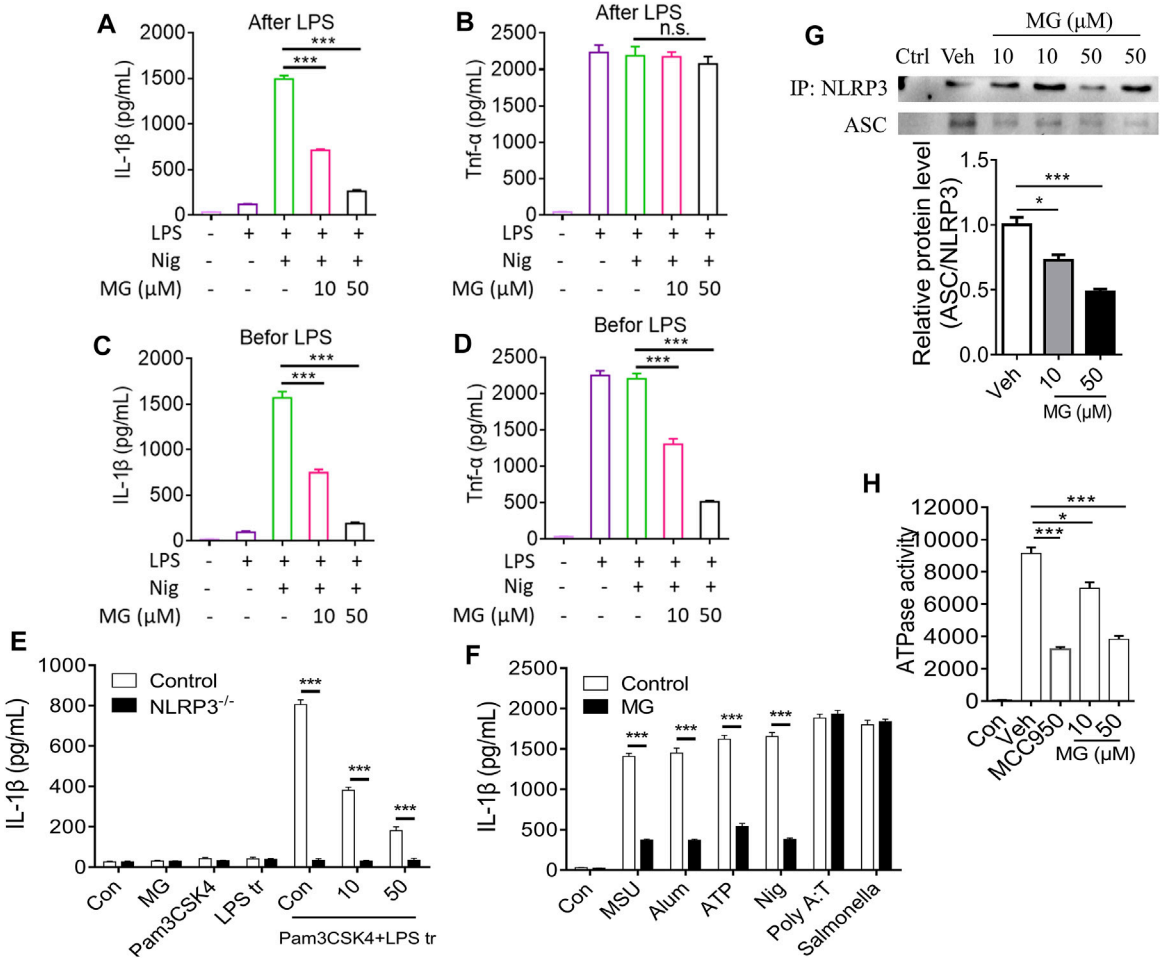

FIGURE 4 | Methyl gallate specifically inhibits activation of NLRP3 by blocking the oligomerization of NLRP3 inflammasome in BMDMs. **(A,B)** BMDMs were treated with different doses of MG for 0.5 h and then stimulated with LPS for 3 h. After that, the cells were stimulated with nigericin. Medium supernatants (SN) were analyzed by ELISA for IL-1β and TNF-α release. **(C,D)** BMDMs were primed with LPS for 3 h and then stimulated with different doses of MG 0.5 h, then the cells were stimulated with nigericin. SN were analyzed by ELISA for IL-1β and TNF-α release. **(E)** The release of IL-1β in BMDMs stimulated with the TLR2/4 agonist Pam3CSK4, and then transfected Wild type and NLRP3 effective cells with LPS. Treatment with MG (10, 50 μM) can reduce the release of IL-1β in BMDMs cells. Cells lacking NLRP3 showed low or no IL-1β production. **(F)** ELISA of IL-1β in SN of LPS-primed BMDMs treated with MG (50 μM) and then stimulated with MSU, nigericin, ATP, Alum, poly A:T and Salmonella. **(G)** Immunoprecipitation (IP, Up) and analysis (Down, mean ± SEM) of the NLRP3-ASC association in BMDMs cells stimulated with LPS/nigericin. **(H)** ATPase activity of recombinant NLRP3 in the presence of MG (n = 3), MCC950 (1 μM) (n = 3). MG: methyl gallate, Veh: Vehicle, Con: Control. Data are expressed as mean ± S.D. (n = 6). Statistical differences were calculated by single-factor ANOVA with Tukey HSD test **(A–D,G,H)**, and unpaired Student's t-test **(E,F)**: $^{*}p < 0.05$, $^{***}p < 0.001$.

the activation of NLRP3 inflammasomes and the subsequent production of IL-1β.

We next used immunoprecipitation (IP) of the NLRP3-ASC association to study the effect of methyl gallate on the formation of NLRP3 inflammasome in BMDMs stimulated by LPS/nigericin. Following the stimulation of LPS and nigericin, ASC was immunoprecipitated with NLRP3 confirming the oligomer formation (**Figure 4G**). Methyl gallate led to a reduction in the NLRP3-mediated ASC recruitment (**Figure 4G**, top and bottom). Using the full-length recombinant human NLRP3 protein, we next gauged the effect of methyl gallate on the nucleotide binding domain of NLRP3. Recombinant NLRP3 exhibited ATPase activity and was inhibited by methyl gallate at 10 and 50 μM (**Figure 4H**). In the same assay, MCC950, a known inhibitor of the NLRP3 inflammasome, was used as a positive control (Coll et al., 2019). In conclusion, these data suggested that methyl gallate reduced the release of mature IL-1β by blocking the oligomerization of NLRP3 inflammasome.

Methyl Gallate Inhibits NLRP3-dependent Inflammation *in vivo*

We next examined whether methyl gallate could inhibit NLRP3 inflammasome activation *in vivo*. As mentioned above, methyl gallate administration significantly improved PO-induced HN (including renal function, high uric acid levels and FEUA) in wild type C57BL/6 mice, but not in *Nlrp3*$^{-/-}$ mice (**Table.2**). In addition, methyl gallate administration significantly improved

TABLE 2 | The effects of methyl gallate on serum and urinary levels of uric acid and creatinine, as well as FEUA and BUN in PO-induced *wt* and *NLRP3*$^{-/-}$ HN mice.

Group	Dose (mg/kg)	SUA (mg/dl)	SCr (mg/dl)	UUA (mg/dl)	UCr (mg/dl)	BUN (mg/dl)	FEUA
WT	PBS	5.24 ± 0.83	2.63 ± 0.32	31.32 ± 3.89	32.15 ± 3.71	49.52 ± 5.86	39.68 ± 8.02
WT + MG	40	2.67 ± 0.54***	0.85 ± 0.12***	45.63 ± 5.32**	27.20 ± 3.95*	31.45 ± 4.06***	53.66 ± 9.87***
NLRP3$^{-/-}$	PBS	2.45 ± 0.44***	0.83 ± 0.09***	44.23 ± 3.87**	30.15 ± 4.80	32.98 ± 3.85***	55.07 ± 10.14***
NLRP3$^{-/-}$+MG	40	2.29 ± 0.36[a]	0.79 ± 0.11[a]	41.04 ± 4.62[a]	29.03 ± 3.24[a]	33.05 ± 4.19[a]	54.08 ± 9.33[a]

*Uric acid, creatinine and urea nitrogen in serum and urine were detected by kits. MG: methyl gallate. Values are expressed as means ± S.D. (n = 10) Statistical differences were calculated by single-factor ANOVA with Tukey HSD test. Compared with WT: *p < 0.05, **p < 0.01, ***p < 0.001.*

[a]*there was no significant difference compared to* NLRP3$^{-/-}$ *group.*

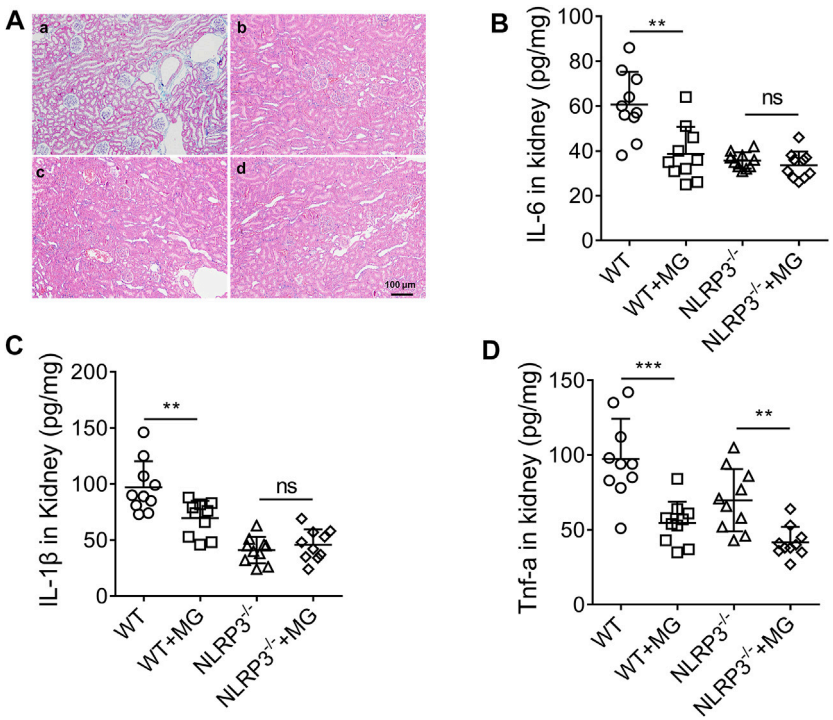

FIGURE 5 | Effect of methyl gallate dependent on NLRP3 pathway in renal tissues. **(A)** HE-staining of renal tissues from mice in different groups. **(B–D)** Cytokines such as IL-6 **(B)**, IL-1β **(C)** and TNF-α **(D)** in renal tissues were detected by ELISA kits. Scale bar, 100 μm. a: WT; b: WT + MG (40 mg/kg); c:*NLRP3*$^{-/-}$; d: *NLRP3*$^{-/-}$ + MG (40 mg/kg). Values are expressed as means ± S.D. (n = 10). Data were analyzed by single-factor ANOVA with Tukey HSD test. Compared with WT or *NLRP3*$^{-/-}$ group: *$^{**}p < 0.01$, $^{***}p < 0.001$.

renal histological changes and reduced renal levels of IL-6 and IL-1β in wild type mice but not in *Nlrp3*$^{-/-}$ mice in PO-induced HN (**Figures 5A–C**). As expected, methyl gallate treatment significantly reduced TNF-a levels in PO-induced wild type mice. In particular, methyl gallate treatment further reduced TNF-a levels in *Nlrp3*$^{-/-}$ mice (**Figure 5D**). Thus, these findings suggested that methyl gallate protected against inflammation and tissue damage by inhibition of NLRP3 inflammasome.

Methyl Gallate has *in vivo* Activity on Cells of Healthy People or Patients With Gout

The recruitment of neutrophils and tissue infiltration are hallmarks of the inflammatory response to injury and infection. Thus, we evaluated the effect of methyl gallate on PBMCs after LPS and ATP treatment. As expected, methyl gallate prevented the release of IL-1β (**Figure 6A**) without affecting the production of TNF-a in PBMCs (**Figure 6B**). Methyl gallate (10 and 50 μM) also reduced caspase-1 activity in PBMCs (**Figure 6C**). Therefore, these results suggested that methyl gallate could prevent the activation of NLRP3 in human cells.

Finally, we assessed whether methyl gallate could affect the pre-activated NLRP3 inflammasomes on patient cells with abnormal NLRP3 activation. As expected, IL-1β secretion could be detected in the culture supernatant from synovial fluid cells (SFCs) isolated from two patients with gout arthritis were cultured in the absence of NLRP3 agonist stimulation (**Figure 6D**). However, when these cells were incubated with methyl gallate (50 μM), IL-1β production

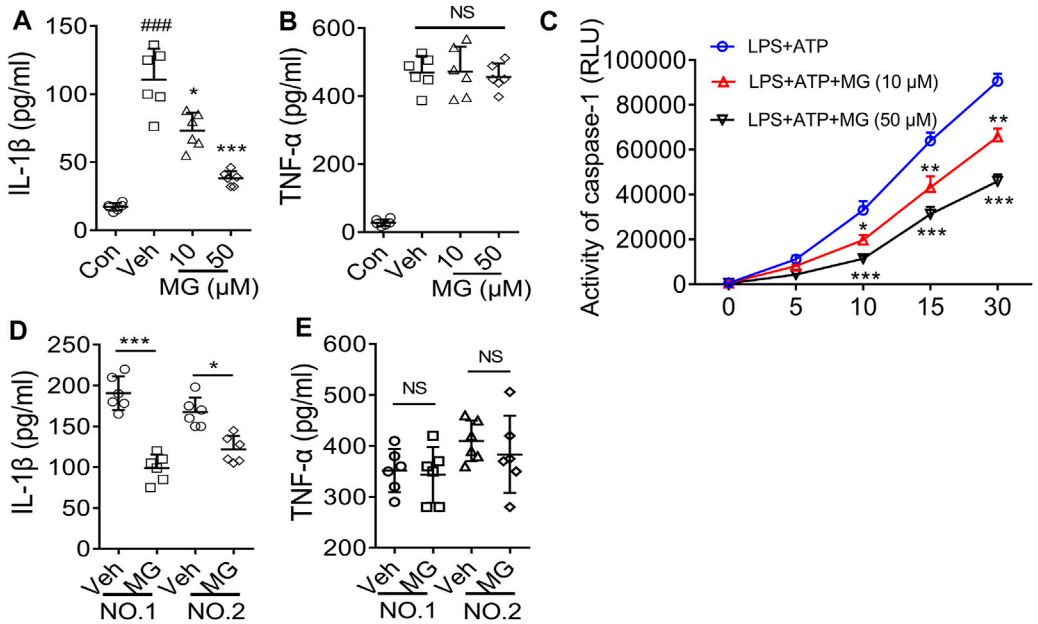

FIGURE 6 | Methyl gallate is active for cells from healthy humans or patients with gout. **(A,B)** ELISA of IL-1β **(A)** or TNF-α **(B)** levels in the supernatants from PBMCs stimulated with LPS and ATP in the presence of concentrations of MG (10 and 50 μM). **(C)** Caspase-1 activity in human PBMCs following LPS + ATP in the presence of MG (10 and 50 μM). **(D,E)** ELISA of IL-1β **(D)** and TNF-α **(E)** in supernatants from SFCs isolated from an individual with gout, treated with MG (50 μM) for 20 h. MG: methyl gallate, Veh: Vehicle, Con: Control. The data are expressed as mean ± S.D. (n = 6) of PBMCs from three healthy donors and the SFCs isolated from two patients were analyzed. Statistical differences were calculated by single-factor ANOVA with Tukey HSD test **(A,B)**, or 2-way ANOVA **(C)** with post hoc Sidak test for multiple comparisons, or unpaired Student's t-test **(D,E)**. $^{*}p < 0.05$, $^{***}p < 0.001$.

were reduced by 65 and 40%, respectively (**Figure 6D**). In reverse, TNF-α production was unaffected by methyl gallate treatment (**Figure 6E**). These results suggested that methyl gallate could inhibit the pre-activated NLRP3 inflammasome in patients' SFCs, supporting the clinical use of methyl gallate for the control of NLRP3-driven disease.

DISCUSSION

Hyperuricemia refers to the state where the blood uric acid level of adult men is ≥ 420 μmol·L^{-1} and the blood uric acid level of adult women is ≥ 324 μmol·L^{-1} (Dalbeth et al., 2016). Hyperuricemia is closely related to the occurrence of HN and is an important stage in patients with gout (Eleftheriadis et al., 2017). Recent studies have shown that hyperuricemia is an important risk factor for gout, hypertension, diabetes, cardiovascular complications, metabolic syndrome, and kidney disease (Obermayr et al., 2008; Weiner et al., 2008; Johnson et al., 2013). More and more evidence indicate that uric acid-induced inflammation is the core mechanism of hyperuricemia rodent kidney injury (Wang et al., 2015; Chen and Lan, 2017), and the NLRP3 pathway may play a central role in it.

As the incidence of HN has been increasing year by year in recent years, the situation of finding drugs to treat related diseases has become increasingly critical. Most of the drugs available on the market have various adverse effects, such as hypersensitivity syndrome and nephrotoxicity of allopurinol; and hepatic and renal toxicity of benzbromarone. (Lee et al., 2008; Chou et al., 2018). Therefore, the search for an effective drug with few adverse effects is one of the future directions of drug development.

In this experiment, we found methyl gallate could remarkably reduce the uric acid level by inhibit XOD activity in liver. These studies are consistent with previous reports (Masuoka et al., 2006; Asnaashari et al., 2014) that methyl gallate reduced uric acid production by inhibiting XOD activity. Creatinine and urea nitrogen levels are commonly used indicators to evaluate renal function. Methyl gallate could reduce levels of Scr, Ucr and BUN in a dose-dependent manner. Subsequent pathological section results showed that methyl gallate could significantly improve the renal pathological changes (including arteriosclerosis, glomerulosclerosis and tubulointerstitial fibrosis). These results above suggest that methyl gallate indeed improve HN.

Patients with hyperuricemia activate the self-inhibited inactive NLRP3 through MSU as an activation signal that is recognized and bound by the leucine-rich repeat (LRR) of NLRP3 (Kim et al., 2015; Wen et al., 2021). Activated NLRP3 recruit's apoptosis-associated speck-like protein containing a CARD (ASC) and caspase-1 to form the NLRP3 inflammasome, which cleaves IL-1β precursor proteins and generates IL-1β by regulating caspase-1 activity. At the same time, it induces cell membrane perforation damage, leading to inflammatory death, which facilitates IL-1β release and causes inflammation occurrence

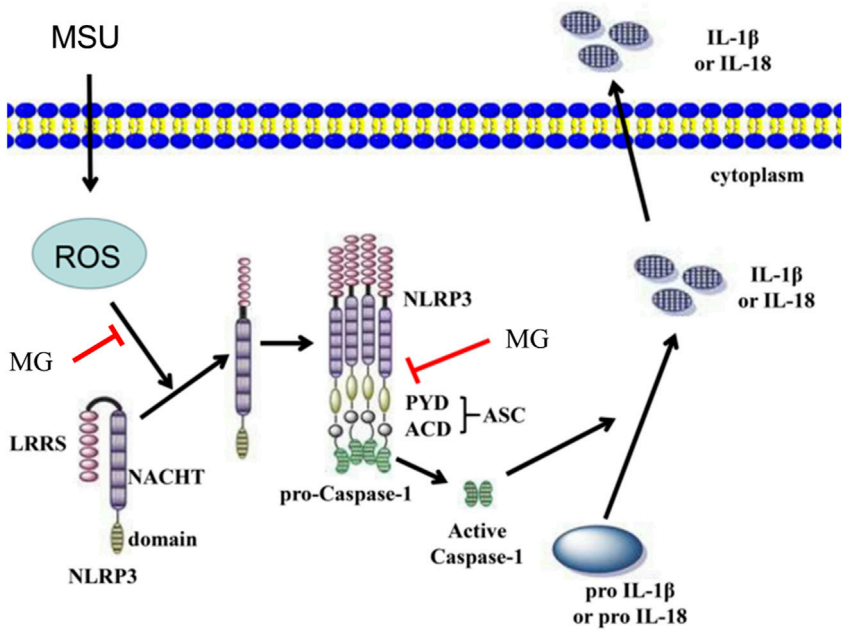

FIGURE 7 | Proposed model for methyl gallate improves PO-induced HN. MG has a protective effect on the kidneys in PO-induced HN. The mechanism may be related to block the overproduction of ROS and prevent NLRP3 inflammasome oligomerization to exert its remarkable anti-inflammatory activity in NLRP3-driven diseases. MG: methyl gallate.

(Franchi et al., 2009). In this study, we found that methyl gallate significantly reduced the NLRP3 inflammasome activation (the protein expression levels of NLRP3, ASC, IL-1β, and caspase-1).

Additionally, we demonstrated that MG had dual inhibition of NLRP3 inflammasome activation. As previously reported (Domanski et al., 2016), firstly, methyl gallate inhibits the activation of NF-κB and suppresses the production of TNF-α, an inflammasome-independent cytokine. Secondly, methyl gallate directly inhibited NLRP3 inflammasome activation to decrease IL-1β production. Interestingly, our findings showed that the beneficial effect of methyl gallate on HN was absent in *Nlrp3*$^{-/-}$ mice, indicating that the anti-inflammatory activity of methyl gallate *in vivo* depended on its inhibition of the NLRP3 inflammasome. These findings showed that methyl gallate binds directly to NLRP3 and displayed significant anti-inflammatory activity both *in vitro* and *in vivo*, and thus methyl gallate may have good therapeutic potential for NLRP3-driven diseases. It is believed that although both NLRP3 inflammasome components and upstream signaling events can be targeted, only targeting NLRP3 itself can specifically block its activation (He et al., 2018). Our results indicated that although NLRP3-activated upstream signaling events such as ROS were influenced by methyl gallate processing, we also found that methyl gallate blocked the interaction between NLRP3 and ASC, an important step in NLRP3 inflammasome assembly (He et al., 2016; Shi et al., 2016). Methyl gallate did not inhibit NLRC4 or AIM2 inflammasome activation, which was consistent with previous reports indicating that ASC interacted with NLRP3 but not with other inflammasome sensors, such as NLRC4 and AIM2 (Shi et al., 2016). Thus, our results indicated that methyl gallate was a classical NLRP3 inhibitor.

Consistent with the results from mouse BMDMs, methyl gallate significantly reduced ATP-induced robust inflammasome activation in cultured PBMCs isolated from healthy subjects and inhibit the pre-activated NLRP3 inflammasome in patients' SFCs. These results indicated that methyl gallate was a specific inhibitor of NLRP3 inflammasome activation in rodent and human innate immune cells.

In conclusion, our research provided a potential new and practical drug candidate for the treatment of HN, the mechanism of methyl gallate may involve blocking NLRP3 activation (**Figure 7**).

DATA AVAILABILITY STATEMENT

The datasets presented in this study can be found in online repositories. The names of the repository/repositories and accession number(s) can be found in the article/ **Supplementary Material**.

ETHICS STATEMENT

The animal study was reviewed and approved by the Animal Ethics Committee of South-Central University for Nationalities.

AUTHOR CONTRIBUTIONS

BX and LC designed the study. PL, WW, QL, XH, CW, and LB performed the experiments. LP, LC, and ZL analyzed the data. LC wrote the manuscript.

FUNDING

This work was financially supported by the National Natural Science Foundation of China grants (82074081 and 81873221); National Major Scientific and Technological Special Project for "Significant New Drugs Development" (No. 2017ZX09301060-007).

SUPPLEMENTARY MATERIAL

The Supplementary Material for this article can be found online at: https://www.frontiersin.org/articles/10.3389/fphar.2021.759040/full#supplementary-material

REFERENCES

Acharyya, S., Sarkar, P., Saha, D. R., Patra, A., Ramamurthy, T., and Bag, P. K. (2015). Intracellular and Membrane-Damaging Activities of Methyl Gallate Isolated from Terminalia Chebula against Multidrug-Resistant Shigella Spp. *J. Med. Microbiol.* 64, 901–909. doi:10.1099/jmm.0.000107

Asnaashari, M., Farhoosh, R., and Sharif, A. (2014). Antioxidant Activity of Gallic Acid and Methyl Gallate in Triacylglycerols of Kilka Fish Oil and its Oil-In-Water Emulsion. *Food Chem.* 159, 439–444. doi:10.1016/j.foodchem.2014.03.038

Azam, S., Jakaria, M., Kim, I. S., Kim, J., Haque, M. E., and Choi, D. K. (2019). Regulation of Toll-like Receptor (TLR) Signaling Pathway by Polyphenols in the Treatment of Age-Linked Neurodegenerative Diseases: Focus on TLR4 Signaling. *Front. Immunol.* 10, 1000. doi:10.3389/fimmu.2019.01000

Chen, L., and Lan, Z. (2017). Polydatin Attenuates Potassium Oxonate-Induced Hyperuricemia and Kidney Inflammation by Inhibiting NF-Kb/nlrp3 Inflammasome Activation via the AMPK/SIRT1 Pathway. *Food Funct.* 8, 1785–1792. doi:10.1039/c6fo01561a

Chen, L., Yin, H., Lan, Z., Ma, S., Zhang, C., Yang, Z., et al. (2011). Anti-hyperuricemic and Nephroprotective Effects of Smilax china L. *J. Ethnopharmacol* 135, 399–405. doi:10.1016/j.jep.2011.03.033

Cho, E. J., Yokozawa, T., Kim, H. Y., Shibahara, N., and Park, J. C. (2004). Rosa Rugosa Attenuates Diabetic Oxidative Stress in Rats with Streptozotocin-Induced Diabetes. *Am. J. Chin. Med.* 32, 487–496. doi:10.1142/S0192415X04002132

Choi, J. G., Kang, O. H., Lee, Y. S., Oh, Y. C., Chae, H. S., Jang, H. J., et al. (2009). Antibacterial Activity of Methyl Gallate Isolated from Galla Rhois or Carvacrol Combined with Nalidixic Acid against Nalidixic Acid Resistant Bacteria. *Molecules* 14, 1773–1780. doi:10.3390/molecules14051773

Chou, H. W., Chiu, H. T., Tsai, C. W., Ting, I. W., Yeh, H. C., Huang, H. C., et al.CMUH Kidney Research Group (2018). Comparative Effectiveness of Allopurinol, Febuxostat and Benzbromarone on Renal Function in Chronic Kidney Disease Patients with Hyperuricemia: a 13-year Inception Cohort Study. *Nephrol. Dial. Transpl.* 33, 1620–1627. doi:10.1093/ndt/gfx313

Coll, R. C., Hill, J. R., Day, C. J., Zamoshnikova, A., Boucher, D., Massey, N. L., et al. (2019). MCC950 Directly Targets the NLRP3 ATP-Hydrolysis Motif for Inflammasome Inhibition. *Nat. Chem. Biol.* 15, 556–559. doi:10.1038/s41589-019-0277-7

Correa, L. B., Pádua, T. A., Seito, L. N., Costa, T. E., Silva, M. A., Candéa, A. L., et al. (2016). Anti-inflammatory Effect of Methyl Gallate on Experimental Arthritis: Inhibition of Neutrophil Recruitment, Production of Inflammatory Mediators, and Activation of Macrophages. *J. Nat. Prod.* 79, 1554–1566. doi:10.1021/acs.jnatprod.5b01115

Crispo, J. A., Piché, M., Ansell, D. R., Eibl, J. K., Tai, I. T., Kumar, A., et al. (2010). Protective Effects of Methyl Gallate on H2O2-Induced Apoptosis in PC12 Cells. *Biochem. Biophys. Res. Commun.* 393, 773–778. doi:10.1016/j.bbrc.2010.02.079

C. S., S., K. G., A., V., V., A., S., and M., H. (2018). Designing of Enzyme Inhibitors Based on Active Site Specificity: Lessons from Methyl Gallate and its Lipoxygenase Inhibitory Profile. *J. Receptors Signal Transduction* 38, 256–265. doi:10.1080/10799893.2018.1478856

Dalbeth, N., Merriman, T. R., and Stamp, L. K. (2016). Gout. *The Lancet* 388, 2039–2052. doi:10.1016/S0140-6736(16)00346-9

Ding, Y. X., Eerduna, G. W., Duan, S. J., Li, T., Liu, R. X., Zhang, L. M., et al. (2021). Escin Ameliorates the Impairments of Neurological Function and Blood Brain Barrier by Inhibiting Systemic Inflammation in Intracerebral Hemorrhagic Mice. *Exp. Neurol.* 337, 113554. doi:10.1016/j.expneurol.2020.113554

Domanski, D., Zegrocka-Stendel, O., Perzanowska, A., Dutkiewicz, M., Kowalewska, M., Grabowska, I., et al. (2016). Molecular Mechanism for Cellular Response to β-Escin and its Therapeutic Implications. *PLoS One* 11, e0164365. doi:10.1371/journal.pone.0164365

Eleftheriadis, T., Golphinopoulos, S., Pissas, G., and Stefanidis, I. (2017). Asymptomatic Hyperuricemia and Chronic Kidney Disease: Narrative Review of a Treatment Controversial. *J. Adv. Res.* 8, 555–560. doi:10.1016/j.jare.2017.05.001

Franchi, L., Eigenbrod, T., Muñoz-Planillo, R., and Nuñez, G. (2009). The Inflammasome: a Caspase-1-Activation Platform that Regulates Immune Responses and Disease Pathogenesis. *Nat. Immunol.* 10, 241–247. doi:10.1038/ni.1703

Franklin, B. S., Mangan, M. S., and Latz, E. (2016). Crystal Formation in Inflammation. *Annu. Rev. Immunol.* 34, 173–202. doi:10.1146/annurev-immunol-041015-055539

Ghaemi-Oskouie, F., and Shi, Y. (2011). The Role of Uric Acid as an Endogenous Danger Signal in Immunity and Inflammation. *Curr. Rheumatol. Rep.* 13, 160–166. doi:10.1007/s11926-011-0162-1

Gross, O., Thomas, C. J., Guarda, G., and Tschopp, J. (2011). The Inflammasome: an Integrated View. *Immunol. Rev.* 243, 136–151. doi:10.1111/j.1600-065X.2011.01046.x

He, H., Jiang, H., Chen, Y., Ye, J., Wang, A., Wang, C., et al. (2018). Oridonin Is a Covalent NLRP3 Inhibitor with strong Anti-inflammasome Activity. *Nat. Commun.* 9, 2550. doi:10.1038/s41467-018-04947-6

He, Y., Zeng, M. Y., Yang, D., Motro, B., and Núñez, G. (2016). NEK7 Is an Essential Mediator of NLRP3 Activation Downstream of Potassium Efflux. *Nature* 530, 354–357. doi:10.1038/nature16959

Johnson, R. J., Nakagawa, T., Sanchez-Lozada, L. G., Shafiu, M., Sundaram, S., Le, M., et al. (2013). Sugar, Uric Acid, and the Etiology of Diabetes and Obesity. *Diabetes* 62, 3307–3315. doi:10.2337/db12-1814

Kamatham, S., Kumar, N., and Gudipalli, P. (2015). Isolation and Characterization of Gallic Acid and Methyl Gallate from the Seed coats of Givotia Rottleriformis Griff. And Their Anti-proliferative Effect on Human Epidermoid Carcinoma A431 Cells. *Toxicol. Rep.* 2, 520–529. doi:10.1016/j.toxrep.2015.03.001

Kang, M. S., Jang, H. S., Oh, J. S., Yang, K. H., Choi, N. K., Lim, H. S., et al. (2009). Effects of Methyl Gallate and Gallic Acid on the Production of Inflammatory Mediators Interleukin-6 and Interleukin-8 by Oral Epithelial Cells Stimulated with Fusobacterium Nucleatum. *J. Microbiol.* 47, 760–767. doi:10.1007/s12275-009-0097-7

Kim, S. M., Lee, S. H., Kim, Y. G., Kim, S. Y., Seo, J. W., Choi, Y. W., et al. (2015). Hyperuricemia-induced NLRP3 Activation of Macrophages Contributes to the Progression of Diabetic Nephropathy. *Am. J. Physiol. Ren. Physiol* 308, F993–F1003. doi:10.1152/ajprenal.00637.2014

Lee, H., Lee, H., Kwon, Y., Lee, J. H., Kim, J., Shin, M. K., et al. (2010). Methyl Gallate Exhibits Potent Antitumor Activities by Inhibiting Tumor Infiltration of CD4+CD25+ Regulatory T Cells. *J. Immunol.* 185, 6698–6705. doi:10.4049/jimmunol.1001373

Lee, M. H., Graham, G. G., Williams, K. M., and Day, R. O. (2008). A Benefit-Risk Assessment of Benzbromarone in the Treatment of Gout. Was its Withdrawal

from the Market in the Best Interest of Patients. *Drug Saf.* 31, 643–665. doi:10.2165/00002018-200831080-00002

Lee, S. H., Kim, J. K., Kim, D. W., Hwang, H. S., Eum, W. S., Park, J., et al. (2013). Antitumor Activity of Methyl Gallate by Inhibition of Focal Adhesion Formation and Akt Phosphorylation in Glioma Cells. *Biochim. Biophys. Acta* 1830, 4017–4029. doi:10.1016/j.bbagen.2013.03.030

Lu, J., Dalbeth, N., Yin, H., Li, C., Merriman, T. R., and Wei, W. H. (2019). Mouse Models for Human Hyperuricaemia: a Critical Review. *Nat. Rev. Rheumatol.* 15, 413–426. doi:10.1038/s41584-019-0222-x

Lu, X., Shi, X., Li, Y., Chi, H., Liao, E., Liu, C., et al. (2020). A Negative Association between Urinary Iodine Concentration and the Prevalence of Hyperuricemia and Gout: a Cross-Sectional and Population-Based Study in Mainland China. *Eur. J. Nutr.* 59, 3659–3668. doi:10.1007/s00394-020-02199-z

Masuoka, N., Nihei, K., and Kubo, I. (2006). Xanthine Oxidase Inhibitory Activity of Alkyl Gallates. *Mol. Nutr. Food Res.* 50, 725–731. doi:10.1002/mnfr.200500250

Mazzali, M., Hughes, J., Kim, Y. G., Jefferson, J. A., Kang, D. H., Gordon, K. L., et al. (2001). Elevated Uric Acid Increases Blood Pressure in the Rat by a Novel crystal-independent Mechanism. *Hypertension* 38, 1101–1106. doi:10.1161/hy1101.092839

Obermayr, R. P., Temml, C., Gutjahr, G., Knechtelsdorfer, M., Oberbauer, R., and Klauser-Braun, R. (2008). Elevated Uric Acid Increases the Risk for Kidney Disease. *J. Am. Soc. Nephrol.* 19, 2407–2413. doi:10.1681/ASN.2008010080

Park, D. J., Jung, H. J., Park, C. H., Yokozawa, T., and Jeong, J. C. (2019). Root Bark of Paeonia Suffruticosa Extract and its Component Methyl Gallate Possess Peroxynitrite Scavenging Activity and Anti-inflammatory Properties through NF-Kb Inhibition in LPS-Treated Mice. *Molecules* 24, 3483. doi:10.3390/molecules24193483

Rahimifard, M., Maqbool, F., Moeini-Nodeh, S., Niaz, K., Abdollahi, M., Braidy, N., et al. (2017). Targeting the TLR4 Signaling Pathway by Polyphenols: A Novel Therapeutic Strategy for Neuroinflammation. *Ageing Res. Rev.* 36, 11–19. doi:10.1016/j.arr.2017.02.004

Rosas, E. C., Correa, L. B., Pádua, Tde. A., Costa, T. E., Mazzei, J. L., Heringer, A. P., et al. (2015). Anti-inflammatory Effect of Schinus Terebinthifolius Raddi Hydroalcoholic Extract on Neutrophil Migration in Zymosan-Induced Arthritis. *J. Ethnopharmacol* 175, 490–498. doi:10.1016/j.jep.2015.10.014

Sattui, S. E., and Gaffo, A. L. (2016). Treatment of Hyperuricemia in Gout: Current Therapeutic Options, Latest Developments and Clinical Implications. *Ther. Adv. Musculoskelet. Dis.* 8, 145–159. doi:10.1177/1759720X16646703

Shi, H., Wang, Y., Li, X., Zhan, X., Tang, M., Fina, M., et al. (2016). NLRP3 Activation and Mitosis Are Mutually Exclusive Events Coordinated by NEK7, a New Inflammasome Component. *Nat. Immunol.* 17, 250–258. doi:10.1038/ni.3333

Wang, M. X., Liu, Y. L., Yang, Y., Zhang, D. M., and Kong, L. D. (2015). Nuciferine Restores Potassium Oxonate-Induced Hyperuricemia and Kidney Inflammation in Mice. *Eur. J. Pharmacol.* 747, 59–70. doi:10.1016/j.ejphar.2014.11.035

Weiner, D. E., Tighiouart, H., Elsayed, E. F., Griffith, J. L., Salem, D. N., and Levey, A. S. (2008). Uric Acid and Incident Kidney Disease in the Community. *J. Am. Soc. Nephrol.* 19, 1204–1211. doi:10.1681/ASN.2007101075

Wen, L., Yang, H., Ma, L., and Fu, P. (2021). The Roles of NLRP3 Inflammasome-Mediated Signaling Pathways in Hyperuricemic Nephropathy. *Mol. Cel Biochem* 476, 1377–1386. doi:10.1007/s11010-020-03997-z

Whang, W. K., Park, H. S., Ham, I. H., Oh, M., Namkoong, H., Kim, H. K., et al. (2005). Methyl Gallate and Chemicals Structurally Related to Methyl Gallate Protect Human Umbilical Vein Endothelial Cells from Oxidative Stress. *Exp. Mol. Med.* 37, 343–352. doi:10.1038/emm.2005.44

Yahfoufi, N., Alsadi, N., Jambi, M., and Matar, C. (2018). The Immunomodulatory and Anti-inflammatory Role of Polyphenols. *Nutrients* 10, 1618. doi:10.3390/nu10111618

Zhang, L., Chen, X., Wu, L., Li, Y., Wang, L., Zhao, X., et al. (2021). Ameliorative Effects of Escin on Neuropathic Pain Induced by Chronic Constriction Injury of Sciatic Nerve. *J. Ethnopharmacol* 267, 113503. doi:10.1016/j.jep.2020.113503

Conflict of Interest: BX was employd by the company Zhejiang Heze Pharmaceutical Technology Co., Ltd.

The remaining authors declare that the research was conducted in the absence of any commercial or financial relationships that could be construed as a potential conflict of interest.

Publisher's Note: All claims expressed in this article are solely those of the authors and do not necessarily represent those of their affiliated organizations, or those of the publisher, the editors and the reviewers. Any product that may be evaluated in this article, or claim that may be made by its manufacturer, is not guaranteed or endorsed by the publisher.

Copyright © 2021 Liu, Wang, Li, Hu, Xu, Wu, Bai, Ping, Lan and Chen. This is an open-access article distributed under the terms of the Creative Commons Attribution License (CC BY). The use, distribution or reproduction in other forums is permitted, provided the original author(s) and the copyright owner(s) are credited and that the original publication in this journal is cited, in accordance with accepted academic practice. No use, distribution or reproduction is permitted which does not comply with these terms.

frontiers in Pharmacology

ORIGINAL RESEARCH
published: 23 December 2021
doi: 10.3389/fphar.2021.800220

Targeting MyD88 Downregulates Inflammatory Mediators and Pathogenic Processes in PBMC From DMARDs-Naïve Rheumatoid Arthritis Patients

Sergio Ramirez-Perez[1,2], *Edith Oregon-Romero*[3], *Itzel Viridiana Reyes-Perez*[4] *and Pallavi Bhattaram*[1,2]*

[1]Department of Orthopaedics, Emory University School of Medicine, Atlanta, GA, United States, [2]Department of Cell Biology, Emory University School of Medicine, Atlanta, GA, United States, [3]Biomedical Sciences Research Institute (IICB), University of Guadalajara, Guadalajara, Mexico, [4]Department of Molecular Biology and Genomics, University of Guadalajara, Guadalajara, Mexico

OPEN ACCESS

Edited by:
Emer S. Ferro,
University of São Paulo, Brazil

Reviewed by:
Bjarne Kuno Møller,
Aarhus University Hospital, Denmark
Shuji Sumitomo,
Kobe City Medical Center General Hospital, Japan

***Correspondence:**
Pallavi Bhattaram
pallavi.bhattaram@emory.edu

Specialty section:
This article was submitted to Inflammation Pharmacology, a section of the journal Frontiers in Pharmacology

Received: 22 October 2021
Accepted: 29 November 2021
Published: 23 December 2021

Citation:
Ramirez-Perez S, Oregon-Romero E, Reyes-Perez IV and Bhattaram P (2021) Targeting MyD88 Downregulates Inflammatory Mediators and Pathogenic Processes in PBMC From DMARDs-Naïve Rheumatoid Arthritis Patients. Front. Pharmacol. 12:800220. doi: 10.3389/fphar.2021.800220

MyD88-dependent intracellular signalling cascades and subsequently NF-kappaB-mediated transcription lead to the dynamic inflammatory processes underlying the pathogenesis of rheumatoid arthritis (RA) and related autoimmune diseases. This study aimed to identify the effect of the MyD88 dimerization inhibitor, ST2825, as a modulator of pathogenic gene expression signatures and systemic inflammation in disease-modifying antirheumatic drugs (DMARDs)-naïve RA patients. We analyzed bulk RNA-seq from peripheral blood mononuclear cells (PBMC) in DMARDs-naïve RA patients after stimulation with LPS and IL-1β. The transcriptional profiles of ST2825-treated PBMC were analyzed to identify its therapeutic potential. Ingenuity Pathway Analysis was implemented to identify downregulated pathogenic processes. Our analysis revealed 631 differentially expressed genes between DMARDs-naïve RA patients before and after ST2825 treatment. ST2825-treated RA PBMC exhibited a gene expression signature similar to that of healthy controls PBMC by downregulating the expression of proinflammatory cytokines, chemokines and matrix metalloproteases. In addition, B cell receptor, IL-17 and IL-15 signalling were critically downregulated pathways by ST2825. Furthermore, we identified eight genes (*MMP9*, *CXCL9*, *MZB1*, *FUT7*, *TGM2*, *IGLV1-51*, *LINC01010*, and *CDK1*) involved in pathogenic processes that ST2825 can potentially inhibit in distinct cell types within the RA synovium. Overall, our findings indicate that targeting MyD88 effectively downregulates systemic inflammatory mediators and modulates the pathogenic processes in PBMC from DMARDs-naïve RA patients. ST2825 could also potentially inhibit upregulated genes in the RA synovium, preventing synovitis and joint degeneration.

Keywords: rheumatoid arthritis, MyD88, DMARDs, downregulation, inflammatory mediators, pathogenic processes

INTRODUCTION

Rheumatoid arthritis (RA) is an autoimmune, inflammatory-chronic and systemic disease of multifactorial etiology. The presence of circulating autoantibodies and increased production of inflammatory mediators are the most important immunological changes in RA. Inflammatory mediators play an essential role in the joint pathology of RA by promoting synovitis, articular cartilage degeneration and bone loss. These critical mediators include the tumor necrosis factor (TNF)-α, interleukin (IL)-1β, and IL-6 (Aletaha and Smolen, 2018; Smolen et al., 2018). In order to mitigate the joint damage caused by systemic inflammation in RA patients, chemical and biological therapies directed against these crucial cytokines have been established. The development of biological disease-modifying antirheumatic drugs (DMARDs), including anti-TNF, anti-IL-1 and anti-IL-6 antibodies, have contributed to ameliorating patients' disease status and delaying the RA progression (Brzustewicz and Bryl, 2015). However, a significant proportion of RA patients fail to show the desired response to the biological DMARDs, highlighting the need to develop additional therapeutics (Aletaha, 2020).

The proinflammatory cytokine IL-1β, is among the critical mediators of inflammatory damage in RA. It exerts its activity via interaction with its receptors (IL-1R), which subsequently leads to the presentation of an intracellular Toll-IL-1-receptor (TIR) domain and activation of downstream signalling cascades that converge into large scale transcriptomic changes (Migliorini et al., 2020; Haque et al., 2021). Myeloid Differentiation Primary Response 88 (Myd88) is a significant constituent of the signalling cascade downstream of IL-1β-IL-1R interaction, which ultimately converges with the canonical NF-κB signalling pathway leading to the further amplification of the inflammatory mediator production in RA (Avbelj et al., 2011; Chen et al., 2020). Another important proinflammatory promoter is the bacterial lipopolysaccharide (LPS), which activates MyD88-dependent intracellular signalling cascades and, subsequently NF-κB-mediated transcription, leading to the activation of inflammatory processes underlying RA (Balka and De Nardo, 2019).

Targeting MyD88 by the effect of the synthetic chemical compound ST2825 has shown a significant decrease in the production of proinflammatory cytokines such as IL-1β, IL-6, TNF-α and IL-12 after LPS stimulation in macrophages (Long et al., 2018), kidney epithelial cells (Qi et al., 2016) and PBMC from healthy subjects (Ramírez-Pérez et al., 2020). The precise ST2825 mechanism-of-action for inhibiting MyD88 is mediated by interfering with homo-oligomerization of BB loop in the MyD88 TIR domain and thereby affecting its dimerization and downstream signalling activation (Loiarro et al., 2007; Loiarro et al., 2013; Chen et al., 2020). In addition, different studies have reported that ST2825 leads to a decrease in the recruitment and activation of IRAK1, IRAK4, TRAF6, IKK complex, p-BTK, p-IκB, NF-κB (p65) and HIF-1α, factors involved in the activation of inflammatory processes (Qi et al., 2016; Yao et al., 2016; Yang et al., 2018; Wang et al., 2019). Together, these studies suggest that inhibition of MyD88 is a potential RA therapeutic strategy. We, therefore, initiated this study to obtain an indepth understanding of the effect of MyD88 inhibition by ST2825 on systemic inflammation generated by the peripheral blood mononuclear cells (PBMC) from RA patients. In order to decipher the effect of MyD88 inhibition independent of DMARDs, we performed our studies on DMARDs-naïve RA patients. Dysregulated pathways and the expression of genes involved in inflammation were evaluated by performing a transcriptomic analysis of healthy and RA PBMC sensitized to various proinflammatory stimuli. We thus identified the MyD88-dependent immunopathological gene expression signature that is downregulated by its specific inhibitor ST2825. Our studies on DMARDs-naïve patients might provide invaluable information on transcriptional changes that contribute to identifying specific immunopathological pathways implicated in the presentation and progression of RA.

MATERIALS AND METHODS

Study Design

We aimed to identify inflammatory mediators and fundamental signalling pathways in RA, which cause sustained inflammation after stimulation with important mitogens and proinflammatory cytokines such as LPS and IL-1β. The potential effect of ST2825 as an inhibitor of MyD88-dependent inflammatory mechanisms could represent a critical strategy to modulate the inflammatory process in RA. Our working hypothesis is that the chemical molecule ST2825 inhibits the signalling pathways mediated by the activation of peripheral blood mononuclear cells (PBMC) stimulated with bacterial lipopolysaccharides (LPS) and recombinant human IL-1β (hrIL-1β) in treatment-naïve RA patients.

Reagents

LPS from *Escherichia coli* (CAT-L-2880, SIGMA®), Recombinant Human IL-1 beta/IL-1F2 Protein (201-LB-005, R&D Systems®), and ST2825 Inhibitor of MyD88 dimerization (Cat. No. A3840, APExBIO) were used for PBMC stimulation. All reagents were reconstituted according to the manufacturer's instructions.

PBMC and Cell Culture

PBMC samples from DMARDs-naïve RA patients and healthy subjects were purchased from STEMCELL Technologies Inc. and Precision For Medicine Inc. (**Supplementary Table S1**). Frozen PBMC were thaw according to STEMCELL Technologies instructions. PBMC were cultured in 6-well plates after the density adjustment at 1×10^6 cells/mL (final volume of 2000 μL). A serum-free system was implemented for PBMC culturing by using X-VIVO™ 15 Hematopoietic Serum-Free Culture Media (Lonza) supplemented with 1% penicillin/streptomycin. PBMC were cultured for 48 h before stimulation. Subsequently, PBMC stimulation was performed by adding LPS (30 ng/ml), LPS (30 ng/ml) plus ST2825 (30 μM), rhIL-1β (10 ng/ml), rhIL-1β (10 ng/ml) plus ST2825 (30 μM) or ST2825 (30 μM). Unstimulated PBMC were taken as the control group. The MyD88 inhibitor ST2825 was added to the

corresponding well 30 min before stimulation with LPS or rhIL-1β. A treatment concentration of 30 μM ST2825 was chosen based on our previous study in healthy PBMC (Ramírez-Pérez et al., 2020). Experiments were done in duplicates, and PBMC were incubated for 24 h at 37°C in a humidified 5% CO_2 atmosphere.

Bulk RNA Sequencing

PBMC were collected 24 h after stimulation, and total RNA was extracted and purified using Direct-zol RNA MicroPrep (Zymo Research) following manufacturers' protocol. RNA quality and quantity were assessed using a 2100 Bioanalyzer (Agilent Technologies). Only samples with an RNA integrity number (RIN) > 7 were used. Libraries were generated from 250 ng RNA using TruSeq Stranded Total RNA Sample Prep Kit (Illumina). Sequencing was carried out using the NovaSeq 6000 system (Novogene UC Davis Sequencing Center, Novogene Corporation Inc.). FASTQ files from these samples were uploaded in Strand NGS software (version 4.0) for analysis (**Supplementary Table S3**). Paired-end reads were mapped to the hg19 human genome assembly. RNA levels were normalized using DESeq. The lower cut-off for RNA levels was = 2 NRPKM (normalized reads per kilobase of exon model per million mapped sequence).

Bioinformatics Analysis of RNA Sequencing Data

Differentially expressed (DE) genes were identified through Strand NGS software (version 4.0). QIAGEN Ingenuity Pathway Analysis (IPA) was used to identify canonical pathways, upstream regulators, predicted diseases and functions dysregulated between different conditions in our study. Data visualization and DE analysis was performed in GraphPad Prism version 9. Networks of relevant DE genes were identified and analyzed in STRING version 11.5 and Cytoscape version 3.8.2. For bulk RNA-seq data analysis from the Accelerating Medicines Partnership (AMP) (Zhang et al., 2019), synovial tissue was obtained from 14 OA, 17 leukocyte-poor RA and 18 leukocyte-rich RA, synovial cell populations were sorted by flow cytometry. RNA-seq from AMP was performed on sorted cells using the following surface markers: $CD45^-$ $Podoplanin^+$ for fibroblasts, $CD45^+$ $CD14^+$ for monocytes, $CD45^+$ $CD3^+$ for T cells, and $CD45^+$ $CD3^-$ $CD19^+$ for B cells; data were visualized using Immunogenomics.io.

Statistical Analysis

Differential gene expression changes in RNA-seq were calculated by Audic Claverie test and Benjamini-Hochberg false discovery rate (FDR) for multiple testing corrections. Hierarchical cluster analysis of biological replicates was performed on normalized intensity values from RNA sequenced samples; similarities were determine by using Euclidean distance measure and Wards methods. For bulk RNA-seq data analysis from the Accelerating Medicines Partnership (AMP) Kruskal–Wallis test was performed to observe differences among groups. The p-value cut-off was set at 0.05.

RESULTS

Identification of Gene Expression Signatures and Distinct Canonical Pathways in DMARDs-Naïve RA Patients

In order to identify critical gene expression signatures in PBMC from DMARDs-naïve RA patients, differential expression analysis was performed (**Figure 1A**, **Supplementary Figure S1A**). We identified 796 differentially expressed (DE) genes by 2-fold change ($p < 0.05$) between RA patients and healthy subjects. The analysis showed 180 downregulated and 616 upregulated genes. Upregulated genes are exemplified in the heatmap (**Figure 1B**) and the top 5 pathways associated with the upregulated genes identified by IPA analysis are shown in **Figure 1C**. Interestingly, granulocyte adhesion, phagosome formation, IL-8 signalling, osteoarthritis pathway and neuroinflammation were important pathways associated with DMARDs-naïve RA patients. Furthermore, DE genes were used to identify IPA-predicted disease associations and functions upregulated in DMARDs-naïve RA patients compared with healthy subjects (**Figure 1D**) and as expected the top 5 IPA-predicted disease associations related to the upregulated genes were directly associated with RA or rheumatic disease processes, which fortify the successful characterization of samples used for this study.

MyD88 Inhibition Significantly Modulates Gene Expression and Pathogenic Features in PBMC From DMARDs-Naïve RA Patients

To address specific MyD88 dimerization inhibition, we took advantage of the synthetic chemical compound ST2825, which has previously been reported in several cell studies to downregulate important MyD88-dependent inflammatory signalling pathways. PBMC from DMARDs-naïve RA patients were treated with ST2825, and DE genes were identified. Hierarchical cluster analysis of normalized gene expression from DMARDs-naïve RA after ST2825 treatment is shown in **Supplementary Figures S3A–B**. Our analysis revealed 631 DE genes between DMARDs-naïve RA patients before and after ST2825 treatment (**Figure 2A**). The most interesting finding we observed from this analysis was that ST2825-treated RA PBMC exerted a gene expression signature similar to that observed in healthy controls by downregulating the expression of several genes such as *C1QA* (Complement C1q subcomponent subunit A), *C2* (Complement C2), *CR1* (Complement receptor type 1), *CCL22* (C-C motif chemokine 22), *CX3CR1* (CX3C chemokine receptor 1), and *CXCL9* (C-X-C motif chemokine 9). However, ST2825 treatment did not completely normalize RA expression values to the levels seen in healthy control PBMC, where several upregulated genes were downregulated by the effect of MyD88 inhibition. Another exciting finding was attributed to the top 5 downregulated IPA-predicted disease associations in PBMC from DMARDs-naïve RA patients by the effect of ST2825 (**Figure 2B**), where systemic autoimmune syndrome, rheumatic

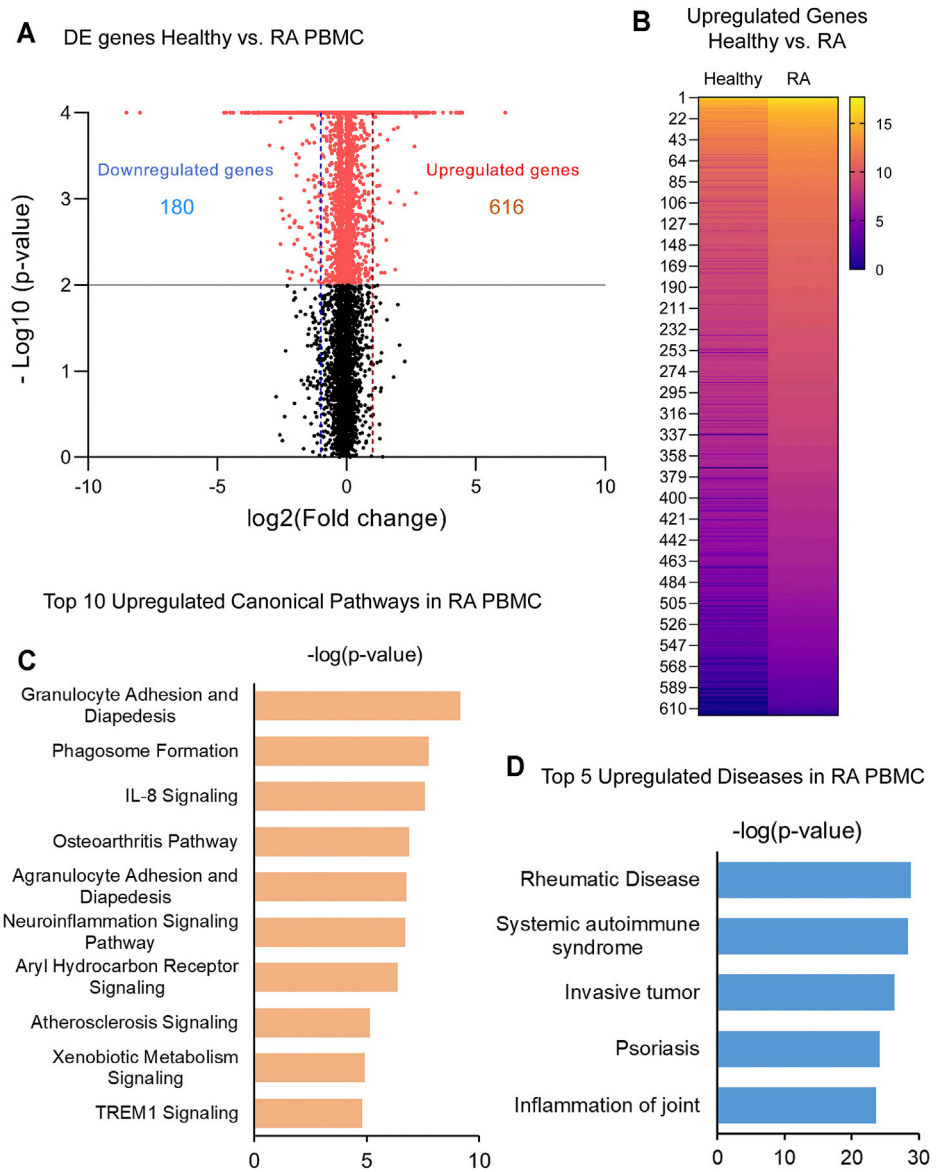

FIGURE 1 | Identification of upregulated genes and canonical pathways in DMARDs-naïve RA patients. **(A)** Volcano plot shows differentially expressed genes between unstimulated PBMC from healthy subjects vs. DMARDs-naïve RA patients (RA). Downregulated genes are shown on the left hand (doted blue line represents 2-fold change) and upregulated genes are shown on the right hand (doted red line represents 2-fold change) of the volcano plot. Grey line represents cut-off of p-value = 0.05. **(B)** Upregulated genes from healthy subjects vs. RA were included in the heatmap (averaged expression patterns of biological replicates are shown). **(C)** Top 10 canonical pathways and **(D)** top 5 of IPA-predicted disease associations were identified from upregulated genes between healthy subjects and DMARDs-naïve RA PBMC.

disease, joint inflammation, and rheumatoid arthritis were significantly inhibited. These results strongly suggest that ST2825 successfully modulates crucial pathogenic hallmarks of RA. We next performed an *in silico* upstream regulatory analysis to identify the main upstream regulators of those upregulated genes in DMARDs-naïve RA patients *vs.* healthy controls. Our analysis found that 34 upregulated genes from DMARDs-naïve RA patients were predicted to be activated by MyD88 (z-score = 5.384; *p*-value = 1.23E-16), which we referred to as MyD88-dependent genes (**Figure 2C**) (Interaction confidence = 0.9; PPI enrichment *p*-value < 1.1E-13). To determine the effectiveness of ST2825 in reverting the inflammatory transcriptome of the RA PBMC, we compared the top 30 genes that were downregulated by ST2825 in RA PBMC (**Figure 2D**). The analysis indeed revealed that ST2825 reverted the expression of different transcription factor subunits, receptors, and enzymes involved in inflammatory pathways to levels similar in healthy PBMC. These included *MMP9* (Matrix metalloproteinase-9), *FOS* (Fos proto-oncogene), *ALDH1A1* (Aldehyde Dehydrogenase 1 Family Member A1), *SPP1* (Secreted Phosphoprotein 1), *CTSK*

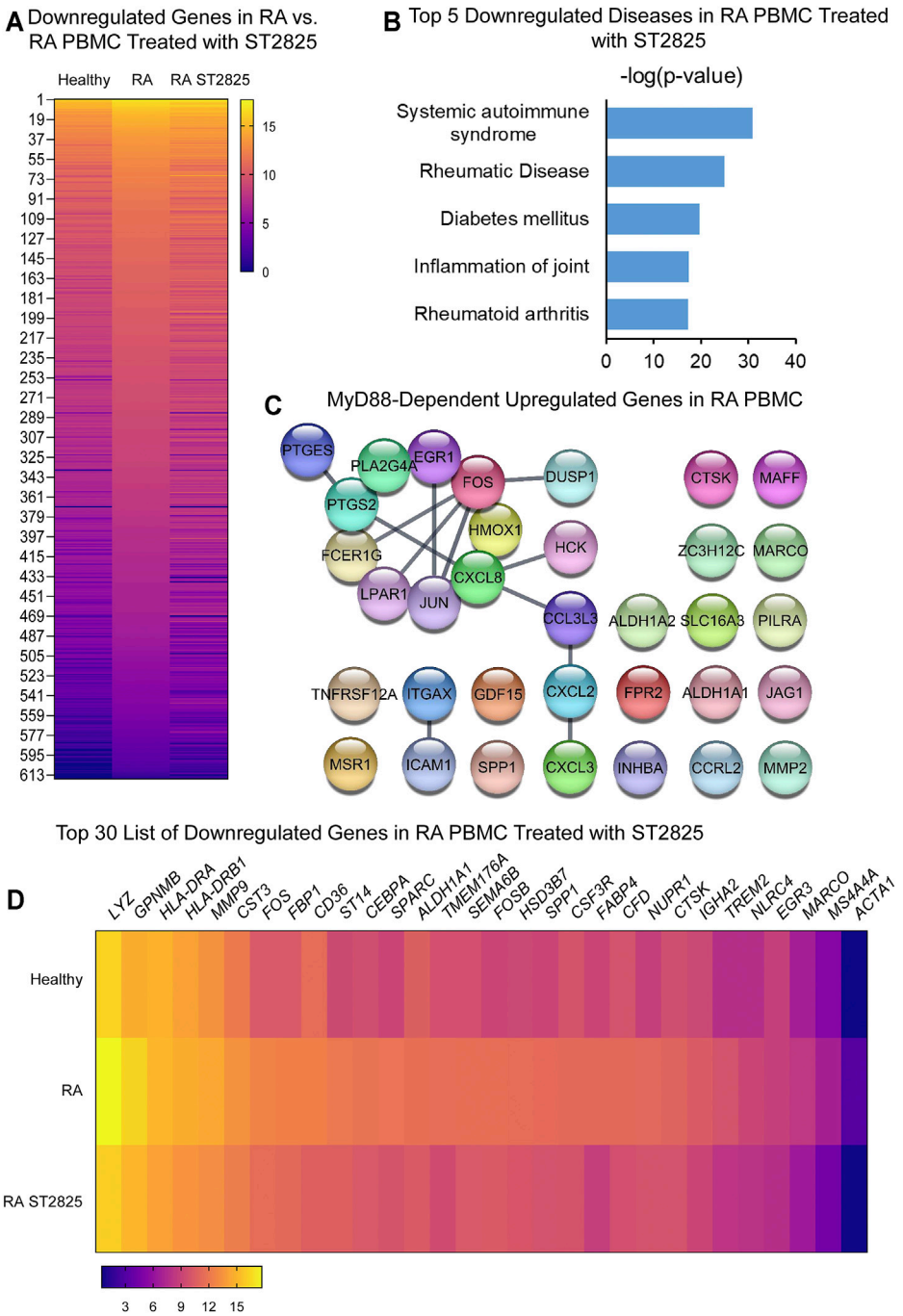

FIGURE 2 | MyD88 inhibition by ST2825 downregulates critical molecules and IPA-predicted disease associations in PBMC from DMARDs-naïve RA patients. **(A)** Transcriptomic signatures from healthy subjects, RA and RA PBMC treated with ST2825 are shown in the heatmap (averaged expression patterns of biological replicates are shown). **(B)** MyD88-predicted target gene network was identified from upregulated genes expressed in RA PBMC vs. healthy subjects. **(C)** Top 5 of IPA-predicted disease associations were determined based on downregulated genes by effect of ST2825. **(D)** Top 30 downregulated genes by effect of ST2825 involved in the inflammatory response are illustrated in the heatmap (averaged expression patterns of biological replicates are shown).

(Cathepsin K), *NLRC4* (NLR family CARD domain-containing protein 4), and *MARCO* (Macrophage Receptor With Collagenous Structure). Downregulated genes by effect of ST2825 are mainly expressed by classical, non-classical and intermediate monocytes, as well as myeloid and plasmacytoid dendritic cells (DCs). In addition, other PBMCs such as natural killer (NK), T and B cells are able to express these genes as well. Principal component analysis (PCA) of the gene expression data from DMARDs-naïve RA patients shows that ST2825 treatment clustered similarly in principal component space. Therefore,

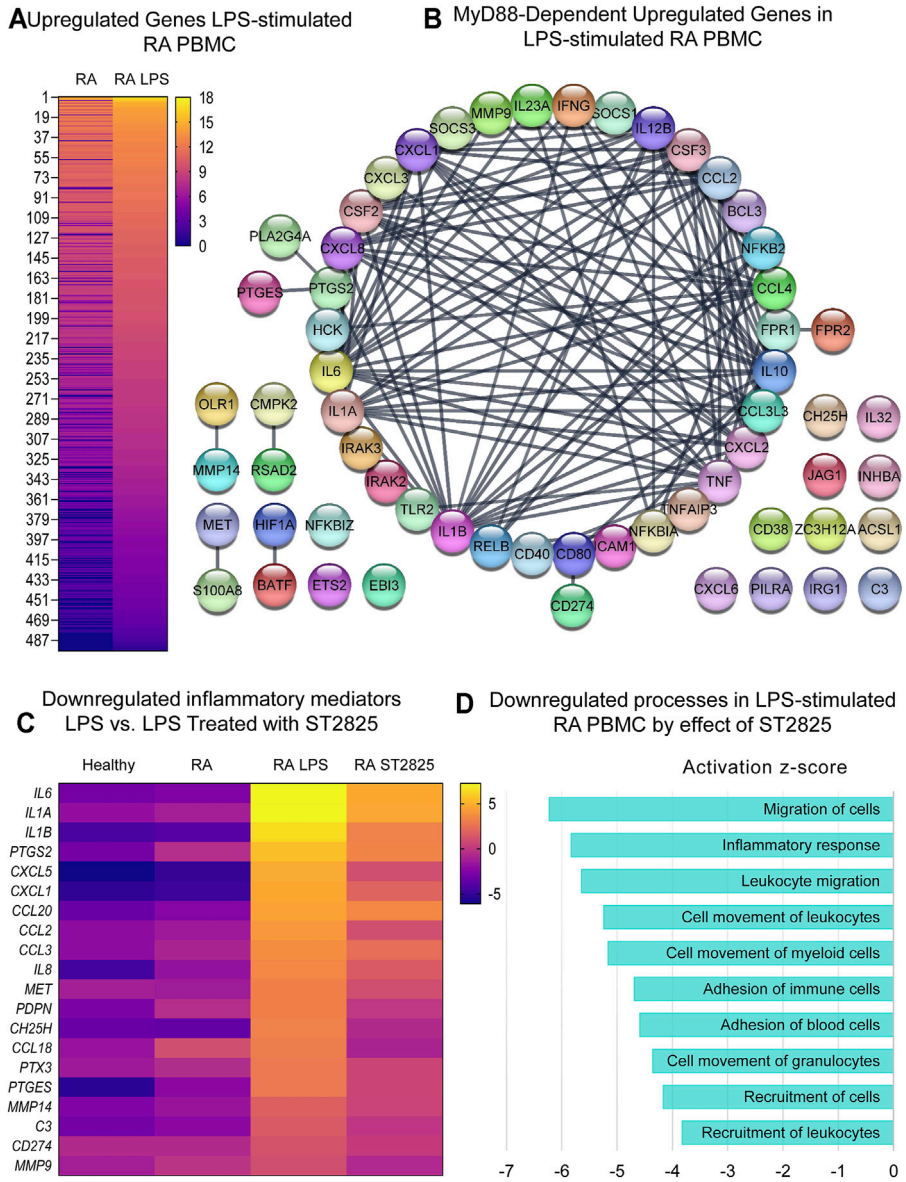

FIGURE 3 | MyD88 inhibition by ST2825 downregulates key inflammatory mediators and pathogenic processes in LPS-stimulated PBMC from DMARDs-naïve RA patients. **(A)** Transcriptomic signatures from RA PBMC and RA LPS-stimulated PBMC are presented in the heatmap (averaged expression patterns of biological replicates are shown). **(B)** MyD88-predicted target gene network was identified from upregulated genes expressed in RA PBMC vs. RA LPS-stimulated PBMC. **(C)** Top 20 downregulated inflammatory mediators by effect of ST2825 are illustrated in the heatmap (averaged expression patterns of biological replicates are shown). **(D)** Top 10 downregulated pathogenic processes were determined based on downregulated genes by effect of ST2825.

these data demonstrate a similar molecular signature of gene expression after MyD88 inhibition (**Supplementary Figure S1A**). Canonical pathway analysis of genes downregulated by ST2825 identified IL-15 signalling, B cell receptor signalling, communication between innate and adaptive immune cells, dendritic cell maturation, and complement system activation as the targets of ST2825 (**Supplementary Figure S1B**). Together, these data show that inhibition of MyD88 has the potential to mitigate and, to some extent, revert multiple critical pathogenic features that drive RA pathogenesis.

Targeting MyD88 Effectively Downregulates Inflammatory Gene Expression Signatures and Pathogenic Processes in LPS-Stimulated PBMC From DMARDs-Naïve RA Patients

Since RA PBMCs are constantly under the influence of proinflammatory mediators, we wanted to determine if MyD88 inhibition has the potential to inhibit the deleterious effects of LPS stimulation. Hierarchical cluster analysis of normalized expression from DMARDs-naïve RA LPS-stimulated PBMC treated with

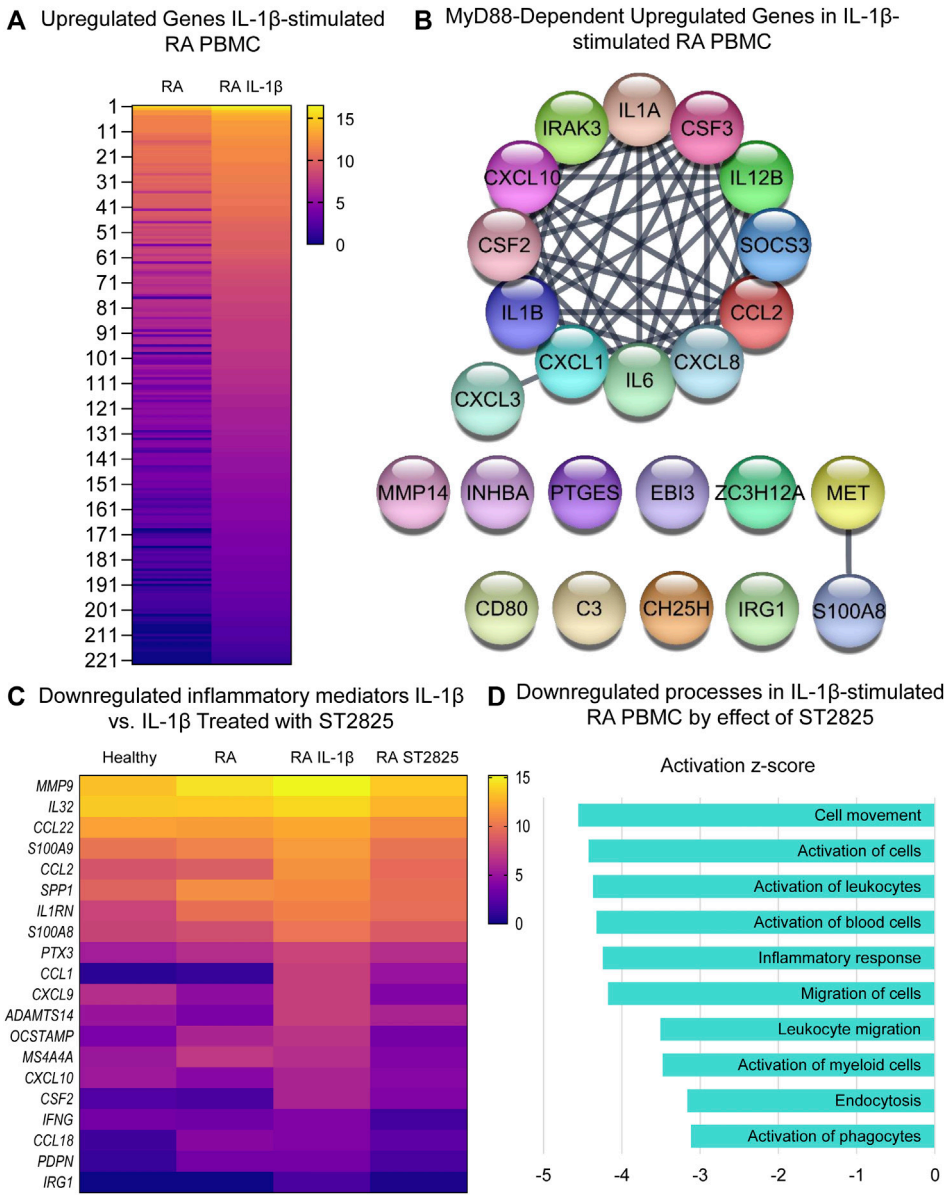

FIGURE 4 | MyD88 inhibition by ST2825 downregulates key inflammatory mediators and pathogenic processes in IL-1β-stimulated PBMC from DMARDs-naïve RA patients. **(A)** Transcriptomic signatures from RA PBMC and RA IL-1β-stimulated PBMC are presented in the heatmap (averaged expression patterns of biological replicates are shown). **(B)** MyD88-predicted target gene network was identified from upregulated genes expressed in RA PBMC vs. RA IL-1β-stimulated PBMC. **(C)** Top 20 downregulated inflammatory mediators by effect of ST2825 are exemplified in the heatmap (averaged expression patterns of biological replicates are shown). **(D)** Top 10 downregulated pathogenic processes were determined based on downregulated genes by effect of ST2825.

ST2825 is shown in **Supplementary Figures S3C,D**. As expected, LPS induced 950 DE genes; 454 downregulated genes and 496 upregulated genes were identified on LPS-stimulated PBMC compared with unstimulated cells from DMARDs-naïve RA patients. Upregulated genes are presented in **Figure 3A**. A subsequent analysis established the top 10 upregulated canonical pathways by the effect of LPS; granulocyte adhesion and diapedesis, IL-17 signalling, TREM1 signalling, and tumor microenvironment were observed in our study (**Supplementary Figure S2A**). Upstream regulatory analysis indeed predicted that 60 of the LPS upregulated genes were downstream targets of MyD88. The protein interaction network predicted for these 60 MyD88-dependent genes is illustrated in **Figure 3B** at an Interaction confidence = 0.900; PPI enrichment p-value < 1.0E-16. We next evaluated the effect of ST2825 on LPS-stimulated PBMC. We identified 471 DE genes between LPS-stimulated RA PBMC and LPS-stimulated RA PBMC treated with ST2825. The analysis also showed 121 up and 350 downregulated genes. The most relevant finding was the downregulation of crucial inflammatory mediators such as proinflammatory cytokines, chemokines, and matrix

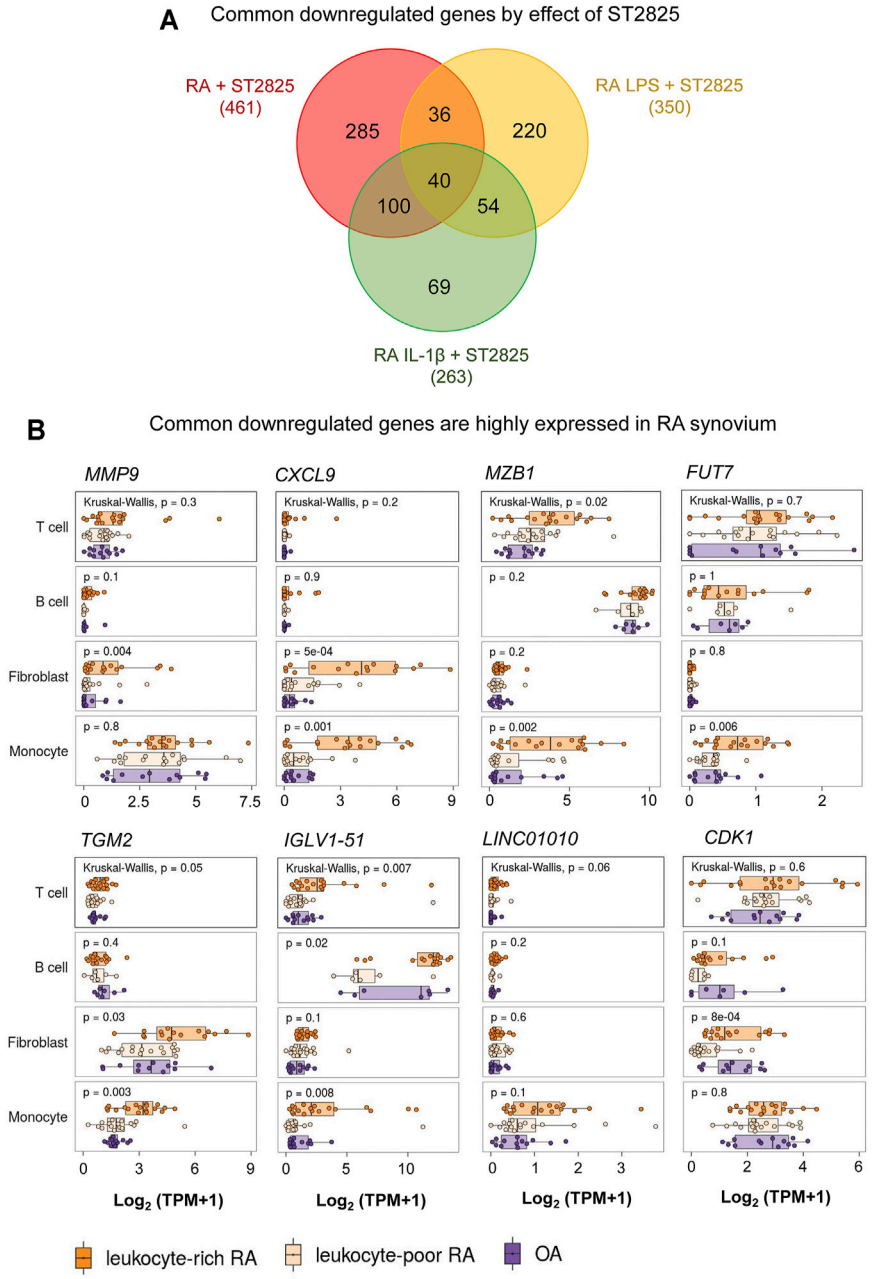

FIGURE 5 | RNA-seq comparison reveals that highly expressed genes in RA synovium could be potentially downregulated by ST2825. **(A)** Venn diagram shows overlap among all sets of downregulated genes from RA PBMC (red), RA LPS-stimulated PBMC (yellow), and RA IL-1β-stimulated PBMC (green) after treatment with ST2825. **(B)** Eight common downregulated genes by effect of ST2825 identified from RA PBMC were highly expressed by different cell types in the synovium of leukocyte-rich RA (orange), leukocyte-poor RA (tan) and OA (purple) patients.

metalloproteinases (MMP) by the effect of ST2825 (**Figure 3C**). Of importance, several MyD88-dependent genes such as the cytokines *IL6*, *IL1A*, *IL1B*, *PTGS2*, chemokines *CXCL1*, *CCL2*, matrix-degrading enzymes *MMP14*, *MMP9*, and complement *C3* were downregulated by ST2825. The significantly downregulated processes (-3 to -6 z-scores) were associated with (**Figure 3D**) migration of cells, inflammatory response, leucocyte migration, adhesion of immune cells, and recruitment of leukocytes. Canonical pathway analysis further supported these findings by revealing that B cell receptor, IL-15 and IL-17 signalling were critically downregulated pathways by the effect of ST2825 (**Supplementary Figure S2B**). Together, these findings suggest that ST2825 effectively downregulates MyD88-dependent gene expression and pathogenic processes orchestrated by the effect of LPS in PBMC from DMARDs-naïve RA patients.

ST2825 Downregulates IL-1β-Dependent Inflammatory Response in PBMC From DMARDs-Naïve RA Patients

Since IL-1β is an important cytokine capable of activating pathogenic mechanisms upstream of MyD88 in RA, we asked whether ST2825 effectively inhibits the pathological gene expression induced by IL-1β on DMARDs-naïve RA PBMC. Hierarchical cluster analysis of normalized expression from DMARDs-naïve RA IL-1β-stimulated PBMC treated with ST2825 is shown in **Supplementary Figures S3E,F**. IL-1β-stimulation resulted in 375 DE genes. Heatmap illustrates gene expression signatures from 222 upregulated genes by the effect of IL-1β **(Figure 4A)**. The main upregulated canonical pathways associated with the upregulated gene signature were granulocyte adhesion and diapedesis, IL-17 signalling in psoriasis and RA, and pattern recognition receptor signalling (**Supplementary Figure S2C**). Besides, analysis of upstream regulators predicted twenty-four IL-1β target genes to be MyD88-dependent (z-score = 4.786, *p*-value = 9.33E-20), and were predicted to form an interactive protein network at a high degree of statistical confidence (**Figure 4B,** confidence = 0.900 and a PPI enrichment *p*-value < 1.0E-16). Similar to the LPS treatment, heatmap analysis revealed that ST2825 was at least partially successful in reverting the IL-1β-induced transcriptomic changes to be comparable to healthy PBMC (**Figure 4C**). The global inhibitory effect of ST2825 was evident from the downregulated processes (**Figure 4D**), which included: cell movement, activation of cells, inflammatory response, leucocyte migration, endocytosis, and activation of phagocytes. In addition, IL-15 signalling, B cell receptor signalling, granulocyte adhesion and diapedesis, and the role of macrophages, fibroblasts and endothelial cells in RA were the main downregulated canonical pathways identified in this study (**Supplementary Figure S2D**). Overall, our observations suggest that dimerization inhibition of MyD88 is an effective target for downregulating the IL-1β-dependent inflammatory response in PBMC from DMARDs-naïve RA patients.

Targeting MyD88 Could Potentially Inhibit Upregulated Genes in the RA Synovium

The *in vivo* inflammatory environment constitutes multiple types of inflammatory mediators that feed forward on to the MyD88 and NF-κB pathways and their targets. We, therefore, hypothesized that the most clinically relevant targets of ST2825 could overlap between the LPS and IL-1β. By overlapping the genes downregulated by ST2825 among different treatment conditions tested in this study we identified 40 common genes (**Figure 5A**, **Supplementary Table S2**). Since, joint degeneration and synovitis are a major part of RA pathology, we asked whether the 40 common ST2825 target genes could also play a role in the RA synovium. Taking advantage of a published RNA-seq data set from synovial tissue cells freshly sorted from RA and OA patients (Zhang et al., 2019), we found that eight of the 40 common ST2825 target genes were highly expressed in the inflammatory leukocyte-rich RA compared to the OA synovium (**Figure 5B**). It is relevant to highlight that some genes such as *MMP9* and *CXCL9* essential for maintaining and promoting inflammatory and pathogenic processes in RA were upregulated in fibroblasts and monocytes from the inflammatory leukocyte-rich RA synovium. We also identified six genes that are highly expressed in the various cell types of the inflamed synovium for which a specific role has not yet been attributed in the context of RA; *MZB1* (Marginal zone B and B1 cell-specific protein), *FUT7* (Fucosyltransferase 7), *TGM2* (Transglutaminase 2), *IGLV1-51* (Immunoglobulin Lambda Variable 1–51), *LINC01010* (Long Intergenic Non-Protein Coding RNA 1010), and *CDK1* (cyclin-dependent kinase 1). Overall, our findings suggest that targeting MyD88 not only effectively downregulates known systemic inflammatory mediators but also could potentially inhibit upregulated genes in the RA synovium, preventing synovitis and joint degeneration.

DISCUSSION

Genome wide studies represent the most powerful and valuable tools to identify global transcriptional changes and dysregulated biological processes in RA. These approaches have allowed molecular stratification of RA patients and resulted in the identification of novel therapeutic targets (Teixeira et al., 2009; Shchetynsky et al., 2017; Lewis et al., 2019; Lee et al., 2020). However, an important limitation of these studies has been the sample variability in terms of differences in the administration of DMARDs. This limitation may have affected the gene expression signatures and interfered with the interpretation of the fundamental role of some genes in RA pathogenesis. Only a few studies have considered the analysis of treatment-naïve RA patients to identify gene expression signatures in response to treatment and to characterize better the RA transcriptional profiles obtaining insightful results (Shchetynsky et al., 2017; Boutet et al., 2021; Wang et al., 2021).

In this study, we performed RNA-seq analysis from DMARDs-naïve RA patients to decipher the effect of MyD88 inhibition independent on the impact of DMARDs. Due to the large number of genes overexpressed in our data set, the presentation of single genes was unsuitable. Instead, to get a functional overview and integration of the complex gene expression changes, we showed a global view of DE gene signatures and focused on pathways associated with those overexpressed genes. Despite the potential differences in the percentages of various cell types between the PBMC, the differentially expressed genes from healthy PBMC, RA PBMC and the PBMC under various treatments clustered together into their respective groups suggesting that our sample sets are representative of their treatment group or condition. As expected, the upregulated IPA-predicted disease associations in our study related to rheumatic disease, systemic autoimmune disorder, invasive tumor, psoriasis, and inflammation of joint were consistent pathogenic hallmarks in RA. Known canonical pathways in RA such as chemoattraction promoted by IL-8/CXCL8 signalling, granulocyte adhesion and diapedesis of immune cells, and high expression of degrading enzymes and

growth factors in the osteoarthritis pathway were observed. We identified the neuroinflammation pathway as a primary mediator of pain in RA (Fuggle et al., 2014; Süß et al., 2020). In addition, the Aryl hydrocarbon receptor, known as Th17 cell differentiation promoter (Nakahama et al., 2011; Talbot et al., 2018), and TREM1 signalling involved in systemic and local inflammatory process activation (Kuai et al., 2009; Peng et al., 2019; Inanc et al., 2021), were also processes identified to be associated with the DMARDs-naïve RA PBMC. Based on our previous findings of the role of ST2825 in downregulating the release of proinflammatory cytokines in PBMC from healthy subjects (Ramírez-Pérez et al., 2020); we tested whether this chemical compound could modulate gene expression signatures and canonical pathways on PBMC from RA patients. Our findings indicate that ST2825 downregulates an enormous number of genes that are increased in RA patients compared with healthy subjects. Indeed, the genes downregulated by MyD88 inhibition were consistent with the IPA-predicted disease associations directly related to RA, such as systemic autoimmune syndrome, rheumatic disease, inflammation of joint, and rheumatoid arthritis. Both innate and adaptive immune responses were inhibited by ST2585.

The vital role of IL-17 in maintaining and promoting destructive processes in RA has been widely described (Tang et al., 2020; Miossec, 2021); however, only a few studies have explored the central role of MyD88 signalling in IL-17-driven inflammatory arthritis. In this regard, Abdollahi-Roodsaz et al. reported that IL-17 production and pathogenic changes such as joint swelling, inflammation and cartilage degeneration were significantly reduced in a MyD88 knockout mice model of inflammatory arthritis (Abdollahi-Roodsaz et al., 2012). Furthermore, MyD88 knockout also resulted in the downregulation of B cell signalling pathways and decreased production of autoantibodies. Other studies reported that the inhibition of MyD88 dimerization by ST2825 blocked the induction of plasma cell differentiation and antibody production from the PBMC of systemic lupus erythematosus (SLE) patients (Capolunghi et al., 2010). In corroboration with previous reports, we here showed that ST2825-mediated inhibition of MyD88 in PBMC also resulted in the downregulation of IL-17 signalling, antibody production, plasma cell activation and Th17 cell differentiation pathways. Indeed, our previous report suggested that ST2825 can decrease the secretion of IL-17A in PBMC from healthy donors; however, the results were not statistically significant (Ramírez-Pérez et al., 2020). Thus, we speculate that ST2825-mediated MyD88 inhibition could prevent the adverse effects of IL-17 signalling on RA PBMC; in parallel, we propose that future studies should be focused on identifying ST2825-mediated effects on Th17 cells from RA patients.

Critical canonical pathways typical for granulocytes, fibroblasts and endothelial cells in RA were downregulated on RA PBMC treated with ST2825. In support of this observation, a recent study identified a specific set of genes in blood samples from RA patients related to cartilage morphogenesis, endochondral bone growth and extracellular matrix organization. The authors concluded that those processes were observed due to the presence the presence of circulating preinflammatory mesenchymal (PRIME) cells in blood samples predicting flares in RA patients (Orange et al., 2020). It is also worth noting that PBMC are obtained by density centrifugation. On this matter, neutrophils are usually localized on the top of the erythrocyte pellet; however, in autoimmune diseases, a particular neutrophil population known as low-density granulocyte has been described (Carmona-Rivera and Kaplan, 2013; Wright et al., 2017; Ostendorf et al., 2019). This portion of low-density granulocyte is generally co-purified with the PBMC. We are not able to corroborate that those populations are present in our samples since we did not perform immune phenotyping; nevertheless, those previously reported findings may explain the identification of typical pathways for granulocyte adhesion and diapedesis, fibroblasts, or endothelial cells in PBMC samples.

MyD88 has also shown promising results by downregulating cytokines and chemokines and modulating LPS-induced mechanical hyperalgesia in the joint (Guerrero et al., 2016). Several large-scale transcriptomic changes have been identified in different joint-resident cell types under IL-1β stimulation (Gao et al., 2021; Haque et al., 2021). For this reason, inhibition of IL-1β and LPS signalling pathways is imperative. Our study identified overlapping of downregulated genes by the effect of ST2825 under distinct inflammatory conditions: 1) RA PBMC, LPS-stimulated RA PBMC, and 3) IL-1β-stimulated RA PBMC, where 461, 350 and 263 genes were significantly downregulated, respectively.

Our analysis revealed 40 commonly downregulated genes among conditions. We took advantage of an RNA-seq published data set from the Accelerating Medicines Partnership Rheumatoid Arthritis (RA) Phase I project (Zhang et al., 2019) to identify whether these genes may play a role in T and B cells, monocytes, and fibroblasts from RA synovium and shot listed 8 MyD88 target genes with potential roles in RA synovium. One of the shot listed genes *MMP9*, is known to be highly expressed in synovial fibroblasts in RA with therapeutic potential (Gossage et al., 2018; Shatunova et al., 2020). *CXCL9* was significantly overexpressed in fibroblasts and monocytes from the RA synovium and according to previous reports, its knockdown by exosomes containing miR-320a suppressed the activation, migration, and invasion of RA-FLS and decreased the arthritis index and inflammatory score in the CIA model (Meng and Qiu, 2020). We found that *MZB1* was highly upregulated in T cells and monocytes from leukocyte-rich RA synovium compared with OA. Although the role of *MZB1* in RA is yet to be clarified; its previously described role in SLE during the maintenance of splenic marginal zone B cells, plasma cells and autoantibody production (Miyagawa-Hayashino et al., 2018), suggest this molecule could play a central role in maintaining ectopic lymphoid structures, in the RA synovium. Fucosyltransferase 7 is (*FUT7*) is yet another MyD88 common target that was significantly increased in monocytes from RA synovial tissue. Zhang *et al.* showed that *FUT7* might play a role in inducing monocyte-endothelial adhesion, promoting atherosclerosis progression (Zhang et al., 2018), and FUT7 knockdown inhibited cell proliferation, migration, and invasion in metastatic follicular thyroid carcinoma cell lines (Qin et al., 2020). We, therefore, predict that *FUT7* may play a role in the proliferation, migration, and invasion of synovial fibroblasts and monocyte infiltration.

The other MyD88 target genes that were upregulated in RA synovium were *TGM2* (Transglutaminase 2), *CDK1* (Cyclin-dependent kinase 1), *IGLV1-51* (Immunoglobulin lambda

variable 1–51) and *LINC01010* (long-non coding RNA *LINC01010*). In support of a role for *TGM2* in RA, its knockdown resulted in a reduction of cartilage degradation and invadopodia formation in CIA model (Lauzier et al., 2012). Interestingly, high expression of *CDK1* positively correlated with interferon type 1 (IFN-1) serum levels and presence of anti-citrullinated protein antibodies (ACPA), which suggests a possible pathogenic role for *CDK1* in RA (Fattah et al., 2020). Finally, the roles of *IGLV1-51* and *LINC01010* in RA are yet to be defined.

Some limitations in our study were sample size sequencing; future studies must consider evaluation of a greater number of DMARDs-naïve RA patients in order to obtain a more robust estimation of ST2825 effects. The treatment of the patients in our data set with other non-DMARDs drugs could be an important variable as well. Our study did not take into consideration the disease stage or disease activity, which are relevant clinical variables in RA. Another limitation of the study is that the bulk RNA-sequencing of the unsorted PBMC population does not reveal the identity of the cell type that is most responsive to ST2825 treatment since immune phenotyping was not performed. The differential percentages of $CD4^+$ T cells, $CD8^+$ T cells, B cells, classical, intermediate, and non-classical monocytes, DCs, NK cells could potentially dictate the response to ST2825 in each individual patient. Therefore, future studies must consider the analysis of single-cell RNA sequencing to decipher whether specific immune cell populations contribute to the downregulation of inflammatory mediators and pathogenic processes observed in this study. Finally, although our analysis *in silico* revealed distinct genes that might be downregulated by ST2825 in the inflamed synovium of RA patients, this analysis might not represent the biological response of stromal and immune cells within the joint and further analysis should be carried out to corroborate these findings.

In summary, our study provides comprehensive evidence supporting the potential application of the MyD88 inhibitor, ST2825, as a modulator of systemic inflammatory processes in PBMC from DMARDs-naïve RA patients. Our indepth analysis of RNA-seq data will serve as a valuable resource containing the inflammatory gene expression signatures and pathogenic processes regulated by MyD88. Our findings also suggest that ST2825 might potentially downregulate crucial genes overexpressed in the RA synovium and function as an emerging therapeutic strategy for RA patients.

DATA AVAILABILITY STATEMENT

The datasets presented in this study can be found in online repositories. The names of the repository/repositories and accession number(s) can be found below: Gene Expression Omnibus (GEO/NCBI); GSE189136.

ETHICS STATEMENT

Ethical review and approval was not required for the study on human participants in accordance with the local legislation and institutional requirements. Written informed consent was not provided because PBMC samples from patients and healthy subjects were purchased from STEMCELL Technologies Inc. and Precision For Medicine Inc..

AUTHOR CONTRIBUTIONS

SR-P and PB contributed to the study conception and design. SR-P and PB performed material preparation, data collection and analysis. SR-P and PB drafted the article. EO-R and IR-P performed critical revision of the manuscript. All authors contributed to the article and approved the submitted version.

ACKNOWLEDGMENTS

We thank the support from the National Institutes of Health/ National Institute of Arthritis, Musculoskeletal and Skin Disease grant (R01 AR070736) and Startup funds from the Department of Orthopaedics, Emory University School of Medicine assigned to PB. We also thank the support from the National Council of Science and Technology (CONACYT-Mexico) grant (770696) assigned to SR-P (CVU: 660472).

SUPPLEMENTARY MATERIAL

The Supplementary Material for this article can be found online at: https://www.frontiersin.org/articles/10.3389/fphar.2021.800220/full#supplementary-material

REFERENCES

Abdollahi-Roodsaz, S., van de Loo, F. A., Koenders, M. I., Helsen, M. M., Walgreen, B., van den Bersselaar, L. A., et al. (2012). Destructive Role of Myeloid Differentiation Factor 88 and Protective Role of TRIF in Interleukin-17-dependent Arthritis in Mice. *Arthritis Rheum.* 64, 1838–1847. doi:10.1002/art.34328

Aletaha, D. (2020). Precision Medicine and Management of Rheumatoid Arthritis. *J. Autoimmun.* 110, 102405. doi:10.1016/j.jaut.2020.102405

Aletaha, D., and Smolen, J. S. (2018). Diagnosis and Management of Rheumatoid Arthritis: A Review. *Jama* 320, 1360–1372. doi:10.1001/jama.2018.13103

Avbelj, M., Horvat, S., and Jerala, R. (2011). The Role of Intermediary Domain of MyD88 in Cell Activation and Therapeutic Inhibition of TLRs. *J. Immunol.* 187, 2394–2404. doi:10.4049/jimmunol.1100515

Balka, K. R., and De Nardo, D. (2019). Understanding Early TLR Signaling through the Myddosome. *J. Leukoc. Biol.* 105, 339–351. doi:10.1002/JLB.MR0318-096R

Boutet, M. A., Nerviani, A., Lliso-Ribera, G., Leone, R., Sironi, M., Hands, R., et al. (2021). Circulating and Synovial Pentraxin-3 (PTX3) Expression Levels Correlate with Rheumatoid Arthritis Severity and Tissue Infiltration Independently of Conventional Treatments Response. *Front. Immunol.* 12, 686795. doi:10.3389/fimmu.2021.686795

Brzustewicz, E., and Bryl, E. (2015). The Role of Cytokines in the Pathogenesis of Rheumatoid Arthritis--Practical and Potential Application of Cytokines as Biomarkers and Targets of Personalized Therapy. *Cytokine* 76, 527–536. doi:10.1016/j.cyto.2015.08.260

Capolunghi, F., Rosado, M. M., Cascioli, S., Girolami, E., Bordasco, S., Vivarelli, M., et al. (2010). Pharmacological Inhibition of TLR9 Activation Blocks

Autoantibody Production in Human B Cells from SLE Patients. *Rheumatology (Oxford)* 49, 2281–2289. doi:10.1093/rheumatology/keq226

Carmona-Rivera, C., and Kaplan, M. J. (2013). Low-density Granulocytes: a Distinct Class of Neutrophils in Systemic Autoimmunity. *Semin. Immunopathol* 35, 455–463. doi:10.1007/s00281-013-0375-7

Chen, L., Zheng, L., Chen, P., and Liang, G. (2020). Myeloid Differentiation Primary Response Protein 88 (MyD88): The Central Hub of TLR/IL-1R Signaling. *J. Med. Chem.* 63, 13316–13329. doi:10.1021/acs.jmedchem.0c00884

Fattah, S. A., Abdel Fattah, M. A., Mesbah, N. M., Saleh, S. M., Abo-Elmatty, D. M., and Mehanna, E. T. (2020). The Expression of Zinc finger 804a (ZNF804a) and Cyclin-dependent Kinase 1 (CDK1) Genes Is Related to the Pathogenesis of Rheumatoid Arthritis. *Arch. Physiol. Biochem.* 1, 6.

Fuggle, N. R., Howe, F. A., Allen, R. L., and Sofat, N. (2014). New Insights into the Impact of Neuro-Inflammation in Rheumatoid Arthritis. *Front. Neurosci.* 8, 357. doi:10.3389/fnins.2014.00357

Gao, C., Pu, H., Zhou, Q., Tao, T., Liu, H., Sun, X., et al. (2021). Two Reactive Behaviors of Chondrocytes in an IL-1β-induced Inflammatory Environment Revealed by the Single-Cell RNA Sequencing. *Aging (Albany NY)* 13, 11646–11664. doi:10.18632/aging.202857

Gossage, D. L., Cieslarová, B., Ap, S., Zheng, H., Xin, Y., Lal, P., et al. (2018). Phase 1b Study of the Safety, Pharmacokinetics, and Disease-Related Outcomes of the Matrix Metalloproteinase-9 Inhibitor Andecaliximab in Patients with Rheumatoid Arthritis. *Clin. Ther.* 40, 156–e5. doi:10.1016/j.clinthera.2017.11.011

Guerrero, A. T., Pinto, L. G., Cunha, F. Q., Ferreira, S. H., Alves-Filho, J. C., Verri, W. A., Jr., et al. (2016). Mechanisms Underlying the Hyperalgesic Responses Triggered by Joint Activation of TLR4. *Pharmacol. Rep.* 68, 1293–1300. doi:10.1016/j.pharep.2016.08.006

Haque, M., Singh, A. K., Ouseph, M. M., and Ahmed, S. (2021). Regulation of Synovial Inflammation and Tissue Destruction by Guanylate Binding Protein 5 in Synovial Fibroblasts from Patients with Rheumatoid Arthritis and Rats with Adjuvant-Induced Arthritis. *Arthritis Rheumatol.* 73, 943–954. doi:10.1002/art.41611

Inanc, N., Mumcu, G., Can, M., Yay, M., Silbereisen, A., Manoil, D., et al. (2021). Elevated Serum TREM-1 Is Associated with Periodontitis and Disease Activity in Rheumatoid Arthritis. *Sci. Rep.* 11, 2888. doi:10.1038/s41598-021-82335-9

Kuai, J., Gregory, B., Hill, A., Pittman, D. D., Feldman, J. L., Brown, T., et al. (2009). TREM-1 Expression Is Increased in the Synovium of Rheumatoid Arthritis Patients and Induces the Expression of Pro-inflammatory Cytokines. *Rheumatology (Oxford)* 48, 1352–1358. doi:10.1093/rheumatology/kep235

Lauzier, A., Charbonneau, M., Paquette, M., Harper, K., and Dubois, C. M. (2012). Transglutaminase 2 Cross-Linking Activity Is Linked to Invadopodia Formation and Cartilage Breakdown in Arthritis. *Arthritis Res. Ther.* 14, R159. doi:10.1186/ar3899

Lee, E. J., Lilja, S., Li, X., Schäfer, S., Zhang, H., and Benson, M. (2020). Bulk and Single Cell Transcriptomic Data Indicate that a Dichotomy between Inflammatory Pathways in Peripheral Blood and Arthritic Joints Complicates Biomarker Discovery. *Cytokine* 127, 154960. doi:10.1016/j.cyto.2019.154960

Lewis, M. J., Barnes, M. R., Blighe, K., Goldmann, K., Rana, S., Hackney, J. A., et al. (2019). Molecular Portraits of Early Rheumatoid Arthritis Identify Clinical and Treatment Response Phenotypes. *Cell Rep* 28, 2455–e5. doi:10.1016/j.celrep.2019.07.091

Loiarro, M., Capolunghi, F., Fantò, N., Gallo, G., Campo, S., Arseni, B., et al. (2007). Pivotal Advance: Inhibition of MyD88 Dimerization and Recruitment of IRAK1 and IRAK4 by a Novel Peptidomimetic Compound. *J. Leukoc. Biol.* 82, 801–810. doi:10.1189/jlb.1206746

Loiarro, M., Ruggiero, V., and Sette, C. (2013). Targeting the Toll-like Receptor/interleukin 1 Receptor Pathway in Human Diseases: Rational Design of MyD88 Inhibitors. *Clin. Lymphoma Myeloma Leuk.* 13, 222–226. doi:10.1016/j.clml.2013.02.003

Long, T., Liu, Z., Shang, J., Zhou, X., Yu, S., Tian, H., et al. (2018). Polygonatum Sibiricum Polysaccharides Play Anti-cancer Effect through TLR4-Mapk/nf-Kb Signaling Pathways. *Int. J. Biol. Macromolecules* 111, 813–821. doi:10.1016/j.ijbiomac.2018.01.070

Meng, Q., and Qiu, B. (2020). Exosomal MicroRNA-320a Derived from Mesenchymal Stem Cells Regulates Rheumatoid Arthritis Fibroblast-like Synoviocyte Activation by Suppressing CXCL9 Expression. *Front. Physiol.* 11, 441. doi:10.3389/fphys.2020.00441

Migliorini, P., Italiani, P., Pratesi, F., Puxeddu, I., and Boraschi, D. (2020). The IL-1 Family Cytokines and Receptors in Autoimmune Diseases. *Autoimmun. Rev.* 19, 102617. doi:10.1016/j.autrev.2020.102617

Miossec, P. (2021). Local and Systemic Effects of IL-17 in Joint Inflammation: a Historical Perspective from Discovery to Targeting. *Cell Mol Immunol* 18, 860–865. doi:10.1038/s41423-021-00644-5

Miyagawa-Hayashino, A., Yoshifuji, H., Kitagori, K., Ito, S., Oku, T., Hirayama, Y., et al. (2018). Increase of MZB1 in B Cells in Systemic Lupus Erythematosus: Proteomic Analysis of Biopsied Lymph Nodes. *Arthritis Res. Ther.* 20, 13. doi:10.1186/s13075-018-1511-5

Nakahama, T., Kimura, A., Nguyen, N. T., Chinen, I., Hanieh, H., Nohara, K., et al. (2011). Aryl Hydrocarbon Receptor Deficiency in T Cells Suppresses the Development of Collagen-Induced Arthritis. *Proc. Natl. Acad. Sci. U S A.* 108, 14222–14227. doi:10.1073/pnas.1111786108

Orange, D. E., Yao, V., Sawicka, K., Fak, J., Frank, M. O., Parveen, S., et al. (2020). RNA Identification of PRIME Cells Predicting Rheumatoid Arthritis Flares. *N. Engl. J. Med.* 383, 218–228. doi:10.1056/NEJMoa2004114

Ostendorf, L., Mothes, R., van Koppen, S., Lindquist, R. L., Bellmann-Strobl, J., Asseyer, S., et al. (2019). Low-Density Granulocytes Are a Novel Immunopathological Feature in Both Multiple Sclerosis and Neuromyelitis Optica Spectrum Disorder. *Front. Immunol.* 10, 2725. doi:10.3389/fimmu.2019.02725

Peng, A., Lu, X., Huang, J., He, M., Xu, J., Huang, H., et al. (2019). Rheumatoid Arthritis Synovial Fibroblasts Promote TREM-1 Expression in Monocytes via COX-2/PGE2 Pathway. *Arthritis Res. Ther.* 21, 169. doi:10.1186/s13075-019-1954-3

Qi, M., Yin, L., Xu, L., Tao, X., Qi, Y., Han, X., et al. (2016). Dioscin Alleviates Lipopolysaccharide-Induced Inflammatory Kidney Injury via the microRNA let-7i/TLR4/MyD88 Signaling Pathway. *Pharmacol. Res.* 111, 509–522. doi:10.1016/j.phrs.2016.07.016

Qin, H., Liu, J., Yu, M., Wang, H., Thomas, A. M., Li, S., et al. (2020). FUT7 Promotes the Malignant Transformation of Follicular Thyroid Carcinoma through α1,3-fucosylation of EGF Receptor. *Exp. Cel Res* 393, 112095. doi:10.1016/j.yexcr.2020.112095

Ramírez-Pérez, S., Hernández-Palma, L. A., Oregon-Romero, E., Anaya-Macías, B. U., García-Arellano, S., González-Estevez, G., et al. (2020). Downregulation of Inflammatory Cytokine Release from IL-1β and LPS-Stimulated PBMC Orchestrated by ST2825, a MyD88 Dimerisation Inhibitor. *Molecules* 25.

Shatunova, E. A., Korolev, M. A., Omelchenko, V. O., Kurochkina, Y. D., Davydova, A. S., Venyaminova, A. G., et al. (2020). Aptamers for Proteins Associated with Rheumatic Diseases: Progress, Challenges, and Prospects of Diagnostic and Therapeutic Applications. *Biomedicines* 8. doi:10.3390/biomedicines8110527

Shchetynsky, K., Diaz-Gallo, L. M., Folkersen, L., Hensvold, A. H., Catrina, A. I., Berg, L., et al. (2017). Discovery of New Candidate Genes for Rheumatoid Arthritis through Integration of Genetic Association Data with Expression Pathway Analysis. *Arthritis Res. Ther.* 19, 19. doi:10.1186/s13075-017-1220-5

Smolen, J. S., Aletaha, D., Barton, A., Burmester, G. R., Emery, P., Firestein, G. S., et al. (2018). Rheumatoid Arthritis. *Nat. Rev. Dis. Primers* 4, 18001. doi:10.1038/nrdp.2018.1

Süß, P., Rothe, T., Hoffmann, A., Schlachetzki, J. C. M., and Winkler, J. (2020). The Joint-Brain Axis: Insights from Rheumatoid Arthritis on the Crosstalk between Chronic Peripheral Inflammation and the Brain. *Front. Immunol.* 11, 612104.

Talbot, J., Peres, R. S., Pinto, L. G., Oliveira, R. D. R., Lima, K. A., Donate, P. B., et al. (2018). Smoking-induced Aggravation of Experimental Arthritis Is Dependent of Aryl Hydrocarbon Receptor Activation in Th17 Cells. *Arthritis Res. Ther.* 20, 119. doi:10.1186/s13075-018-1609-9

Tang, M., Lu, L., and Yu, X. (2020). Interleukin-17A Interweaves the Skeletal and Immune Systems. *Front. Immunol.* 11, 625034. doi:10.3389/fimmu.2020.625034

Teixeira, V. H., Olaso, R., Martin-Magniette, M. L., Lasbleiz, S., Jacq, L., Oliveira, C. R., et al. (2009). Transcriptome Analysis Describing New Immunity and Defense Genes in Peripheral Blood Mononuclear Cells of Rheumatoid Arthritis Patients. *PLoS One* 4, e6803. doi:10.1371/journal.pone.0006803

Wang, X., Tan, Y., Huang, Z., Huang, N., Gao, M., Zhou, F., et al. (2019). Disrupting Myddosome Assembly in Diffuse Large B-cell L-ymphoma C-ells

U-sing the MYD88 D-imerization I-nhibitor ST2825. *Oncol. Rep.* 42, 1755–1766. doi:10.3892/or.2019.7282

Wang, Y., Xie, X., Zhang, C., Su, M., Gao, S., Wang, J., et al. (2021). Rheumatoid Arthritis, Systemic Lupus Erythematosus and Primary Sjögren's Syndrome Shared Megakaryocyte Expansion in Peripheral Blood. *Ann. Rheum. Dis.*.

Wright, H. L., Makki, F. A., Moots, R. J., and Edwards, S. W. (2017). Low-density Granulocytes: Functionally Distinct, Immature Neutrophils in Rheumatoid Arthritis with Altered Properties and Defective TNF Signalling. *J. Leukoc. Biol.* 101, 599–611. doi:10.1189/jlb.5A0116-022R

Yang, X., Chen, G. T., Wang, Y. Q., Xian, S., Zhang, L., Zhu, S. M., et al. (2018). TLR4 Promotes the Expression of HIF-1α by Triggering Reactive Oxygen Species in Cervical Cancer Cells In vitro-Implications for Therapeutic Intervention. *Mol. Med. Rep.* 17, 2229–2238. doi:10.3892/mmr.2017.8108

Yao, H., Hu, C., Yin, L., Tao, X., Xu, L., Qi, Y., et al. (2016). Dioscin Reduces Lipopolysaccharide-Induced Inflammatory Liver Injury via Regulating TLR4/MyD88 Signal Pathway. *Int. Immunopharmacol* 36, 132–141. doi:10.1016/j.intimp.2016.04.023

Zhang, F., Wei, K., Slowikowski, K., Fonseka, C. Y., Rao, D. A., Kelly, S., et al. (2019). Defining Inflammatory Cell States in Rheumatoid Arthritis Joint Synovial Tissues by Integrating Single-Cell Transcriptomics and Mass Cytometry. *Nat. Immunol.* 20, 928–942. doi:10.1038/s41590-019-0378-1

Zhang, J., Ju, N., Yang, X., Chen, L., and Yu, C. (2018). The α1,3-fucosyltransferase FUT7 Regulates IL-1β-induced Monocyte-Endothelial Adhesion via Fucosylation of Endomucin. *Life Sci.* 192, 231–237. doi:10.1016/j.lfs.2017.11.017

Conflict of Interest: The authors declare that the research was conducted in the absence of any commercial or financial relationships that could be construed as a potential conflict of interest.

Publisher's Note: All claims expressed in this article are solely those of the authors and do not necessarily represent those of their affiliated organizations, or those of the publisher, the editors, and the reviewers. Any product that may be evaluated in this article, or claim that may be made by its manufacturer, is not guaranteed or endorsed by the publisher.

Copyright © 2021 Ramirez-Perez, Oregon-Romero, Reyes-Perez and Bhattaram. This is an open-access article distributed under the terms of the Creative Commons Attribution License (CC BY). The use, distribution or reproduction in other forums is permitted, provided the original author(s) and the copyright owner(s) are credited and that the original publication in this journal is cited, in accordance with accepted academic practice. No use, distribution or reproduction is permitted which does not comply with these terms.

frontiers in Pharmacology

ORIGINAL RESEARCH
published: 17 January 2022
doi: 10.3389/fphar.2021.782095

Laser Photobiomodulation 808 nm: Effects on Gene Expression in Inflammatory and Osteogenic Biomarkers in Human Dental Pulp Stem Cells

Elaine A. da Rocha[1], *Marcela M. P. Alvarez*[2], *Agatha M. Pelosine*[3], *Marcela Rocha O. Carrilho*[4], *Ivarne L. S. Tersariol*[2] *and Fábio D. Nascimento*[1,2,3]*

[1]Technology Research Center, Mogi das Cruzes University, Mogi das Cruzes, Brazil, [2]Department of Biochemistry, Federal University of São Paulo, São Paulo, Brazil, [3]Interdisciplinary Center of Biochemical Investigation, University of Mogi das Cruzes, Mogi das Cruzes, Brazil, [4]College of Dental Medicine-Illinois, Midwestern University, Downers Grove, IL, United States

OPEN ACCESS

Edited by:
Emer S. Ferro, University of São Paulo, Brazil

Reviewed by:
Paulo Jorge Palma, University of Coimbra, Portugal
Camila Squarzoni Dale, University of São Paulo, Brazil

***Correspondence:**
Fábio D. Nascimento
fdnascimento@gmail.com

Specialty section:
This article was submitted to Inflammation Pharmacology, a section of the journal Frontiers in Pharmacology

Received: *23 September 2021*
Accepted: *19 October 2021*
Published: *17 January 2022*

Citation:
Rocha EA, Alvarez MMP, Pelosine AM, Carrilho MRO, Tersariol ILS and Nascimento FD (2022) Laser Photobiomodulation 808 nm: Effects on Gene Expression in Inflammatory and Osteogenic Biomarkers in Human Dental Pulp Stem Cells. Front. Pharmacol. 12:782095. doi: 10.3389/fphar.2021.782095

The tissue engineering of dental oral tissue is tackling significant advances and the use of stem cells promises to boost the therapeutical approaches of regenerative dentistry. Despite advances in this field, the literature is still scarce regarding the modulatory effect of laser photobiomodulation (PBM) on genes related to inflammation and osteogenesis in Postnatal Human Dental Pulp Stem cells (DPSCs). This study pointedly investigated the effect of PBM treatment in proliferation, growth and differentiation factors, mineralization, and extracellular matrix remodeling genes in DPSCs. Freshly extracted human third molars were used as a source for DPSCs isolation. The isolated DPSCs were stimulated to an inflammatory state, using a lipopolysaccharide (LPS) model, and then subjected or not to laser PBM. Each experiment was statistically evaluated according to the sample distribution. A total of 85 genes related to inflammation and osteogenesis were evaluated regarding their expression by RT-PCR. Laser PBM therapy has shown to modulate several genes expression in DPSCs. PBM suppressed the expression of inflammatory gene TNF and RANKL and downregulated the gene expression for VDR and proteolytic enzymes cathepsin K, MMP-8 and MMP-9. Modulation of gene expression for proteinase-activated receptors (PARs) following PBM varied among different PARs. As expected, PBM blocked the odontoblastic differentiation of DPSCs when subjected to LPS model. Conversely, PBM has preserved the odontogenic potential of DPSCs by increasing the expression of TWIST-1/RUNEX-2/ALP signaling axis. PBM therapy notably played a role in the DPSCs genes expression that mediate inflammation process and tissue mineralization. The present data opens a new perspective for PBM therapy in mineralized dental tissue physiology.

Keywords: human dental pulp stem cells, photobiomodualtion therapy, gene expreesion, dental pulp stem cells, inflammation, bone osteogenesis

INTRODUCTION

A primary objective of regenerative medicine and tissue engineering is to support the reinstatement of tissues and/or organ's functions by means an *in situ* substitution/repair of their injured structures. However, intrinsic morphological complexities such as those found, for instance, in dental pulp can substantially compromise this tissue successful remodeling and repair. Dental pulp is a unique and specialized mesenchymal tissue that, by being confined inside a mineralized rigid chamber in the core of teeth, has limited or virtually no chance to expand as part of the inflammatory response to accommodate an uneventful tissue turnover. Stromal fibroblasts and odontoblasts are the main regenerative/formative cells in dental pulp tissue (Nor, 2006). Interestingly, the pulp tissue also harbors mesenchymal stem cells with self-renewal capacity and multidifferentiation potential (Botelho et al., 2017).

Postnatal stem cells have proven to be an excellent resource in regenerative medicine. Among mesenchymal postnatal cells found in dental pulp, the Dental pulp stem cells (DPSCs) (Kerkis et al., 2006) have shown to exhibit promising tissue regenerative cues, such as a more mature phenotype in comparison to stem cells derived from exfoliated deciduous teeth (SHEDs) (Goldberg and Smith, 2004), and higher plasticity (i.e. proliferative and differentiation capacity to turn into various cells) than Bone marrow stem cells (BMSCs) (Miura et al., 2003).

Overall, the inflammatory process is generally accompanied by imbalance in gene expression and signaling, as well as by the release of proinflammatory cytokines, such as tumor necrosis factor-alpha (TNF-α), reactive oxygen, nitrogen species and, interleukin-1β (IL-1β) and IL-6 (Hanisch, 2002). LPS can activate the NF-κB signalling pathway in DPSCs. NF-κB is a transcription factor that regulates a large variety of inflammatory cytokines, including TNF-α, IL-1, IL-6, and IL-8 (Baldwin, 2001). The LPS induces the production of pro-inflammatory cytokines in dental pulp fibroblasts (Nakane et al., 1995). Also, it has been shown that LPS can promote odontoblastic differentiation of human DPSCs via TLR-4, ERK, and P38 MAPK signalling pathways (He et al., 2015). The inflammatory interleukin(s)-1. -6. -11 (IL-1. IL-6. IL-11), and TNF-α can stimulate osteoclast development and thereby the process of bone resorption (Manolagas, 1995).

In addition to these canonical inflammatory pathways, cell signaling *via* Proteinase-activated receptors (PARs) are emerging as an important path in the study of inflammatory responses in various tissues (Russell and McDougall, 2009). PARs are part of the family of G-protein-coupled receptors that are activated by proteinases secreted into extracellular matrix (ECM) during inflammation. Whilst first described as thrombin receptors, various other proteinases are able to signal *via* PARs. While PAR-1, PAR-3, and PAR-4 are canonically activated by thrombin, PAR-2 is mainly activated by trypsin. Furthermore, it can be activated by tryptase, matrix metalloproteinases (MMPs), and tissue factor-VIIa-Xa complex (Vu et al., 1991; Bohm et al., 1996; Ruf and Mueller, 2006). PARs are also known to participate on extracellular matrix pathophysiological processes. Collagenase hydrolysis showed an antagonistic behavior on PAR2 activation, proposing an relevant negative feedback mechanism whereby canonical PAR2 activation induces MMP expression, and MMP activity can subsequently antagonize PAR2 (Falconer et al., 2019). PARs 1 and 2 have been recently demonstrated to play a role in inflamed odontoblasts (Alvarez et al., 2017).

Low-level laser therapy, also known as Photobiomodulation Therapy (PBM) (Hamblin, 2016), had its onset in the 1960's and it relies on the use of light devices–lasers or light-emitting diodes (LEDs) - as resource to trigger tissue biological/medical responses (i.e. healing, immunity enhancement, anti-inflammatory and antibiotic properties) (Vu et al., 1991; Conlan et al., 1996; Bjordal et al., 2003; Yu et al., 2003; Ruf and Mueller, 2006; Ghanaat, 2010; Alvarez et al., 2017; Falconer et al., 2019). Studies have showed that PBM can significantly reduce inflammation, by inhibiting inflammatory cytokines expression and activity in different tissues (Sakurai et al., 2000; Arany et al., 2007; de Lima et al., 2011). Moreover, the use of lasers and LEDs demonstrated to be effective in modulating the cell viability and growth in different cell models, including mesenchymal stem cells (Kim et al., 2009; Li et al., 2010; Alghamdi et al., 2012; Ginani et al., 2015). Research that evaluated the effect of PBM on SHED cells has shown for instance that infrared LEDs (850 nm 40mW/cm^2) could promote an *in vitro* increase in the levels of phosphates, synthesis of collagen and dentinal sialoprotein (Turrioni et al., 2014), and induce a significant increase in cells viability, proliferation, and production of mineralized tissues for SHEDs that remained in nutrient starvation after PBM (Turrioni et al., 2015).

To better understand DPSC's features for tissue regenerative applications, such as vital pulp therapy or regenerative endodontic procedures, we believe it is important to assess their biological responses when exposed to light sources under PBM parameters. As far as we know, this is the first study that assessed the potential for laser irradiation to modulate the gene expression for PARs and other genes related to the inflammatory process and osteogenesis using a DPSCs model. This study hypothesis was that PBM can interfere in inflammatory gene expression and in osteogenesis related genes.

METHODS

Dental Pulp Tissues Obtainment

Approval for this protocol was obtained from the local Human Research Ethics Committee (# 98511618.8.0000.5497) to use five freshly extracted third molars from patients ages 19–39 years. The use of the third molars is the most convenient source of adult stem cells as they contain sufficient amount of dental pulp tissue to ensure proper isolation of DPSCs (Liu et al., 2006). After extraction teeth were copiously washed with deionized water and placed in a sterile solution containing saline, subsequently they were rinsed with 70% ethanol to reduce the biofilm contamination. Then, the dental elements were rinsed 5 times with sodium phosphate buffer (PBS) to remove ethanol. Subsequently, decontaminated teeth were cut with a sterile Zekrya (Dentsplay Sirona, United States) drill using a high-speed device to expose the pulp chamber and, consequently,

provide access to the pulp tissue. The pulp tissue was gently removed from the pulp chamber with a sterile endodontic file and immediately transferred to a sterile screw-capped tube containing α-MEM cell culture medium without calf bovine serum (FCS).

Isolation of Postnatal Human Dental Pulp Stem Cells

Excised pulp tissue was digested in a solution containing 3 mg/ml collagenase type I (Merck KGaA, Darmstadt, Germany) and 4 mg/ml dispase (Merck KGaA, Darmstadt, Germany) for 1 h at 37°C. After digestion, 5 volumes of α-MEM medium containing 10% FCS were added. This solution was centrifuged at 120 × g for 10 min, at room temperature. The precipitated material was resuspended in α-MEM medium and filtered through filters with pores of 70 μM. This procedure resulted in a single-cell suspension for *in vitro* culture. The cells were seeded into culture flasks with α-MEM, supplemented with 10% FCS, 100 μM L-ascorbic acid, 2 mM L-glutamine and penicillin (100 U/mL)/streptomycin (100 mg/ml) and incubated at 37°C with 5% CO_2. In the initial stage, after adhering to culture flasks, cells grew slowly. Cell colonies were identified after 10–14 days, with their fibroblastoid appearance, which showed to be dependent on the cell density obtained in initial plating. After reach 70% of confluence, cells were considered ready to proceed with experiments. Accordingly, isolated DPSCs were randomly assigned to the following experimental groups: Group 1–LPS stimulus and laser irradiation; Group 2–LPS stimulus and no laser irradiation; Group 3–Control group, no LPS or laser treatment.

Human Dental Pulp Stem Cells Inflammation Induction by Lipopolysaccharides Assay

The lipopolysaccharides induces the production of pro-inflammatory cytokines such as interleukins (IL-1β, IL-6 and IL-8), tumor necrosis factor (TNF-), platelet and prostaglandin activating factors by macrophages and neutrophils present in areas infected by bacteria (Lindemann et al., 1988; Wilson et al., 1996). To promote *in vitro* cellular inflammatory response, 2×10^6 of DPSCs were seeded in six wells plates with α-MEM, supplemented with 10% FCS, 100 μM L-ascorbic acid, 2 mM L-glutamine and penicillin (100U/mL)/streptomycin (100 mg/ml) and incubated from 24 h at 37°C with 5% CO_2 for complete adhesion. Previous to the experiment cells were starved for 6hs in α-MEM without FCS. After starvation period, 10 μg/ml of LPS were added in α-MEM, supplemented with 10% FCS, 100 μM L-ascorbic acid, 2 mM L-glutamine and penicillin (100 U/mL)/streptomycin (100 mg/ml), for 24 hs.

Part of these cells was further irradiated (see PBM protocol following) with a laser device (Group 1); while the other part remained not irradiated for subsequent analysis (Group 2).

Photobiomodulation Irradiation Protocol

DPSCs assigned for Group 1 were irradiated using the Laser Duo device (MM Optics, São Carlos, BR), containing 1 light-emitting diode, in the infrared wavelength (808 nm) that delivered a total energy of 6 J (100 mW × 60 s). 0.4×10^5 cells per well were seeded in a 96 wells plate 24 hs before the experiment. All the three experimental groups were evaluated in triplicates. The plate cover and the culture medium were removed prior irradiation to avoid any interference related to light refraction. The laser probe was placed perpendicularly from bottom of the well with a 0.5 cm of distance for 60 s, in order to be sure that all cells received the radiation. After the treatment, the culture medium was replaced for 30 min before the genetic material be assessed. Device specifications: laser type, InGaAIP; wavelength, 808 nm; irradiation type, Infrared; laser beam output area, 0.3 cm^2; Continuous; power output, 100 mW ± 20%; irradiance, 0.33 W/cm^2; fluence, 6 J/cm^2 (**Table 1**).

TABLE 1 | mRNA expression of cell adhesion and extracellular matrix proteins in DPSCs after and before laser irradiation.

Gene	LPS	LPS + Laser	Gene Fold (Change Factor)
ACVR1	1.15	0.66	−1.74
AHSG	1.21	0.53	−2.28*
ALPL	2.85	6.15	2.16*
ANXA5	1.99	1.48	−1.34
BGLAP	0.61	0.26	−2.35*
BGN	1.31	1.13	−1.16
CDH11	1.33	1.30	−1.02
CD36	0.11	0.06	−1.83
COL10A1	2.89	5.84	2.02*
COL14A1	0.82	0.79	−1.04
COL15A1	1.21	1.27	1.04
COL1A1	1.12	0.83	−1.35
COL1A2	1.00	0.77	−1.29
COL2A1	1.21	0.53	−2.28*
COL3A1	1.02	0.99	−1.03
COL5A1	1.65	0.98	−1.68
COMP	1,21	0.53	−2,28*
FN1	1.04	0.83	−1.25
ICAM1	29.32	30.55	1.04
ITGA1	4.73	2.98	−1.59
ITGA2	3.20	1.95	−1.64
ITGA3	0.61	0.60	−1.02
ITGAM	1.96	0.53	−3.70*
ITGB1	2.00	1.48	−1.35
SPP1	0.95	0.56	−1.70
VCAM1	6.07	3.67	−1.65

Proteinase-Activated Receptors Gene Expression Quantification

The tRNA from DPSCs was extracted using the TRIzol® (Thermo Fischer Scientific, Waltham, United States) reagent. The complementary DNA (cDNA) was obtained from the tRNA by reverse-transcription using the ImProm-II Reverse transcriptase System kit (Promega, Madison, United States) according to the manufacturer's protocol. The gene expression evaluation was performed by Real-time quantitative polymerase chain reaction (qRT-PCR) assays, using the SYBR Green PCR Master Mix® (Thermo Fisher Scientific, Waltham, United States). The reaction cycling parameters were adjusted to 50°C for 2 min and 95°C for 10 min, followed by 40 cycles at 95°C for 15 s and 60°C for 1 min in an Real Time PCR System ABI PRISM 7500 (Applied Biosystems, Foster City, United States). Relative quantification was carried out using the ΔCt method. This method results in ratios between the target genes and the housekeeping reference gene, in this case, the

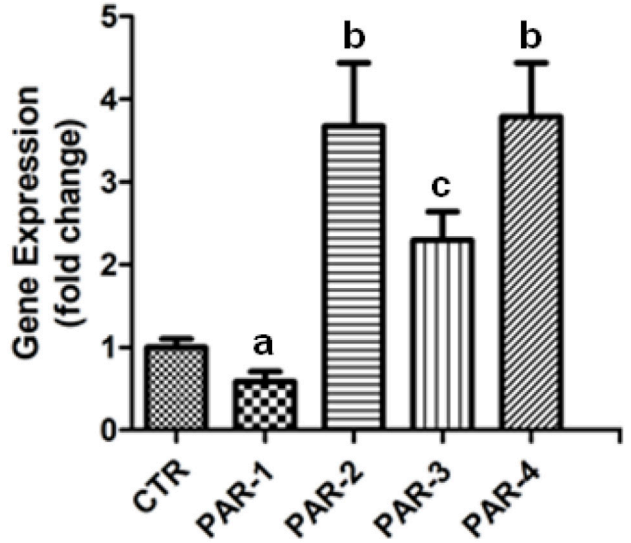

FIGURE 1 | PBM modulate PARs genes expression in DPSCs. Real-time quantitative PCR (qRT-PCR) analysis of gene expression in LPS stimulated DPSCs irradiated with the infrared wavelength (808 nm) with total energy of 6 J (100mW × 60s). The bars represent the mean expression levels of the four PARs genes and standard error. The qRT-PCR analysis of gene expressions was normalized to the housekeeping gene enzyme β-2-microglobulin for DPSCs (control); the relative quantification of the expression levels (experimental/control) was determined based on the 2-ΔCt method. Experiments were performed in triplicate. Different letters indicate statistically significant differences ($p < 0.05$) in gene expression.

enzyme β-2-microglobulin (positive control) for DSPCs. This assay is based on gene fold-Regulation approach, that represents in fold-change (fc) results of the evaluated genes. Fold-change values greater than one indicates a positive- or an up-regulation in gene expression, while fold-change values less than one indicate a negative or down-regulation, of the evaluated gene. The *p*-values were calculated based on a Student's t-test of the replicate $2^{\hat{}}(\Delta Ct)$ values for each gene in the experimental or control groups. All primers sequences used in PARs genes evaluation were manufactured by Exxtend (São Paulo, SP, Brazil). The melting curve analysis was used to determine the specificity of the reaction. All experiments were run in triplicates.

Inflammation and Osteogeneses Genes Expression Array

Likewise, DPSCs from the 3 experimental groups were assessed for expression of eighty-five (85) genes related to inflammation and osteogenesis the RT^2 Profiler ™ PCR array (Qiagen, Hilden, GER) was used. This device allows gene expression profiling technology by analyzing focused panels of genes using real-time PCR. Each experimental kit contains a set of the inflammatory/osteogenesis pathway-converged genes, and five housekeeping (positive controls) genes. The array also contains a panel of other reaction controls to monitor real-time PCR efficiency (PPC), genomic DNA contamination (GDC) as well as the first strand synthesis (RTC). All experiments were run in triplicates.

TABLE 2 | mRNA expression of proteolytic enzymes related to organic matrix remodeling in the DPSCs before and after laser irradiation.

Gene	LPS	LPS + Laser	Gene Fold (Change Factor)
CTSK	1,70	1.14	−1.49
MMP2	1.30	0.96	−1.35
MMP8	1.60	0.53	−3.02*
MMP9	1.42	0.53	−2.68*
MMP10	0.54	0.98	1.81
PHEX	0.26	0.18	−1.44
SERPINH1	1.30	0.99	−1.31

Statistical Analysis

Raw data for each experiment (PARs, inflammation and osteogenesis gene expression) was transformed in a fractional number as function of the data from control group, using a single rule of 3, wherein the gene expression values of control groups for each experiment were considered = 1. Lack of normal distribution demanded the application of non-parametric Kruskal–Wallis tests, complemented by Mann–Whitney tests for pairwise comparison, at a 5% level of significance.

RESULTS

Proteinase-Activated Receptor Expression

Four PARs have been identified so far (PAR-1–4) and evidence shows that they can exhibit both anti- and pro-inflammatory properties. **Figure 1** shows that PBM treatment can modulate the gene expression of all PARs members. While PAR-1 showed a downregulation in the gene expression, the other PARs show a significant increase in the number of gene copies.

Photobiomodulation Effect on Gene Expression of Human Dental Pulp Stem Cells After Lipopolysaccharide Inflammatory Stimulus

PBM therapy showed a wide range of effects at the tissue, cellular, and molecular levels. LPS-inflamed DPSCs demonstrated to be sensitive to PBM irradiation with several genes related to inflammation and osteogenesis being modulated either up or down after treatment. Among the genes analyzed, **Table 1** depicts the DPSCs genes related to proteins involved in the extracellular matrix (ECM) organization that were modulated by LPS inducement and/or then regulated or inhibited by PBM irradiation.

Photobiomodulation Effect on Expression of Proteolytic Enzymes Genes of Human Dental Pulp Stem Cells

Both *in vivo* and *in vitro* have used PBM because it is an important tool to positively stimulate bone. However, little is known about its association with anti-inflammatory and neoformative events taking place in human stem cells

TABLE 3 | mRNA expression of growth and differentiation factors in the DPSCs before and after laser irradiation.

Gene	LPS	LPS + Laser	Gene Fold (Change Factor)
BMP1	3.05	0.83	–3.67*
BMP2	2.85	1.82	–1.47
BMP3	1.21	1.94	1.60
BMP4	1.53	0.41	–3.73*
BMP5	0.52	0.57	1.90
BMP6	1.50	1.59	1.06
BMP7	1.21	0.53	–2.28*
CHRD	1.21	0.53	–2.28*
CSF1	1.36	1.28	–1.06
CSF2	0.13	0.16	1.23
CSF3	0.77	0.49	–1.57
EGF	1.21	1.53	1.26
FGF1	3.51	1.29	–2.72*
FGF2	2.63	2.09	–1.26
GDF10	1.21	0.53	–2.28*
IGF1	0.37	0.51	1.38
IGF2	1.21	0.53	–2.28*
IHH	1.21	0.53	–2.28*
NOG	2.80	2.79	–1.00
PDGFA	1.22	1.24	1.01
TGFB1	1.79	0.88	–2.03*
TGFB2	2.19	1.12	–1.96
TGFB3	0.47	0.52	1.11
TNF	1.21	0.53	–2.28*
VEGFA	1.52	1.16	–1.31
VEGFB	2.64	0.28	–9.43*

TABLE 4 | mRNA Expression of Cellular Receptors Related to Osteogenesis in the DPSCs After and Before Laser Irradiation.

Gene	LPS	LPS + Laser	Gene Fold (Change Factor)
ACVR1	1.15	0.66	–1.74
BMPR1A	2.02	1.40	–1.44
BMPR1B	1.11	0.55	–2.02*
BMPR2	1.81	1.40	–1.29
CALCR	1.21	0.53	–2.28*
EGFR	1.33	1.11	–1.20
FGFR1	1.24	0.95	–1.31
FGFR2	0.78	0.13	–6.00*
FLT1	0.19	0.55	2.89*
IGF1R	3.88	1.90	–2.04*
TGFBR1	1.36	0.92	–1.48
TGFBR2	1.31	0.81	–1.62
TNFSF11	0.58	0.37	–1.57
VDR	15.44	0.41	–37.66*

*(ACVR1) Activin A receptor type I. (BMPR1A) Bone morphogenetic protein receptor, type IA. (BMPR1B) Bone morphogenetic protein receptor, type IB. (BMPR2) Bone morphogenetic protein receptor, type II. (CALCR) Calcitonin receptor. (EGFR) Epidermal growth factor receptor. (FGFR1) Fibroblast growth factor receptor 1. (FGFR2) Fibroblast growth factor receptor 2. (FLT1) Fms-related tyrosine kinase. (IGF1R) Insulin-like growth factor 1 receptor. (TGFBR1) Transforming growth factor, beta receptor 1. (TGFBR2) Transforming growth factor, beta receptor II. (TNFSF11) Tumor necrosis factor (ligand) superfamily, member 11. (VDR) Vitamin D (1.25- dihydroxyvitamin D3) receptor. The numbers represent the quantification of the gene expression variation in fold change, and the * represents genes that were modulated + or – 2.00-fold* ($p<0.05$).

derived from a mineralized tissue. The data presented in **Table 2** show the expression of proteolytic enzymes genes related to organic matrix remodeling in mineralized tissues that were upregulated in the inflammatory state and then, mainly downregulated after PBM therapy. From all enzymes evaluated only MMP-10 showed an increase in the expression (1.81-fold), while MMP-8 and MMP-9 gene expression were significantly reduced -3.03 and -2.68-fold, respectively.

TABLE 5 | mRNA expression of transcription factors in the DPSCs before and after laser irradiation.

Gene	LPS	LPS + Laser	Gene Fold (Change Factor)
DLX5	1.21	0.53	–2.28*
GLI1	1.51	0.53	–2.85*
NFKB1	1.21	1.27	1.05
RUNX2	0.83	0.80	–1.04
SMAD1	1.51	0.66	–2.29*
SMAD2	1.68	1.09	–1.54
SMAD3	1.55	0.79	–1.96
SMAD4	2.80	1.36	–2.06*
SMAD5	1.99	1.76	–1.13
SOX9	3.68	3.20	–1.15
SP7	1.74	0.53	–3.28*
TWIST1	1.56	3.78	2.35*

Photobiomodulation Effects on Genes Expression of Growth and Differentiation Factors in Human Dental Pulp Stem Cells

Initially known as an active secreted molecule that can affect the growth of the cells, the growth factors family has been expanded his activities to include secreted molecules that can affect cellular differentiation and promote or inhibit mitosis. **Table 3** show the expression profile of genes that can act on specific cell surface receptors that subsequently transmit their growth signals to other intracellular components, after inflammatory stimulus, and after PBM treatment. Our results clearly show that the growth factors were predominantly upregulated by LPS, while PBM treatment lowered the gene expression of proteins related to tissue mineralization, such as BMP-1 (-3.67-fold), BMP-4 (-3.73-fold), and BMP-7 (-2.28-fold). In the same sense, VEGF-B was significantly downregulated by laser treatment (-9.43-fold).

Photobiomodulation-Modulating Effect on Gene Expression of Cell Surface Receptors

Once the expression of growth factors was evaluated, the gene expression for cell receptors related to these specific ligands was also evaluated. As expected, the expression of the cellular receptors followed the trend profiling found as far expression of their respective ligands. For most of evaluated cellular receptors, it was observed an increase in their gene expression after induction with LPS, while PBM treatment downregulated all evaluated genes. Interestingly, the most significantly inhibited receptors were those related to tissue mineralization processes (**Table 4**), including: Calcium Receptor (-2.28-fold), and Vitamin D Receptor (-37.66-fold).

Photobiomodulation-Modulating Effect on Gene Expression of Transcription Factors

Transcription factors are proteins that regulates the transcription of genes. They have DNA-binding sequences that give them the ability to bind to specific of DNA domains called enhancer sequences. The evaluated members of this family were basically not modulated by LPS (**Table 5**). Except for the SOX-9 gene that showed a 3.68-fold increase in expression levels. Conversely, the PBM treatment downregulated the expression of all analyzed genes with the SP-7 (−3.28-fold), GLI-1 (−2.85-fold), and TWIST-1 (−2.35-fold) showing to be the most sensitive genes to laser irradiation.

DISCUSSION

In the regenerative dentistry field researchers face two major challenges, both related to the pulp tissue pathophysiology. The first is the tissue ability to turn back to a healthy metabolic state after a transitory inflammation. The second concerns to its intrinsic potential to produce mineralized tissue through its specialized cells, the odontoblasts. The appreciation of human dental pulp stem cells (DPSCs) as suitable for dental tissue engineering applications (Kaigler and Mooney, 2001; Young et al., 2005; Duailibi et al., 2008; Zhang et al., 2009) renders the overall ambition of tissue regeneration in dentistry more accomplishable. The PBM therapy or PBM treatment has been used in medicine and dentistry for its well demonstrated analgesic, anti-inflammatory, and biostimulation effects (Reddy, 2004; Silveira et al., 2007; Moosavi et al., 2016). In addition, the present study has shown, for the first time, that such modulatory physio-biological effects of PBM is accompanied by a modulation on the gene expression of inflammation and osteogenic biomarkers in DPSCs.

Proteinase-activated receptors (PARs) have a distinct mechanism of activation that involves limited proteolysis and unmasking of a receptor activating motif called tethered ligand (Huesa et al., 2016). PAR-1 and PAR-4 are canonically described as thrombin-activated receptors, while PAR-2 is activated by trypsin. Interestingly, PAR-3 was related to play role during embryonic development (Gieseler et al., 2013). Our results clearly showed that PBM therapy can increase the expression of PAR-2 (3.7-fold), PAR-3 (2.3-fold), and PAR-4 (3.8-fold) while decreasing the expression of PAR-1 (-0.6-fold). Interestingly, matrix metalloproteinases (MMPs), which genes have shown to be upregulated by PBM in the present study, have been described to activate PARs in a noncanonical way (Alvarez et al., 2017). Thus, taken in conjunction, these results strongly suggest that PARs can play a role in the anti-inflammatory process promoted by PBM therapy by not only increasing their expression, but also by increasing the MMPs expression levels.

Even under basal conditions DPSCs produce these molecular markers, including but not limited to CD-36, BMPs, NOG, Type II collagen, RUNX2, SOX-9 that are responsible for maintenance of pluripotency in early embryos and embryonic stem cells (Govindasamy et al., 2010; Karaoz et al., 2010; Martinez-Sarra et al., 2017), which indicate a promising primitiveness and multipotency of DPSCs for regenerative dentistry.

The osteogenic gene profile analysis was performed to provide better understanding on the underlying mechanisms for DPSCs differentiation and modulation of mineralization process upon the effects of an inflammatory model (LPS) and PBM (**Tables 2–5**). The treatment of DPSCs with LPS was capable to remarkably induce the gene expression of odontoblastic differentiation biomarkers, BMP-1, BMP-2, BMPR-1A, FGF-1, FGF-2, TGF-B2, IGF-1R, SMAD-4, SMAD-5, COL-10A1, ITG-A1, ITG-A2, ITG-B, ITG-A, and Alkaline phosphatase (ALP) in DPSCs. ALP is a widely accepted as an earlier marker for the differentiation of cells forming mineralized tissues. It has been shown that BMP-2 is required to induce the differentiation of DPSCs into odontoblast (Casagrande et al., 2010), and in mesenchymal stem cells, BMP-2 efficiently induced the expression of transcriptional factor Sox9 responsible for chondrogenic differentiation via BMP-2/Smad (Pan et al., 2008). Transforming growth factor-beta (TGF-β), also via SMAD pathways, plays a major role in tooth development and the reparative process by regulating cell proliferation, differentiation, and reparative dentinogenesis (Niwa et al., 2018). FGF-1 and TGF-β1 have a synergic effect to promote morphological and functional features of differentiated odontoblasts, whereas FGF-2 seems to modulate TGF-β1 action (Unda et al., 2000). TGF-β1 and TGF-β3 are predominantly expressed in odontoblasts, whereas TGF-β2 is high expressed in dental pulp (Niwa et al., 2018). IGF-I stimulate osteoblast differentiation in human mesenchymal stem cells (HMSCs), it stimulates the biosynthesis of 1α.25(OH)2D in synergy with 25OHD3. Osteoblast differentiation and skeletal homeostasis may be regulated by autocrine/paracrine actions of 25(OH)D (3) in HMSCs (Geng et al., 2011). Here, we demonstrate that LPS can increases both IGF-1R and VDR expression in DPSCs favoring odontoblast differentiation. Taken together, our data suggest that LPS treatment induced odontoblastic differentiation of human DPSCs.

RANKL is a tumor necrosis factor (TNF)-like factor produced by mesenchymal cells, osteoblast derivatives, and T cells that is essential for osteoclastogenesis. In osteoblasts, RANKL expression is regulated by two major calcemic hormones, 1.25-dihydroxyvitamin D (3) [1.25(OH) (2)D (3)] and parathyroid hormone (PTH), as well as by several inflammatory/osteoclastogenic cytokines (Kim et al., 2006).

It is important to mention that 1.25(OH)2 vitamin D stimulates osteoblast maturation, increasing expression of the mature osteoblast marker osteocalcin (BGLAP) in osteoblasts, and 1.25(OH)2 vitamin D also stimulates the expression of the osteoclast differentiation factor RANKL (Pereira et al., 2019). The biological actions of 1.25-(OH)2D3 are mediated by the vitamin D receptor (VDR), a protein that binds to target genes and alters their expression. 1.25-(OH)2D3 is also able of inducing transcription of the VDR gene itself (Zella et al., 2006). VDR signaling in osteoprogenitors cells increases RANKL expression and stimulates osteoclastogenesis (Kim et al., 2006).

In this sense, PBM treatment significantly suppressed the mRNA expression of TNF and RANKL (TNFSF11) triggered by LPS in DSPC. Interesting, PBM treatment greatly decreased (37.66-fold) the expression Vitamin D Receptor (VDR) triggered by LPS in the cell model. PBM treatment can inhibit the transcriptional activity of NF-κB in human periodontal ligament cells (Lee et al., 2018), which is a crucial transcription factor involved in the regulation of the inflammatory process triggered by LPS in dental pulp stem cells (Baldwin, 2001). PBM decreased cell death and attenuated the NLRP3 inflammasome in the ischemic brain. In mice experimental model with ischemic stroke, PBM therapy showed suppressed TLR-2 levels, MAPK signaling and NF-kB activation. The suppression of NF-kB activation induced by PBM is related to the major anti-inflammatory activity of Laser (Lee et al., 2017).

Our data suggest that the decrease in the VDR expression promoted by PBM treatment can lead to inhibition of $1.25(OH)_2D_3$/VTR signaling, and downregulating RANKL expression in DPSCs (Kim et al., 2006). PBM therapy also decreased the expression of proteolytic enzymes cathepsin K, MMP-8 and MMP-9 after LPS assay. Overall, PBM blocked the odontoblastic differentiation of human dental pulp stem cells subjected to LPS assay that were dependent on BMP, FGF, IGF and TGFB signaling, decreasing the expression of the transcriptional factor DLX-5 and SP-7 as expected. SP-7 and Dlx5, in turn, was shown to drive the differentiation of mesenchymal precursor cells into osteoblasts (Nakashima et al., 2002). Conversely, it is important to mention that PBM did not block the mRNA expression of ALP, Twist homolog 1 (TWIST-1) and Runt-related transcription factor 2 (RUNX-2) in DPSCs, even in the presence of LPS. TWIST-1 protein regulates several genes that are known to be key players in bone formation, including the FGF-R2 and RUNX-2 genes. In conjunction, our data strongly suggest that PBM decreased inflammatory mineral matrix resorption in DPSCs by decreasing the activation of RANKL expression via inhibition of $1.25(OH)_2D_3$/VTR signaling. Moreover, PBM treatment preserved the odontogenic potential of DPSCs by increasing the expression of TWIST-1/RUNEX-2/ALP signaling axis.

In spite of the study limitations, were possible to conclude that biomodulation of DPSCs by irradiation with laser device at the infrared wavelength (808 nm) showed not only to mediate the gene expression related to habitual anti-inflammatory molecular canons, but also participate in the regulation of genes that can express signaling molecules and factors associated with other non-classic inflammation molecules (i.e. PARs, cell receptors and transcription factors) as well as with molecules of bone tissue protection from resorption, even if it has not clearly shown yet to influence the expression of genes that stimulate bone neoformation. Further studies still need to be performed to better elucidate the role of PBM therapy on the DPSCs and bone. However, this study certainly brings new data to tissue engineering related to the regenerative pulp therapy field.

DATA AVAILABILITY STATEMENT

The datasets presented in this study can be found in online repositories. The data can be accessed from the Gene Expression Omnibus (GEO) database, using accession number GSE193448.

ETHICS STATEMENT

The studies involving human participants were reviewed and approved by Approval for this protocol was obtained from the University of Mogi das Cruzes Human Research Ethics Committee (protocol # 98511618.8.0000.5497). The patients/participants provided their written informed consent to participate in this study.

AUTHOR CONTRIBUTIONS

ER contributed to conception, design, data acquisition and interpretation, drafted and critically revised the manuscript and project administration; MA contributed to data acquisition and interpretation, drafted and critically revised the manuscript; AP contributed to data acquisition, interpretation and analyses, drafted and critically revised the manuscript; MM contributed to conception, data curation and analyses, drafted and critically revised the manuscript; SO contributed to data acquisition, interpretation and analyses and critically revised the manuscript; MRC contributed to data interpretation, drafted and critically revised the manuscript. IT contributed to data interpretation, drafted and critically revised the manuscript; and FN contributed to conception, design and data acquisition, drafted and critically revised the manuscript and funding acquisition. All authors gave their final approval and agreed to be accountable for all aspects of the work.

FUNDING

This study was funded with grant FAPESP (13/05822-9 and 2017/07687-2 P.I. Nascimento).

REFERENCES

Alghamdi, K. M., Kumar, A., and Moussa, N. A. (2012). Low-level Laser Therapy: a Useful Technique for Enhancing the Proliferation of Various Cultured Cells. *Lasers Med. Sci.* 27, 237–249. doi:10.1007/s10103-011-0885-2

Alvarez, M. M. P., Moura, G. E., Machado, M. F. M., Viana, G. M., De Souza Costa, C. A., Tjäderhane, L., et al. (2017). PAR-1 and PAR-2 Expression Is Enhanced in Inflamed Odontoblast Cells. *J. Dent. Res.* 96, 1518–1525. doi:10.1177/0022034517719415

Arany, P. R., Nayak, R. S., Hallikerimath, S., Limaye, A. M., Kale, A. D., and Kondaiah, P. (2007). Activation of Latent TGF-Beta1 by Low-Power Laser *In Vitro* Correlates

with Increased TGF-Beta1 Levels in Laser-Enhanced Oral Wound Healing. *Wound Repair Regen.* 15, 866–874. doi:10.1111/j.1524-475X.2007.00306.x

Baldwin, A. S., Jr. (2001). Series Introduction: the Transcription Factor NF-kappaB and Human Disease. *J. Clin. Invest.* 107, 3–6. doi:10.1172/JCI11891

Bjordal, J. M., Couppé, C., Chow, R. T., Tunér, J., and Ljunggren, E. A. (2003). A Systematic Review of Low Level Laser Therapy with Location-specific Doses for Pain from Chronic Joint Disorders. *Aust. J. Physiother.* 49, 107–116. doi:10.1016/s0004-9514(14)60127-6

Bohm, S. K., Kong, W., Bromme, D., Smeekens, S. P., Anderson, D. C., Connolly, A., et al. (1996). Molecular Cloning, Expression and Potential Functions of the Human Proteinase-Activated Receptor-2. *Biochem. J.* 314 (Pt 3), 1009–1016. doi:10.1042/bj3141009

Botelho, J., Cavacas, M. A., Machado, V., and Mendes, J. J. (2017). Dental Stem Cells: Recent Progresses in Tissue Engineering and Regenerative Medicine. *Ann. Med.* 49, 644–651. doi:10.1080/07853890.2017.1347705

Casagrande, L., Demarco, F. F., Zhang, Z., Araujo, F. B., Shi, S., and Nör, J. E. (2010). Dentin-derived BMP-2 and Odontoblast Differentiation. *J. Dent. Res.* 89, 603–608. doi:10.1177/0022034510364487

Conlan, M. J., Rapley, J. W., and Cobb, C. M. (1996). Biostimulation of Wound Healing by Low-Energy Laser Irradiation. A Review. *J. Clin. Periodontol.* 23, 492–496. doi:10.1111/j.1600-051x.1996.tb00580.x

De Lima, F. M., Villaverde, A. B., Albertini, R., Corrêa, J. C., Carvalho, R. L., Munin, E., et al. (2011). Dual Effect of Low-Level Laser Therapy (LLLT) on the Acute Lung Inflammation Induced by Intestinal Ischemia and Reperfusion: Action on Anti- and Pro-inflammatory Cytokines. *Lasers Surg. Med.* 43, 410–420. doi:10.1002/lsm.21053

Duailibi, S. E., Duailibi, M. T., Zhang, W., Asrican, R., Vacanti, J. P., and Yelick, P. C. (2008). Bioengineered Dental Tissues Grown in the Rat Jaw. *J. Dent. Res.* 87, 745–750. doi:10.1177/154405910808700811

Falconer, A. M. D., Chan, C. M., Gray, J., Nagashima, I., Holland, R. A., Shimizu, H., et al. (2019). Collagenolytic Matrix Metalloproteinases Antagonize Proteinase-Activated Receptor-2 Activation, Providing Insights into Extracellular Matrix Turnover. *J. Biol. Chem.* 294, 10266–10277. doi:10.1074/jbc.RA119.006974

Geng, S., Zhou, S., and Glowacki, J. (2011). Effects of 25-hydroxyvitamin D(3) on Proliferation and Osteoblast Differentiation of Human Marrow Stromal Cells Require CYP27B1/1α-Hydroxylase. *J. Bone Miner. Res.* 26, 1145–1153. doi:10.1002/jbmr.298

Ghanaat, M. (2010). Types of Hair Loss and Treatment Options, Including the Novel Low-Level Light Therapy and its Proposed Mechanism. *South. Med. J.* 103, 917–921. doi:10.1097/SMJ.0b013e3181ebcf71

Gieseler, F., Ungefroren, H., Settmacher, U., Hollenberg, M. D., and Kaufmann, R. (2013). Proteinase-activated Receptors (PARs) - Focus on Receptor-Receptor-Interactions and Their Physiological and Pathophysiological Impact. *Cell Commun. Signal.* 11, 86. doi:10.1186/1478-811X-11-86

Ginani, F., Soares, D. M., Barreto, M. P., and Barboza, C. A. (2015). Effect of Low-Level Laser Therapy on Mesenchymal Stem Cell Proliferation: a Systematic Review. *Lasers Med. Sci.* 30, 2189–2194. doi:10.1007/s10103-015-1730-9

Goldberg, M., and Smith, A. J. (2004). Cells and Extracellular Matrices of Dentin and Pulp: A Biological Basis for Repair and Tissue Engineering. *Crit. Rev. Oral Biol. Med.* 15, 13–27. doi:10.1177/154411130401500103

Govindasamy, V., Abdullah, A. N., Ronald, V. S., Musa, S., Ab Aziz, Z. A., Zain, R. B., et al. (2010). Inherent Differential Propensity of Dental Pulp Stem Cells Derived from Human Deciduous and Permanent Teeth. *J. Endod.* 36, 1504–1515. doi:10.1016/j.joen.2010.05.006

Hamblin, M. R. (2016). Photobiomodulation or Low-Level Laser Therapy. *J. Biophotonics* 9, 1122–1124. doi:10.1002/jbio.201670113

Hanisch, U. K. (2002). Microglia as a Source and Target of Cytokines. *Glia* 40, 140–155. doi:10.1002/glia.10161

He, W., Wang, Z., Luo, Z., Yu, Q., Jiang, Y., Zhang, Y., et al. (2015). LPS Promote the Odontoblastic Differentiation of Human Dental Pulp Stem Cells via MAPK Signaling Pathway. *J. Cel. Physiol.* 230, 554–561. doi:10.1002/jcp.24732

Huesa, C., Ortiz, A. C., Dunning, L., Mcgavin, L., Bennett, L., Mcintosh, K., et al. (2016). Proteinase-activated Receptor 2 Modulates OA-Related Pain, Cartilage and Bone Pathology. *Ann. Rheum. Dis.* 75, 1989–1997. doi:10.1136/annrheumdis-2015-208268

Kaigler, D., and Mooney, D. (2001). Tissue Engineering's Impact on Dentistry. *J. Dent. Educ.* 65, 456–462. doi:10.1002/j.0022-0337.2001.65.5.tb03415.x

Karaöz, E., Doğan, B. N., Aksoy, A., Gacar, G., Akyüz, S., Ayhan, S., et al. (2010). Isolation and *In Vitro* Characterisation of Dental Pulp Stem Cells from Natal Teeth. *Histochem. Cel. Biol.* 133, 95–112. doi:10.1007/s00418-009-0646-5

Kerkis, I., Kerkis, A., Dozortsev, D., Stukart-Parsons, G. C., Gomes Massironi, S. M., Pereira, L. V., et al. (2006). Isolation and Characterization of a Population of Immature Dental Pulp Stem Cells Expressing OCT-4 and Other Embryonic Stem Cell Markers. *Cells Tissues Organs* 184, 105–116. doi:10.1159/000099617

Kim, H. K., Kim, J. H., Abbas, A. A., Kim, D. O., Park, S. J., Chung, J. Y., et al. (2009). Red Light of 647 Nm Enhances Osteogenic Differentiation in Mesenchymal Stem Cells. *Lasers Med. Sci.* 24, 214–222. doi:10.1007/s10103-008-0550-6

Kim, S., Yamazaki, M., Zella, L. A., Shevde, N. K., and Pike, J. W. (2006). Activation of Receptor Activator of NF-kappaB Ligand Gene Expression by 1,25-dihydroxyvitamin D3 Is Mediated through Multiple Long-Range Enhancers. *Mol. Cel. Biol.* 26, 6469–6486. doi:10.1128/MCB.00353-06

Lee, H. I., Lee, S. W., Kim, N. G., Park, K. J., Choi, B. T., Shin, Y. I., et al. (2017). Low-level Light Emitting Diode (LED) Therapy Suppresses Inflammasome-Mediated Brain Damage in Experimental Ischemic Stroke. *J. Biophotonics* 10, 1502–1513. doi:10.1002/jbio.201600244

Lee, J. H., Chiang, M. H., Chen, P. H., Ho, M. L., Lee, H. E., and Wang, Y. H. (2018). Anti-inflammatory Effects of Low-Level Laser Therapy on Human Periodontal Ligament Cells: *In Vitro* Study. *Lasers Med. Sci.* 33, 469–477. doi:10.1007/s10103-017-2376-6

Li, W. T., Leu, Y. C., and Wu, J. L. (2010). Red-light Light-Emitting Diode Irradiation Increases the Proliferation and Osteogenic Differentiation of Rat Bone Marrow Mesenchymal Stem Cells. *Photomed. Laser Surg.* 28 (Suppl. 1), S157–S165. doi:10.1089/pho.2009.2540

Lindemann, R. A., Economou, J. S., and Rothermel, H. (1988). Production of Interleukin-1 and Tumor Necrosis Factor by Human Peripheral Monocytes Activated by Periodontal Bacteria and Extracted Lipopolysaccharides. *J. Dent. Res.* 67, 1131–1135. doi:10.1177/00220345880670081401

Liu, H., Gronthos, S., and Shi, S. (2006). Dental Pulp Stem Cells. *Methods Enzymol.* 419, 99–113. doi:10.1016/S0076-6879(06)19005-9

Manolagas, S. C. (1995). Role of Cytokines in Bone Resorption. *Bone* 17, 63S–67S. doi:10.1016/8756-3282(95)00180-l

Martínez-Sarrà, E., Montori, S., Gil-Recio, C., Núñez-Toldrà, R., Costamagna, D., Rotini, A., et al. (2017). Human Dental Pulp Pluripotent-like Stem Cells Promote Wound Healing and Muscle Regeneration. *Stem Cel. Res. Ther.* 8, 175. doi:10.1186/s13287-017-0621-3

Miura, M., Gronthos, S., Zhao, M., Lu, B., Fisher, L. W., Robey, P. G., et al. (2003). SHED: Stem Cells from Human Exfoliated Deciduous Teeth. *Proc. Natl. Acad. Sci. U S A.* 100, 5807–5812. doi:10.1073/pnas.0937635100

Moosavi, H., Arjmand, N., Ahrari, F., Zakeri, M., and Maleknejad, F. (2016). Effect of Low-Level Laser Therapy on Tooth Sensitivity Induced by In-Office Bleaching. *Lasers Med. Sci.* 31, 713–719. doi:10.1007/s10103-016-1913-z

Nakane, A., Yoshida, T., Nakata, K., Horiba, N., and Nakamura, H. (1995). Effects of Lipopolysaccharides on Human Dental Pulp Cells. *J. Endod.* 21, 128–130. doi:10.1016/s0099-2399(06)80437-1

Nakashima, K., Zhou, X., Kunkel, G., Zhang, Z., Deng, J. M., Behringer, R. R., et al. (2002). The Novel Zinc finger-containing Transcription Factor Osterix Is Required for Osteoblast Differentiation and Bone Formation. *Cell* 108, 17–29. doi:10.1016/s0092-8674(01)00622-5

Niwa, T., Yamakoshi, Y., Yamazaki, H., Karakida, T., Chiba, R., Hu, J. C., et al. (2018). The Dynamics of TGF-β in Dental Pulp, Odontoblasts and Dentin. *Sci. Rep.* 8, 4450. doi:10.1038/s41598-018-22823-7

Nör, J. E. (2006). Tooth Regeneration in Operative Dentistry. *Oper. Dent.* 31, 633–642. doi:10.2341/06-000

Pan, Q., Yu, Y., Chen, Q., Li, C., Wu, H., Wan, Y., et al. (2008). Sox9, a Key Transcription Factor of Bone Morphogenetic Protein-2-Induced Chondrogenesis, Is Activated through BMP Pathway and a CCAAT Box in the Proximal Promoter. *J. Cel Physiol* 217, 228–241. doi:10.1002/jcp.21496

Pereira, R. C., Salusky, I. B., Bowen, R. E., Freymiller, E. G., and Wesseling-Perry, K. (2019). Vitamin D Sterols Increase FGF23 Expression by Stimulating Osteoblast and Osteocyte Maturation in CKD Bone. *Bone* 127, 626–634. doi:10.1016/j.bone.2019.07.026

Reddy, G. K. (2004). Photobiological Basis and Clinical Role of Low-Intensity Lasers in Biology and Medicine. *J. Clin. Laser Med. Surg.* 22, 141–150. doi:10.1089/104454704774076208

Ruf, W., and Mueller, B. M. (2006). Thrombin Generation and the Pathogenesis of Cancer. *Semin. Thromb. Hemost.* 32 (Suppl. 1), 61–68. doi:10.1055/s-2006-939555

Russell, F. A., and Mcdougall, J. J. (2009). Proteinase Activated Receptor (PAR) Involvement in Mediating Arthritis Pain and Inflammation. *Inflamm. Res.* 58, 119–126. doi:10.1007/s00011-009-8087-0

Sakurai, Y., Yamaguchi, M., and Abiko, Y. (2000). Inhibitory Effect of Low-Level Laser Irradiation on LPS-Stimulated Prostaglandin E2 Production and Cyclooxygenase-2 in Human Gingival Fibroblasts. *Eur. J. Oral Sci.* 108, 29–34. doi:10.1034/j.1600-0722.2000.00783.x

Silveira, P. C., Streck, E. L., and Pinho, R. A. (2007). Evaluation of Mitochondrial Respiratory Chain Activity in Wound Healing by Low-Level Laser Therapy. *J. Photochem. Photobiol. B* 86, 279–282. doi:10.1016/j.jphotobiol.2006.10.002

Turrioni, A. P., Basso, F. G., Montoro, L. A., Almeida, Lde. F., Costa, C. A., and Hebling, J. (2014). Phototherapy Up-Regulates Dentin Matrix Proteins Expression and Synthesis by Stem Cells from Human-Exfoliated Deciduous Teeth. *J. Dent.* 42, 1292–1299. doi:10.1016/j.jdent.2014.07.014

Turrioni, A. P., Montoro, L. A., Basso, F. G., de Almeida, Lde. F., Costa, C. A., and Hebling, J. (2015). Dose-responses of Stem Cells from Human Exfoliated Teeth to Infrared LED Irradiation. *Braz. Dent. J.* 26, 409–415. doi:10.1590/0103-6440201300148

Unda, F. J., Martín, A., Hilario, E., Bègue-Kirn, C., Ruch, J. V., and Aréchaga, J. (2000). Dissection of the Odontoblast Differentiation Process *In Vitro* by a Combination of FGF1, FGF2, and TGFbeta1. *Dev. Dyn.* 218, 480–489. doi:10.1002/1097-0177(200007)218:3<480:AID-DVDY1011>3.0.CO;2-O

Vu, T. K., Hung, D. T., Wheaton, V. I., and Coughlin, S. R. (1991). Molecular Cloning of a Functional Thrombin Receptor Reveals a Novel Proteolytic Mechanism of Receptor Activation. *Cell* 64, 1057–1068. doi:10.1016/0092-8674(91)90261-v

Wilson, M., Reddi, K., and Henderson, B. (1996). Cytokine-inducing Components of Periodontopathogenic Bacteria. *J. Periodontal Res.* 31, 393–407. doi:10.1111/j.1600-0765.1996.tb00508.x

Young, C. S., Abukawa, H., Asrican, R., Ravens, M., Troulis, M. J., Kaban, L. B., et al. (2005). Tissue-engineered Hybrid Tooth and Bone. *Tissue Eng.* 11, 1599–1610. doi:10.1089/ten.2005.11.1599

Yu, H. S., Wu, C. S., Yu, C. L., Kao, Y. H., and Chiou, M. H. (2003). Helium-neon Laser Irradiation Stimulates Migration and Proliferation in Melanocytes and Induces Repigmentation in Segmental-type Vitiligo. *J. Invest. Dermatol.* 120, 56–64. doi:10.1046/j.1523-1747.2003.12011.x

Zella, L. A., Kim, S., Shevde, N. K., and Pike, J. W. (2006). Enhancers Located within Two Introns of the Vitamin D Receptor Gene Mediate Transcriptional Autoregulation by 1,25-dihydroxyvitamin D3. *Mol. Endocrinol.* 20, 1231–1247. doi:10.1210/me.2006-0015

Zhang, W., Abukawa, H., Troulis, M. J., Kaban, L. B., Vacanti, J. P., and Yelick, P. C. (2009). Tissue Engineered Hybrid Tooth-Bone Constructs. *Methods* 47, 122–128. doi:10.1016/j.ymeth.2008.09.004

Conflict of Interest: The authors declare that the research was conducted in the absence of any commercial or financial relationships that could be construed as a potential conflict of interest.

Publisher's Note: All claims expressed in this article are solely those of the authors and do not necessarily represent those of their affiliated organizations, or those of the publisher, the editors and the reviewers. Any product that may be evaluated in this article, or claim that may be made by its manufacturer, is not guaranteed or endorsed by the publisher.

Copyright © 2022 Rocha, Alvarez, Pelosine, Carrilho, Tersariol and Nascimento. This is an open-access article distributed under the terms of the Creative Commons Attribution License (CC BY). The use, distribution or reproduction in other forums is permitted, provided the original author(s) and the copyright owner(s) are credited and that the original publication in this journal is cited, in accordance with accepted academic practice. No use, distribution or reproduction is permitted which does not comply with these terms.

frontiers in Pharmacology

ORIGINAL RESEARCH
published: 31 January 2022
doi: 10.3389/fphar.2022.790712

CB2R Deficiency Exacerbates Imiquimod-Induced Psoriasiform Dermatitis and Itch Through the Neuro-Immune Pathway

Li Li[1†], Xin Liu[1†], Wenqiang Ge[2], Chao Chen[2], Yuqiong Huang[1], Zilin Jin[1], Muouyang Zhan[2], Xiaoru Duan[3], Xinxin Liu[1], Yi Kong[1], Jian Jiang[1], Xuemei Li[4], Xin Zeng[4], Fei Li[4], Shibin Xu[4], Man Li[2] and Hongxiang Chen[1,4,5]**

[1]Department of Dermatology, Union Hospital, Tongji Medical College, Huazhong University of Science and Technology, Wuhan, China, [2]Department of Neurobiology, School of Basic Medicine, Tongji Medical College, Huazhong University of Science and Technology, Wuhan, China, [3]Department of Rheumatology, Union Hospital, Tongji Medical College, Huazhong University of Science and Technology, Wuhan, China, [4]Department of Dermatology, Union Shenzhen Hospital, Huazhong University of Science and Technology, Shenzhen, China, [5]Department of Dermatology, The 6th Affiliated Hospital of Shenzhen University Health Science Center, Shenzhen, China

OPEN ACCESS

Edited by:
Soraia K. P. Costa,
University of São Paulo, Brazil

Reviewed by:
Andrzej T. Slominski,
University of Alabama at Birmingham, United States
Sara Gonzalez-Rodriguez,
University of Oviedo, Spain
Laure Favot,
University of Poitiers, France

***Correspondence:**
Man Li
liman7322@hotmail.com
Hongxiang Chen
hongxiangchen@hotmail.com

[†]These authors have contributed equally to this work

Received: 07 October 2021
Accepted: 05 January 2022
Published: 31 January 2022

Citation:
Li L, Liu X, Ge W, Chen C, Huang Y, Jin Z, Zhan M, Duan X, Liu X, Kong Y, Jiang J, Li X, Zeng X, Li F, Xu S, Li M and Chen H (2022) CB2R Deficiency Exacerbates Imiquimod-Induced Psoriasiform Dermatitis and Itch Through the Neuro-Immune Pathway. Front. Pharmacol. 13:790712. doi: 10.3389/fphar.2022.790712

Background: Cannabinoid receptor 2 (CB2R) is a potential target for anti-inflammatory and pain therapeutics given its significant immunomodulatory and analgesic effects. However, the role of CB2R in imiquimod (IMQ)-induced psoriasiform dermatitis (PsD) and itch is poorly understood.

Objective: To investigate the function and mechanism of CB2R in PsD and itch in mice.

Methods: Following daily treatment with topical IMQ cream for 5-7 consecutive days in C56BL/6 wild-type (WT) and CB2R gene knockout (KO) mice, we assessed the Psoriasis Area and Severity Index (PASI) scores and the scratch bouts every day, and hematoxylin and eosin (H&E) staining, toluidine blue staining were used to observe the histological changes. mRNA levels were analyzed by quantitative real-time polymerase chain reaction (qRT-PCR). Protein levels were detected by western blotting (WB), immunohistochemistry (IHC), immunofluorescence (IF) and cytometric bead array (CBA). Flow cytometry (FCM) was used to examine the proportion of Th17/Treg cells.

Results: We found that CB2R expression levels were increased in mice with psoriasis. Compared with WT mice, CB2R deficiency exacerbated IMQ-induced PsD and scratching bouts and upregulated the expression of proinflammatory cytokines by increasing the infiltration of $CD4^+$ T cells and the Th17/Treg ratio. Obvious proliferation and prolongation of nerve fibers and high expression of nerve growth factor (NGF) were observed in PsD and CB2R KO mice. Pretreatment with the CB2R agonist, JWH-133 significantly reversed inflammation and scratching bouts. CB2R didn't participate in the induction of itch in psoriasis by regulating the expression of IL-31, thymic stromal lymphopoietin (TSLP) and mast cells in mouse skins.

Conclusion: Our results demonstrate that CB2R plays a pivotal role in the pathophysiology of psoriasis, providing a new potential target for anti-inflammatory and antipruritic drugs.

Keywords: psoriasis, the cannabinoid receptor 2, inflammation, itch (pruritus), nerve fiber

INTRODUCTION

Psoriasis is a chronic, immune-mediated skin disease caused by the interaction of multiple factors. The most characteristic skin lesions of psoriasis are erythematosus plaques covered with silvery scales, and a greatly thickened epidermis with elongated rete ridges into the dermis (Julià et al., 2012; Boehncke and Schön, 2015). In addition, it has been reported that approximately 70–90% of patients with psoriasis suffer from itch (Szepietowski and Reich, 2016), which can easily be ignored by clinicians. It is currently widely accepted that the pathophysiology of psoriasis is related to the activation and dysregulation of the innate and adaptive immune systems. Various immune cells secrete cytokines, which can directly or indirectly aggravate or even induce itch by increasing the inflammatory response (Komiya et al., 2020). Given the lack of available treatments for psoriatic patients, it is urgent to develop more effective and safer anti-inflammatory and antipruritic therapies.

Cannabinoids are chemical substances that exert their therapeutic effects by binding to cannabinoid receptors. Cannabinoid receptor-2 (CB2R) is a G-protein-coupled receptor and is primarily located on immune organs and cells (Munro et al., 1993; Galiègue et al., 1995). Studies have shown that CB2R is involved in the pathophysiological processes of skin cell proliferation and differentiation, immune regulation, and sensory conduction (Sheriff et al., 2020). In addition, CB2R activation exerts analgesic effects and inhibits the scratching behaviour of rodents (Phan et al., 2010; Haruna et al., 2015). Thus, CB2R agonists may act as potential candidates for new anti-inflammatory and antipruritic drugs by interfering with the occurrence and progression of inflammatory skin diseases. However, to date, it remains unknown whether targeting CB2R can alleviate inflammation and itch in psoriasis. The molecular biological mechanism of its antipruritic effect also needs further study.

Regulatory T cells (Tregs) regulate the inflammatory response in autoimmune diseases and are important in maintaining immune tolerance (Kanda et al., 2021). Peripheral Tregs and Th17 cells are formed by the differentiation of $CD4^+$ T cells, of which Tregs are differentiated depending on the activity of forkhead/winged helix transcription factor (FOXP3), which is regulated by transforming growth factor-β (TGF-β) or IL-2 (von Knethen et al., 2020). Th17 cells are differentiated according to retinoid-related orphan nuclear receptor γt (RORγt) activity regulated by TGF-β, IL-1 or IL-6 (Pandiyan and McCormick, 2021). The functional defect of Tregs in psoriasis cannot sufficiently inhibit the proliferation of Th17 cells or inflammatory cytokines production, which may lead to the development and exacerbation of psoriasis. Compared with healthy skin, the ratio of Th17/Treg cells is higher in psoriatic skin lesions. Therefore, we selected Th17/Treg cells as the main research object.

Chronic itch is associated with increased levels of nerve growth factor (NGF). NGF belongs to the neurotrophic factor family (Yamaguchi et al., 2009) and influences the inflammatory reaction. On the other hand, NGF causes the elongation and branching of epidermal nerve fibers, which leads to hypersensitivity of itch and inflammation aggravation in psoriasis (Jaworecka et al., 2021). However, previous studies yielded contradictory results. Some researchers have observed that compared with nonpruritic skin, NGF content was increased in pruritic psoriasis skin lesions (Yamaguchi et al., 2009) accompanied by increased nerve density in the skin (Tan et al., 2019), whereas others did not see such a correlation (Taneda et al., 2011). Further studies are needed to clarify its exact role in psoriasis.

To that end, this study sought to investigate whether CB2R deficiency modifies skin nerve fibers hyperreactivity and the itch-related scratching observed in psoriatic mice by regulating NGF. This study also assessed the role and mechanism of CB2R in IMQ-induced psoriasis inflammation and itch.

MATERIALS AND METHODS

Chemicals and Reagents

AM-630 (A3168), JWH-133 (B7941) were purchased from APExBIO (United States). Dimethyl- sulfoxide (DMSO) was purchased from Sigma. AM-630 and JWH-133 were dissolved in 10% DMSO, 20% Tween-80 and 70% saline. Mice were injected intraperitoneally with AM-630 (1/3/5 mg/kg/day), JWH-133 (1/3/5 mg/kg/day), and intradermally with them 2.5 mg/kg/day respectively, or an equal volume of solvent (control group) every day.

Human Sample Collection

Skin sample were obtained through surgical biopsy from Union Hospital, Tongji Medical College of Huazhong University of Science and Technology in Wuhan, China. All patients involved signed informed consent. The research protocols conformed to the declaration of Helsinki Principles and were approved by the medical ethics committee of Tongji Medical College of Huazhong University of Science and Technology.

Animals

All the animal experimental protocols in this study were conducted in accordance with the ARRIVE guidelines and were approved by the Institutional Animal Care and Use Committee of Tongji Medical College of Huazhong University of Science and Technology (Wuhan, China). Male CB2R$^{-/-}$ mice on C57BL/6 background and C57BL/6 wild-type mice aged 6–8 weeks were purchased from Jackson Laboratories. Experimental groups consisted of five mice each and the studies were repeated three times.

Induction of Psoriasiform Skin Inflammation by Imiquimod

A daily topical dose of 62.5 mg of commercially available imiquimod cream (5%) (Mingxin Pharmaceuticals, Sichuan, China) was applied to the shaved back skin (2.5 cm × 2 cm) of mice for seven consecutive days (days 0–6) (Moos et al., 2019).

Control mice were treated similarly with vaseline jelly as the control vehicle cream. Disease severity was assessed by using a scoring system based on the clinical Psoriasis Area and Severity Index (PASI). To be precise, erythema, scaling, and thickening were scored independently on a scale from 0 to 4 (0, none; 1, slight; 2, moderate; 3, marker; 4, very marked), and the cumulative score was used as a total score (scale 0–12). Disease severity was assessed by two researchers in a blinded manner. On day 8, serum samples and skin tissues were taken from the sacrificed mice for subsequent studies.

Behavioral Scratching Testing

The behavioral scratching was recorded by video. Mice were habituated individually to an observation chamber for 30 min before testing for five consecutive days. Twenty to 22 hours after each topical application of IMQ, mice were videotaped from below for 60 min. The number of videotaped scratch bouts was counted by two trained observers blinded to the treatment condition. A scratch bout was defined as one or more rapid back-and-forth hind paw motions directed toward and contacting the treated area or scratched directly at the area around the injection site continuously for any length of time and lasted, ending with licking or biting of the toes or placement of the hind paw on the floor (Sakai et al., 2016). The use of each fore paw was classified as grooming behavior and was not considered scratching.

Histology and Immunohistochemistry

Animals were euthanized under sodium pentobarbital anesthesia, and the skin was acutely dissected on the ice. Skin was fixed in 4% paraformaldehyde, embedded in paraffin and cut in 15-μm sections on a microtome. The sections were partly stained with hematoxylin and eosin (H&E) or toluidine blue, or prepared for rabbit monoclonal anti-CD4 (1:1000, Abcam) for IHC. Means of epidermal thickness, the number of mast cells and the degranulation mast cell from toluidine blue staining were calculated based on five randomly selected fields of view per mouse as previously described (Liu et al., 2017). And stained cells were counted under high original magnification (×200) power fields of a light microscope by ImageJ software. Each section was examined independently by two investigators in a blinded manner.

Immunofluorescence Analysis

Skin was fixed in 4% paraformaldehyde for 24 h and dehydrated with 30% sucrose, frozen in optimal cutting temperature (OCT) compound (Tissue-Tek, Sakura Finetek, Torrance, CA), and cut in 15-μm sections on a cryostat. The sections were incubated with 5% donkey serum and then immunofluorescent staining with a rabbit CB2R (1:200, Abcam, Cambrige, United Kingdom), PGP 9.5 (1:500, ABclonal), c-kit (1:500, RD system) at 4°C overnight, followed by incubation with the corresponding secondary antibody conjugated with Alexa Fluor 594 (1:500; Jackson Laboratory) at 37°C for an hour. All sections were counterstained with 4′,6-diamino-2-phenylindole (DAPI) at room temperature for 5 min. Images were captured from 3-4 skin sections from each animal and were imaged at 20× magnification.

The PGP 9.5-immunoreactive nerve fibers crossing the epidermis from the dermis were quantified by IENFD (expressed as fibers/linear mm) as described previously (Gylfadottir et al., 2022).

Western Blotting

Total proteins samples from the mouse tissues were extracted using lysis buffer for 30 min and the lysates were centrifuged at 12,000 rpm for 15 min at 4°C. The concentrations of proteins in the supernatants were measured using a BCA protein assay kit. Equal amounts of protein were separated by SDS-PAGE gel electrophoresis and then transferred to PVDF membranes. After blocking with 5% skim milk powder for 1 h at room temperature, the membranes were incubated with primary antibodies against CB2R (1:500, ABclonal), NGF (1:500, Affinity) and β-actin (1:20,000, ABclonal) at 4°C overnight. Secondary antibodies were labeled with horseradish peroxidase and incubated for 1 h at room temperature. The antigen-antibody complexes formed were detected by enhanced chemiluminescence in accordance with the manufacturer's instructions. Band signal intensities of the western blot films were assessed using the ImageJ software. Relative protein expression levels were normalized to that of β-actin (internal control).

RNA Isolation and Quantitative Real-Time PCR

RNA isolation was performed using Trizol reagent (Vazyme Biotech Co. Ltd, Nanjing, China). Conversion of total RNA to cDNA was performed with cDNA Reverse Transcription Kit (Vazyme Biotech Co. Ltd, Nanjing, China). All real-time PCR reactions were performed using the Real Time PCR System and the quantitative reverse-transcription PCR assay was carried out using SYBR Green PCR Master Mix (Vazyme Biotech Co. Ltd, Nanjing, China) on StepOne v2.3 detection system (Life Technologies, CA, United States). Forty cycles of amplification were performed involving sequential denaturation at 95°C for 30 s, annealing at 60°C for 5 s, and extension at 72°C for 30 s. The messenger RNA (mRNA) levels were normalized to those of the β-actin gene. Real-time PCR analysis was performed using the $2^{-\triangle\triangle CT}$ method. All primer pairs are listed in **Table 1**.

Flow Cytometry Analysis

Spleens from the individual mice were freshly isolated and mechanically dissociated. RBCs were lysed with lysis buffer (Biosharp, Beijing Labgic Technology Co. Ltd). Single cell suspensions of spleen were passed through a 40-μm sterile wire screen. Cell suspensions were washed twice in RPMI 1640 (Gibco, ThermoFisher Biochemical Products Co. Ltd) and stored in media containing 10% FBS on ice until used within 2 h. Splenocytes were stimulated with 50 μL phorbol 12-myeistate 13-acetate (PMA) (1 μg/ml), 40 μL ionomycin (50 μg/ml), and 20 μL monensin (0.1 mg/ml) for 5 h at 37°C humidified incubator. For cell surface antigen staining, cells

TABLE 1 | Primer sequences for real-time quantitative PCR.

Name	Forward 5′ - 3′	Reverse 5′ - 3′
CB2	CGTGATCTTCGCCTGCAACT	GTCAACAGCGGTTAGCAGCA
β-actin	TGGCACCCAGCACAATGAA	TAAGTCATAGTCCGCCTAGAAGCA
GAPDH	TCTCCTGCGACTTCAACA	TGTAGCCGTATTCATTGTCA
NGF	AAGGCTTTGCCAAGGACG	GTGATGTTGCGGGTCTGC
IL-1β	CTTCAGGCAGGCAGTATC	CAGCAGGTTATCATCATCATC
TNF-α	TGTCCATTCCTGAGTTCTG	GGAGGCAACAAGGTAGAG
IL-17A	ACTACCTCAACCGTTCCA	GAATCTGCCTCTGAATCCA
IL-17F	TGCTACTGTTGATGTTGGGAC	AATGCCCTGGTTTTGGTTGAA
IL-17C	ATGCTTGTGTCGTGGATG	GTGCCTGGAATGTCTGTC
IL-23A	ACCTGCTTGACTCTGACA	CCACTGCTGACTAGAACTC
IL-10	TTTGAATTCCCTGGGTGAGAA	ACAGGGGAGAAATCGATGACA
IL-6	CCGCTATGAAGTTCCTCTC	GGTATCCTCTGTGAAGTCTC
CXCL-1	CTGGGATTCACCTCAAGAACATC	CAGGGTCAAGGCAAGCCTC
CCL-20	GCCTCTCGTACATACAGACGC	CCAGTTCTGCTTTGGATCAGC
TGF-β	TTGCTTCAGCTCCACAGAGA	TGGTTGTAGAGGGCAAGGAC
ROR-γt	GTGGAGCAGAGCTTAAACCCC	ATGACTGAGAACTTGGCTCCC
Foxp-3	CACCTATGCCACCCTTATCCG	CATGCGAGTAAACCAATGGTAGA
IL-31	TCAGCAGACGAATCAATACAGC	TCGCTCAACACTTTGACTTTCT
TSLP	ACTGCCATGATGAGGTGGTC	GTCCTGGGTCTGAACCCTTT

were pre-blocked for Fc receptors (BD, Pharmingen) for 15 min at 4°C. The cells were then washed with staining buffer following by staining with Abs for 1 h at 37°C. The cells were washed with staining buffer, then resuspended in 300 μL of staining buffer. Flow cytometry was carried out using a FACS Canto II flow cytometer (BD) and the ratio of Th17 cells and Treg cells were analyzed. All the antibodies information were listed in **Supplementary Table S1**.

Cytometric Beads Array for Detecting Mouse Th1/Th2/Th17 Cytokines

The content of Th1/Th2/Th17 cytokines including IL-2, IL-4, IL-6, IL-10, TNF-α, IFN-γ and IL-17A concentrations was measured by the CBA kits (BD, Pharmingen, United States) according to the manufacturer's protocols. Data were acquired on FACS Canto-II flow cytometer (BD Bioscience, United States) and analyzed using FCAP Array software (BD Bioscience).

Statistics

The data were expressed as mean ± SD and analyzed by Graph Prism 8.2 software (GraphPad Software, San Diego, CA, United States). One-way analysis of variance (ANOVA) analyses was used to evaluate changes in groups by SPSS 25.0 software (SPSS Software, United States). Results were considered statistically significant if $^{*}p$ values were <0.05, $^{**}p$ values were <0.01 or $^{***}p$ values were <0.001 between the control and experimental groups.

RESULTS

CB2R Deficiency Exacerbated Psoriasiform Dermatitis Induced by IMQ Treatment

Although major CB2R immunoreactivity in basal keratinocytes of the epidermis in human skin has been observed (Ständer et al., 2005), reports about CB2R expression in PsD and human psoriasis lesions are lacking. We first analyzed CB2R localization in psoriatic skin tissues by immunofluorescence staining. We observed that the fluorescence intensity of CB2R in the epidermis of psoriatic lesions was greater than that of normal skin. These cells were mainly located in the cytoplasm of the epithelial cells and diffusely distributed in the suprabasal keratinocytes of the epidermal stratum spinosum and stratum granulosum in psoriasiform skin and psoriatic lesion biopsies (**Figure 1A**). Strong positive staining for CB2R was also observed in the dermis in human compared with negative control (**Supplementary Figure S1**). Next, we measured CB2R protein and mRNA expression levels in psoriasiform skin inflammation and normal skin tissues using WB and qRT-PCR analysis. **Figures 1B–D** showed that CB2R levels were significantly increased in the IMQ group compared with the normal control group. These data showed dysregulation of CB2R in psoriasis.

Then, we investigated the clinical and histopathological features of WT and CB2R KO mice following IMQ treatment. CB2R KO mice exhibited worse clinical outcomes with more severe erythema and scales and increased skin thickness by IMQ application than WT mice (**Figure 1E**). Hematoxylin-eosin (H&E) staining performed on the dorsal skin of the mice on Day 7 revealed more severe epidermal hyperplasia, significantly increased acanthosis and parakeratosis and more intense inflammatory cell infiltration in CB2R KO mice than in WT mice after IMQ application (**Figure 1F**). Consistently, the average Psoriasis Area and Severity Index (PASI) scores of the four groups were graded daily to assess their clinical changes. Compared with WT mice, the total PASI scores of CB2R KO mice were increased after IMQ application (**Figure 1G**). We measured epidermal thickness with ImageJ analysis of H&E skin sections. Epidermal hyperplasia was significantly increased in CB2R KO mice compared with WT mice (**Figure 1H**). Thus, CB2R deficiency exacerbated IMQ-induced PsD.

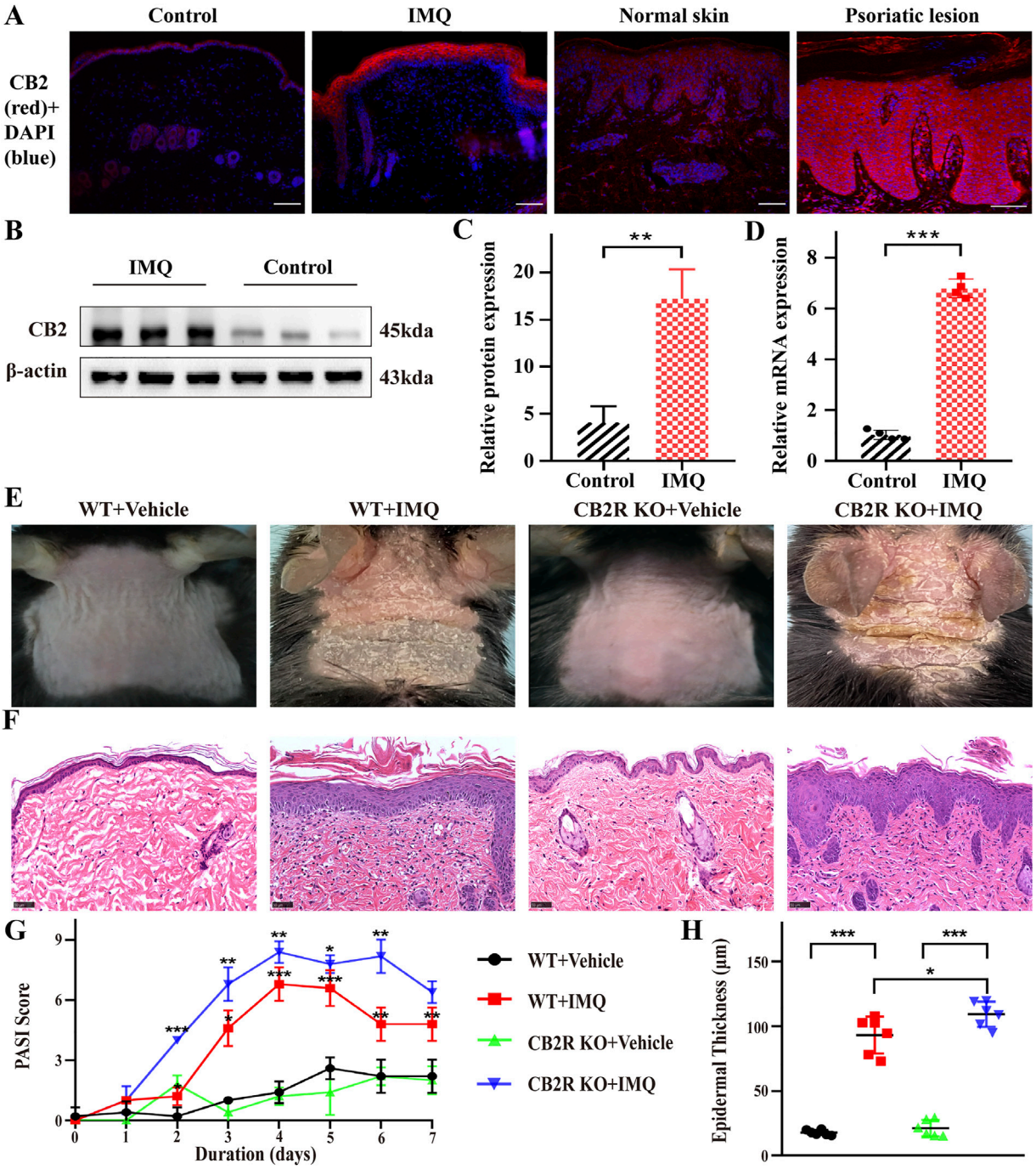

FIGURE 1 | CB2R was upregulated throughout the epidermis, and CB2R deficiency exacerbated the morphological and histological features of psoriasiform dermatitis induced by IMQ treatment. **(A)** Immunofluorescence was used to detect the protein level of CB2R in psoriasiform dermatitis, human normal skin and psoriasis lesions (scale bar: 100 μm). blue, DAPI; red, CB2R. **(B, C)** Protein levels of CB2R were quantified by western blotting. β-actin was used as a loading control. Relative protein expression was normalized to that of the internal control. **(D)** mRNA levels of CB2R in skin tissues from the normal and psoriasis groups were analyzed by real-time quantitative PCR. **(E)** Representative phenotype manifestation of WT and CB2R KO mouse back skin induced by IMQ application at day 7. **(F)** H&E staining of cross-sectional slices of the dorsal skin of C57BL/6 mice on the seventh day. Scale bar represents 50 μm. **(G)** Clinical scores for disease severity were calculated daily of epidermal erythema, scales, and thickening of the dorsal skin. The PASI score was calculated by adding the scores of three independent criteria (ranging from 0 to 12). **(H)** The epidermal thickness of the dorsal skin on the seventh day was measured by four randomly selected fields per section of each mouse. Results are representative of three independent experiments. Error bars represent mean ± SD. (n = 5 for each group). *p < 0.05, **p < 0.01, and ***p < 0.001 when compared.

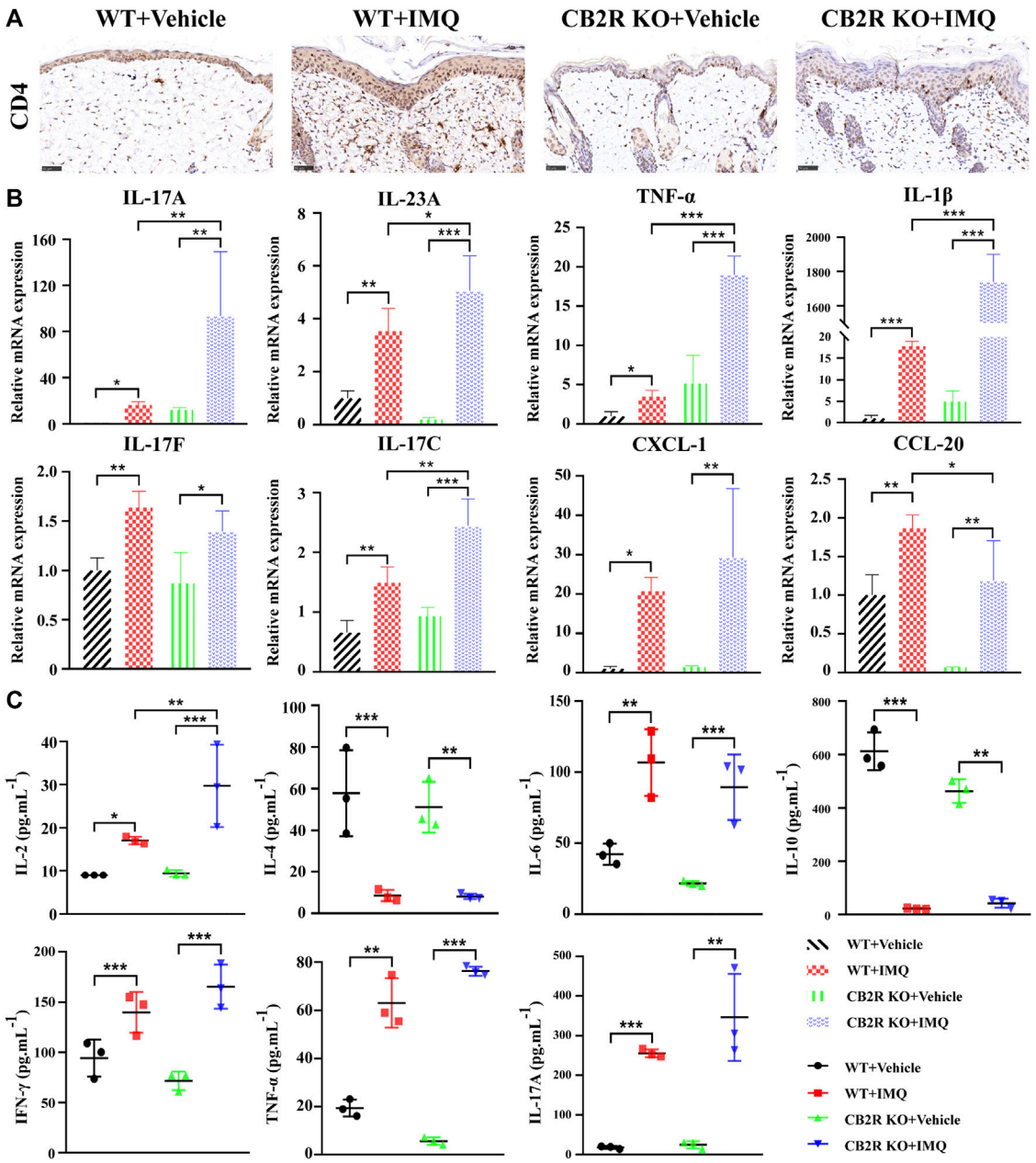

FIGURE 2 | Effects of CB2R on the infiltration of CD4$^+$ T cell and expression levels of inflammatory cytokines in mice with IMQ-induced psoriasiform dermatitis. **(A)** The representative immunohistochemical staining images of IMQ- and vehicle- treated skin in WT and CB2R KO mice at day 7. Scale bar represents 50 μm.**(B)** Real-time quantitative PCR was performed to quantify the mRNA level of IL-17A, IL-23A, TNF-α, IL-1β, IL-17F, IL-17C, CXCL-1, CCL-20 in the skin biopsies from mice. Data are obtained from duplicate samples from five mice in each group. **(C)** CBA assay was performed to quantify the protein level of IL-2, IL-4, IL-6, IL-10, IFN-γ, TNF-α and IL-17A in the serum from mice. All the assays were repeated three times with consistent results. Error bars represent mean ± SD. *$p < 0.05$, **$p < 0.01$, and ***$p < 0.001$ when compared.

CB2R Deficiency Increased CD4$^+$ T Cells Infiltration and Proinflammatory Cytokines Expression in IMQ Mice

In both psoriasis and relevant mouse models, the IL-23/Th17 axis and Th1/Th2/Th17 balance play a major role in disease (Gauld et al., 2019). To appraise the effects of CB2R on IMQ-induced local and systemic inflammation, we used IHC to observe the infiltration of CD4$^+$ T cells, which are the main source that induce differentiation into various subtypes of T cells in psoriasis. The numbers of CD4$^+$ T cells in IMQ-treated CB2R KO mice were significantly increased compared with those in IMQ-treated WT mice (**Figure 2A** and **Supplementary Figure S2A**). We also examined the mRNA expression of key inflammation genes

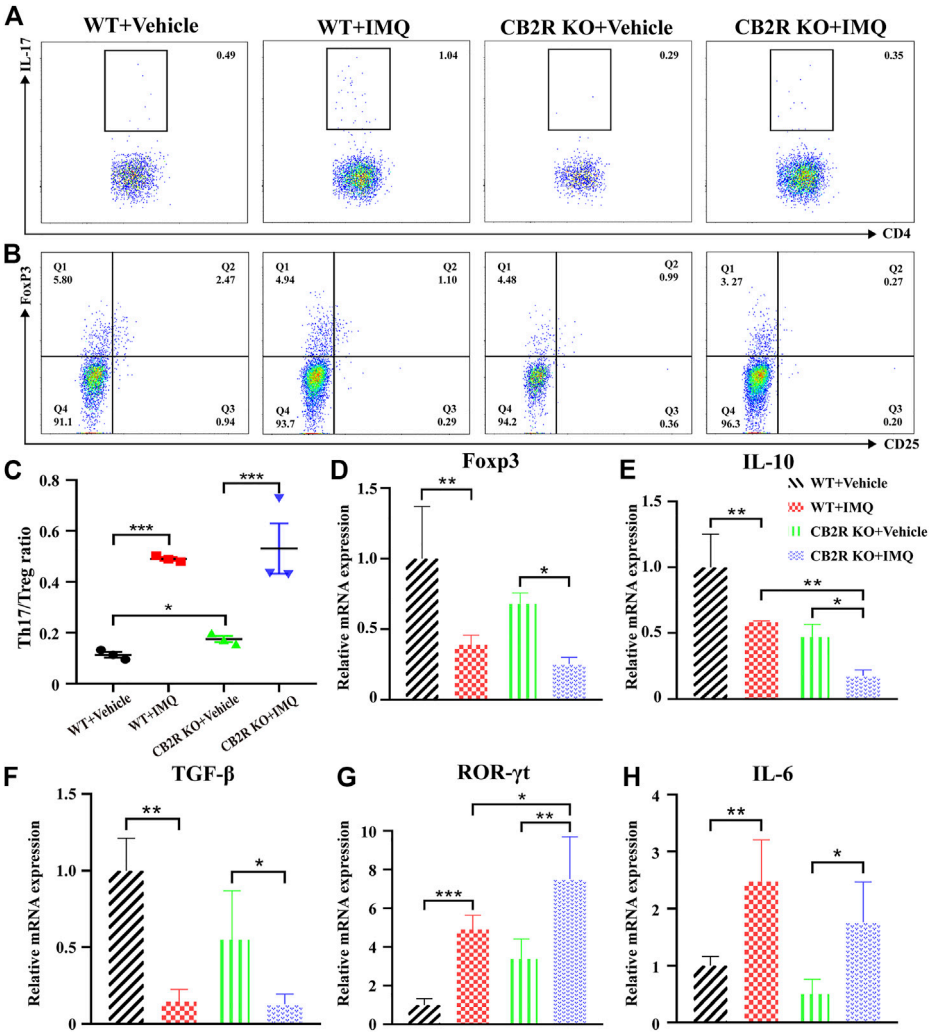

FIGURE 3 | Effects of CB2R deficiency on differentiation proportion of Th17/Treg in IMQ-induced PsD. **(A)** Flow cytometric analysis of the proportion of Th17 cells ($CD4^+$, $IL\text{-}17A^+$ cells) in single cell suspensions of spleen of IMQ- and vehicle- treated skin in WT and CB2R KO mice. **(B)** Flow cytometric analysis of the proportion of Treg cells ($CD4^+$, $CD25^+$, and $Foxp3^+$ cells) in single cell suspensions of spleen of IMQ- and vehicle- treated skin in WT and CB2R KO mice. **(C)** The ratio of Th17/Treg cells. **(D-H)** The mRNA expression levels of Foxp3 **(D)**, IL-10 **(E)**, TGF-β **(F)**, ROR-γt **(G)**, IL-6 **(H)**. Error bars represent mean ± SD. $^*p < 0.05$, $^{**}p < 0.01$, and $^{***}p < 0.001$ when compared.

that are known to regulate psoriatic skin inflammation. As shown in **Figure 2B**, relatively increased mRNA levels of IL-17A, IL-23A, TNF-α, IL-1β, and IL-17C were noted in the psoriasiform skin lesions of CB2R KO mice as compared with WT mice. Although the expression of IL-17F, CXCL-1, and CCL-20 in IMQ-treated CB2R KO PsD mice was higher than that in CB2R KO vehicle mice, there was no significant difference in PsD between CB2R KO mice and WT mice, and CCL-20 mRNA levels were somewhat lower in the two groups. In addition, the CBA assay showed that the levels of Th1 (IL-2, IFN-γ, TNF-α) and Th17 (IL-17A) cell-related cytokines in the serum were markedly increased, whereas the levels of Th2 cell-related cytokines (IL-4, IL-10) were significantly decreased in PsD mice compared with normal mice in both the WT and CB2R KO groups. Interestingly, CB2R deficiency exhibited the greatest impact on the expression of IL-2 in the serum after applying IMQ, given that the changes in several other cytokines were not statistically significant (**Figure 2C**). These results indicated that CB2R deficiency exacerbated the IMQ-induced skin inflammation by regulating inflammatory cell infiltration and the release of local and systemic inflammatory cytokines.

CB2R Deficiency Promoted the Differentiation Proportion of Th17/Treg Cells Among $CD4^+$ T Cells

It is well known that psoriasis may result from massive inflammatory cellular infiltrates and/or an imbalance in T cells, especially in Th17/Treg cells (Shi et al., 2019). Furthermore, it has been reported that CB2R activation may change the balance of

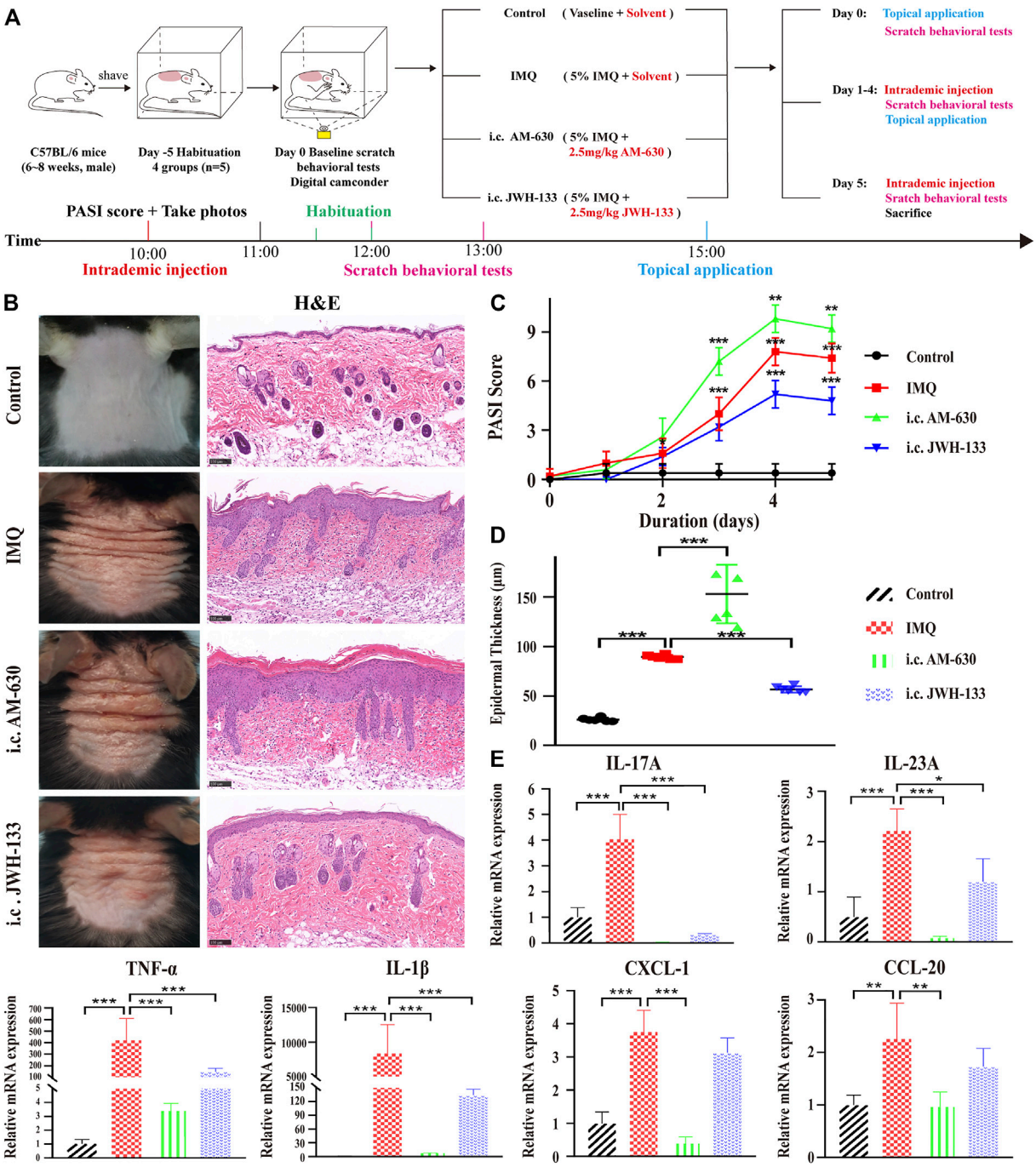

FIGURE 4 | The selective agonist of CB2R, JWH-133, could alleviate PsD in IMQ-induced mice. **(A)** Schematic diagram of the animal experiment protocol for the control, IMQ, i.c. AM-630 and i.c. JWH-133 groups ($n = 5$). **(B)** Representative macroscopic view and H&E staining of cross-sectional slices of the dorsal skin of C57BL/6 mice on the fifth day. Scale bar represents 100 μm. **(C)** Daily assessment of epidermal erythema, scales, and thickening of the dorsal skin. The PASI score was calculated by adding the scores of three independent criteria (ranging from 0 to 12). **(D)** The epidermal thickness of the dorsal skin on the fifth day was measured by four randomly selected fields per section of each mouse. **(E)** The mRNA expression levels of IL-17A, IL-23A, TNF-α, IL-1β, CXCL-1 and CCL-20 were measured by qRT-PCR. Error bars represent mean ± SD. ($n = 5$ for each group). $^{*}p < 0.05$, $^{**}p < 0.01$, and $^{***}p < 0.001$ when compared. All the assays were repeated three times with consistent results.

Th17/Treg cells in lung tissues (Wei et al., 2021), but it remains unclear whether it plays the same role in psoriasis. To probe the effect of CB2R in regulating the Th17/Treg cell balance on IMQ-induced systemic inflammation, we next performed flow cytometric analysis of splenic single cells. We found that the proportion of Th17/Treg cells was increased in IMQ-induced

PsD mice compared with vehicle-induced control mice. However, CB2R deficiency slightly increased the ratio of Th17/Treg cells in the spleen compared to that of WT mice after IMQ application. However, this effect was more obvious in vehicle mice (**Figures 3A–C**). We also verified the mRNA expression levels of ROR-γt, TGF-β, IL-6, Foxp3 and IL-10, which play a critical role in the differentiation of Th17 and Treg cells, respectively. Importantly, the mRNA levels of Treg-related transcription factors and cytokines, including Foxp3, IL-10, and TGF-β, were significantly decreased in CB2R KO-PsD mice compared with CB2R KO-vehicle mice (**Figures 3D–F**). In contrast, Th17-related transcription factors and cytokines, including ROR-γt and IL-6, were significantly increased in the two groups (**Figures 3G,H**). Compared with WT mice, CB2R deficiency had a more obvious effect on IL-10 and ROR-γt expression after applying IMQ. In summary, the experiments demonstrated that CB2R deficiency promoted the proportion of Th17/Treg cells among $CD4^+$ T cells.

The CB2R Agonist JWH-133, was Effective Against IMQ-Induced PsD

We further applied the CB2R agonist JWH-133 and the CB2R antagonist AM-630 to observe their effects on PsD. JWH-133, AM-630 or solvent (10% DMSO+20% Tween-80 + 70% saline) was intraperitoneally (i.p.) injected into WT mice during IMQ treatment. We first found that 5 mg/kg was the optimum dose because 1 and 3 mg/kg were not effective. Intraperitoneal treatment with 5 mg/kg JWH-133 improved the PASI score. Because CB2R was mainly located on the epidermis, then we observed that mice received 2.5 mg/kg JWH-133 intracutaneously (i.c.) showed a significant attenuation of psoriasis inflammation compared with those that received an intraperitoneal injection. Thus, an IMQ-induced PsD mouse model and simultaneous intracutaneous injection pretreatment with AM-630 or JWH-133 were conducted to verify the role of CB2R *in vivo* (**Figure 4A**). Compared with the IMQ group, JWH-133 visibly alleviated the clinical phenotype of IMQ-induced PsD but did not completely eliminate the macroscopic clinical symptoms, which included redness and thickening of the skin reduction. Histological results showed that JWH-133 significantly improved the histologic changes, which showing less parakeratosis and less inflammatory cell infiltration than the IMQ group. In contrast, AM-630 had the opposite effect (**Figure 4B**). Similarly, the i.c. JWH-133 group showed lower PASI scores (**Figure 4C**) and less epidermal thickening (**Figure 4D**). Consistently, JWH-133 also significantly reduced the mRNA expression levels of proinflammatory cytokines, including IL-17A, IL-23A, TNF-α, IL-1β, CXCL-1 and CCL-20, in skin lesions (**Figure 4E**). Of note, the expression levels of proinflammatory cytokines also decreased after i.c. administration of AM-630. It is possible that the dose was insufficient or the pharmacological effect of the antagonist was not as thorough as knocking out the receptor. These results demonstrated that CB2R activation alleviated inflammation in IMQ-induced PsD.

CB2R Deficiency Intensified the Scratching Behaviour of IMQ-Induced Psoriatic Mice

It has been reported that CB2R agonists significantly suppress scratching behaviour induced by compound 48/80, histamine, substance P or serotonin in mice or rats (Odan et al., 2012; Haruna et al., 2015), but all of those compounds are the pruritogens of acute itch. Spontaneous scratching and psoriasiform skin lesions can be induced by topical stimulation of IMQ (Sakai et al., 2016), which simulates the chronic itch of psoriasis. To investigate the effect of CB2R on the chronic itch in psoriasis, we followed the schematic experimental protocol (**Figure 4A**). The results showed that mice treated with IMQ indeed exhibited more scratching bouts than the control group. Both CB2R deficiency and i.c. AM-630 injection intensified the scratching behaviour, whereas i.c. JWH-133 alleviated the scratching behaviour compared with that in the IMQ model group (**Figures 5A,B**). We next examined the sensory nerve fibers in lesion skin and untreated skin from WT mice and CB2R KO mice. Nerve fibers density was analyzed using immunofluorescence to visualize protein gene product 9.5 (PGP 9.5)-positive nerve fibers, which are known as peripheral sensory nerve markers (Feld et al., 2016). As shown in **Figure 5C** and **Supplementary Figure S2B**, CB2R KO showed that dermal nerve fibers extended to the epidermis, and a significant increase in the density of PGP 9.5-positive nerve fibers at the junction of the dermis and epidermis was noted in IMQ-induced PsD skin compared with WT mice or vehicle-treated skin. To further explore the mechanism of itch, we hypothesized that the changes in nerve fibers involved NGF-induced neuronal growth. Western blot and qRT-PCR revealed an increase in NGF expression levels in the IMQ group compared with the normal control group. However, CB2R KO only affected NGF gene expression level but did not significantly influence NGF protein expression (**Figures 5D,E**). Taken together, these results suggested that the extension of nerve fibers into the epidermis could be involved in the itch-related scratching of mice, and CB2R deficiency intensified the scratching behaviour of IMQ-induced psoriatic mice by regulating the expression of nerve fibers. Moreover, all of these effects could be reversed by JWH-133, but the effects of the antagonists AM-630 were not as significant as those of the knockout mice.

The Regulation of CB2R on Psoriatic Itch was Independent of IL-31, TSLP and Mast Cells

IL-31, thymic stromal lymphopoietin (TSLP) and mast cells have recently attracted much attention as targets for chronic itch therapy (Agarwala et al., 2016). However, whether CB2R is involved in psoriatic itch by regulating these cytokines and mast cells remains unclear. We used immunofluorescence to label the mast cells surface marker c-kit and toluidine lube staining to observe the changes in the number and activation of mast cells in the skin. As shown in **Figures 6A–E**, the infiltration and degranulation rate of mast cells increased after IMQ treatment in WT mice. However, we found no difference in

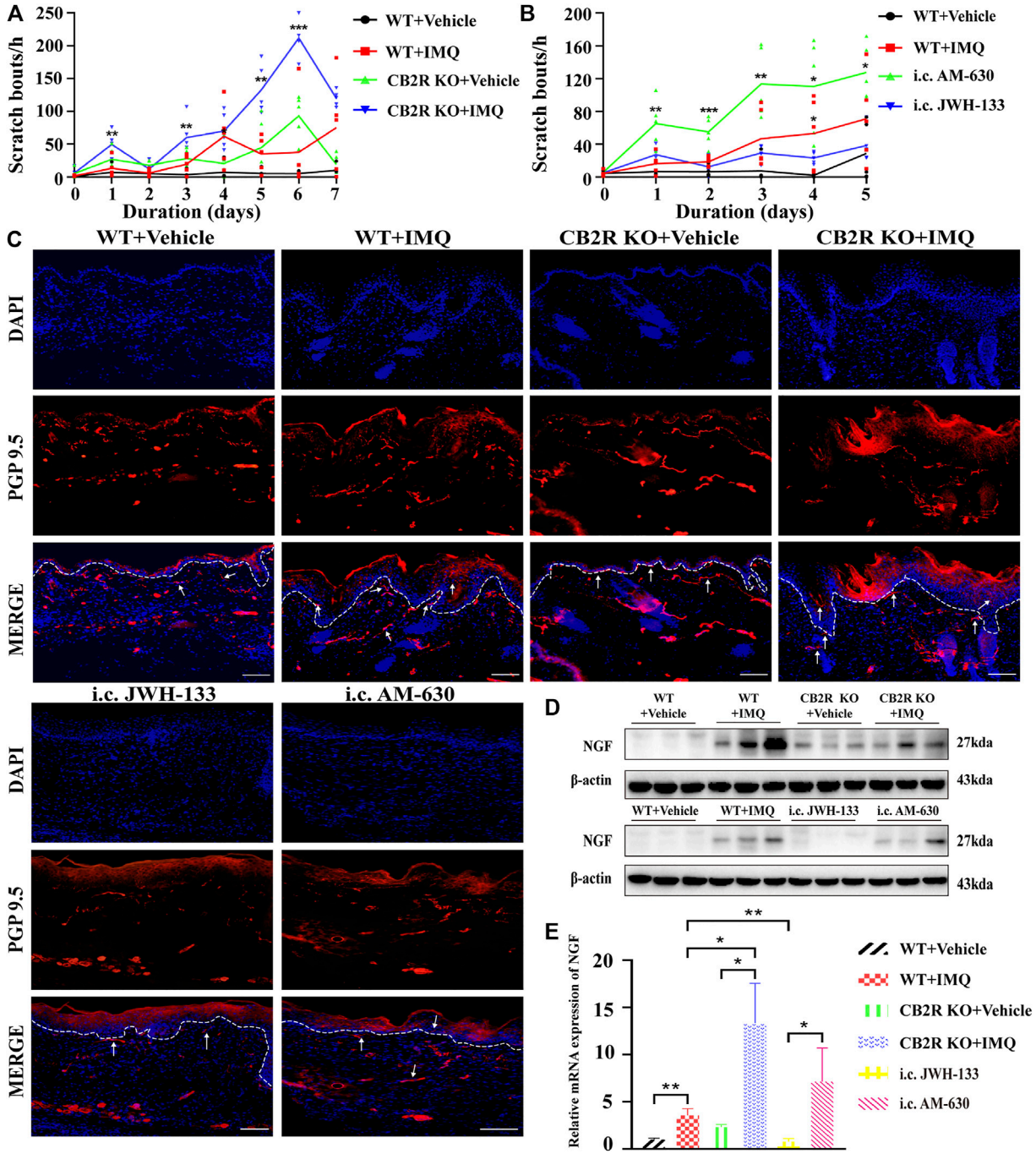

FIGURE 5 | Effects of CB2R on the scratching behavior and expression of nerve fibers in IMQ-induced PsD. **(A, B)** The behavior results of mice in different groups. **(C)** PGP 9.5 stained (red fluorescence) nerve fibers in the skin biopsies from mice, co-stained with DAPI (blue fluorescence) to detect the nucleus. Scale bar represents 100 μm. **(D)** Protein level of NGF was analyzed by western blotting in the six groups of mice. β-actin served as the loading control. **(E)** The mRNA expression levels of NGF was measured by qRT-PCR. Error bars represent mean ± SD. ($n = 5$ for each group). *$p < 0.05$, **$p < 0.01$, and ***$p < 0.001$ when compared. All the assays were repeated three times with consistent results.

mast cells between IMQ-treated CB2R KO mice and WT mice. Interestingly, CB2R KO significantly reduced the mRNA expression of IL-31 and TSLP after IMQ application compared with WT mice (**Supplementary Figures S2C,D**), showing an opposite trend to scratching bouts. Intradermal JWH-133 reversed the expression of IL-31and TSLP and the activation of mast cells in PsD mice. Collectively, these data suggested that CB2R didn't participate in the induction of itch in psoriasis by regulating the expression of IL-31, TSLP and mast cells in mice.

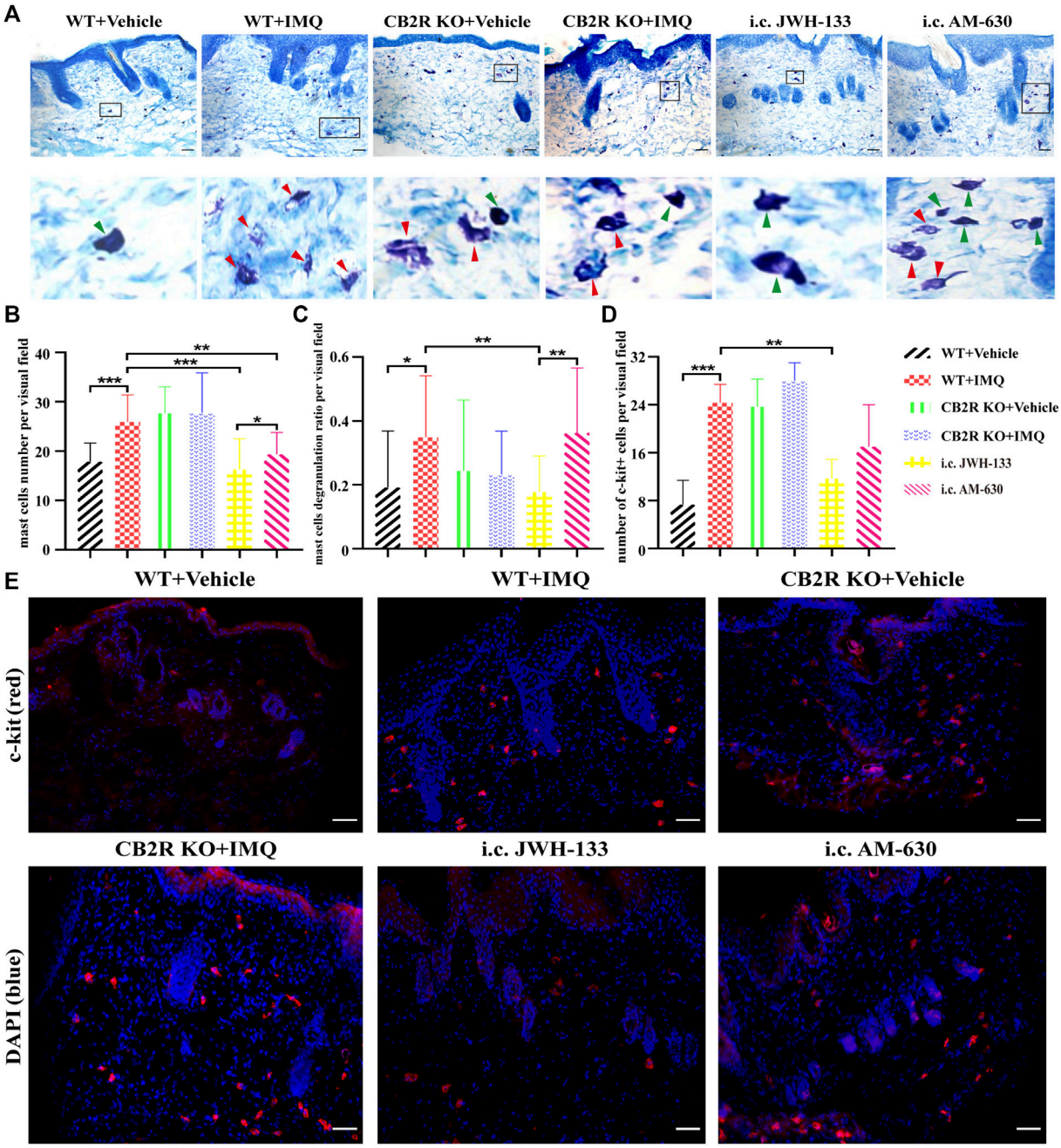

FIGURE 6 | Regulation of mast cells number and degranulation by CB2R in IMQ-induced psoriasis. **(A–C)** Toluidine bule staining to detect the number and the degranulation of mast cells, green arrows pointed to non-degranulated mast cells, red arrows pointed to degranulated mast cells. **(D, E)** Immunofluorescence to analysis of c-kit (mast cell marker) expression and quantification of mast cells number in the skin. Error bars represent mean ± SD. *$p < 0.05$, **$p < 0.01$, and ***$p < 0.001$ when compared. Scale bar represents 100 μm.

DISCUSSION

In recent years, an emerging concept has been proposed that the skin serves as a neuro-endocrine-immune organ to maintain global and local homeostasis through multidirectional communication among the brain, the endocrine and immune systems, and peripheral organs (Slominski and Wortsman, 2000). This homeostasis can be unbalanced due to environmental stress, trauma and metabolic disorders, underscoring the pathogenesis of some skin diseases, such as atopic dermatitis and psoriasis (Slominski et al., 2012; Slominski et al., 2013). It is known that the pathogenesis of psoriasis is a result of complex interactions

among the neuroendocrine, immune and vascular systems (Armstrong and Read, 2020). Evidence suggests that CB2R plays a critical role in immune modulation and sensory conduction (Sheriff et al., 2020; Graczyk et al., 2021). Although CB2R-mediated immune responses have been observed in other inflammatory skin diseases, including skin wound healing (Wang et al., 2016; Du et al., 2018), allergic contact dermatitis (Karsak et al., 2007) and artificially induced dermatitis (Haruna et al., 2017), little is known about their role in psoriasis. We first found that CB2R expression levels were significantly increased in psoriatic lesions compared with normal skin. CB2R was mainly expressed in the suprabasal epidermis, indicating that endocannabinoid signaling is implicated in the regulation of the epidermal permeability barrier homeostasis (Roelandt et al., 2012). Positive staining for CB2R was also observed in the dermis, which may be due to it located in cutaneous nerve fiber bundles, mast cells, macrophages, the epithelial cells of hair follicles, sebocytes and eccrine sweat glands (Ständer et al., 2005). These findings were consistent with the concept that CB2R expression increased by greater than 100 times the base level due to the inflammation (Lu and Mackie, 2016). CB2R overexpression in psoriatic skin tissues may be a synergistic action of acanthosis cell layer thickening, or it may be a self-protective response of reactive upregulation to inhibit keratinocyte proliferation. CB2R deficiency unexpectedly exacerbated psoriasiform skin inflammation.

The balance of Th17/Treg cells plays a critical role in the pathogenesis of psoriasis. Some studies have shown that Treg cells are easily converted into Th17 cells under psoriatic inflammatory conditions (Bovenschen et al., 2011). Shi et al. confirmed the existence of an imbalance of Th17/Treg cells in psoriasis patients (Shi et al., 2019). CB2R is expressed in B lymphocytes, neutrophils, leucocytes CD8 and CD4, allowing cannabinoids to mitigate the inflammatory response (Graczyk et al., 2021). A previous *in vitro* study found that the CB2R selective agonist O-1966 activated Tregs and promoted increased IL-10 secretion in the mixed lymphocyte reaction culture supernatant (Robinson et al., 2015). In the present study, we found that CB2R KO contributed to the pathogenesis of psoriasis by promoting $CD4^+$ T cell proliferation; upregulating Th17 cytokines, such as IL-17A, IL-23A, and IL-17C; and downregulating IL-10. In addition, CB2R KO aggravated the imbalance of Th17 and Treg cells by regulating the expression of key transcription factors ROR-γt and Foxp3. The changes in these cytokines at the protein level were confirmed by CBA assay. The protein results showed the same trends as the mRNA results, suggesting that CB2R has a regulatory effect on systemic and local inflammation. Thus, future studies should focus on the molecular mechanism of CB2R activation in regulating $CD4^+$ T cell differentiation at the cellular level as a more representative comparison to our murine studies.

Although it has been reported that a variety of endogenous and exogenous CB2R agonists can suppress acute itch-associated scratching behaviour in rodents through inhibition of itch signal transmission (Haruna et al., 2015; Avila et al., 2020), the relationship between CB2R and chronic itch is poorly understood, especially in psoriasis itch. Previous studies have demonstrated that the increase in nerve fiber density and the prolongation of nerve fiber endings to the epidermis could promote itch hypersensitivity, which subsequently leads to psoriasis pruritus (Tominaga et al., 2007). We found that the immunoreactive nerve fibers treated with anti-PGP 9.5 antibody were markedly increased in the epidermis of IMQ-induced WT and CB2R deficiency mice on Day 7. Thus, these results appear to indicate that CB2R KO could lead to increased nerve ending density and length, and the changes in nerve fibers may be related to the frequency of scratching in psoriatic mice. Our work also provided evidence for the involvement of CB2R in the regulation of chronic itch.

The mechanisms by which nerve fibers extend in psoriatic mice and CB2R deficiency modulates itching remain unclear. Various studies provide evidence that some neurotrophins can contribute to neural extension (Menezes et al., 2019; Sultan et al., 2021). NGF is abundantly released from human keratinocytes in culture, and is highly expressed in the epidermis of psoriatic mice (Pincelli et al., 1994). Some researchers have observed that compared with nonpruritic skin, NGF content in pruritic psoriasis skin lesions was increased (Yamaguchi et al., 2009) and accompanied by increased nerve density in the skin (Tan et al., 2019). Furthermore, NGF expression in astrocytes and microglia was markedly upregulated by local tissue injury, inflammation and cytokines (Pöyhönen et al., 2019). Bozkurt et al. reported that CB1R activation could continuously modify neuronal airway hyperreactivity by inhibiting neuronal growth induced by NGF (Bozkurt et al., 2016). Whether CB2R has a similar effect on NGF expression has not yet been reported. Our results showed that NGF expression levels were significantly upregulated in psoriasis skin lesions. CB2R deficiency significantly increased NGF mRNA but not protein expression, and the translation of mRNA to protein might be inhibited by CB2R. We assumed that in pruritus psoriasis skin, the number of nerve fibers increases, and the new nerve fibers promote the continued secretion of NGF, resulting in abnormal hyperplasia of nerve fibers and more sensitive sensation. In addition, the local high expression of a variety of inflammatory factors for NGF secretion and nerve fiber hyperplasia are also effective stimuli, leading to pruritus paresthesia. Together, NGF expression and nerve fiber changes may represent the essential changes that are responsible for itching in CB2R-deficient psoriatic mice. However, there may be other factors in addition to NGF that cause nerve fiber changes and itch in psoriasis. The mechanism by which CB2R regulates NGF expression also needs to be further elucidated.

CB2R is mainly present in immune cells such as mast cells (Rom and Persidsky, 2013), and the latter have been implicated as key mediators of itch (Siiskonen and Harvima, 2019). Although it has been reported that the number and degranulation of mast cells elevated in pruritic psoriatic lesions (Harvima et al., 2008; Cho et al., 2017), lack of study investigate the correlation between CB2R and mast cells in psoriasis. Our data demonstrated that there was indeed an increase in the number and degranulation of mast cells in PsD. CB2R deficiency increased mast cells activation in normal control mice, but had no effect on

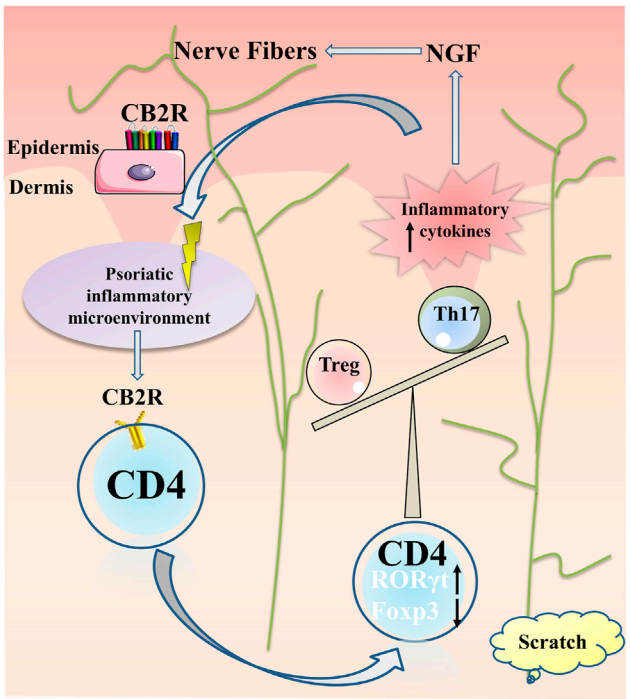

FIGURE 7 | Summary of CB2R actions in psoriatic inflammation and itch. Under the psoriatic inflammatory microenvironment, CB2R regulated proliferation and differentiation of $CD4^+$ T cell, increased ROR-γt expression and decreased Foxp3 expression, resulting in imbalance of Th17 and Treg cells, further aggravating the inflammatory microenvironment of psoriasis. The local high expression of a variety of inflammatory factors stimulated the keratinocytes secreting NGF for nerve fiber hyperplasia, resulting in pruritus paresthesia.

IMQ-induced psoriasis mice. IL-31 and TSLP are key cytokines directly promoting itch (Dillon et al., 2004; Wilson et al., 2013). Recent studies demonstrated that IL-31 and TSLP appear to be partially involved not only in the pathogenesis of psoriasis, but also in the induction of itch in psoriasis (Nattkemper et al., 2018; Gago-Lopez et al., 2019; Gibbs et al., 2019; Suwarsa et al., 2019). Our study was consistent with previous findings in WT mice. However, CB2R deficiency contributed to opposite results. Combined with the results of i.c. JWH-133 group, we cannot exclude the possibility that location of CB2R in other cells other than keratinocytes and mast cells might be involved in the pathogenesis. The generation of tissue - or cell-specific knockout CB2R mice is necessary for further studies.

In conclusion, our results suggested that CB2R may play a protective role in mediating immunosuppression by regulating the proliferation and differentiation of $CD4^+$ T cells and reducing the production of cytokines and chemokines. In addition, the reduction of the release of inflammatory factors may weaken the NGF secreted by keratinocytes, reduce the proliferation and elongation of nerve fibers, and have an antipruritic effect (**Figure 7**). The neuro-immune pathway may be involved in the regulation of inflammation and itch in psoriasis. Given CB2R's localized expression, most of the adverse side effects associated with systemic therapy can be avoided. Topical preparations are readily absorbed through the skin, which is traditionally the preferred route of delivery for treating psoriasis. These considerations have led to the hypothesis that topical selective CB2R agonists may have potential therapeutic applications for the treatment of psoriasis.

DATA AVAILABILITY STATEMENT

The original contributions presented in the study are included in the article/**Supplementary Material**, and at the following link, further inquiries can be directed to the corresponding authors: https://www.jianguoyun.com/p/Db79a-YQuImUChjCoqYE.

ETHICS STATEMENT

The studies involving human participants were reviewed and approved by Tongji Medical College of Huazhong University of Science and Technology. The patients/participants provided their written informed consent to participate in this study. The animal study was reviewed and approved by The Institutional Animal Care and Use Committee of Tongji Medical College of Huazhong University of Science and Technology.

AUTHOR CONTRIBUTIONS

LL, LM and CHX conceived and designed the study. LL, LX, WGQ, CC and ZMOY completed the experiments. HYQ, JLZ, KY, JJ, LF and LXM collected and analyzed data. DXR, LXX, ZX and XSB collected the psoriatic lesions. LL wrote the paper. LM and CHX reviewed and edited the manuscript. All authors read and approved the manuscript.

FUNDING

This work was supported by National Nature Science Foundation of China (Nos. 81974475, 82173423 and 82103731); Shenzhen Basic Research Project (Natural Science Foundation) (No. JCYJ20190809103805589; JCYJ20210324112213036).

ACKNOWLEDGMENTS

The authors thank all patients and healthy individuals who participated in this study.

SUPPLEMENTARY MATERIAL

The Supplementary Material for this article can be found online at: https://www.frontiersin.org/articles/10.3389/fphar.2022.790712/full#supplementary-material

REFERENCES

Agarwala, M. K., George, R., Pramanik, R., and McGrath, J. A. (2016). Olmsted Syndrome in an Indian Male with a New De Novo Mutation in TRPV3. *Br. J. Dermatol.* 174 (1), 209–211. doi:10.1111/bjd.13910

Armstrong, A. W., and Read, C. (2020). Pathophysiology, Clinical Presentation, and Treatment of Psoriasis: A Review. *JAMA* 323 (19), 1945–1960. doi:10.1001/jama.2020.4006

Avila, C., Massick, S., Kaffenberger, B. H., Kwatra, S. G., and Bechtel, M. (2020). Cannabinoids for the Treatment of Chronic Pruritus: A Review. *J. Am. Acad. Dermatol.* 82 (5), 1205–1212. doi:10.1016/j.jaad.2020.01.036

Boehncke, W.-H., and Schön, M. P. (2015). Psoriasis. *The Lancet* 386 (9997), 983–994. doi:10.1016/S0140-6736(14)61909-7

Bovenschen, H. J., van de Kerkhof, P. C., van Erp, P. E., Woestenenk, R., Joosten, I., and Koenen, H. J. (2011). Foxp3+ Regulatory T Cells of Psoriasis Patients Easily Differentiate into IL-17A-producing Cells and Are Found in Lesional Skin. *J. Invest. Dermatol.* 131 (9), 1853–1860. doi:10.1038/jid.2011.139

Bozkurt, T. E., Larsson, O., and Adner, M. (2016). Stimulation of Cannabinoid CB1 Receptors Prevents Nerve-Mediated Airway Hyperreactivity in NGF-Induced Inflammation in Mouse Airways. *Eur. J. Pharmacol.* 776, 132–138. doi:10.1016/j.ejphar.2016.02.045

Cho, K. A., Park, M., Kim, Y. H., and Woo, S. Y. (2017). Th17 Cell-Mediated Immune Responses Promote Mast Cell Proliferation by Triggering Stem Cell Factor in Keratinocytes. *Biochem. Biophys. Res. Commun.* 487 (4), 856–861. doi:10.1016/j.bbrc.2017.04.141

Dillon, S. R., Sprecher, C., Hammond, A., Bilsborough, J., Rosenfeld-Franklin, M., Presnell, S. R., et al. (2004). Interleukin 31, a Cytokine Produced by Activated T Cells, Induces Dermatitis in Mice. *Nat. Immunol.* 5 (7), 752–760. doi:10.1038/ni1084

Du, Y., Ren, P., Wang, Q., Jiang, S. K., Zhang, M., Li, J. Y., et al. (2018). Cannabinoid 2 Receptor Attenuates Inflammation during Skin Wound Healing by Inhibiting M1 Macrophages rather Than Activating M2 Macrophages. *J. Inflamm. (Lond)* 15, 25. doi:10.1186/s12950-018-0201-z

Feld, M., Garcia, R., Buddenkotte, J., Katayama, S., Lewis, K., Muirhead, G., et al. (2016). The Pruritus- and TH2-Associated Cytokine IL-31 Promotes Growth of Sensory Nerves. *J. Allergy Clin. Immunol.* 138 (2), 500–e24. doi:10.1016/j.jaci.2016.02.020

Gago-Lopez, N., Mellor, L. F., Megías, D., Martín-Serrano, G., Izeta, A., Jimenez, F., et al. (2019). Role of Bulge Epidermal Stem Cells and TSLP Signaling in Psoriasis. *EMBO Mol. Med.* 11 (11), e10697. doi:10.15252/emmm.201910697

Galiègue, S., Mary, S., Marchand, J., Dussossoy, D., Carrière, D., Carayon, P., et al. (1995). Expression of Central and Peripheral Cannabinoid Receptors in Human Immune Tissues and Leukocyte Subpopulations. *Eur. J. Biochem.* 232 (1), 54–61. doi:10.1111/j.1432-1033.1995.tb20780.x

Gauld, S. B., Jacquet, S., Gauvin, D., Wallace, C., Wang, Y., McCarthy, R., et al. (2019). Inhibition of Interleukin-23-Mediated Inflammation with a Novel Small Molecule Inverse Agonist of RORγt. *J. Pharmacol. Exp. Ther.* 371 (1), 208–218. doi:10.1124/jpet.119.258046

Gibbs, B. F., Patsinakidis, N., and Raap, U. (2019). Role of the Pruritic Cytokine IL-31 in Autoimmune Skin Diseases. *Front. Immunol.* 10, 1383. doi:10.3389/fimmu.2019.01383

Graczyk, M., Lewandowska, A. A., and Dzierżanowski, T. (2021). The Therapeutic Potential of Cannabis in Counteracting Oxidative Stress and Inflammation. *Molecules* 26 (15), 4551. doi:10.3390/molecules26154551

Gylfadottir, S. S., Itani, M., Kristensen, A. G., Tankisi, H., Jensen, T. S., Sindrup, S. H., et al. (2022). Analysis of Macrophages and Peptidergic Fibers in the Skin of Patients with Painful Diabetic Polyneuropathy. *Neurol. Neuroimmunol Neuroinflamm* 9 (1), e1111. doi:10.1212/NXI.0000000000001111

Haruna, T., Soga, M., Morioka, Y., Hikita, I., Imura, K., Furue, Y., et al. (2015). S-777469, a Novel Cannabinoid Type 2 Receptor Agonist, Suppresses Itch-Associated Scratching Behavior in Rodents through Inhibition of Itch Signal Transmission. *Pharmacology* 95 (1-2), 95–103. doi:10.1159/000371890

Haruna, T., Soga, M., Morioka, Y., Imura, K., Furue, Y., Yamamoto, M., et al. (2017). The Inhibitory Effect of S-777469, a Cannabinoid Type 2 Receptor Agonist, on Skin Inflammation in Mice. *Pharmacology* 99 (5-6), 259–267. doi:10.1159/000455916

Harvima, I. T., Nilsson, G., Suttle, M. M., and Naukkarinen, A. (2008). Is There a Role for Mast Cells in Psoriasis? *Arch. Dermatol. Res.* 300 (9), 461–478. doi:10.1007/s00403-008-0874-x

Jaworecka, K., Muda-Urban, J., Rzepko, M., and Reich, A. (2021). Molecular Aspects of Pruritus Pathogenesis in Psoriasis. *Int. J. Mol. Sci.* 22 (2), 858. doi:10.3390/ijms22020858

Julià, A., Tortosa, R., Hernanz, J. M., Cañete, J. D., Fonseca, E., Ferrándiz, C., et al. (2012). Risk Variants for Psoriasis Vulgaris in a Large Case-Control Collection and Association with Clinical Subphenotypes. *Hum. Mol. Genet.* 21 (20), 4549–4557. doi:10.1093/hmg/dds295

Kanda, N., Hoashi, T., and Saeki, H. (2021). The Defect in Regulatory T Cells in Psoriasis and Therapeutic Approaches. *J. Clin. Med.* 10 (17), 3880. doi:10.3390/jcm10173880

Karsak, M., Gaffal, E., Date, R., Wang-Eckhardt, L., Rehnelt, J., Petrosino, S., et al. (2007). Attenuation of Allergic Contact Dermatitis through the Endocannabinoid System. *Science* 316 (5830), 1494–1497. doi:10.1126/science.1142265

Komiya, E., Tominaga, M., Kamata, Y., Suga, Y., and Takamori, K. (2020). Molecular and Cellular Mechanisms of Itch in Psoriasis. *Int. J. Mol. Sci.* 21 (21), 8406. doi:10.3390/ijms21218406

Liu, X., Wang, X., Duan, X., Poorun, D., Xu, J., Zhang, S., et al. (2017). Lipoxin A4 and its Analog Suppress Inflammation by Modulating HMGB1 Translocation and Expression in Psoriasis. *Sci. Rep.* 7 (1), 7100. doi:10.1038/s41598-017-07485-1

Lu, H. C., and Mackie, K. (2016). An Introduction to the Endogenous Cannabinoid System. *Biol. Psychiatry* 79 (7), 516–525. doi:10.1016/j.biopsych.2015.07.028

Menezes, R., Hashemi, S., Vincent, R., Collins, G., Meyer, J., Foston, M., et al. (2019). Investigation of Glycosaminoglycan Mimetic Scaffolds for Neurite Growth. *Acta Biomater.* 90, 169–178. doi:10.1016/j.actbio.2019.03.024

Moos, S., Mohebiany, A. N., Waisman, A., and Kurschus, F. C. (2019). Imiquimod-Induced Psoriasis in Mice Depends on the IL-17 Signaling of Keratinocytes. *J. Invest. Dermatol.* 139 (5), 1110–1117. doi:10.1016/j.jid.2019.01.006

Munro, S., Thomas, K. L., and Abu-Shaar, M. (1993). Molecular Characterization of a Peripheral Receptor for Cannabinoids. *Nature* 365 (6441), 61–65. doi:10.1038/365061a0

Nattkemper, L. A., Tey, H. L., Valdes-Rodriguez, R., Lee, H., Mollanazar, N. K., Albornoz, C., et al. (2018). The Genetics of Chronic Itch: Gene Expression in the Skin of Patients with Atopic Dermatitis and Psoriasis with Severe Itch. *J. Invest. Dermatol.* 138 (6), 1311–1317. doi:10.1016/j.jid.2017.12.029

Odan, M., Ishizuka, N., Hiramatsu, Y., Inagaki, M., Hashizume, H., Fujii, Y., et al. (2012). Discovery of S-777469: An Orally Available CB2 Agonist as an Antipruritic Agent. *Bioorg. Med. Chem. Lett.* 22 (8), 2803–2806. doi:10.1016/j.bmcl.2012.02.072

Pandiyan, P., and McCormick, T. S. (2021). Regulation of IL-17A-Producing Cells in Skin Inflammatory Disorders. *J. Invest. Dermatol.* S0022-202X (21), 01673. doi:10.1016/j.jid.2021.06.036

Phan, N. Q., Siepmann, D., Gralow, I., and Ständer, S. (2010). Adjuvant Topical Therapy with a Cannabinoid Receptor Agonist in Facial Postherpetic Neuralgia. *J. Dtsch Dermatol. Ges* 8 (2), 88–91. doi:10.1111/j.1610-0387.2009.07213.x

Pincelli, C., Sevignani, C., Manfredini, R., Grande, A., Fantini, F., Bracci-Laudiero, L., et al. (1994). Expression and Function of Nerve Growth Factor and Nerve Growth Factor Receptor on Cultured Keratinocytes. *J. Invest. Dermatol.* 103 (1), 13–18. doi:10.1111/1523-1747.ep12388914

Pöyhönen, S., Er, S., Domanskyi, A., and Airavaara, M. (2019). Effects of Neurotrophic Factors in Glial Cells in the Central Nervous System: Expression and Properties in Neurodegeneration and Injury. *Front. Physiol.* 10, 486. doi:10.3389/fphys.2019.00486

Robinson, R. H., Meissler, J. J., Fan, X., Yu, D., Adler, M. W., and Eisenstein, T. K. (2015). A CB2-Selective Cannabinoid Suppresses T-Cell Activities and Increases Tregs and IL-10. *J. Neuroimmune Pharmacol.* 10 (2), 318–332. doi:10.1007/s11481-015-9611-3

Roelandt, T., Heughebaert, C., Bredif, S., Giddelo, C., Baudouin, C., Msika, P., et al. (2012). Cannabinoid Receptors 1 and 2 Oppositely Regulate Epidermal Permeability Barrier Status and Differentiation. *Exp. Dermatol.* 21 (9), 688–693. doi:10.1111/j.1600-0625.2012.01561.x

Rom, S., and Persidsky, Y. (2013). Cannabinoid Receptor 2: Potential Role in Immunomodulation and Neuroinflammation. *J. Neuroimmune Pharmacol.* 8 (3), 608–620. doi:10.1007/s11481-013-9445-9

Sakai, K., Sanders, K. M., Youssef, M. R., Yanushefski, K. M., Jensen, L., Yosipovitch, G., et al. (2016). Mouse Model of Imiquimod-Induced Psoriatic Itch. *Pain* 157 (11), 2536–2543. doi:10.1097/j.pain.0000000000000674

Sheriff, T., Lin, M. J., Dubin, D., and Khorasani, H. (2020). The Potential Role of Cannabinoids in Dermatology. *J. Dermatolog Treat.* 31 (8), 839–845. doi:10.1080/09546634.2019.1675854

Shi, Y., Chen, Z., Zhao, Z., Yu, Y., Fan, H., Xu, X., et al. (2019). IL-21 Induces an Imbalance of Th17/Treg Cells in Moderate-To-Severe Plaque Psoriasis Patients. *Front. Immunol.* 10, 1865. doi:10.3389/fimmu.2019.01865

Siiskonen, H., and Harvima, I. (2019). Mast Cells and Sensory Nerves Contribute to Neurogenic Inflammation and Pruritus in Chronic Skin Inflammation. *Front Cel Neurosci* 13, 422. doi:10.3389/fncel.2019.00422

Slominski, A., and Wortsman, J. (2000). Neuroendocrinology of the Skin. *Endocr. Rev.* 21 (5), 457–487. doi:10.1210/edrv.21.5.0410

Slominski, A. T., Zmijewski, M. A., Skobowiat, C., Zbytek, B., Slominski, R. M., and Steketee, J. D. (2012). Sensing the Environment: Regulation of Local and Global Homeostasis by the Skin's Neuroendocrine System. *Adv. Anat. Embryol. Cel Biol* 212, 1–115. doi:10.1007/978-3-642-19683-6_1

Slominski, A. T., Zmijewski, M. A., Zbytek, B., Tobin, D. J., Theoharides, T. C., and Rivier, J. (2013). Key Role of CRF in the Skin Stress Response System. *Endocr. Rev.* 34 (6), 827–884. doi:10.1210/er.2012-1092

Ständer, S., Schmelz, M., Metze, D., Luger, T., and Rukwied, R. (2005). Distribution of Cannabinoid Receptor 1 (CB1) and 2 (CB2) on Sensory Nerve Fibers and Adnexal Structures in Human Skin. *J. Dermatol. Sci.* 38 (3), 177–188. doi:10.1016/j.jdermsci.2005.01.007

Sultan, N., Amin, L. E., Zaher, A. R., Grawish, M. E., and Scheven, B. A. (2021). Dental Pulp Stem Cells Stimulate Neuronal Differentiation of PC12 Cells. *Neural Regen. Res.* 16 (9), 1821–1828. doi:10.4103/1673-5374.306089

Suwarsa, O., Dharmadji, H. P., Sutedja, E., Herlina, L., Sori, P. R., Hindritiani, R., et al. (2019). Skin Tissue Expression and Serum Level of Thymic Stromal Lymphopoietin in Patients with Psoriasis Vulgaris. *Dermatol. Rep.* 11 (1), 8006. doi:10.4081/dr.2019.8006

Szepietowski, J. C., and Reich, A. (2016). Pruritus in Psoriasis: An Update. *Eur. J. Pain* 20 (1), 41–46. doi:10.1002/ejp.768

Tan, Y., Ng, W. J., Lee, S. Z. X., Lee, B. T. K., Nattkemper, L. A., Yosipovitch, G., et al. (2019). 3-Dimensional Optical Clearing and Imaging of Pruritic Atopic Dermatitis and Psoriasis Skin Reveals Downregulation of Epidermal Innervation. *J. Invest. Dermatol.* 139 (5), 1201–1204. doi:10.1016/j.jid.2018.11.006

Taneda, K., Tominaga, M., Negi, O., Tengara, S., Kamo, A., Ogawa, H., et al. (2011). Evaluation of Epidermal Nerve Density and Opioid Receptor Levels in Psoriatic Itch. *Br. J. Dermatol.* 165 (2), 277–284. doi:10.1111/j.1365-2133.2011.10347.x

Tominaga, M., Ozawa, S., Tengara, S., Ogawa, H., and Takamori, K. (2007). Intraepidermal Nerve Fibers Increase in Dry Skin of Acetone-Treated Mice. *J. Dermatol. Sci.* 48 (2), 103–111. doi:10.1016/j.jdermsci.2007.06.003

von Knethen, A., Heinicke, U., Weigert, A., Zacharowski, K., and Brüne, B. (2020). Histone Deacetylation Inhibitors as Modulators of Regulatory T Cells. *Int. J. Mol. Sci.* 21 (7), 2356. doi:10.3390/ijms21072356

Wang, L. L., Zhao, R., Li, J. Y., Li, S. S., Liu, M., Wang, M., et al. (2016). Pharmacological Activation of Cannabinoid 2 Receptor Attenuates Inflammation, Fibrogenesis, and Promotes Re-Epithelialization during Skin Wound Healing. *Eur. J. Pharmacol.* 786, 128–136. doi:10.1016/j.ejphar.2016.06.006

Wei, C., Huang, L., Zheng, Y., and Cai, X. (2021). Selective Activation of Cannabinoid Receptor 2 Regulates Treg/Th17 Balance to Ameliorate Neutrophilic Asthma in Mice. *Ann. Transl Med.* 9 (12), 1015. doi:10.21037/atm-21-2778

Wilson, S. R., Thé, L., Batia, L. M., Beattie, K., Katibah, G. E., McClain, S. P., et al. (2013). The Epithelial Cell-Derived Atopic Dermatitis Cytokine TSLP Activates Neurons to Induce Itch. *Cell* 155 (2), 285–295. doi:10.1016/j.cell.2013.08.057

Yamaguchi, J., Aihara, M., Kobayashi, Y., Kambara, T., and Ikezawa, Z. (2009). Quantitative Analysis of Nerve Growth Factor (NGF) in the Atopic Dermatitis and Psoriasis Horny Layer and Effect of Treatment on NGF in Atopic Dermatitis. *J. Dermatol. Sci.* 53 (1), 48–54. doi:10.1016/j.jdermsci.2008.08.011

Conflict of Interest: The authors declare that the research was conducted in the absence of any commercial or financial relationships that could be construed as a potential conflict of interest.

Publisher's Note: All claims expressed in this article are solely those of the authors and do not necessarily represent those of their affiliated organizations, or those of the publisher, the editors, and the reviewers. Any product that may be evaluated in this article, or claim that may be made by its manufacturer, is not guaranteed or endorsed by the publisher.

Copyright © 2022 Li, Liu, Ge, Chen, Huang, Jin, Zhan, Duan, Liu, Kong, Jiang, Li, Zeng, Li, Xu, Li and Chen. This is an open-access article distributed under the terms of the Creative Commons Attribution License (CC BY). The use, distribution or reproduction in other forums is permitted, provided the original author(s) and the copyright owner(s) are credited and that the original publication in this journal is cited, in accordance with accepted academic practice. No use, distribution or reproduction is permitted which does not comply with these terms.

frontiers | Frontiers in Pharmacology

ORIGINAL RESEARCH
published: 16 May 2022
doi: 10.3389/fphar.2022.848957

Astilbin Activates the Reactive Oxidative Species/PPARγ Pathway to Suppress Effector CD4$^+$ T Cell Activities *via* Direct Binding With Cytochrome P450 1B1

Shizhen Ding[1,2†], Guotao Lu[1†], Biying Wang[2], Jie Xiang[3], Chunxia Hu[2], Zhijie Lin[2,4], Yanbing Ding[1,4], Weiming Xiao[1,4,5] and Weijuan Gong[1,2,4,5*]*

[1]Department of Gastroenterology, Affiliated Hospital of Yangzhou University, Yangzhou University, Yangzhou, China, [2]Department of Immunology, School of Medicine, Yangzhou University, Yangzhou, China, [3]Department of Pharmacology, School of Medicine, Yangzhou University, Yangzhou, China, [4]Jiangsu Key Laboratory of Integrated Traditional Chinese and Western Medicine for Prevention and Treatment of Senile Diseases, Yangzhou University, Yangzhou, China, [5]Jiangsu Key Laboratory of Zoonosis, Jiangsu Co-innovation Center for Prevention and Control of Important Animal Infectious Diseases and Zoonoses, Yangzhou University, Yangzhou, China

OPEN ACCESS

Edited by:
Soraia K. P. Costa,
University of São Paulo, Brazil

Reviewed by:
Chao-Zhan Lin,
Guangzhou University of Chinese Medicine, China
Andreas von Knethen,
Goethe University Frankfurt, Germany

***Correspondence:**
Weijuan Gong
wjgong@yzu.edu.cn
Weiming Xiao
wmxiao@yzu.edu.cn

[†]These authors have contributed equally to this work

Specialty section:
This article was submitted to Inflammation Pharmacology, a section of the journal Frontiers in Pharmacology

Received: 05 January 2022
Accepted: 29 April 2022
Published: 16 May 2022

Citation:
Ding S, Lu G, Wang B, Xiang J, Hu C, Lin Z, Ding Y, Xiao W and Gong W (2022) Astilbin Activates the Reactive Oxidative Species/PPARγ Pathway to Suppress Effector CD4$^+$ T Cell Activities via Direct Binding With Cytochrome P450 1B1. Front. Pharmacol. 13:848957. doi: 10.3389/fphar.2022.848957

Astilbin, as a compound of flavonoids, exerts anti-inflammation, antioxidation, and immune-suppression activities. Decreased activation of NF-κB and p38 MAPK and increased activation of SOCS3 and AMPK have been found in astilbin-treated cells. However, what molecules are docked by astilbin to initiate signaling cascades and result in functional changes remains unknown. In the study, we found that astilbin efficiently suppressed TNF-α production and increased CCR9 and CD36 expression of CD4$^+$ T cells. *In vivo* administration of astilbin repressed the occurrence of type 1 diabetes mellitus in non-obese diabetic mice. The PPARγ/SOCS3, PPARγ/PTEN, and PPARγ/AMPK signaling pathways were substantially activated and played key roles in astilbin-induced downregulation of CD4$^+$ T cell functions. Transcriptome sequencing results confirmed the changes of signaling molecules involved in the immune system, inflammatory responses, and indicated variations of multiple enzymes with oxidant or antioxidant activities. Astilbin directly induced cytoplasmic ROS production of CD4$^+$ T cells *ex vivo*, but had no effects on mitochondrial ROS and mitochondrial weight. When cellular ROS was depleted, astilbin-treated CD4$^+$ T cells remarkably reversed the expression of TNF-α, IFN-γ, CCR9, CD36, and signaling molecules (PPARγ, PTEN, p-AMPK, and SOCS3). Based on bioinformatics, two P450 enzymes (CYP1B1 and CYP19A1) were selected as candidate receptors for astilbin. CYP1B1 was identified as a real docking protein of astilbin in ROS production by AutoDock Vina software analysis and surface plasmon resonance assay. Collectively, astilbin downregulates effector CD4$^+$ T cell activities *via* the CYP1B1/ROS/PPARγ pathway, which firmly supports its potential use in the treatment of inflammation.

Keywords: astilbin, ROS, CD4$^+$T cell, cytochrome P450 1B1, anti-inflammation, PPARγ

INTRODUCTION

Astilbin is a flavonoid compound that can be extracted from *Smilax glabra* rhizomes, *Hypericum perforatum*, and various French vines (0.78–15.12 mg/dl) (Sharma et al., 2020). It possesses strong anti-inflammation, immunosuppression, anti-microorganism, and antioxidation activities (Panche et al., 2016) and plays a therapeutic role in various disorders, such as diabetes (Perez-Najera et al., 2018), liver injury (Wang et al., 2004), lung injury (H. B. Zhang H B et al., 2017), cardiovascular infarction (Diao et al., 2014), depression (Lv et al., 2014), myasthenia gravis (Meng et al., 2016), neurodegenerative diseases (Wang et al., 2017; Zhu et al., 2019), renal dysfunction (Chen et al., 2018), contact hypersensitivity (Fei et al., 2005), psoriasis (Di et al., 2016), burn wound healing (Kimura et al., 2007), androgenic alopecia (Nagasawa et al., 2016), systemic lupus erythematosus (Guo et al., 2015), transplant arteriosclerosis (Zhao et al., 2009), and arthritis (Cai et al., 2003). Astilbin also inhibits the activities of angiotensin-converting enzyme, glucose-6-phosphatase, aldose reductase, α-glucosidase, horseradish peroxidase, and myeloperoxidase and amplifies lipoprotein lipase activity, thus exerting modulatory effects on blood pressure and metabolism (Sharma et al., 2020).

The mechanisms of astilbin-mediated anti-inflammation and immunosuppression are involved with downregulating the activities of macrophages, dendritic cells (Ding et al., 2014), and effector T cells and inducing regulatory B cells (Xu et al., 2020) and T cells (Han et al., 2020). Astilbin suppresses the function of inflammatory cells by inhibiting the PI3K/AKT, TLR4/MyD88/NF-κB (Li et al., 2019), and MAPK signaling pathways and promoting the expression of SOCS3 and activating AMPK, leading to less production of IL-1β, IL-6, TNF-α, IFN-γ, and MMPs (Sharma et al., 2020; Yang et al., 2021). Astilbin is also verified to have strong capacity for scavenging reactive oxidative species (ROS) directly or indirectly (Wang et al., 2019). Astilbin promotes Nrf2 nucleus translocation in skin cells (HaCaT) to reduce ROS accumulation, VEGF expression, and HaCaT cell proliferation (C. Zhang et al., 2017). However, what molecules have dock sites for astilbin and how astilbin modifies the actions of its receptors to induce downstream signaling events in cells, remains unknown.

Astilbin was firstly identified to inhibit effector $CD4^+$ T cell function in concanavalin A-induced liver injury (Wang et al., 2004). Astilbin efficiently suppresses TNF-α and MMP-9 production and adhesion of $CD4^+$ T cells, as well as Th17 differentiation (Meng et al., 2016). Given the key role of effector $CD4^+$ T cells in inflammation-associated diseases, the accurate elucidation of the effects and mechanisms of astilbin on $CD4^+$ T cells would promote its clinical application. In the present study, we profoundly investigated the molecular mechanisms behind the inhibitory effects of astilbin on effector $CD4^+$ T cells and found that CYP1B1 was one dock molecule of astilbin associated with its ability to modulate $CD4^+$ T cell function.

MATERIALS AND METHODS

Animals and Reagents

Non-obese diabetic (NOD) mice and *Nrf2*$^{-/-}$ mice were obtained from the Model Animal Research Center of Nanjing University (Nanjing, China). C57BL/6 mice were from Comparative Medical Center of Yangzhou University (Yangzhou, China). Experiments used 6–12-week-old and sex-matched mice, unless otherwise indicated. All animal care and handling procedures were conducted in accordance with the protocols approved by the Institutional Animal Care and Use Committee (IACUC) at Yangzhou University (Yangzhou, China).

The following reagents were used: Astilbin (HY-N0509); 1-aminobenzotriazole (ABT, HY-103389), a nonspecific and irreversible inhibitor of CYP enzymes; etomoxir (HY-50202), an inhibitor of CPT1α; SF1670 (HY-15842), an inhibitor of PTEN; N-Acetyl-L-cysteine (NAC, HY-B0215), a GSH-related antioxidant; GW9662 (HY-16578), a potent and selective PPARγ antagonist; and dorsomorphin (Compound C, HY-13418A), a selective and ATP-competitive AMPK inhibitor (MedChemExpress, NJ, United States).

Cell Culture

$CD3^+$ $CD4^+$ cells were isolated from the spleen by magnetic bead sorting (Miltenyi Biotec GmbH, BG, Germany). Isolated $CD4^+$ T cells and unlabeled cells were counted and then cultured in RPMI containing 10% FBS and penicillin/streptomycin in a humidified atmosphere containing 5% CO_2 at 37°C. Cells were further stimulated *in vitro* with astilbin, with or without IL-12 (20 U/ml), plate-bound anti-CD3 (2 μg/ml) and soluble anti-CD28 (1 μg/ml) antibodies, GW9662, NAC, SPF1670, dorsomorphin, ABT, and etomoxir according to the experimental design. After 12 h, 24 h, or 2 days, cells were harvested for flow cytometric analysis.

Flow Cytometry

Cells were stained with the indicated antibodies for 30 min at 4°C. The following antibodies for flow cytometry were obtained from BioLegend, CA, United States: anti-mouse CD4 (GK1.5), anti-mouse CCR6 (29-2L17), anti-mouse CCR9 (9B1), anti-mouse CD36 (HM36), and anti-human CD4 (OKT4). For intracellular cytokine analysis, cells were stimulated with PMA and ionomycin for 30 min and treated with brefeldin A for 4 h before staining Fixation/Permeabilization Solution Kit (BD, NJ, United States) followed by anti-mouse TNF-α (MP6-XT22, BioLegend, CA, United States), anti-mouse IFN-γ (XMG1.2, BD, NJ, United States), anti-human TNF-α (Mab11, BioLegend, CA, United States), or anti-human IFN-γ (4S.B3, BioLegend, CA, United States). Cell apoptosis was detected with an Annexin V staining kit (BD, NJ, United States) according to the manufacturer's instructions. For cell proliferation, cells were labeled with 5 μM CFDA-SE (CFSE) (Invitrogen, CA, United States). Seventy-two hours later, they were collected and analyzed by flow cytometry. Acquisition was carried out

on FACSVerse (BD, NJ, United States), and analysis was performed with FlowJo v10 software.

Evaluation of Type 1 Diabetes Mellitus

NOD mice were randomly divided into three groups, and each group was intraperitoneal injected twice weekly with PBS or astilbin (50, 100 mg/kg) for 7 weeks. Body weight and blood glucose of NOD mice were monitored once a week until the end of the observation period. NOD mice were characterized as diabetic when blood glucose readings were >13.9 mmol/L for two consecutive measurements. The indexes of dead mice were shown as the last blood glucose or weight data. At the end of the observation period, mice were euthanized by cervical dislocation, and pancreatic $CD4^+$ T cells were measured by flow cytometry.

Western Blot

Total protein was extracted and boiled for 5 min, resolved by electrophoresis, and transferred to PVDF membranes. Blots were blocked for 1 h with 5% milk in TBST followed by incubation with antibodies (dilution 1:500 to 1:2000) at 4°C overnight. The following antibodies were used for western blot: ACC (Cat# 3676, RRID:AB_2219397), p-ACC (Cat# 11818, RRID:AB_2687505), HKII (Cat# 2867, RRID:AB_2232946), mTOR (Cat# 2983, RRID:AB_2105622), p-mTOR (Cat# 5536, RRID:AB_10691552), Akt (Cat# 4691, RRID: AB_915783), p-Akt (Cat# 4060, RRID:AB_2315049), AMPK (Cat# 5831, RRID:AB_10622186), p-AMPK (Cat# 50081, RRID:AB_2799368), LKB1 (Cat# 3047, RRID:AB_2198327), p-LKB1 (Cat# 3482, RRID:AB_2198321), PTEN (Cat# 9188, RRID:AB_2253290), PPAR-γ (Cat# 2443, RRID:AB_823598), PI3K p110α (Cat# 4249, RRID:AB_2165248), β-actin (Cat# 4970, RRID:AB_2223172), NF-κB p65 (Cat# 8242, RRID: AB_10859369), NF-κB p-p65 (Cat# 3033, RRID: AB_331284), p38 (Cat# 8690, RRID:AB_10999090), p-p38 (Cat# 4511, RRID:AB_2139682), JNK (Cat# 9252, RRID: AB_2250373), p-JNK (Cat# 4668, RRID:AB_823588), Erk (Cat# 4695, RRID:AB_390779), p-Erk (Cat# 4370, RRID: AB_2315112), Stat3 (Cat# 4904, RRID:AB_331269), p-Stat3 (Cat# 9145, RRID:AB_2491009), SOCS3 (Cat# 52113, RRID: AB_2799408) (Cell Signaling Technology, MA, United States), Glut1 (Cat# ab115730, RRID:AB_10903230), CPT1α (Cat# ab234111, RRID:AB_2864319), LPL (Cat# ab21356, RRID: AB_446221) (Abcam, Cambridge, Britain), CYP1B1 (Cat# 18505-1-A, RRID:AB_2878548) (Proteintech, IL, United States), CYP19A1 (Cat# YT1190, RRID: AB_2864736) (Immunoway, DE, United States) and P-PPARγ (abs130911, absin, Shanghai China). HRP-conjugated anti-rabbit (Cat# 7074, RRID:AB_2099233, Cell Signaling Technology, MA, United States) secondary antibodies were used at 1:5000 dilution for 1 h at room temperature. The bands were detected by developing with chemiluminescent HRP substrate (Thermo Scientific, MA, United States), and the intensity of bands was determined by imaging with a molecular imager (Bio-Rad, CA, United States). Bands quantified using the ImageJ software. All results were normalized to those of β-actin, which was used as a loading control, and phosphorylated proteins is compared to the total amount of proteins and housekeeping genes (β-actin).

Detection of Reactive Oxidative Species and Mitochondria

To determine the mitochondrial mass and the levels of intracellular and mitochondrial ROS (mROS), the cells were incubated with 100 nM MitoTracker Green (Beyotime, Shanghai, China) (De Nicola et al., 2011), 10 μM DCFH-DA (Beyotime, Shanghai, China), and 10 μM MitoSOX Indicator (Thermo Fisher Scientific, MA, United States) for 15 min in a CO_2 incubator at 37°C. After washing twice, the data were acquired on a FACSVerse (BD, NJ, United States) and analyzed with FlowJo v10 software.

Transcriptome Sequencing

Total RNA was isolated from mouse $CD4^+$ T cells with TRIzol (1 ml) reagent and purified using Quick-RNA Miniprep columns and RNase-free DNase digestion. RNA integrity was assessed with the Agilent 2100 Bioanalyzer (Agilent Technologies, CA, United States). RNA purity and quantity were evaluated with a NanoDrop 2000 spectrophotometer (Thermo Scientific, MA, United States). Only samples with RIN scores above nine and a minimum total RNA of 500 ng were used for library preparation. Then, the libraries were constructed using TruSeq Stranded mRNA LT Sample Prep Kit (Illumina, CA, United States) according to the manufacturer's instructions. Subsequently, the transcriptome sequencing data were used for a series of analyses, including differential expression analysis, gene enrichment analysis, and expression level analysis.

Prediction of Potential Targets of Astilbin

The potential targets of astilbin were predicted using the PharmMapper database (http://www.lilab-ecust.cn/pharmmapper/index.php) by performing Druggable Pharmacophore Models and SwissTargetPrediction (http://www.swisstargetprediction.ch/) on the basis of the principle that chemicals with similar structures may have similar functions. All the screened targets were input into the UniProt database (http://www.uniprot.org/) to exclude the same targets and non-Homo sapiens targets. The corresponding predicted target information obtained was collected and sorted according to fit score and probability.

Docking Study

The chemical structure of astilbin was obtained from the PubChem compound database (http://pubchem.ncbi.nlm.nih.gov/) with ID 29838-67-3. The crystal structures of CYP1B1 and CYP19A1 proteins with PDB IDs 3PM0 and 3S79, respectively, were obtained from the Research Collaboratory for Structural Bioinformatics (RCSB) Protein Data Bank. The crystal water molecules, ligand atoms, and ions that were bound to the proteins were removed. Hydrogen atoms were subsequently added using AutoDock Tool

program version 1.5.6. Molecular docking between astilbin and human cytochrome P450 1B1 (CYP1B1) was performed using AutoDock Vina on the basis of the Lamarckian genetic algorithm, which combines energy evaluation through grids of affinity potential to find a suitable binding position for a ligand on a given protein. The grid box for docking was positioned properly at the active binding site in the center. The genetic algorithm and its run were set to 1000, as the docking algorithms were set on default. Finally, the results were retrieved as binding energy, and docking with binding energies lower than −5 kcal/mol was selected as a significant binding event and was visualized using PyMOL version 1.5.0. 3. software for obtaining hydrogen bond, hydrophobic, and electrostatic interactions.

Surface Plasmon Resonance

SPR experiments were performed with a Biacore T200 (GE Healthcare, MA, United States). CYP1B1 coupling protein (ImmunoClone, NY, United States) was diluted in 10 mM sodium acetate (pH 5.0) and immobilized on the sensor chip CM7 by primary amine coupling kit (Biacore, GE Healthcare, MA, United States) to a final response level of approximately 6000 resonance units. A blank channel was used as the negative control. All data were collected at 25°C with HBS-EP running buffer (10 mM HEPES, 150 mM NaCl, 3 mM EDTA, 0.05% surfactant polysorbate 20, pH 7.4) at a flow rate of 30 μl/min. Concentration series of the original astilbin (two-fold dilutions starting from a top concentration of 200 μM) was injected over immobilized proteins for a contact time of 180 s and dissociation time of 300 s. The resulting data were fit to a 1:1 binding model using Biacore Evaluation Software v3.2, and the Kd value was determined.

Knockdown of Cytochrome P450 1B1

Silencing of CYP1B1 in $CD4^+$ T cells was achieved using lentivirus. The specific lentivirus CYP1B1-shRNA (5′-GCC TGACCATTAAGCCCAAGTCTCGAGACTTGGGCTTAA TGGTCAG GCTTTTT-3′) and negative control lentivirus shRNA were designed and synthesized by Genecreate, Wuhan, China. Lentiviral plasmid vectors and packaging vectors were co-transfected in 293T cells with Lipofectamine 3000 Reagent (Thermo Fisher, MA, United States). For lentiviral infection, $CD4^+$ T cells were mixed with the virus and 10 μg/ml of polybrene (Sigma-Aldrich, MS, United States). The knockdown effect of CYP1B1 in $CD4^+$ T cells was confirmed by RT-PCR and Western blot analysis.

Statistical Analysis

All data are presented as the means ± SD or means ± SEM. Comparisons between two groups were assessed using the unpaired two-tailed student's *t* test. Comparison of multiple groups was performed using one-way ANOVA or two-way ANOVA. All statistical tests were two-sided. Statistical differences are significant for *, $p \leq 0.05$; **, $p \leq 0.01$; ***, $p \leq 0.001$.

RESULTS

Astilbin Suppressed $CD4^+$ T Cell Function Involved in Ameliorating Type 1 Diabetes Mellitus

After the IC_{50} of astilbin on $CD4^+$ T cells (181 μg/ml) was verified *ex vivo* (**Supplementary Figure S1A**), the effects of astilbin treatment at various doses on TNF-α and IFN-γ, two key inflammatory cytokines produced by effector $CD4^+$ T cells, were checked. As shown in **Figure 1A**, TNF-α production could be substantially inhibited in a dose-dependent manner. Although IFN-γ secretion was also downregulated statistically, the extent was weak. CCR9 expression of lymphocytes indicates the gut-homing activity. Consistent with the effect of astilbin on $NK1.1^-$ $CD4^+$ $NKG2D^+$ regulatory T cells (Han et al., 2020), the expression of CCR9 on $CD4^+$ T cells was also enhanced with astilbin treatment in a dose-dependent manner. Unexpectedly, no changes in the expression of IL-10 and CCR6 in astilbin-treated $CD4^+$ T cells were observed (**Supplementary Figures S1B,C**). Astilbin slightly decreased TGF-β1 secretion of $CD4^+$ T cells (**Supplementary Figure S1D**). We also did not observe any effects of astilbin on the proliferation (**Figures 1B,C**) and apoptosis of $CD4^+$ T cells at doses of 40–160 μg/ml (**Figure 1D**; **Supplementary Figure S1E**).

IFN-γ, IL-1β, and TNF-α production by autoreactive Th1 cells is involved in the destruction of insulin-secreting β-cells in type 1 diabetes (Kaufmann et al., 2019). Since we noted that astilbin could reduce IFN-γ and TNF-α in $CD4^+$T cells, we then analyzed whether astilbin could repress the onset of type 1 diabetes in NOD mice by regulating $CD4^+$T cells. Compared with control group, blood glucose levels and body weights were significantly controlled after the administration of astilbin (50 or 100 mg/kg) (**Figures 1E,F**). When mononuclear cells of the pancreas from mice were isolated, less $CD4^+$ T cells infiltrated the pancreas of astilbin-administered mice (**Figure 1G**). These results demonstrated that astilbin ameliorated T1DM involved with the downregulation of $CD4^+$ T cell activities. Finally, astilbin also efficiently decreased TNF-α and IFN-γ production of peripheral blood $CD4^+$ T cells from human healthy individuals as displayed in **Figures 1H,I**. Therefore, we identified that astilbin exerted immune-suppressive activities *via* downregulating inflammatory cytokine secretions of $CD4^+$ T cells.

PPARγ/SOCS3 Pathway Involved in Astilbin-Mediated Inhibition

Several studies have found that astilbin treatment increases the expression of SOCS3 (Wang et al., 2016; Han et al., 2020; Sharma et al., 2020). Variations of SOCS3 were first measured in freshly isolated, IL-12-activated, or α-CD3/α-CD28-activated $CD4^+$ T cells treated by astilbin. Astilbin could increase SOCS3 expression of freshly isolated and activated $CD4^+$ T cells. The critical role of SOCS3 is manifested by its binding to both the JAK kinase and the cytokine receptor, which can result in the inhibition of STAT3 phosphorylation. Consequently, as

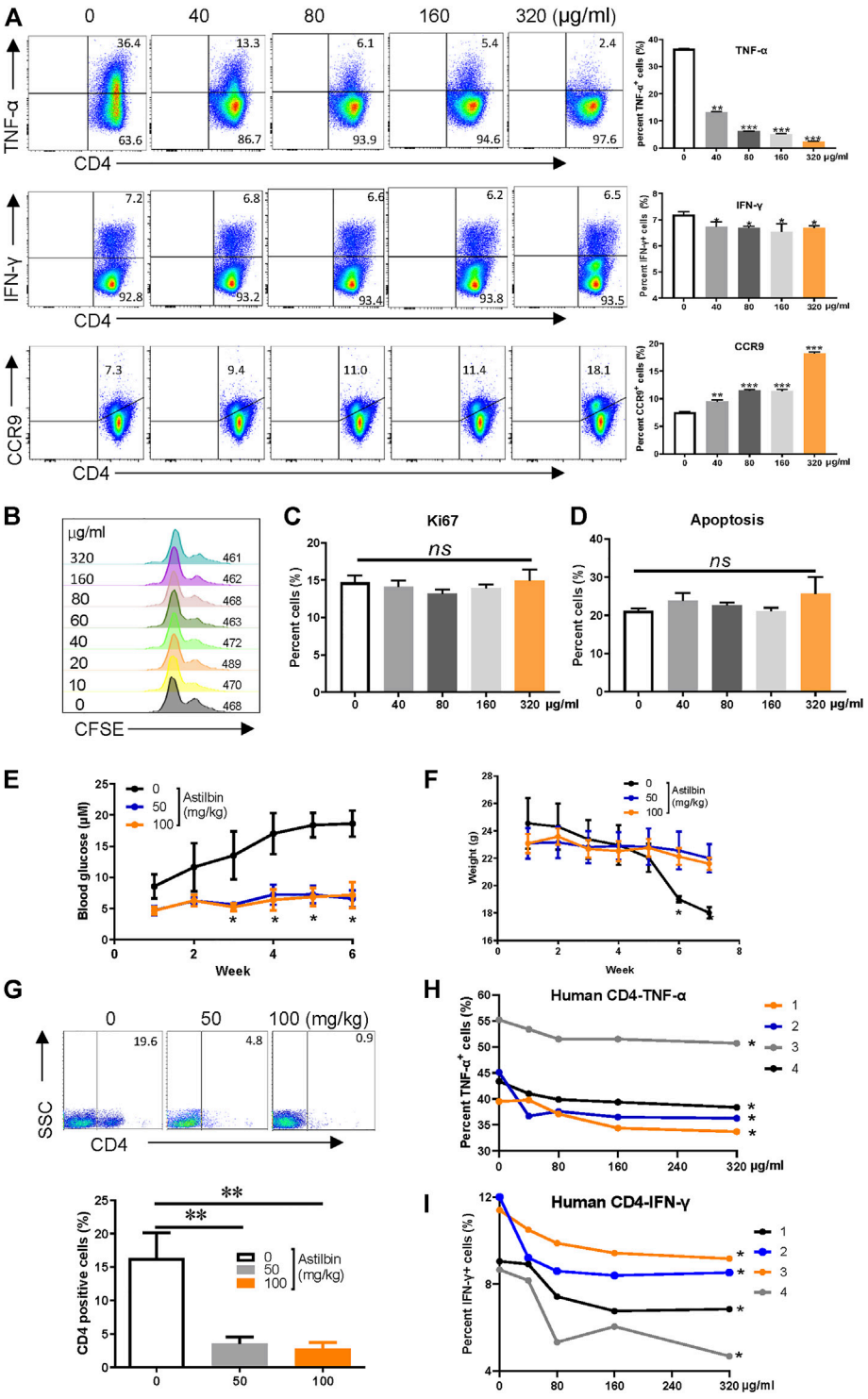

FIGURE 1 | Astilbin decreases $CD4^+$ T cell functions. **(A)** TNF-α^+, IFN-γ^+, and $CCR9^+$ of $CD4^+$T cells treated with various doses of astilbin. Mean ± SD; $n = 3$. **(B)** $CD4^+$ T cell division by CFSE dilution. **(C)** Proliferative capacity of $CD4^+$ T cells evaluated by Ki67. Mean ± SD; $n = 3$. **(D)** Apoptosis of astilbin-treated $CD4^+$ T cells stained by Annexin V and PI. Mean ± SD; $n = 3$. **(E)** Blood glucose levels of NOD mice intraperitoneally injected with astilbin. Mean ± SEM; $n = 10$. **(F)** Weight curves of NOD mice. Mean ± SEM; $n = 10$. **(G)** Infiltrated $CD4^+$ cells in the pancreas of NOD mice. Mean ± SD; $n = 10$. Variations of TNF-α **(H)** and IFN-γ **(I)** in human $CD4^+$ T cells as treated by astilbin for 24 h. Mean ± SEM; $n = 4$. All *ex vivo* experiments were repeated at least three times. Experiments of astilbin-treated NOD mice were conducted twice. *p* values (*$p \leq 0.05$; **$p \leq 0.01$; ***$p \leq 0.001$; ns, no significant difference) determined by one-way ANOVA **(A–C,G)**, two-way ANOVA **(E,F,H,I)**.

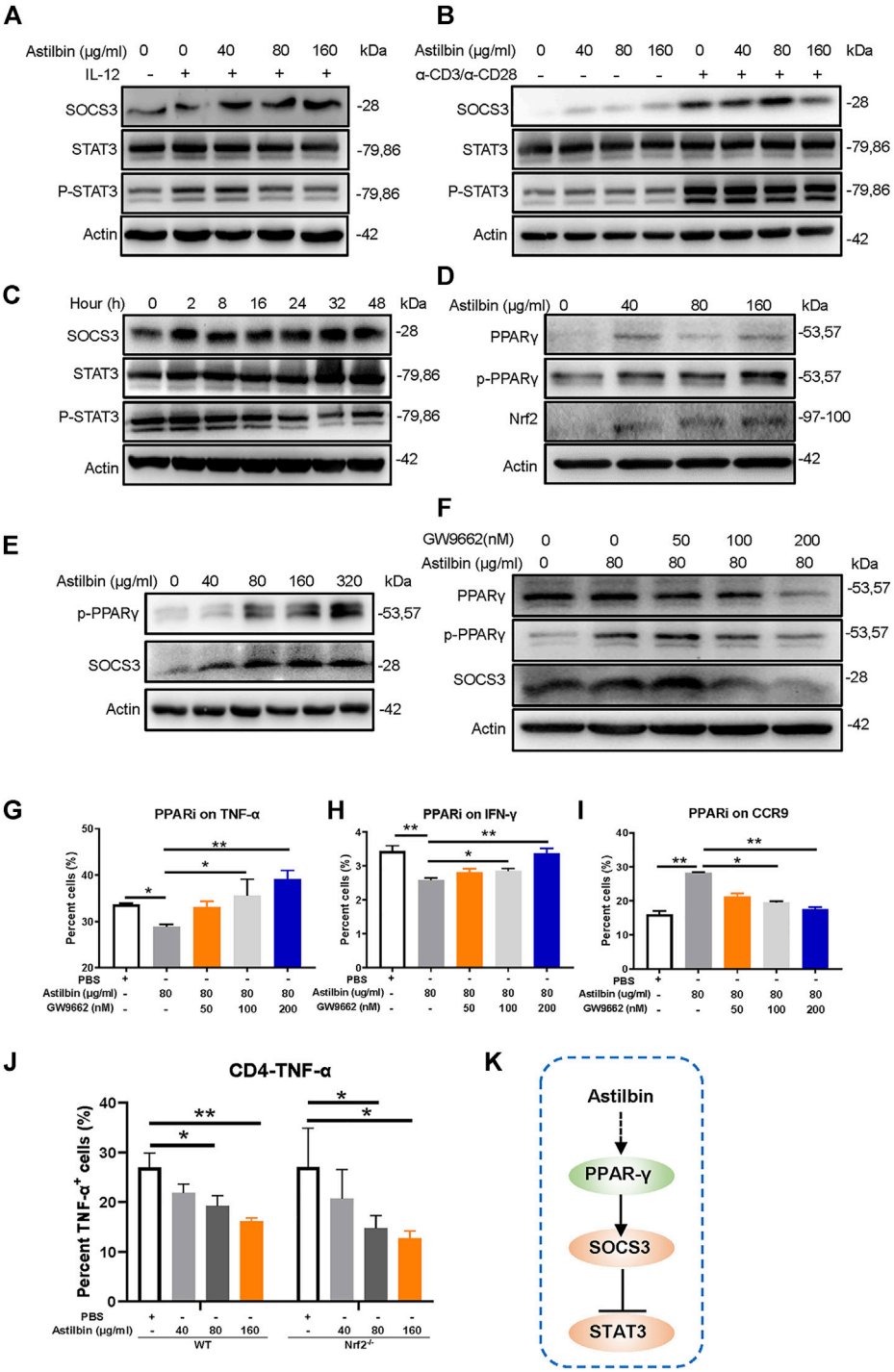

FIGURE 2 | PPARγ/SOCS3 pathway in astilbin-treated CD4$^+$ T cells. Effects of astilbin on the expression of SOCS3 and STAT3/p-STAT3 of unstimulated, IL-12- **(A)**, or α-CD3/α-CD28– **(B)** stimulated CD4$^+$ T cells by Western blot analysis. **(C)** Effects of 80 μg/ml astilbin on SOCS3 and STAT3/p-STAT3 of activated CD4$^+$ T cells at different time points. **(D)** Variations of PPARγ/p-PPARγ and Nrf2 in astilbin-treated CD4$^+$ T cells. **(E)** Parallel expression of p-PPARγ and SOCS3 in astilbin-treated CD4$^+$ T cells. **(F)** Inhibiting PPARγ by GW9662 decreased SOCS3 expression. Effects of GW9662 on TNF-α **(G)**, IFN-γ **(H)**, and CCR9 **(I)** expression in astilbin-treated CD4$^+$ T cells. Mean ± SD; $n = 3$. **(J)** TNF-α production of astilbin-treated *Nrf2*$^{-/-}$ CD4$^+$ T cells. Mean ± SD; $n = 3$. **(K)** Diagram of PPAR/SOCS3 pathway on CD4$^+$ T cells by astilbin. Each experiment was repeated at least three times. The inhibitor of PPAR, GW9662, is abbreviated as PPARi. p values (*$p \leq 0.05$; **$p \leq 0.01$) determined by one-way ANOVA **(G–J)**.

expected phosphorylated STAT3 (p-Y705) levels were downregulated in astilbin-treated $CD4^+$ T cells (**Figures 2A,B**; **Supplementary Figures S2A,B**). However, when variations of SOCS3 were further detected after $CD4^+$ T cells were treated by astilbin (80 μg/ml) at different time courses. SOCS3 expression was increased by 2-h coculture of astilbin and maintained high levels even at 48 h. In parallel, p-STAT3 level was decreased by 2-h treatment, maintained low levels at 8–16 h, and reversed to normal levels at 24 h (**Figure 2C**; **Supplementary Figure S2C**). This trend of p-STAT3 changes may indicate that STAT3 activation could be regulated by other factors, besides SOCS3.

In general, SOCS3 and STAT3 are mutually regulated in cells (Carow and Rottenberg, 2014). Considering the decreased activation of STAT3 and the upregulation of SOCS3, p-STAT3 might not have promoted SOCS3 transcription in astilbin-treated $CD4^+$ T cells. SOCS3 transcription is also activated by PPARγ to prevent IL-17-derived cancer growth (Berger et al., 2013). We determined whether the increased SOCS3 of $CD4^+$ T cells was promoted by PPARγ. As expected, total and phosphorylated PPARγ (p-PPARγ) were remarkably increased in astilbin-treated $CD4^+$ T cells (**Figure 2D**; **Supplementary Figure S2D**). Moreover, astilbin treatment at different doses resulted in parallel variations of p-PPARγ and SOCS3 expression (**Figure 2E**; **Supplementary Figure S2E**) and the expression of SOCS3 decreased significantly after the addition of PPARγ inhibitor GW9662 in $CD4^+$ T cells, which was similar to the changes of p-PPARγ (**Figure 2F**; **Supplementary Figure S2F**). Next, GW9662 was used simultaneously to analyze the effects on functional changes of $CD4^+$ T cells, which were cotreated by astilbin. Treatment of GW9662 reversed TNF-α (**Figure 2G**) and IFN-γ (**Figure 2H**) production and decreased CCR9 expression (**Figure 2I**) of astilbin-treated $CD4^+$ T cells (**Supplementary Figure S2G**).

Another prominent regulator of antioxidant signaling pathways, that is, positively associated with PPARγ regulation is nuclear factor erythroid 2-related factor 2 (Nrf2) (Annie-Mathew et al., 2021). We then tested the expression of Nrf2 in astilbin-treated $CD4^+$T cells. Interestingly, Nrf2 was also enhanced by astilbin treatment (**Figure 2D**). However, when $CD4^+$ T cells derived from *Nrf2*$^{-/-}$ mice were treated by astilbin, the decreased TNF-α production was not almost affected (**Figure 2J**; **Supplementary Figure S2H**), indicating that astilbin-mediated immunoregulatory effect was independent on Nrf2. Collectively, the above results demonstrated the key role of the PPARγ/SOCS3 pathway in astilbin-downregulated $CD4^+$ T cells (**Figure 2K**).

PPARγ/Phosphatase and Tensin Homolog Pathway Involved in Astilbin-Treated $CD4^+$ T Cells

Given that astilbin conducts anti-inflammatory activity *via* downregulating the phosphorylation of PI3K/Akt, NF-κB, and p38 MAPK signaling pathways, some molecules with diphosphatase activity might be stimulated by astilbin. Both phosphatase and tensin homolog (PTEN) was a phosphatase that efficiently inhibits the activation of PI3K/Akt, NF-κB, and p38 MAPK (Worby and Dixon, 2014). Through astilbin treatment, PTEN is remarkably induced in physiological $CD4^+$ T cells and IL-12-stimulated $CD4^+$ T cells. Given that PTEN is more increased in $CD4^+$ T cells by the stimulation of α-CD3/α-CD28, the induction of PTEN by astilbin may be sheltered in α-CD3/α-CD28-stimulated $CD4^+$ T cells. Correspondingly, phosphorylated Akt, NF-κB p65, and p38 decreased in activated $CD4^+$T cells treated by astilbin (**Figures 3A,B**; **Supplementary Figures S3A,B**). In addition, 2-h astilbin treatment increased PTEN expression, and the increased expression lasted for 48 h. Similarly, induced PPARγ expression was observed after 2–24-h stimulation (**Figure 3C**; **Supplementary Figure S3C**).

When astilbin-treated $CD4^+$ T cells were co-cultured with a PTEN inhibitor (SF1670), TNF-α (**Figure 3D**) production was partially reversed (**Supplementary Figure S3D**), and IFN-γ (**Figure 3E**) production was restored, confirming that decreased cytokine secretion of $CD4^+$ T cells is induced by astilbin dependent on the induction of PTEN. On the other hand, incomplete restoration of TNF-α indicated that PTEN was only one of the signal molecules involved in astilbin-induced downregulation. Given that PTEN expression is transactivated by PPARγ (Worby and Dixon, 2014), we determined whether the inhibition of PPARγ affected PTEN and its downstream signaling molecules. As shown in **Figure 3F**, when $CD4^+$ T cells were cotreated by astilbin and GW9662, increased PTEN expression was blocked, and the decreased expression of phosphorylated Akt, NF-κB p65, and p38 was recovered (**Supplementary Figure S3E**). Taken together, astilbin promoted the PPARγ/PTEN pathway to downregulate TNF-α and IFN-γ production of $CD4^+$ T cells (**Figure 3G**).

Involvement of the PPARγ/AMPK Axis in Astilbin-Treated $CD4^+$ T Cells

Astilbin decreases lipid accumulation in high-fat-diet-induced obese mice (Perez-Najera et al., 2018) and inhibits proliferation and improves differentiation in HaCaT keratinocytes *via* activating AMPK (C. Zhang et al., 2017). The LKB1/AMPK/mTOR signaling pathway was also checked in astilbin-treated $CD4^+$ T cells. Although no substantial changes of total LKB1, AMPK, and mTOR level were observed, phosphorylated LKB1 and AMPK were increased, and phosphorylated mTOR was decreased in $CD4^+$ T cells (**Figure 4A**; **Supplementary Figure S4A**). Moreover, the increased expression of phosphorylated LKB1 and AMPK was observed given that $CD4^+$ T cells were treated with astilbin for 2 h, accompanied by the decreased activation of mTOR (**Figure 4B**; **Supplementary Figure S4B**).

Given the metabolic role regulated by AMPK, key molecules associated with glycolipid metabolism in $CD4^+$ T cells were further analyzed. Through astilbin treatment, glucose transporter of T cells (Glut1) decreased with no obvious changes of HK2, indicating decreased glucose intake. Meanwhile, ACC1 (a key enzyme in fatty acid synthesis) was decreased, while CPT1a and pACC1 representing fatty acid oxidation (FAO) were increased (**Figure 4C**; **Supplementary Figure S4C**). The CD36 receptor for the intake of fatty acid

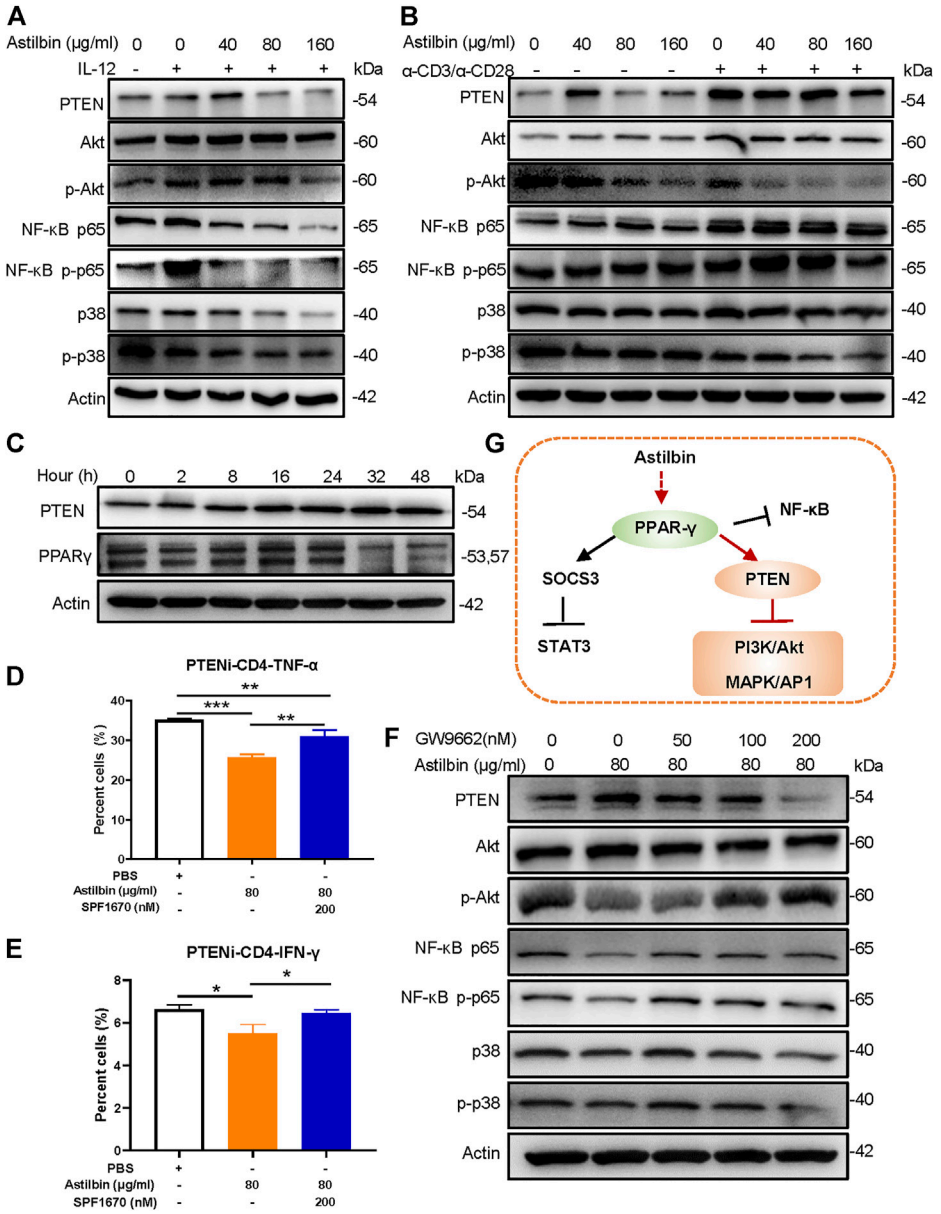

FIGURE 3 | PPARγ/PTEN pathway in astilbin-treated CD4$^+$ T cells. Effects of astilbin on the expression of PTEN, Akt/p-Akt, NF-κB p65/NF-κB p-p65, and p38/p-p38 of unstimulated, IL-12- **(A)**, or α-CD3/α-CD28– **(B)** stimulated CD4$^+$ T cells by Western blot analysis. **(C)** Effects of astilbin (80 μg/ml) on PTEN and PPARγ of CD4$^+$ T cells at different time points. Effects of PTEN inhibitor (SF1670) on TNF-α **(D)** and IFN-γ **(E)** production in astilbin-treated CD4$^+$ T cells. Mean ± SD; $n = 3$. **(F)** Effects of GW9662 on PTEN, Akt/p-Akt, NF-κB p65/NF-κB p-p65, and p38/p-p38 of astilbin-treated CD4$^+$ T cells. **(G)** Diagram of PPAR/PTEN pathway on CD4$^+$T cells by astilbin. Each experiment was conducted at least three times. The inhibitor of PTEN, SF1670 is abbreviated as PTENi. *p* values (*$p \leq 0.05$; **$p \leq 0.01$; ***$p \leq 0.001$) determined by one-way ANOVA **(D,E)**.

was also increased in a dose-dependent manner by astilbin treatment for 24 (**Figures 4D,E**) or 36 h (**Supplementary Figure S4D**). These data demonstrated that astilbin treatment induced metabolic reprogramming of CD4$^+$ T cells, namely, the upregulation of lipid oxidation and downregulation of lipid synthesis and glucose catabolism.

PPARγ activation can transactivate CD36 expression (Marechal et al., 2018). When CD4$^+$ T cells were cotreated with astilbin and GW9662, the upregulation of CD36 was remarkably inhibited (**Figure 4F**; **Supplementary Figure S4E**). Next, we determined whether decreased CPT1a and p-AMPK exerted inhibitory effects on CD4$^+$ T cell function. When a CPT1a inhibitor (etomoxir) was added, IFN-γ production could be partially increased, but TNF-α downregulation could not be reversed at all. On the contrary, etomoxir synergized with astilbin to promote CD36 and CCR9 expression (**Figure 4G**; **Supplementary Figure S4F**). Simultaneously, etomoxir had no effects on PTEN expression (**Figure 4I**; **Supplementary Figure**

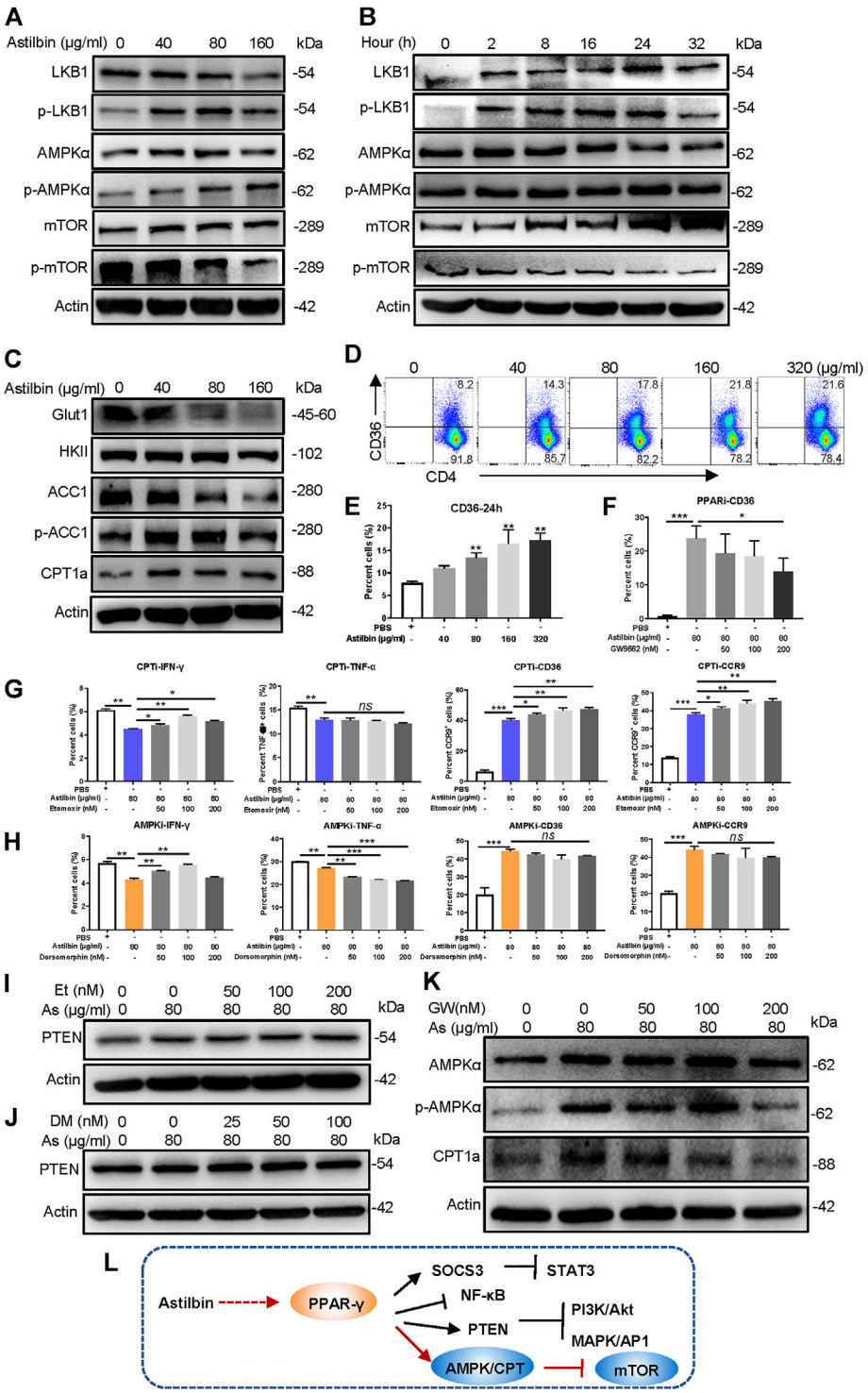

FIGURE 4 | PPARγ/AMPK pathway in astilbin-treated CD4$^+$ T cells. Variations of LKB1/p-LKB1, AMPK/p-AMPK, and mTOR/p-mTOR in CD4$^+$ T cells treated with various doses of astilbin **(A)** or at different time points **(B)**. **(C)** Variations of proteins involved in glucose and lipid metabolism. CD36 of CD4$^+$ T cells affected by astilbin **(D, E)**. Mean ± SD; $n = 3$. **(F)** Effects of PPARγ inhibition on CD36 expression. Mean ± SD; $n = 3$. Effects of CPT inhibition (etomoxir) **(G)** or AMPK inhibition (dorsomorphin) **(H)** on IFN-γ, TNF-α, CD36, and CCR9 of astilbin-treated CD4$^+$ T cells. Mean ± SD; $n = 3$. Effects of etomoxir **(I)** or dorsomorphin **(J)** on PTEN expression of astilbin-treated CD4$^+$ T cells. **(K)** Effects of PPARγ inhibition on AMPK and CPT1a expression of astilbin-treated CD4$^+$ T cells. **(L)** Diagram of PPAR/PTEN pathway on CD4$^+$ T cells by astilbin. Each experiment was performed at least three times. The inhibitor of CPT, etomoxir, is abbreviated as CPTi. The inhibitor of AMPK, dorsomorphin, is abbreviated as AMPKi. p values (*$p \leq 0.05$; **$p \leq 0.01$; ***$p \leq 0.001$; ns, no significant difference) determined by one-way ANOVA **(E–H)**.

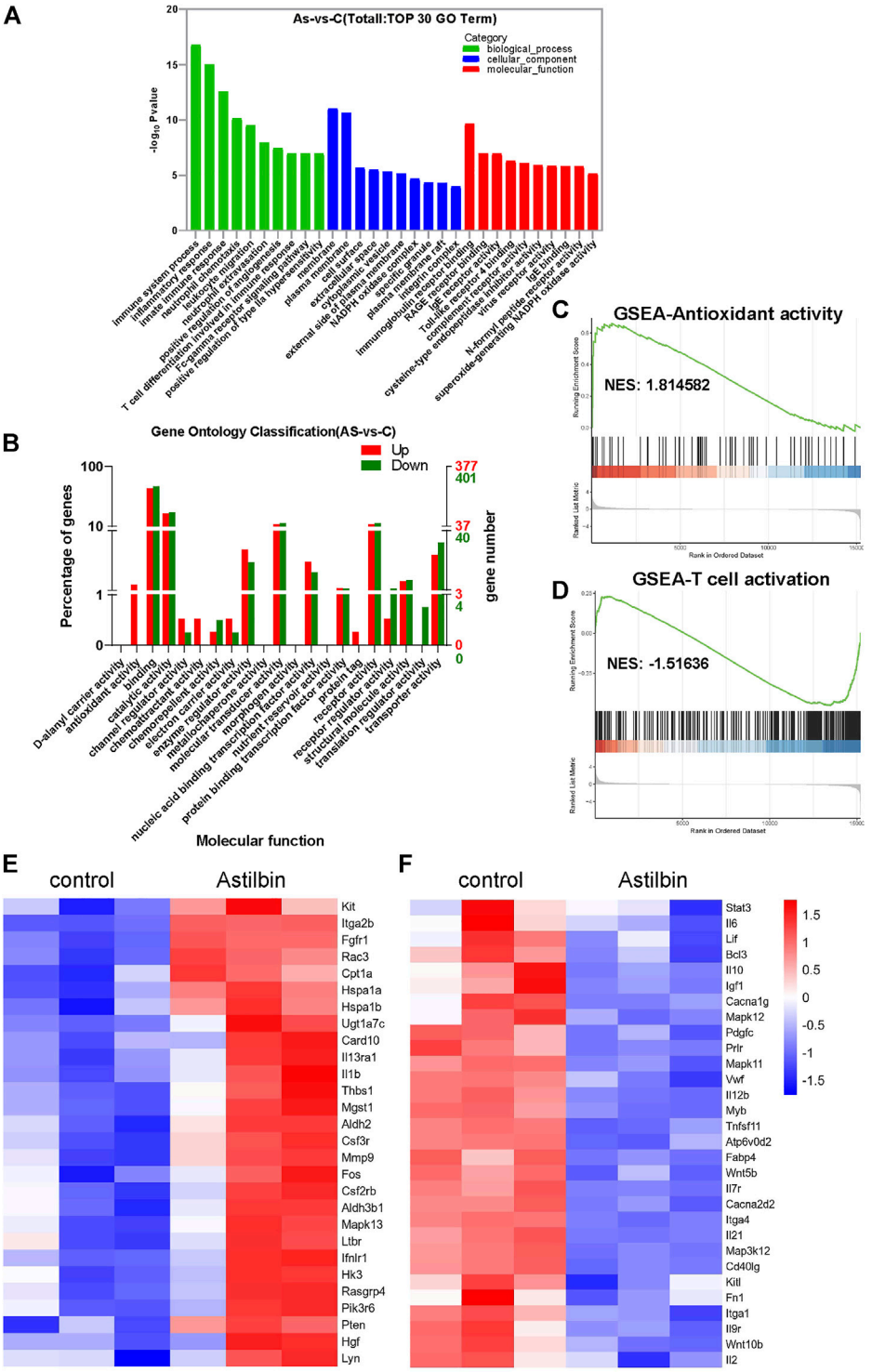

FIGURE 5 | Transcriptome analysis of astilbin-treated CD4$^+$ T cell functions. **(A)** Top 10 changed genes in biological process, cellular component, and molecular function. **(B)** Numbers of differentially expressed genes in molecular function by gene ontology analysis. GSEA of signaling molecules involved in antioxidant activity **(C)** and T cell activation **(D)**. Heatmap of upregulated **(E)** or downregulated **(F)** genes involved in immune function.

S4H). Thus, the increased CPT1a expression in $CD4^+$ T cells was only a stimulatory effect induced by astilbin, not a cause for the downregulation of $CD4^+$ T cell function.

Unexpectedly, when an inhibitor of AMPK (dorsomorphin) was expected to block astilbin-induced activation of AMPK, decreased IFN-γ production could be reversed, whereas TNF-α production was more decreased (**Figure 4H**; **Supplementary Figure S4G**). Meanwhile, treatment with dorsomorphin had no effects on the increased expression of CD36 and CCR9 induced by astilbin (**Figure 4H**; **Supplementary Figure S4G**). Dorsomorphin even synergized astilbin to express PTEN (**Figure 4J**; **Supplementary Figure S4I**), which could explain the deeper inhibition of TNF-α production by cotreatment of astilbin and dorsomorphin. It could be inferred that although the expression of TNF-α, IFN-γ, CCR9, and CCR6 of $CD4^+$ T cells could be regulated by metabolic intervention, functional changes are very different when using different small molecules with metabolic modulatory activity. Given that the CD36 and CCR9 expression of astilbin-treated $CD4^+$T cells was dependent on PPARγ (**Figures 2I**, **4F**), the expression of p-AMPK and CPT1a was inhibited in $CD4^+$ T cells by the cotreatment of GW9662 (**Figure 4K**; **Supplementary Figure S4J**). Collectively, astilbin stimulated the PPARγ/AMPK axis to induce metabolic reprogramming and downregulate the activities of $CD4^+$ T cells (**Figure 4L**).

Differential Expression Genes of $CD4^+$ T Cells by Astilbin Treatment

The transcriptome profiles of $CD4^+$ T cells were further compared before and after astilbin treatment. The heatmap of mRNA sequencing results is displayed in **Supplementary Figure S5A**. Based on KEGG pathway analysis, the top three pathways were in the immune system (108 genes), signal transduction (104 genes), and signaling molecules and interaction (76 genes) (**Supplementary Figure S5B**). The most changed biological processes were immune system process, inflammatory process, and leukocyte migration by gene ontology analysis. Of note, the NADPH oxidase complex and superoxide-generating NADPH oxidase activity were among the top changed pathways of cellular component and molecular function, respectively (**Figures 5A,C**).

When the numbers of upregulated or downregulated genes associated with molecular function were checked, multiple genes were upregulated, but almost no genes related to the functions of antioxidant activity and chemoattraction were downregulated (**Figure 5B**). As expected, the JAK-STAT3, MAPK, and TNF signaling pathways which were associated with T cell activation, showed substantial changes (**Figure 5D**; **Supplementary Table S1**).

In addition, transcriptions of *PTEN*, *CPT1a*, and *microsomal glutathione S transferase 1* with antioxidase activity were upregulated in astilbin-treated $CD4^+$ T cells (**Figure 5E**), while those of *Tnfsf11*, *Mapk11*, *IL-12*, *Mapk12*, *IL-12b*, *IL-2*, *STAT3*, and *IL-6* were decreased (**Figure 5F**). These results confirmed the downregulated expression of genes involved in inflammation and indicated the upregulation of genes with antioxidase activity in astilbin-treated $CD4^+$ T cells.

Astilbin Induced Cytoplasmic Reactive Oxidative Species Production to Activate PPARγ

Given that the transcriptions of NADPH oxidase complex and enzymes with antioxidant activity were increased in astilbin-treated $CD4^+$ T cells, cytoplasmic and mROS of $CD4^+$ T cells were measured after astilbin treatment. cROS were increased at astilbin doses of 40 and 80 μg/ml and peaked at 160 μg/ml (**Figure 6A**) after 24-h treatment. cROS also displayed similar patterns of variation after 36-h treatment (**Supplementary Figure S6A**). Unexpectedly, no obvious changes of mROS and mitochondrial weight were observed after 24-h treatment (**Figure 6A**); even mildly decreased mROS levels were observed after 36-h treatment (**Supplementary Figure S6A**). Human $CD4^+$ T cells of peripheral blood from four healthy individuals also showed increased cROS production after astilbin treatment (**Figure 6B**).

Furthermore, Cellular ROS in astilbin-treated $CD4^+$ T cells could be depleted by NAC (2 mM) (**Figure 6C**; **Supplementary Figure S6B**). When astilbin-treated $CD4^+$ T cells were treated with NAC, decreased IFN-γ production and increased CCR9 and CD36 expression were completely restored (**Figure 6D**; **Supplementary Figure S6C,D**). PPAR expression is strongly induced and activated by ROS-oxidized lipids (Marion-Letellier et al., 2016). When NAC was added into $CD4^+$ T cells, astilbin-increased expression of p-PPARγ, PTEN, p-AMPK, and SOCS3 was completely reversed (**Figure 6E**; **Supplementary Figure S6E**), confirming that PPARγ activation in astilbin-treated $CD4^+$ T cells was dependent on cellular ROS production. Of note, TNF-α secretion was only partially reversed (**Figure 6D**; **Supplementary Figure S6C,D**), indicating that other factors were involved in this astilbin-induced downregulation.

Next, we determined whether inhibiting PPARγ, p-AMPK, or CPT1a would impact ROS production in astilbin-treated $CD4^+$ T cells. When GW9662 was used to inhibit PPARγ activation, the increased ROS level induced by astilbin did not have any changes in $CD4^+$ T cells (**Figure 6F**; **Supplementary Figure S6F**), indicating that the ROS production of $CD4^+$ T cells was the upstream event of PPARγ activation as treated by astilbin. When FAO of $CD4^+$ T cells was inhibited by CPT1a inhibitor (etomoxir) or AMPK inhibitor (dorsomorphin), ROS production induced by astilbin decreased (**Figure 6G**; **Supplementary Figure S6F**), indicating that the upregulated FAO induced by astilbin had a positive feedback for cellular ROS production. Taken together, astilbin induced cROS production in $CD4^+$ T cells to activate the PPARγ signaling pathway.

Astilbin Interacted With Cytochrome P450 1B1 to Stimulate Reactive Oxidative Species Production

Finally, we aimed to investigate the molecular mechanisms of elevated ROS production in astilbin-treated $CD4^+$ T cells. In general, cellular ROS is mainly produced by oxidative

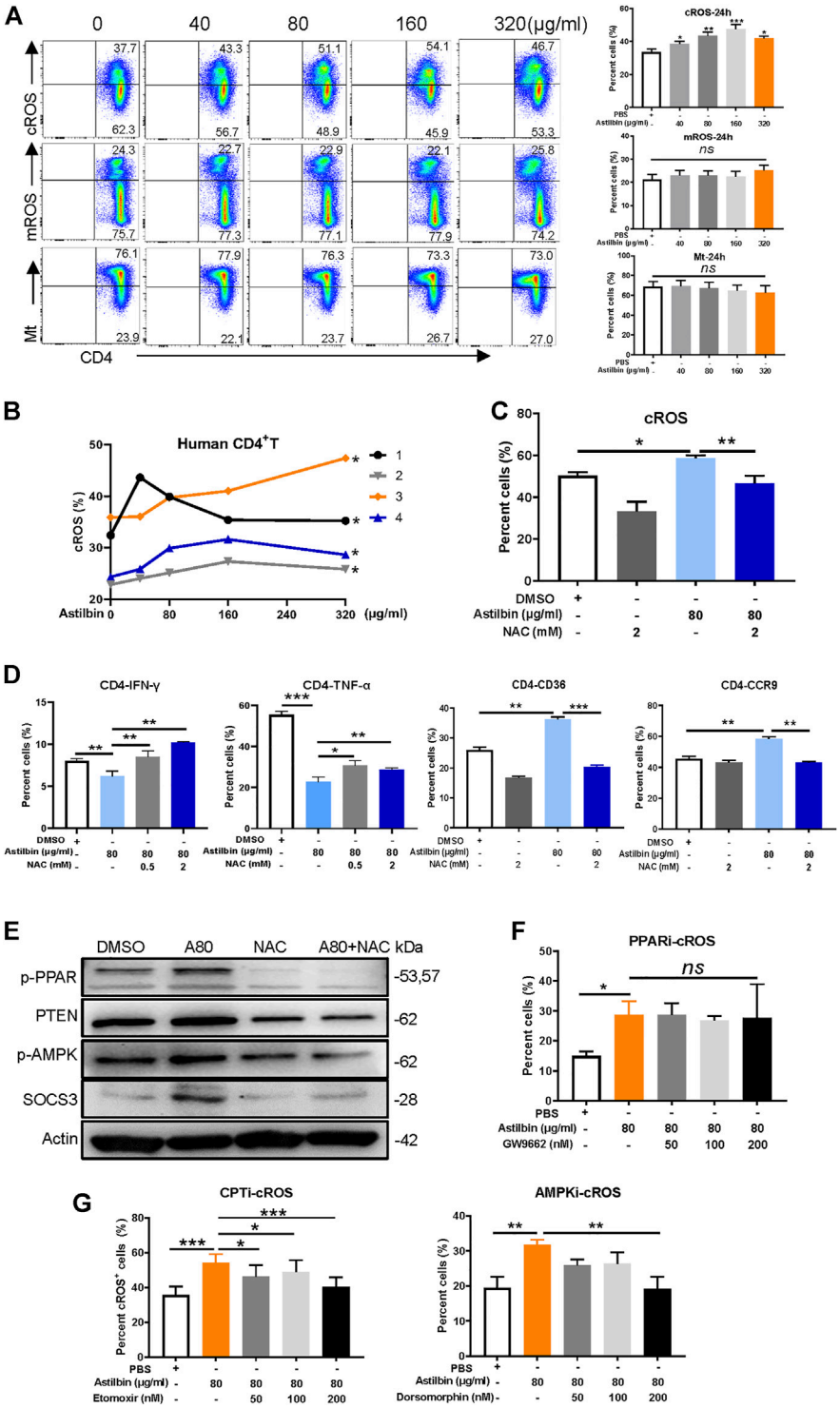

FIGURE 6 | cROS production induced by astilbin in CD4$^+$ T cells. **(A)** Variations of cytoplasmic ROS, mROS, and mitochondrial weight in murine CD4$^+$ T cells treated with astilbin for 24 h. Mean ± SD; $n = 3$. **(B)** Variations of cROS in human CD4$^+$ T cells treated with astilbin. Mean ± SEM; $n = 4$. **(C)** Depletion of ROS by NAC (2 mM). Mean ± SD; $n = 3$. **(D)** Effects of ROS depletion on IFN-γ, TNF-α, CD36, and CCR9 of astilbin-treated CD4$^+$ T cells. Mean ± SD; $n = 3$. **(E)** Effects of ROS depletion on p-PPARγ, PTEN, p-AMPK, and SOCS3 of astilbin-treated CD4$^+$ T cells. Effects of PPARγ inhibition **(F)** and CPT or AMPK inhibition **(G)** on cellular ROS production of astilbin-treated CD4$^+$ T cells. Mean ± SD; $n = 3$. All experiments were conducted at least three times. p values (*$p \leq 0.05$; **$p \leq 0.01$; ***$p \leq 0.001$; ns, no significant difference) determined by one-way ANOVA **(A,C,D,F,G)** and two-way ANOVA **(B)**.

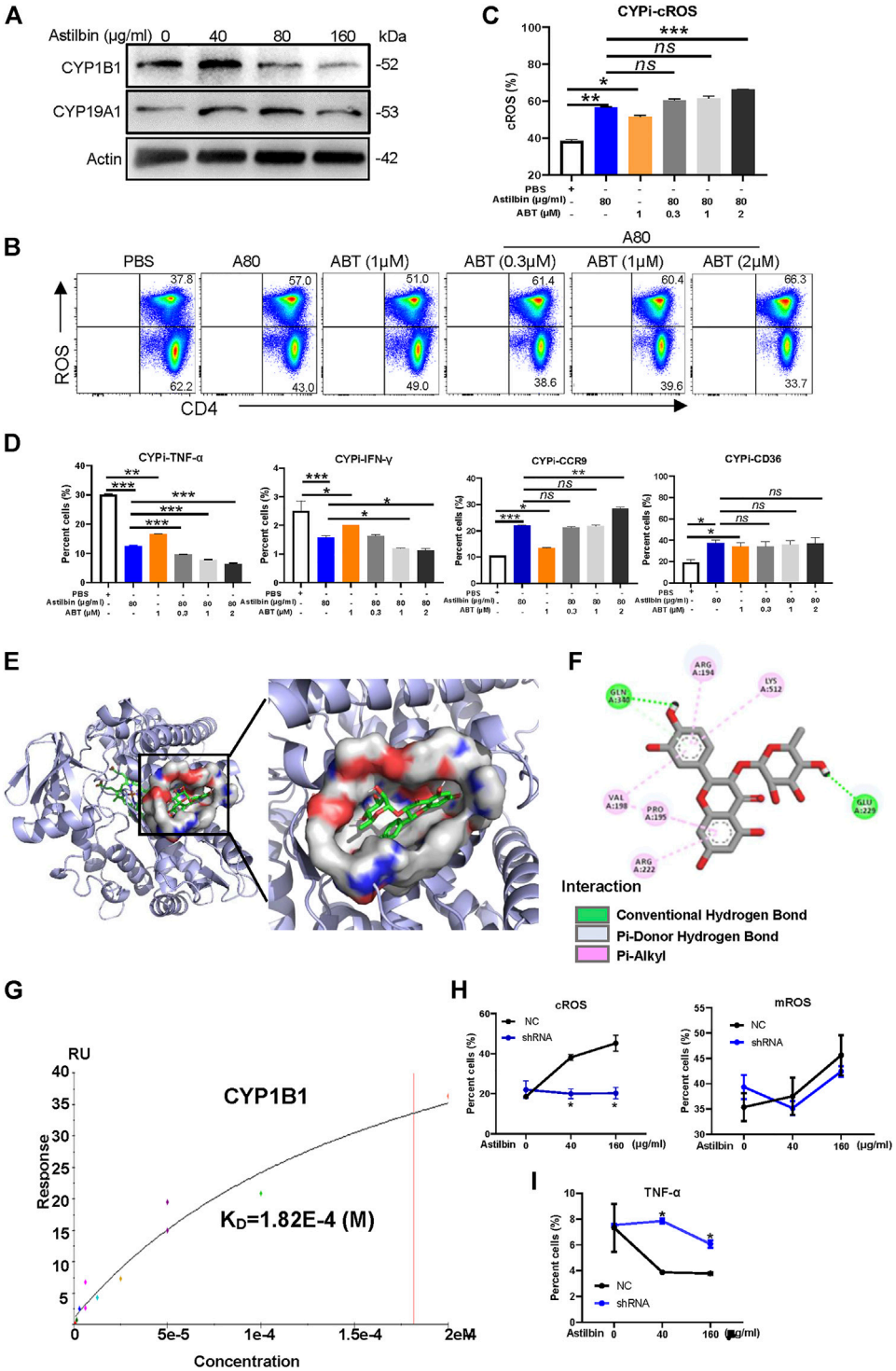

FIGURE 7 | CYP1B1 provides a dock site for astilbin. **(A)** Variations of CYP1B1 and CYP19A1 in astilbin-treated CD4$^+$ T cells. **(B,C)** Astilbin promotes cellular ROS production similar to ABT (a non-specific inhibitor of CYP). Mean ± SD; $n = 3$. **(D)** Effects of astilbin on IFN-γ, TNF-α, CD36, and CCR9 of CD4$^+$ T cells similar to ABT. Mean ± SD; $n = 3$. **(E)** Three-dimensional model of the CYP1B1 active site with bound astilbin. **(F)** Binding of CYP1B1 with astilbin and the inset showing the principal interactive residues of astilbin at the CYP1B1 binding pocket. Green dashed lines represent hydrogen bonds. The hydrophobic interaction is depicted by pink dashed lines. **(G)** Real binding of CYP1B1 with astilbin confirmed by SPR assay. Production of cROS and mROS **(H)** and TNF-α **(I)** in CYP1B1 shRNA-transfected CD4$^+$ T cells. Mean ± SEM; $n = 3$. All experiments were performed three times. The inhibitor of CYP, ABT, is abbreviated as CYPi. p values (*$p \leq 0.05$; **$p \leq 0.01$; ***$p \leq 0.001$; ns, no significant difference) determined by one-way ANOVA **(C,D)** and two-way ANOVA **(H,I)**.

phosphorylation in mitochondria, cytochrome P450 (CYP) oxidases and endoplasmic reticulum oxidoreduction-1 in microsome, polyamine oxidases in cytoplasm, and cell membrane-coupled NADPH oxidases (Zhao et al., 2019). According to the integrated results predicted by the PharmMapper and UniProt databases, 33 candidate proteins of astilbin targets were determined, which are listed in **Supplementary Table S2**. Given that astilbin mainly induced cROS production of $CD4^+$ T cells, we observed that two P450 enzymes (CYP1B1 and CYP19A1) were possibly docked by astilbin. Of note, the expression of CYP1B1 and CYP19A1 could be induced with astilbin (40 μg/ml), but downregulated (160 μg/ml) in $CD4^+$ T cells (**Figure 7A**; **Supplementary Figure S7A,B**).

Next, ABT, a nonselective and irreversible inhibitor of CYP enzymes (Parrish et al., 2016), was used alone or in combination with astilbin to treat $CD4^+$ T cells. As expected, ABT increased cROS production in $CD4^+$ T cells. Compared with astilbin treatment (80 μg/ml) alone, a slightly lower level of cROS was observed in $CD4^+$T cells treated by ABT (1 μM) alone. When low dose of ABT (0.3 or 1 μM) combined with astilbin (80 μg/ml) was used to treat $CD4^+$ T cells, no enhancements of cROS were observed in the cytoplasm of $CD4^+$ T cells compared with astilbin treatment (80 μg/ml) alone. However, cotreatment of high-dose ABT (2 μM) with astilbin (80 μg/ml) substantially increased cROS production (**Figures 7B,C**). This phenomenon indicated that astilbin promoted ROS production with similar molecular pattern to ABT.

As expected, ABT treatment (1 μM) alone reduced TNF-α and IFN-γ production to a lesser degree compared with the astilbin (80 μg/ml)-induced downregulation. In addition, there were obviously synergistic effects in TNF-α and IFN-γ production similar to cotreatment with astilbin (80 μg/ml) and ABT (1, 2 μM). Similar to astilbin, ABT (1 μM) alone increased CCR9 and CD36 expression. More increased CCR9 expression was only observed when ABT (2 μM) and astilbin (80 μg/ml) were both used. ABT and astilbin had no synergistic effects on CD36 expression, even if the ABT dose was 2 μM (**Figure 7D**; **Supplementary Figure S7C**). Thus, it was inferred that astilbin could use other molecular mechanisms to downregulate TNF-α and IFN-γ production besides ROS production; however, it induced CCR9 and CD36 expression dependent on ROS production.

The molecular docking study was conducted using AutoDock Vina 4.2.6. Binding affinity and presence of hydrogen or hydrophobic bonds between astilbin and CYP1B1 or CYP19A1 were predicted. Astilbin had higher binding affinity with CYP1B1 (−6.4 kcal/mol) than CYP19A1 (−3.3 kcal/mol). Then, we used computer-assisted modeling to further investigate whether astilbin interacted with CYP1B1 directly (**Figure 7E**). Three hydrogen bonds were formed in the astilbin–CYP1B1 complex of Glu229 and Gln340 residues (**Figure 7F**). In addition, six hydrophobic contacts contributed to the binding, namely, Pro195, Val198, Arg222, Arg194, Val198, and Lys512 (**Supplementary Table S3**). These interactions helped CYP1B1 and astilbin form stable complexes. Recombinant CYP1B1 and CYP19A1 proteins were used to detect the interaction with astilbin by SPR assay. CYP1B1 stably docked astilbin with a dissociation rate (K_D) of 18.2 (μM) (**Figure 7G**), but CYP19A1 could not bind astilbin efficiently (data not shown). When CYP1B1 was specifically knocked down by shRNA, the increase of cROS in astilbin-treated $CD4^+$T cells disappeared with no variations of mROS production (**Figure 7H**; **Supplementary Figure S7D**). The decreased CYP1B1 expression in shRNA-transfected $CD4^+$ T cells was confirmed in **Supplementary Figure S7E,F**. Consequently, the decrease of TNF-α production in $CD4^+$ T cells induced by astilbin was reversed after being transfected with CYP1B1 shRNA (**Figure 7I**; **Supplementary Figure S7G**). Taken together, we identified that astilbin directly binds CYP1B1 to promote ROS production for the decreased secretion of inflammatory cytokines in $CD4^+$ T cells.

DISCUSSION

The effects and molecular mechanisms of astilbin on modulating effector $CD4^+$ T cell functions were comprehensively analyzed in this study. Astilbin decreased TNF-α and IFN-γ production and increased CCR9 expression of $CD4^+$ T cells, and played a protective role in the onset of type 1 diabetes. PPARγ activation was the upstream event induced by astilbin, leading to stimulate the downstream PTEN and SOCS3 expression and LKB1/AMPK activation. Correspondingly, signaling molecules in mediating the effector function of $CD4^+$ T cells, such as STAT3, NF-κB, Akt, p38 MAPK, and mTOR, were downregulated. Transcriptome sequencing results confirmed the changes of signaling molecules involved in immune systems and inflammatory responses and indicated key variations of enzymes with oxidant or antioxidant activities. Finally, with the help of bioinformatics analysis and SPR assay, we identified that CYP1B1 had a docking pocket for astilbin and that after astilbin interacted with CYP1B1, cellular ROS would be sharply induced to downregulate $CD4^+$ T cell functions, similar to the effects mediated by a nonspecific inhibitor of P450 (ABT). These results elucidated that CYP1B1 is one docking receptor used by astilbin to promote ROS production for the downregulation of effector $CD4^+$T cell function.

CYP1B1 is a member of the CYP superfamily of enzymes localized in the endoplasmic reticulum. The CYP proteins are monooxygenases that catalyze many reactions involved in drug metabolism and synthesis of cholesterol, steroids, and other lipids. CYP1B1 catalyzes the hydroxylation of aryl compounds, thus generating more polar metabolites. About 30 flavonoid compounds have been demonstrated to inhibit CYP1B1 activity (Dutour and Poirier, 2017). Here, we found that astilbin was another inhibitor of CYP1B1. Compared with other CYP1B1 inhibitors derived from flavones, astilbin bound CYP1B1 less potently due to the relatively low affinity (K_D = 18.2 μM). Possibly, the lower binding affinity led to moderate but not high levels of ROS production in $CD4^+$ T cells as treated by astilbin (~80 μg/ml). The moderate or appropriate levels of ROS in cells could efficiently produce oxidized lipids to stimulate PPARγ activation, induce antioxidant expression, and avoid

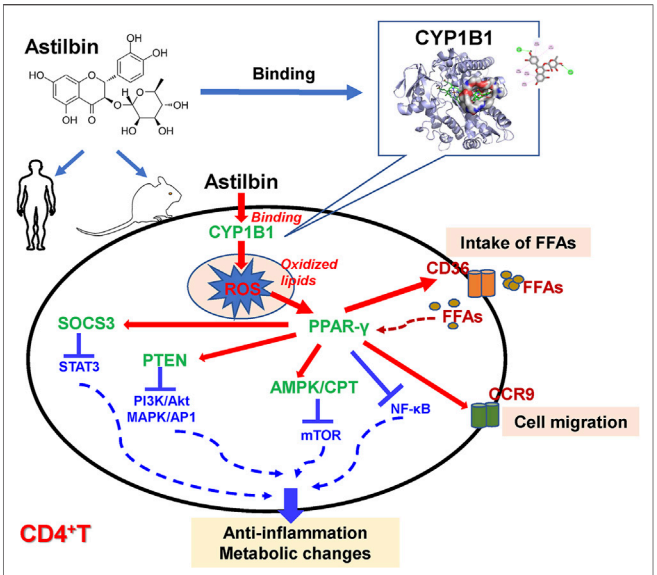

FIGURE 8 | Diagram of astilbin-modulated functions of $CD4^+$ T cells.

cell apoptosis induced by high levels of ROS in cells. Considering the IC_{50} (181 μg/ml), astilbin treatment at a dose of 40–80 μg/ml is safe and effective in the downregulation of $CD4^+$ T cell activities.

Inhibiting PAPRγ activation by GW9662 could almost restore the TNF-α, IFN-γ, and CCR9 expression of astilbin-treated $CD4^+$ T cells. Moreover, GW9662 treatment restored the expression of SOCS3, PTEN, p-Akt, NF-κB pp65, pp38 MAPK, p-AMPK, and CPT1a. It could be concluded that PPARγ activation was a key molecular event in astilbin-induced downregulation of $CD4^+$ T cells. Meanwhile, PPARγ directly transactivated the expression of CCR9 and CD36. The enhancement of CD36 would promote $CD4^+$ T cells to take in free fatty acids (FFAs), and as a positive feedback, intracellular FFAs would promote more PPAR expression. The diagram of key molecular pathways involved in astilbin-treated $CD4^+$ T cells is shown in **Figure 8**. Meanwhile, another antioxidant transcriptional factor, Nrf2, was also induced by astilbin treatment. However, astilbin still downregulated TNF-α production of *Nrf2*$^{-/-}$ $CD4^+$T cells, demonstrating that Nrf2 did not play the key role in the process.

Astilbin was shown to promote the induction of regulatory $NK1.1^-$ $CD4^+$ $NKG2D^+$ T cells and induce regulatory B cells if in combination with LPS dependent on the STAT3 pathway. In astilbin-induced $NK1.1^-$ $CD4^+$ $NKG2D^+$ T cells, STAT3, and SOCS3 were upregulated (21). However, pSTAT3 (Tyr 705) was increased at a dose of 40 μg/ml but decreased at 160 μg/ml when B cells were treated with astilbin alone. However, no changes in SOCS3 expression were observed. Considering the increased SOCS3 and decreased pSTAT3 expression in astilbin-treated effector $CD4^+$ T cells, it was inferred that astilbin used distinct molecular mechanisms to modulate the functions of different cells. Meanwhile, our results confirmed that STAT3 activation in different cell types impacts different effects on cell function.

PTEN expression was decreased by using the PPARγ inhibitor (GW9662) but was increased by the AMPK inhibitor (dorsomorphin) in astilbin-treated $CD4^+$T cells, indicating that PTEN expression was regulated by multiple factors. Although the mROS and mitochondrial weight of $CD4^+$ T cells treated with astilbin for 24 h showed no obvious changes, they decreased after 36-h treatment (**Supplementary Figure S6**), confirming the protective role of astilbin in cerebral ischemia/reperfusion injury by downregulating ROS-NLPR3 activation (Li et al., 2020). Mild decrease of TGF-β1 was also observed in astilbin-treated $CD4^+$ T cells, which was possibly due to decreased STAT3 activation (Dai et al., 2021). The downregulation of TGF-β1 at the transcriptional level is also involved in renal damage in adenine-induced chronic renal failure rats mediated by astilbin-included Erhuang Formula (C. Y. Zhang C Yet al., 2017). Given the key role of TGF-β1 in fibrosis-associated diseases, this effect may be one mechanism in anti-fibrosis activity mediated by astilbin (Sun et al., 2021).

According to multiple spectroscopic coupled with molecular docking analysis, astilbin has strong binding ability to human CYP2D6 (Tao et al., 2021). Ultrahigh-performance liquid chromatography and triple quadrupole mass spectrometry have been used to confirm the interaction of human CYP3A4 and CYP2D6 with astilbin (Shi et al., 2021). In the present study, astilbin efficiently stimulated the ROS of human $CD4^+$ T cells, indicating the inhibition of CYP3A4 and CYP2D6 by astilbin. However, whether astilbin can bind human CYP1B1 or mouse CYP3A4/CYP2D6 still needs further study. In addition, cotreatment of astilbin and the CYP non-selective inhibitor exerted synergistic effects on TNF-α and IFN-γ production in $CD4^+$ T cells. We could not exclude the inhibitory effects mediated by other candidate targets such as STAT1 or MAPKp38 as predicted by bioinformatics (**Supplementary Table S2**).

$CD4^+$ T cells have been regarded as playing a key role in the pathogenesis of T1D (Haskins and Cooke, 2011). The relevance of Th1 cells to T1D in humans has been confirmed by many studies on $CD4^+$ T cells isolated from human patients. Studies have shown that reactive oxygen species (ROS) act as signaling molecules contributing to T cell fate and function (Chavez and Tse, 2021). Eliminating autoreactive T cells by targeting ROS production is a potential strategy to inhibit autoreactive T cell activation without compromising systemic immune function. Recently, more attention has been focused on various treatments to prevent the destructive activity of $CD4^+$ T cells (Bediaga et al., 2022), as our study showed that astilbin can effectively inhibit the activity of $CD4^+$ T cells in NOD mice and humans, providing a new idea for the treatment of T1D. However, it is still necessary to further explore how astilbin inhibits $CD4^+$ T cells activity and whether it targets ROS production in T1D.

In conclusion, we demonstrated that murine CYP1B1 was one P450 receptor of astilbin in $CD4^+$ T cells. The CYP1B1 inhibition by astilbin promoted ROS production and induced the expression of PPAR and antioxidant enzymes. PPAR activation led to the

decreased expression of inflammatory cytokines and increased expression of CD36 and CCR9 in $CD4^+$ T cells *via* the stimulation of PTEN, SOCS3, and AMPK pathways (**Figure 8**). Given that elevated levels of CYP1B1 were observed in multiple cancers (Li et al., 2017), astilbin could also exert anti-tumor activity *via* targeting CYP1B1 to induce apoptosis by producing high levels of ROS.

DATA AVAILABILITY STATEMENT

The datasets presented in this study can be found in online repositories. The names of the repository/repositories and accession number(s) can be found below: https://www.ncbi.nlm.nih.gov/, PRJNA798859.

ETHICS STATEMENT

The studies involving human participants were reviewed and approved by the ethical review committees of Yangzhou University. The patients/participants provided their written informed consent to participate in this study. The animal study was reviewed and approved by the Institutional Animal Care and Use Committee (IACUC) at Yangzhou University.

AUTHOR CONTRIBUTIONS

Study design by WX and WG; data acquisition and analysis by SD, GL, CH, and ZL; bioinformatics by JX; manuscript drafting by SD, BW, and YD; manuscript revision by XW and WG. All authors read and approved the manuscript.

FUNDING

This work was supported by the National Natural Science Foundation of China (grant Nos. 81873866, 81671547, and 81873867), the Natural Science Foundation of Jiangsu Province, China (grant No. BK20180925); the "Six peaks" Talent Project of Jiangsu Province; the "333" Talent Project of Jiangsu Province.

SUPPLEMENTARY MATERIAL

The Supplementary Material for this article can be found online at: https://www.frontiersin.org/articles/10.3389/fphar.2022.848957/full#supplementary-material

REFERENCES

Annie-Mathew, A. S., Prem-Santhosh, S., Jayasuriya, R., Ganesh, G., Ramkumar, K. M., and Sarada, D. V. L. (2021). The Pivotal Role of Nrf2 Activators in Adipocyte Biology. *Pharmacol. Res.* 173, 105853. doi:10.1016/j.phrs.2021.105853

Bediaga, N. G., Garnham, A. L., Naselli, G., Bandala-Sanchez, E., Stone, N. L., Cobb, J., et al. (2022). Cytotoxicity-Related Gene Expression and Chromatin Accessibility Define a Subset of CD4+ T Cells that Mark Progression to Type 1 Diabetes. *Diabetes.* 71 (3), 566–577. doi:10.2337/db21-0612

Berger, H., Végran, F., Chikh, M., Gilardi, F., Ladoire, S., Bugaut, H., et al. (2013). SOCS3 Transactivation by PPARγ Prevents IL-17-driven Cancer Growth. *Cancer Res.* 73 (12), 3578–3590. doi:10.1158/0008-5472.CAN-12-4018

Cai, Y., Chen, T., and Xu, Q. (2003). Astilbin Suppresses Collagen-Induced Arthritis *via* the Dysfunction of Lymphocytes. *Inflamm. Res.* 52 (8), 334–340. doi:10.1007/s00011-003-1179-3

Carow, B., and Rottenberg, M. E. (2014). SOCS3, a Major Regulator of Infection and Inflammation. *Front. Immunol.* 5, 58. doi:10.3389/fimmu.2014.00058

Chávez, M. D., and Tse, H. M. (2021). Targeting Mitochondrial-Derived Reactive Oxygen Species in T Cell-Mediated Autoimmune Diseases. *Front. Immunol.* 12, 703972. doi:10.3389/fimmu.2021.703972

Chen, F., Sun, Z., Zhu, X., and Ma, Y. (2018). Astilbin Inhibits High Glucose-Induced Autophagy and Apoptosis through the PI3K/Akt Pathway in Human Proximal Tubular Epithelial Cells. *Biomed. Pharmacother.* 106, 1175–1181. doi:10.1016/j.biopha.2018.07.072

Dai, W., Liu, S., Wang, S., Zhao, L., Yang, X., Zhou, J., et al. (2021). Activation of Transmembrane Receptor Tyrosine Kinase DDR1-STAT3 Cascade by Extracellular Matrix Remodeling Promotes Liver Metastatic Colonization in Uveal Melanoma. *Signal Transduct. Target Ther.* 6 (1), 176. doi:10.1038/s41392-021-00563-x

DeNicola, G. M., Karreth, F. A., Humpton, T. J., Gopinathan, A., Wei, C., Frese, K., et al. (2011). Oncogene-induced Nrf2 Transcription Promotes ROS Detoxification and Tumorigenesis. *Nature.* 475 (7354), 106–109. doi:10.1038/nature10189

Di, T. T., Ruan, Z. T., Zhao, J. X., Wang, Y., Liu, X., Wang, Y., et al. (2016). Astilbin Inhibits Th17 Cell Differentiation and Ameliorates Imiquimod-Induced Psoriasis-like Skin Lesions in BALB/c Mice *via* Jak3/Stat3 Signaling Pathway. *Int. Immunopharmacol.* 32, 32–38. doi:10.1016/j.intimp.2015.12.035

Diao, H., Kang, Z., Han, F., and Jiang, W. (2014). Astilbin Protects Diabetic Rat Heart against Ischemia-Reperfusion Injury *via* Blockade of HMGB1-dependent NF-Kb Signaling Pathway. *Food Chem. Toxicol.* 63, 104–110. doi:10.1016/j.fct.2013.10.045

Ding, Y., Liang, Y., Deng, B., Qiao, A., Wu, K., Xiao, W., et al. (2014). Induction of TGF-β and IL-10 Production in Dendritic Cells Using Astilbin to Inhibit Dextran Sulfate Sodium-Induced Colitis. *Biochem. Biophys. Res. Commun.* 446 (2), 529–534. doi:10.1016/j.bbrc.2014.02.136

Dutour, R., and Poirier, D. (2017). Inhibitors of Cytochrome P450 (CYP) 1B1. *Eur. J. Med. Chem.* 135, 296–306. doi:10.1016/j.ejmech.2017.04.042

Fei, M., Wu, X., and Xu, Q. (2005). Astilbin Inhibits Contact Hypersensitivity through Negative Cytokine Regulation Distinct from Cyclosporin A. *J. Allergy Clin. Immunol.* 116 (6), 1350–1356. doi:10.1016/j.jaci.2005.08.032

Guo, L., Liu, W., Lu, T., Guo, W., Gao, J., Luo, Q., et al. (2015). Decrease of Functional Activated T and B Cells and Treatment of Glomerulonephitis in Lupus-Prone Mice Using a Natural Flavonoid Astilbin. *Plos One.* 10 (4), e0124002. doi:10.1371/journal.pone.0124002

Han, S., Lin, Z., Wen, J., Wu, K., Xu, Y., Zhang, Y., et al. (2020). Astilbin Promotes the Induction of Regulatory NK1.1- CD4+ NKG2D+ T Cells through the PI3K, STAT3, and MAPK Signaling Pathways. *Int. Immunopharmacol.* 81, 106143. doi:10.1016/j.intimp.2019.106143

Haskins, K., and Cooke, A. (2011). CD4 T Cells and Their Antigens in the Pathogenesis of Autoimmune Diabetes. *Curr. Opin. Immunol.* 23 (6), 739–745. doi:10.1016/j.coi.2011.08.004

Kaufmann, U., Kahlfuss, S., Yang, J., Ivanova, E., Koralov, S. B., and Feske, S. (2019). Calcium Signaling Controls Pathogenic Th17 Cell-Mediated Inflammation by Regulating Mitochondrial Function. *Cell Metab.* 29 (5), 1104–e6. doi:10.1016/j.cmet.2019.01.019

Kimura, Y., Sumiyoshi, M., and Sakanaka, M. (2007). Effects of Astilbe Thunbergii Rhizomes on Wound Healing Part 1. Isolation of Promotional Effectors from Astilbe Thunbergii Rhizomes on Burn Wound Healing. *J. Ethnopharmacol.* 109 (1), 72–77. doi:10.1016/j.jep.2006.07.007

Li, F., Zhu, W., and Gonzalez, F. J. (2017). Potential Role of CYP1B1 in the Development and Treatment of Metabolic Diseases. *Pharmacol. Ther.* 178, 18–30. doi:10.1016/j.pharmthera.2017.03.007

Li, J., Gu, Z., Liu, Y., Wang, Y., and Zhao, M. (2019). Astilbin Attenuates Cerebral Ischemia/reperfusion Injury by Inhibiting the TLR4/MyD88/NF-Kb Pathway. *Toxicol. Res. (Camb)* 8 (6), 1002–1008. doi:10.1039/c9tx00222g

Li, Y., Wang, R., Xue, L., Yang, Y., and Zhi, F. (2020). Astilbin Protects against Cerebral Ischaemia/reperfusion Injury by Inhibiting Cellular Apoptosis and ROS-NLRP3 Inflammasome axis Activation. *Int. Immunopharmacol.* 84, 106571. doi:10.1016/j.intimp.2020.106571

Lv, Q. Q., Wu, W. J., Guo, X. L., Liu, R. L., Yang, Y. P., Zhou, D. S., et al. (2014). Antidepressant Activity of Astilbin: Involvement of Monoaminergic Neurotransmitters and BDNF Signal Pathway. *Biol. Pharm. Bull.* 37 (6), 987–995. doi:10.1248/bpb.b13-00968

Maréchal, L., Laviolette, M., Rodrigue-Way, A., Sow, B., Brochu, M., Caron, V., et al. (2018). The CD36-Pparγ Pathway in Metabolic Disorders. *Int. J. Mol. Sci.* 19 (5). doi:10.3390/ijms19051529

Marion-Letellier, R., Savoye, G., and Ghosh, S. (2016). Fatty Acids, Eicosanoids and PPAR Gamma. *Eur. J. Pharmacol.* 785, 44–49. doi:10.1016/j.ejphar.2015.11.004

Meng, Q. F., Zhang, Z., Wang, Y. J., Chen, W., Li, F. F., Yue, L. T., et al. (2016). Astilbin Ameliorates Experimental Autoimmune Myasthenia Gravis by Decreased Th17 Cytokines and Up-Regulated T Regulatory Cells. *J. Neuroimmunol.* 298, 138–145. doi:10.1016/j.jneuroim.2016.07.016

Nagasawa, A., Wakisaka, E., Kidena, H., Nomura, T., Hotta, M., Taguchi, H., et al. (2016). t-Flavanone Improves the Male Pattern of Hair Loss by Enhancing Hair-Anchoring Strength: A Randomized, Double-Blind, Placebo-Controlled Study. *Dermatol Ther. (Heidelb)* 6 (1), 59–68. doi:10.1007/s13555-016-0101-1

Panche, A. N., Diwan, A. D., and Chandra, S. R. (2016). Flavonoids: an Overview. *J. Nutr. Sci.* 5, e47. doi:10.1017/jns.2016.41

Parrish, K. E., Mao, J., Chen, J., Jaochico, A., Ly, J., Ho, Q., et al. (2016). *In Vitro* and *In Vivo* Characterization of CYP Inhibition by 1-aminobenzotriazole in Rats. *Biopharm. Drug Dispos.* 37 (4), 200–211. doi:10.1002/bdd.2000

Pérez-Nájera, V. C., Gutiérrez-Uribe, J. A., Antunes-Ricardo, M., Hidalgo-Figueroa, S., Del-Toro-Sánchez, C. L., Salazar-Olivo, L. A., et al. (20182018). Smilax Aristolochiifolia Root Extract and its Compounds Chlorogenic Acid and Astilbin Inhibit the Activity of α-Amylase and α-Glucosidase Enzymes. *Evid. Based Complement. Altern. Med.* 2018, 6247306. doi:10.1155/2018/6247306

Sharma, A., Gupta, S., Chauhan, S., Nair, A., and Sharma, P. (2020). Astilbin: A Promising Unexplored Compound with Multidimensional Medicinal and Health Benefits. *Pharmacol. Res.* 158, 104894. doi:10.1016/j.phrs.2020.104894

Shi, Y., Xie, J., Chen, R., Liu, G., Tao, Y., Fan, Y., et al. (2021). Inhibitory Effects of Astilbin, Neoastilbin and Isoastilbin on Human Cytochrome CYP3A4 and 2D6 Activities. *Biomed. Chromatogr.* 35 (4), e5039. doi:10.1002/bmc.5039

Sun, X. H., Zhang, H., Fan, X. P., and Wang, Z. H. (2021). Astilbin Protects against Carbon Tetrachloride-Induced Liver Fibrosis in Rats. *Pharmacology.* 106 (5-6), 323–331. doi:10.1159/000514594

Tao, Y., Fan, Y., Liu, G., Zhang, Y., Wang, M., Wang, X., et al. (2021). Interaction Study of Astilbin, Isoastilbin and Neoastilbin toward CYP2D6 by Multi-Spectroscopy and Molecular Docking. *Luminescence.* 36 (6), 1412–1421. doi:10.1002/bio.4065

Wang, D., Li, S., Chen, J., Liu, L., and Zhu, X. (2017). The Effects of Astilbin on Cognitive Impairments in a Transgenic Mouse Model of Alzheimer's Disease. *Cell Mol. Neurobiol.* 37 (4), 695–706. doi:10.1007/s10571-016-0405-9

Wang, J., Zhao, Y., and Xu, Q. (2004). Astilbin Prevents Concanavalin A-Induced Liver Injury by Reducing TNF-Alpha Production and T Lymphocytes Adhesion. *J. Pharm. Pharmacol.* 56 (4), 495–502. doi:10.1211/0022357023033

Wang, M., Zhao, J., Zhang, N., and Chen, J. (2016). Astilbin Improves Potassium Oxonate-Induced Hyperuricemia and Kidney Injury through Regulating Oxidative Stress and Inflammation Response in Mice. *Biomed. Pharmacother.* 83, 975–988. doi:10.1016/j.biopha.2016.07.025

Wang, W., Yuhai, H., Wang, H., and Bagenna. (2019). Astilbin Reduces ROS Accumulation and VEGF Expression through Nrf2 in Psoriasis-like Skin Disease. *Biol. Res.* 52 (1), 49. doi:10.1186/s40659-019-0255-2

Worby, C. A., and Dixon, J. E. (2014). Pten. *Annu. Rev. Biochem.* 83, 641–669. doi:10.1146/annurev-biochem-082411-113907

Xu, Y. M., Wu, K. Y., Han, S., Ding, S. Z., Lu, G. T., Lin, Z. J., et al. (2020). Astilbin Combined with Lipopolysaccharide Induces IL-10-producing Regulatory B Cells *via* the STAT3 Signalling Pathway. *Biomed. Pharmacother.* 129, 110450. doi:10.1016/j.biopha.2020.110450

Yang, L., Zhu, Y., Zhong, S., and Zheng, G. (2021). Astilbin Lowers the Effective Caffeine Dose for Decreasing Lipid Accumulation *via* Activating AMPK in High-Fat Diet-Induced Obese Mice. *J. Sci. Food Agric.* 101 (2), 573–581. doi:10.1002/jsfa.10669

Zhang, C., Xu, Q., Tan, X., Meng, L., Wei, G., Liu, Y., et al. (2017). Astilbin Decreases Proliferation and Improves Differentiation in HaCaT Keratinocytes. *Biomed. Pharmacother.* 93, 713–720. doi:10.1016/j.biopha.2017.05.127

Zhang, C. Y., Zhu, J. Y., Ye, Y., Zhang, M., Zhang, L. J., Wang, S. J., et al. (2017). Erhuang Formula Ameliorates Renal Damage in Adenine-Induced Chronic Renal Failure Rats *via* Inhibiting Inflammatory and Fibrotic Responses. *Biomed. Pharmacother.* 95, 520–528. doi:10.1016/j.biopha.2017.08.115

Zhang H B, H. B., Sun, L. C., Zhi, L. D., Wen, Q. K., Qi, Z. W., Yan, S. T., et al. (2017). Astilbin Alleviates Sepsis-Induced Acute Lung Injury by Inhibiting the Expression of Macrophage Inhibitory Factor in Rats. *Arch. Pharm. Res.* 40 (10), 1176–1185. doi:10.1007/s12272-016-0857-y

Zhao, J., Li, P., Zhang, Y., Wang, X., Ao, Q., and Gao, S. (2009). The Inhibitory Effect of Astilbin on the Arteriosclerosis of Murine Thoracic Aorta Transplant. *J. Huazhong Univ. Sci. Technol. Med. Sci.* 29 (2), 212–214. doi:10.1007/s11596-009-0215-0

Zhao, R. Z., Jiang, S., Zhang, L., and Yu, Z. B. (2019). Mitochondrial Electron Transport Chain, ROS Generation and Uncoupling (Review). *Int. J. Mol. Med.* 44 (1), 3–15. doi:10.3892/ijmm.2019.4188

Zhu, Y. L., Sun, M. F., Jia, X. B., Cheng, K., Xu, Y. D., Zhou, Z. L., et al. (2019). Neuroprotective Effects of Astilbin on MPTP-Induced Parkinson's Disease Mice: Glial Reaction, Alpha-Synuclein Expression and Oxidative Stress. *Int. Immunopharmacol.* 66, 19–27. doi:10.1016/j.intimp.2018.11.004

Conflict of Interest: The authors declare that the research was conducted in the absence of any commercial or financial relationships that could be construed as a potential conflict of interest.

Publisher's Note: All claims expressed in this article are solely those of the authors and do not necessarily represent those of their affiliated organizations, or those of the publisher, the editors and the reviewers. Any product that may be evaluated in this article, or claim that may be made by its manufacturer, is not guaranteed or endorsed by the publisher.

Copyright © 2022 Ding, Lu, Wang, Xiang, Hu, Lin, Ding, Xiao and Gong. This is an open-access article distributed under the terms of the Creative Commons Attribution License (CC BY). The use, distribution or reproduction in other forums is permitted, provided the original author(s) and the copyright owner(s) are credited and that the original publication in this journal is cited, in accordance with accepted academic practice. No use, distribution or reproduction is permitted which does not comply with these terms.

frontiers | Frontiers in Physiology

MINI REVIEW
published: 19 May 2022
doi: 10.3389/fphys.2022.880422

Inhibition of Serine Proteases as a Novel Therapeutic Strategy for Abdominal Pain in IBS

*Lisse Decraecker, Guy Boeckxstaens and Alexandre Denadai-Souza**

Laboratory of Intestinal Neuro-immune Interaction, Translational Research Center for Gastrointestinal Disorders, Department of Chronic Diseases, Metabolism and Ageing, KU Leuven, Leuven, Belgium

Serine proteases are heavily present in the gastrointestinal tract where they are essential in numerous physiological processes. An imbalance in the proteolytic activity is a central mechanism underlying abdominal pain in irritable bowel syndrome (IBS). Therefore, protease inhibitors are emerging as a promising therapeutic tool to manage abdominal pain in this functional gastrointestinal disorder. With this review, we provide an up-to-date overview of the implications of serine proteases in the development of abdominal pain in IBS, along with a critical assessment of the current developments and prospects of protease inhibitors as a therapeutic tool. In particular, we highlight the current knowledge gap concerning the identity of dysregulated serine proteases that are released by the rectal mucosa of IBS patients. Finally, we suggest a workflow with state-of-the-art techniques that will help address the knowledge gap, guiding future research towards the development of more effective and selective protease inhibitors to manage abdominal pain in IBS.

Keywords: irritable bowel syndrome, visceral hypersensitivity, proteases, protease-activated receptors, protease inhibitors

OPEN ACCESS

Edited by:
Elizabeth S. Fernandes, Pelé Pequeno Príncipe Research Institute, Brazil

Reviewed by:
AisahAniisahAubdool, Queen Mary University of London, United Kingdom
Daniele Maria-Ferreira, Pelé Pequeno Príncipe Research Institute, Brazil

****Correspondence:***
Alexandre Denadai-Souza alexandre.denadai-souza@kuleuven.be

Specialty section:
This article was submitted to Integrative Physiology, a section of the journal Frontiers in Physiology

Received: *21 February 2022*
Accepted: *26 April 2022*
Published: *19 May 2022*

Citation:
Decraecker L, Boeckxstaens G and Denadai-Souza A (2022) Inhibition of Serine Proteases as a Novel Therapeutic Strategy for Abdominal Pain in IBS. Front. Physiol. 13:880422. doi: 10.3389/fphys.2022.880422

INTRODUCTION

Irritable bowel syndrome (IBS) is a highly prevalent disorder of the gut-brain axis affecting 4% of the world population (Sperber et al., 2021). Also according to the Rome IV criteria, IBS is diagnosed when a patient has recurrent abdominal pain that is associated with a change in stool frequency and/or form (Drossman, 2016). Also bloating, gas and cramping are common symptoms, but their presence is not necessary for diagnosis. IBS prevalence is higher in women than in men; female-to-male odds ratio of 1.7 (1.5–1.9), while geographical location does not seem to have an impact (Sperber et al., 2021). Effective therapy to manage the debilitating symptoms is however still lacking and the costs associated with diagnosis and work absenteeism place a heavy burden on both the patient and the health care systems (Drossman et al., 2009; Flacco et al., 2019).

The symptoms of IBS are likely a manifestation of several contributing mechanisms, as depicted in **Figure 1A**. Visceral hypersensitivity (VHS), an increased pain perception in the gastrointestinal tract, is a major contributing factor to abdominal pain in IBS (Farzaei et al., 2016). Mechanical, thermal, or chemical information in the gut wall is sensed by extrinsic, primary afferent neurons with cell bodies in the dorsal root ganglia (DRG). The signal is transduced to different somatosensory areas in the brain via secondary neurons in the spinal cord, where it is subject to central processing to be perceived as noxious or not (Vermeulen et al., 2014). Peripheral sensitization of extrinsic, primary afferents is determined by the expression of specific channels that are involved in sensing noxious

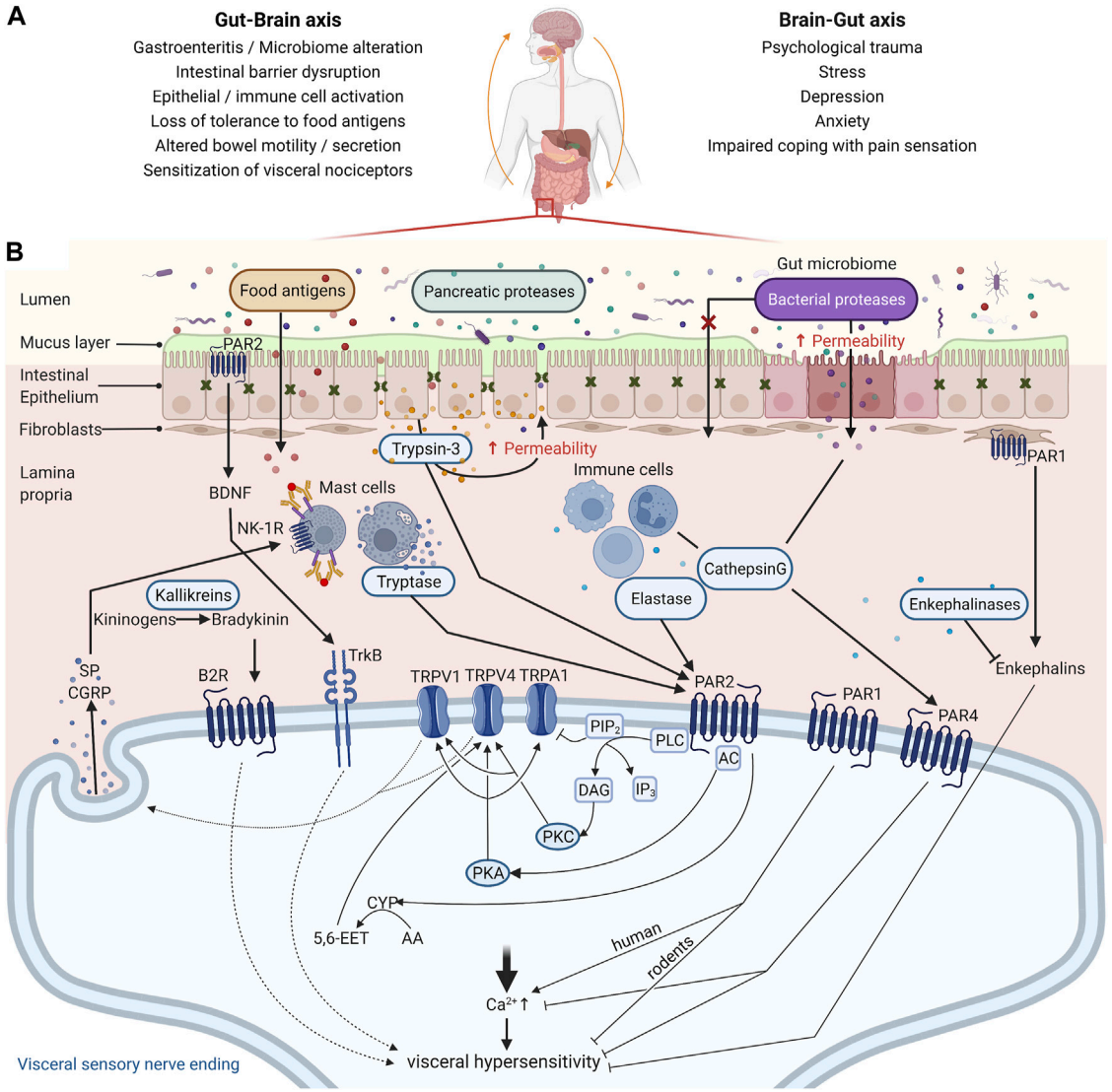

FIGURE 1 | Mechanisms contributing to abdominal pain associated with irritable bowel syndrome (IBS). **(A)** The pathophysiology of IBS is tightly associated with perturbations in the Gut-Brain Axis, which encompasses a bi-directional communication between these organs. Increasing reports indicate that gastroenteritis may promote intestinal barrier disruption, activation of epithelial and immune cells in the gut mucosa, and loss of tolerance to dietary antigens. Upon re-exposure to those dietary antigens, mast cells degranulate and their mediators sensitize nociceptors leading to visceral hypersensitivity. Conversely, IBS is also associated with a higher prevalence of psychiatric disorders such as depression and anxiety, factors that affect coping with pain sensation. A history of psychological trauma and stress are also risk factors for IBS, although the mechanisms involved remain unclear. **(B)** Peripheral sensitization of the gut innervation is a central mechanism underlying abdominal pain in IBS, and proteases are emerging as central mediators in this process. Proteases from the lumen (pancreatic or microbial), epithelial cells (trypsin-3), and immune cells (tryptase, elastase, and cathepsin (G) participate in the disruption of the intestinal barrier and can signal to visceral nociceptors and mediate VHS via protease-activated receptor (PAR) activation. PAR2 activation on the nerve endings of visceral nociceptors induces VHS through TRPV1, TRPV4, and/or TRPA1 sensitization after Gαs or Gαq recruitment, depending on the protease. TRPV1 and TRPV4 on sensory neurons also mediate the release of substance P (SP) and Calcitonin gene-related peptide (CGRP), further contributing to the pain signal. Additionally, proteases modulate synthesis and secretion of respectively bradykinin and brain-derived neurotrophic factor (BDNF), compounds found to be involved in inflammatory pain. On the other hand, activation of PAR1 and PAR4 has an analgesic effect in mice, while in humans PAR1 is emerging as pro-nociceptive. For PAR4 this is likely mediated through reducing intracellular calcium levels. Whether PAR1 mediates VHS due to activation of the receptor in the sensory nerve endings or fibroblasts remains to be investigated in animal models of IBS and patient samples. Unlike the other PARs, PAR3 seems to rather act as a cofactor for PAR1 and PAR4 signaling by potentiating the cleavage by proteases like thrombin, but its role still warrants further investigation. Transient Receptor Potential Cation Channel Subfamily V Member 1 (TRPV1) and 4 (TRPV4); Transient Receptor Potential Cation Channel Subfamily A Member 1 (TRPA1); Adenylyl Cyclase (AC); Protein Kinase A (PKA); Phospholipase C (PLC); Protein Kinase C (PKC); Cytochrome P450 Epoxygenase (CYP); Arachidonic Acid (AA); 5,6-epoxy-8Z,11Z, 14Z-eicosatrienoic acid (5,6-EET); Neurokinin-1 Receptor (NK1-R); Bradykinin Receptor B2 (B2R); Neurotrophic Receptor Tyrosine Kinase 2 (TrkB); Phosphatidylinositol 4,5-bisphosphate (PIP2); Inositol 1,4,5-trisphosphate (IP3); Diacyl Glycerol (DAG). Created with BioRender.com.

stimuli (Anand et al., 2007). In particular, the transient receptor potential (TRP) channels, more specifically TRPA1, TRPV1, and TRPV4, were shown to be sensitized in submucosal neurons of rectal biopsies from IBS patients, thereby contributing to VHS (Wouters et al., 2016; Balemans et al., 2017, 2019). Besides histamine, bradykinin, and serotonin, also proteases have emerged as mediators that can sensitize these channels and consequently contribute to VHS in IBS (Farzaei et al., 2016; Brizuela et al., 2021).

Proteases are enzymes that hydrolyze peptide bonds, which can result not only in the inactivation of the target but also in the activation of signaling molecules and receptors. In the gastrointestinal tract, while proteases are best known for their role in food digestion, they are now emerging as pivotal mediators of increased intestinal epithelial permeability and visceral pain (Cenac, 2013; Van Spaendonk et al., 2017). Among the different classes of proteases, serine proteases are most likely to mediate pain since they are predominantly released to the extracellular milieu (Vergnolle, 2016). This family of proteases is characterized by the presence of a nucleophilic serine in the reactive site and is further subdivided into catalytic groups according to substrate preference as chymotrypsin-, trypsin- and elastase-like serine proteases (Ovaere et al., 2009). This review focuses on the role of serine proteases in the pathophysiology of VHS in IBS, as well as the therapeutic potential of their inhibition.

HOW PROTEASES MEDIATE VISCERAL PAIN IN IBS

Proteases can modulate visceral pain through several mechanisms as illustrated in **Figure 1B**, which are discussed in the following paragraphs. The most extensively studied mechanism to date, is via activation of protease-activated receptors (PARs). PARs belong to a family of cell-surface signaling proteins called G protein-coupled receptors and the four members of the PAR family, PAR1-4, are expressed throughout the body, including various cell types in the intestines, such as epithelial cells, mast cells, and neurons (Vergnolle, 2005). Different proteases can cleave the receptors at different sites and thereby induce different signaling pathways or even inactivate the receptor (Gottesman, 2021). Trypsin and tryptase activate canonical signaling after cleavage of PAR2, leading to G-protein mediated signaling via downstream messengers such as PKC (Dai et al., 2004; Amadesi et al., 2006; Grant et al., 2007). Cathepsin S and elastase cleave elsewhere and activate biased signaling, which includes G-protein mediated activation of cAMP and PKA (Zhao et al., 2015). Hence, the profile of active proteases within a tissue microenvironment is a major determinant of the downstream PAR signaling taking place, with direct consequences for nociception.

Evidence from pre-clinical studies has indicated that proteases can promote VHS in mice via PAR2-mediated sensitization of TRPA1 and TRPV4. Intracolonic administration of PAR2 activating peptide causes visceral hyperalgesia in wild-type mice, but not in TRPA1 knock-out mice, suggesting that TRPA1 is needed to mediate PAR2-induced hyperalgesia (Cattaruzza et al., 2010). Additionally, using TRPV4-targeted siRNA and PAR2 knock-out mice, Cenac and others show that colonic biopsy supernatants from IBS-D patients induce VHS when administered in the colon, in a TRPV4-dependant mechanism by activating PAR2 in sensory neurons (Cenac et al., 2015). A link between PAR2 activation and TRPV1 sensitization has also been shown in murine DRG neurons and models of somatic pain, but this remains to be explored further in visceral pain (Amadesi et al., 2006). PAR1 activation induces antinociceptive effects and even appears to prevent visceral hyperalgesia in mice (Asfaha et al., 2002; Kawao et al., 2004; Martin et al., 2009). However, studies on human enteric and DRG neurons showed that colonic biopsy supernatant from IBS patients could activate the neurons via PAR1, but not PAR2 (Mueller et al., 2011; Kugler et al., 2012; Buhner et al., 2018; Desormeaux et al., 2018). This might suggest very distinct roles for PAR1 and PAR2 in humans versus rodents and might be explained in part by the fact that the class of serine proteases has many lineage-specific differences between humans and mice (Puente et al., 2003). PARs also have other ways to signal than calcium mobilization that would be of interest to investigate in regard to TRP sensitization (Zhao et al.,2014a; 2014b; Sostegni et al., 2015). Interestingly, expression of both PAR1 and PAR4, also suggested to be antinociceptive, was lowered in IBS patients compared to healthy controls, while PAR2 levels were unchanged (Bian et al., 2009; Zhao et al., 2012). To date, there is no data showing co-expression of TRP channels and PARs on human DRGs or sensory nerve endings in human colonic biopsies. Nevertheless, both TRP channels and PARs are broadly expressed in nociceptive neurons; therefore, their co-expression on nerve endings innervating the gut is quite certain (Cenac, 2013; Balemans et al., 2017; Desormeaux et al., 2018).

Proteases can also convert molecules that are active on pain pathways. Bradykinin for example, a potent proinflammatory mediator, is generated through cleavage of kininogens by kallikreins, which are serine proteases, and can induce hyperalgesia via TRPV1 and TRPA1 sensitization (Mizumura et al., 2009). The contribution of the kallikrein-kinin pathway in experimental acute colitis is without controversy, however, there is a lack of studies investigating the role of this mechanism in VHS (Stadnicki, 2011). Endogenous opioids are modulators of nociceptive signaling promoting analgesia of which the activity is also regulated by serine proteases. Enkephalins, one of the endogenous opioid families, are known to promote ion and water absorption in the gut, as well as play a role in visceral nociception (Mosinska et al., 2016). Aminopeptidase N (ANPEP), a metallopeptidase, is an important enzyme involved in the degradation of enkephalins. In colonic biopsies taken from inflamed regions of patients with inflammatory bowel disease (IBD), increased levels of enkephalins were described but protease activity levels were not assessed (Owczarek et al., 2011). To date, reports regarding levels of ANPEP or endogenous opioids in IBS patients are lacking, but levels of opioid receptor expression were significantly lower in the colon of diarrhea-predominant

IBS patients compared to healthy controls (Zielińska et al., 2015).

PROTEASES IN VISCERAL HYPERSENSITIVITY

An increase in serine protease activity, mainly trypsin-like, in colonic tissue or tissue supernatants of IBS patients compared to healthy controls has been reported by several groups (Barbara et al., 2004; Cenac et al., 2007; Buhner et al., 2009; Rolland-Fourcade et al., 2017; Aguilera-Lizarraga et al., 2021). Accordingly, elevated tryptase and trypsin mRNA and protein levels were shown (Zhao et al., 2012; Liang et al., 2016). The increase in tryptase levels was correlated with a higher number of mast cells in the mucosa by some groups (Barbara et al., 2004; Bian et al., 2009; Buhner et al., 2009) although others reported no increase in mast cell count (Cenac et al., 2007; Wouters et al., 2016). Most recently, we provided compelling evidence that mast cells in the rectal mucosa of IBS patients are more sensitized with IgE, thereby more prone to degranulation and tryptase release upon antigen stimulation (Aguilera-Lizarraga et al., 2021). Trypsin-3, as revealed by *in situ* zymography, is expressed by the intestinal epithelium and upregulated in IBS (Rolland-Fourcade et al., 2017). Thrombin, recently identified as upregulated in IBD patients (Denadai-Souza et al., 2018), did not differ, at least in expression levels, between IBS patients and controls (Bian et al., 2009). Interestingly, proteome analysis with LC-MS/MS (liquid chromatography with tandem mass spectrometry) revealed upregulation of elastase-like and not trypsin-like serine proteases in colonic biopsy supernatants from IBS patients (Buhner et al., 2018). However, no complementary experiments were done to confirm this finding. Also, in feces of IBS patients, researchers found an increase in serine protease activity from either the patient or the intestinal bacteria (Annaházi et al., 2009; Tooth et al., 2014; Edogawa et al., 2020). Although these enzymes are less likely to play a direct role in the sensitization of intestinal nociceptors since they would first have to cross the epithelial barrier, they might be involved in barrier dysfunction (Steck et al., 2012; Lomax et al., 2019).

PROTEASE INHIBITORS IN VISCERAL HYPERSENSITIVITY

With increasing evidence that serine proteases contribute to the pathophysiology of IBS, also the search for effective protease inhibitors as therapeutic agents has started. Targeting proteases has resulted in several great success stories in other conditions such as HIV and cardiovascular diseases but it remains a challenging endeavor overall (Turk, 2006; Drag, 2010). To date, no protease inhibitors are marketed or in clinical trials for IBS and only few studies have explored the effects of serine protease inhibitors in experimental models of VHS.

Nafamostat mesylate, also called FUT-175, is a short-acting, synthetic inhibitor of serine proteases with poor oral bioavailability that has been approved in Japan as a treatment for acute pancreatitis and disseminated intravascular coagulation (Cao et al., 2008). FUT-175 could prevent development of VHS in WT mice when co-administered intracolonic with IBS supernatants (Cenac et al., 2007). Additionally, a single intraperitoneal injection of FUT-175 normalized visceral sensitivity in post-colitis rats (Ceuleers et al., 2018). Camostat mesylate, or FOY-305, has similar properties and indications as FUT-175. Intragastric pretreatment with FOY-305 could prevent acute stress-induced VHS in rats (Zhao et al., 2011). Both inhibitors target a broad-spectrum of serine proteases, have anticoagulation activity and are associated with rare, but important side effects such as hyperkalemia, as well as mild complications like headache (Sawada et al., 2016; Quinn et al., 2022). It is important to emphasize that the broad range of targets and intravenous administration (for FUT-175) are crucial determinants of the risk for side effects. Improved targeting of the inhibitors is definitely needed when considering these compounds as treatment options for a chronic and not life-threatening condition such as IBS. Alternatively, oral compounds that act locally and are not systemically absorbed are most likely the safest approach with minimal risk of side effects.

Two newly developed serine protease inhibitors, UAMC-00050 and UAMC-01162, have a more favorable inhibitory profile with a limited inhibition of proteases related to the blood coagulation cascade, but a good inhibition of tryptase (Joossens et al., 2007). Neither had an effect on visceral sensitivity in healthy control animals but successfully reversed VHS in post-colitis rats in the highest dose used (1 mg/kg UAM-00050; 2.5 mg/kg UAMC-01162) (Ceuleers et al., 2018). Plant-derived Bowman-Birk inhibitors are specific toward trypsin and chymotrypsin and are present in vegetables like soybeans. Oral administration of soy germ extract for 15 days resulted in a decrease in visceral sensitivity, fecal protease activity, and PAR2 expression in a stress-induced rat model for VHS (Moussa et al., 2013). However, soy germ extract also contains phytoestrogens and an estrogen-receptor antagonist reversed all effects, except the decrease in fecal proteolytic activity (Moussa et al., 2013). The positive effect of soy germ extract is therefore likely a result of the combination of estrogen-receptor and PAR2 mediated pathways. A randomized, double-blind, placebo-controlled trial done in patients with ulcerative colitis indicated that soy extract is safe although not very effective (Lichtenstein et al., 2008).

Another therapeutic strategy is to increase the bioactive life-span of endogenous opioids in the gut and thereby relieve abdominal pain. Agonists of the μ-opioid receptor are already on the market for diarrhea-predominant IBS, e.g. loperamide, but these drugs can cause severe secondary constipation and do not adequately resolve abdominal pain (Moayyedi et al., 2019). Inhibiting opioid degrading enzymes would have an effect that is restricted in time and space, allowing better control of pharmacological activity. Additionally, repeated administration of RB101, the first dual enkephalinase inhibitor, did not induce tolerance or physical dependence in early animal studies, unlike opioid receptor agonists such as morphine (Noble et al.,1992a; 1992b). Sialorphin, a natural enkephalinase inhibitor, was recently studied for its analgesic potential in a mouse model of

A Generation of specific protease inhibitors

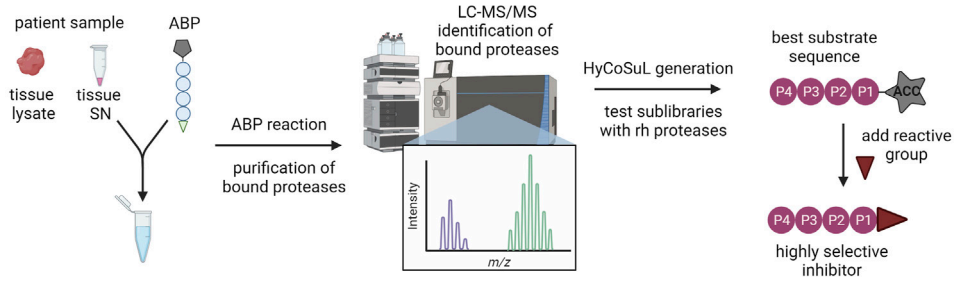

B Animal models for IBS

Model	Species	Affected (studied) regions	Disease mechanism	Visceral sensitization model	Proteases involved in VHS	References
TNBS / post-colitis	Rat, mouse	Colon, stomach	Post-inflammation	acute + chronic (2d-17w)	tryptase-αβ-1 (mRNA), trypsin-like (activity)	Ceuleers et al., 2018; Hughes et al., 2009; Adam et al., 2006; Gschossmann et al., 2004; Winston et al., 2013
Post-infectious OVA intolerance	Mouse	Colon	Break of tolerance to dietary antigen	Transient; during OVA re-exposure (7w post-infection)	tryptase-αβ-1 (mRNA)	Aguilera-Lizarraga et al., 2021
Maternal separation	Rat, mouse (less)	Colon, stomach, CNS	Brain-gut axis dysfunction (early-life stress)	Chronic (1w-12w) Some models require water avoidance to induce VHS (6h-30d)	unknown	Coutinho et al., 2002; Tominaga et al., 2016; O'Mahony et al., 2011; Meleine et al., 2016; Biagini et al., 1998; Ryan et al., 2009; van den Wijngaard et al., 2012
Water avoidance	Rat, mouse	Colon, small intestine, stomach, CNS	Brain-gut axis dysfunction (anxiety inducing)	Transient (acute stress) or chronic (repeated stress)	unknown	Myers et al., 2012; Eutamene et al., 2010; Annahazi et al., 2012; Nozu et al., 2014; Bradesi et al., 2005;

FIGURE 2 | From protease identification to inhibitor design. **(A)** Workflow to develop highly selective protease inhibitors. First, serine proteases present in patient samples, whole tissue lysate or supernatant (SN) containing secreted mediators, will be labeled with desthiobiotin-tagged activity-based probes (ABPs) specific for this class. The desthiobiotin-tag of the ABP is represented as a pentagon, the circles represent the recognition element, and the reactive group that will bind the attacking protease is represented as a triangle. The bound proteases will be isolated with paramagnetic beads conjugated to streptavidin and analyzed by LC-MS/MS. This will unambiguously inform the researcher about the identity of all active serine proteases in the sample and which ones are increased in IBS patients compared to controls. Next, hybrid combinatorial substrate libraries (HyCoSuL) will be developed to determine the substrate specificities of the identified protease(s). For serine proteases, three tetrapeptide sublibraries are made with a fixed amino acid at the P1 position, according to the serine protease of interest. The protease will attack the bond between the amino acid at P1 and the fluorogenic reporter (7-aminocoumarin-4-acetic acid, ACC) at the P1′ position so that hydrolysis can be measured in a plate reader. In each sublibrary, one of the three remaining positions in the tetrapeptide (P2-P4) has a fixed amino acid while the remaining positions contain an equimolar mixture of amino acids. Ultimately, the optimal substrates can be determined using recombinant human (rh) proteases by combining the results from all sublibraries. With prior knowledge about the specificity of the protease, the palette of amino acids can be customized to minimize the number of sublibraries. The best substrate sequence will be used as a scaffold to synthesize highly specific protease inhibitors. **(B)** Animal models of IBS to test the effectiveness of serine protease inhibitors on abdominal pain. TNBS: Trinitrobenzene sulfonic acid; OVA: ovalbumin; CNS: central nervous system (Adam et al., 2006; Annaházi et al., 2012; Biagini et al., 1998; Bradesi et al., 2005; Coutinho et al., 2002; Eutamene et al., 2010; Gschossmann et al., 2004; Hughes et al., 2009; Meleine et al., 2016; Myers and Greenwood-Van Meerveld, 2012; Nozu et al., 2014; O' Mahony et al., 2011; Ryan et al., 2009; Tominaga et al., 2016; van den Wijngaard et al., 2012; Winston and Sarna, 2013). Created with BioRender.com.

visceral pain induced by colorectal distension (Fabisiak et al., 2018). They showed that subcutaneous administration of sialorphin increased the pain threshold comparable to the opioid Leu-enkephalin. Nevertheless, further and more targeted research investigating the potency and side effects of these inhibitors is necessary.

Protease inhibitors with greater specificity have not been tested for their effects on VHS, mainly because the exact targets still need to be identified. However, the following inhibitors might be of interest to explore further. Leupeptin, an organic compound produced by many Actinomycetales bacteria in the human intestinal tract, targets serine proteases (trypsin, plasmin, and kallikrein) and cysteine proteases (papain and cathepsin B), but not thrombin, elastase, or chymotrypsin. This inhibitor was used by Rolland-Fourcade et al. to demonstrate that lipopolysaccharide-stimulation of intestinal epithelial cells results in basolateral release of trypsin-like proteases (Rolland-Fourcade et al., 2017). APC-366 is a tryptase-specific inhibitor and was employed recently to discriminate tryptase activity from total trypsin-like activity (Aguilera-Lizarraga et al., 2021). Initially, it was developed to treat asthma, allergy, and colitis, but it lacked potency and selectivity. This inhibitor also has high affinity for thrombin, a pivotal enzyme in blood coagulation, thus when not applied locally, APC-366 could lead to bleeding. APC-2059 had improved specificity and seemed to be useful as adjuvant

therapy in ulcerative colitis in an open-label, phase two clinical study (Tremaine et al., 2002). However, it needed to be injected and was not developed further.

This indicates that drugability is a critical aspect that requires a lot of attention. For compound UAMC-00050 the efficacy decreased when given locally via an enema versus intraperitoneal injection (Ceuleers et al., 2018; Hanning et al., 2021). Plasma concentrations were very low after intracolonic administration and on average only 5.4% of the plasma concentration after intravenous administration although a five times larger dose was used for local application. This suggests that the inhibitor mainly stays in the lumen or intestinal mucosa. The animals were observed for 3 h after administration of the drug and no side effects were noted. Nonetheless, it would be more relevant for clinical trials if the compounds can be taken orally. Giardina et al. developed a novel inhibitor of human b-tryptase with good oral bioavailability (Giardina et al., 2018). As a dimeric inhibitor, it bridges two active sites resulting in increased affinity and specificity compared to monomeric controls. But unlike previously reported polyvalent inhibitors, this one contains a disiloxane linker, which greatly improves the bioavailability after oral administration. This compound would be of great interest to explore in the context of IBS. The same applies for the use of recombinant lactic acid bacteria to deliver serine protease inhibitors to the intestinal mucosa (Bermúdez-Humarán et al., 2015). However, only biologicals can be delivered via this system and these tend to have a broader selectivity.

TOWARDS MORE SELECTIVE PROTEASE TARGETING

The two major factors hampering the development of specific protease inhibitors are the superficial identification of overactive serine proteases in this disorder, as well as the limited mapping of substrate preferences of relevant proteases. Activity-based probes (ABPs) provide a solution for the first obstacle. The reactive group of the probe binds specifically and irreversibly to the proteases of interest. This allows identification of the bound proteases by mass spectrometry after affinity-based purification. The use of these probes is slowly increasing in the field of inflammatory and functional bowel diseases, which can only be encouraged further (Mayers et al., 2017; Denadai-Souza et al., 2018; Anderson et al., 2019; Solà-Tapias et al., 2020). To tackle the second obstacle; the hybrid combinatorial substrate library (HyCoSuL) using natural and unnatural amino acids, is an efficient way to find highly selective protease substrates (Kasperkiewicz et al., 2014). A HyCoSuL for serine proteases would consist of three sublibraries of tetrapeptides with a fixed amino acid at P1 and amino acid mixtures at the P4-P2 positions as well as an ACC (7-aminocoumarin-4-acetic acid) fluorescent tag occupying the P1' position. Once the tetrapeptide is cleaved, the ACC produces a fluorescent signal.

HyCoSuL has proven to be a valuable tool to study protease substrate preference, however, it is limited to the amino acid residues N-terminal to the cleavage site (Poreba et al., 2018; Anderson et al., 2019). Internally quenched fluorescent substrates are an excellent way to study the specificity of both the prime and non-prime pockets but are inefficient for large screenings. A very good tool for screening a large (up to 10^{10}) and diverse pool of substrates is phage display technology (Kehoe, 2005; Caberoy et al., 2011). Random peptides are expressed on the phage surface and subjected to protease cleavage followed by phage amplification if successfully cleaved. Thus, optimal substrates are enriched over multiple rounds of selection. A major drawback is that the substrates are label-free, so they need to be resynthesized with an appropriate reporter group to compare the kinetics of the best substrates. Label-free substrates are not per se a bad thing; not having a label right next to the cleavage site means it also cannot influence the enzyme-substrate binding interactions. Other approaches to study substrate specificity without the use of reporter tags utilize mass spectrometry (O'Donoghue et al., 2012; Wood et al., 2017; Lapek et al., 2019). A beautiful example by De Bruyn et al. in an acute- and a post-colitis rat model illustrates this is a valuable way to investigate the identity and cleavage patterns of proteases in biological samples (De Bruyn et al., 2021). By applying this method, the authors demonstrated that tryptase and trypsin-3 also unmask PAR1. Nevertheless, also this technique is somewhat biased and requires prior knowledge of the proteases that are being studied. It is important to note that these methods do not exclude each other, on the contrary, they are complementary and provide extra strength where there is overlap.

Combining target identification via ABPs and inhibitor design via HyCoSuL should provide a reliable and accessible toolbox to design highly specific protease inhibitors for the management of abdominal pain in IBS (**Figure 2A**). Testing the effectiveness and safety of promising serine protease inhibitors should be done in animal models of IBS to maximize translational value (**Figure 2B**). Although these models inherently are limited in reflecting the complex disease mechanisms underlying IBS, they are able to induce VHS, an important factor in IBS and the target of these protease inhibitors (Accarie, 2020). It must be noted that the research investigating the role of serine proteases in VHS in these models is in its infancy and the translational value of the results requires further exploration.

CONCLUSION

The investigation of protease dysregulation in gastrointestinal diseases, and more specifically in VHS and IBS, has definitely increased in recent years, bringing protease inhibition to the forefront of one of the most promising novel therapeutic strategies to explore. However, three important factors need to be addressed to advance serine protease inhibitors as a treatment for VHS in IBS. The first is the limited knowledge of the targets. The dysregulated proteases need to be characterized unambiguously and on a patient level, an endeavor that can be achieved with activity-based probes. Secondly, as underlined in this review, proteases have many important physiological roles and any inhibition will have to be carefully targeted to limit side effects. Accurate mapping of substrate specificities of the proteases of interest with a technique like HyCoSuL will facilitate and accelerate the development of highly specific serine protease inhibitors. The third and final limiting factor is that the current oral bioavailability of serine protease inhibitors is poor and improvement of formulations favoring local delivery should be prioritized to give the inhibitors a higher chance to succeed in clinical trials for IBS.

AUTHOR CONTRIBUTIONS

LD prepared the figures and drafted the manuscript; LD and AD-S edited the manuscript; LD, AD-S, and GB revised and approved the final version of the manuscript.

FUNDING

This work was funded by the FWO PhD fellowship no. 11B8920N (to L.D.) and the FWO-SBO grant no. S001017N.

REFERENCES

Accarie, A., and Vanuytsel, T. (2020). Animal Models for Functional Gastrointestinal Disorders. *Front. Psychiatry* 11, 509681. doi:10.3389/fpsyt.2020.509681

Adam, B., Liebregts, T., Gschossmann, J. M., Krippner, C., Scholl, F., Ruwe, M., et al. (2006). Severity of Mucosal Inflammation as a Predictor for Alterations of Visceral Sensory Function in a Rat Model. *Pain* 123, 179–186. doi:10.1016/j.pain.2006.02.029

Aguilera-Lizarraga, J., Florens, M. V., Viola, M. F., Jain, P., Decraecker, L., Appeltans, I., et al. (2021). Local Immune Response to Food Antigens Drives Meal-Induced Abdominal Pain. *Nature* 590, 151–156. doi:10.1038/s41586-020-03118-2

Amadesi, S., Cottrell, G. S., Divino, L., Chapman, K., Grady, E. F., Bautista, F., et al. (2006). Protease-Activated Receptor 2 Sensitizes TRPV1 by Protein Kinase Cε-and A-Dependent Mechanisms in Rats and Mice. *J. Physiol.* 575, 555–571. doi:10.1113/jphysiol.2006.111534

Anand, P., Aziz, Q., Willert, R., and Van Oudenhove, L. (2007). Peripheral and Central Mechanisms of Visceral Sensitization in Man. *Neurogastroenterol. Motil.* 19, 29–46. doi:10.1111/j.1365-2982.2006.00873.x

Anderson, B. M., Poole, D. P., Aurelio, L., Ng, G. Z., Fleischmann, M., Kasperkiewicz, P., et al. (2019). Application of a Chemical Probe to Detect Neutrophil Elastase Activation During Inflammatory Bowel Disease. *Sci. Rep.* 9, 13295. doi:10.1038/s41598-019-49840-4

Annaházi, A., Dabek, M., Gecse, K., Salvador-Cartier, C., Polizzi, A., Rosztóczy, A., et al. (2012). Proteinase-Activated Receptor-4 Evoked Colorectal Analgesia in Mice: An Endogenously Activated Feed-Back Loop in Visceral Inflammatory Pain. *Neurogastroenterol. Motil.* 24, 76–e13. doi:10.1111/j.1365-2982.2011.01805.x

Annaházi, A., Gecse, K., Dabek, M., Ait-Belgnaoui, A., Rosztóczy, A., Róka, R., et al. (2009). Fecal Proteases from Diarrheic-IBS and Ulcerative Colitis Patients Exert Opposite Effect on Visceral Sensitivity in Mice. *Pain* 144, 209–217. doi:10.1016/j.pain.2009.04.017

Asfaha, S., Brussee, V., Chapman, K., Zochodne, D. W., and Vergnolle, N. (2002). Proteinase-Activated Receptor-1 Agonists Attenuate Nociception in Response to Noxious Stimuli. *Br. J. Pharmacol.* 135, 1101–1106. doi:10.1038/sj.bjp.0704568

Balemans, D., Aguilera-Lizarraga, J., Florens, M. V., Jain, P., Denadai-Souza, A., Viola, M. F., et al. (2019). Histamine-Mediated Potentiation of Transient Receptor Potential (TRP) Ankyrin 1 and TRP Vanilloid 4 Signaling in Submucosal Neurons in Patients with Irritable Bowel Syndrome. *Am. J. Physiology-Gastrointestinal Liver Physiology* 316, G338–G349. doi:10.1152/ajpgi.00116.2018

Balemans, D., Boeckxstaens, G. E., Talavera, K., and Wouters, M. M. (2017). Transient Receptor Potential Ion Channel Function in Sensory Transduction and Cellular Signaling Cascades Underlying Visceral Hypersensitivity. *Am. J. Physiology-Gastrointestinal Liver Physiology* 312, G635–G648. doi:10.1152/ajpgi.00401.2016

Barbara, G., Stanghellini, V., De Giorgio, R., Cremon, C., Cottrell, G. S., Santini, D., et al. (2004). Activated Mast Cells in Proximity to Colonic Nerves Correlate with Abdominal Pain in Irritable Bowel Syndrome. *Gastroenterology* 126, 693–702. doi:10.1053/j.gastro.2003.11.055

Bermúdez-Humarán, L. G., Motta, J.-P., Aubry, C., Kharrat, P., Rous-Martin, L., Sallenave, J.-M., et al. (2015). Serine Protease Inhibitors Protect Better Than IL-10 and TGF-β Anti-Inflammatory Cytokines Against Mouse Colitis When Delivered by Recombinant Lactococci. *Microb. Cell Fact.* 14, 26. doi:10.1186/s12934-015-0198-4

Biagini, G., Pich, E. M., Carani, C., Marrama, P., and Agnati, L. F. (1998). Postnatal Maternal Separation During the Stress Hyporesponsive Period Enhances the Adrenocortical Response to Novelty in Adult Rats by Affecting Feedback Regulation in the CA1 Hippocampal Field. *Int. J. Dev. Neurosci.* 16, 187–197. doi:10.1016/s0736-5748(98)00019-7

Bian, Z. X., Li, Z., Huang, Z. X., Zhang, M., Chen, H. L., Xu, H. X., et al. (2009). Unbalanced Expression of Protease-Activated Receptors-1 and -2 in the Colon of Diarrhea-Predominant Irritable Bowel Syndrome Patients. *J. Gastroenterol.* 44, 666–674. doi:10.1007/s00535-009-0058-2

Bradesi, S., Schwetz, I., Ennes, H. S., Lamy, C. M. R., Ohning, G., Fanselow, M., et al. (2005). Repeated Exposure to Water Avoidance Stress in Rats: A New Model for Sustained Visceral Hyperalgesia. *Am. J. Physiology-Gastrointestinal Liver Physiology* 289, G42–G53. doi:10.1152/ajpgi.00500.2004

Brizuela, M., Castro, J., Harrington, A. M., and Brierley, S. M. (2021). Pruritogenic Mechanisms and Gut Sensation: Putting the "Irritant" into Irritable Bowel Syndrome. *Am. J. Physiology-Gastrointestinal Liver Physiology* 320, G1131–G1141. doi:10.1152/ajpgi.00331.2020

Buhner, S., Hahne, H., Hartwig, K., Li, Q., Vignali, S., Ostertag, D., et al. (2018). Protease Signaling Through Protease Activated Receptor 1 Mediate Nerve Activation by Mucosal Supernatants from Irritable Bowel Syndrome but Not from Ulcerative Colitis Patients. *PLoS One* 13, e0193943–16. doi:10.1371/journal.pone.0193943

Buhner, S., Li, Q., Vignali, S., Barbara, G., De Giorgio, R., Stanghellini, V., et al. (2009). Activation of Human Enteric Neurons by Supernatants of Colonic Biopsy Specimens from Patients with Irritable Bowel Syndrome. *Gastroenterology* 137, 1425–1434. doi:10.1053/j.gastro.2009.07.005

Caberoy, N., Alvarado, G., and Li, W. (2011). Identification of Calpain Substrates by ORF Phage Display. *Molecules* 16, 1739–1748. doi:10.3390/molecules16021739

Cao, Y.-g., Zhang, M., Yu, D., Shao, J.-p., Chen, Y.-c., and Liu, X.-q. (2008). A Method for Quantifying the Unstable and Highly Polar Drug Nafamostat Mesilate in Human Plasma with Optimized Solid-Phase Extraction and ESI-MS Detection: More Accurate Evaluation for Pharmacokinetic Study. *Anal. Bioanal. Chem.* 391, 1063–1071. doi:10.1007/s00216-008-2054-4

Cattaruzza, F., Spreadbury, I., Miranda-Morales, M., Grady, E. F., Vanner, S., and Bunnett, N. W. (2010). Transient Receptor Potential Ankyrin-1 Has a Major Role in Mediating Visceral Pain in Mice. *Am. J. Physiology-Gastrointestinal Liver Physiology* 298, G81–G91. doi:10.1152/ajpgi.00221.2009

Cenac, N., Andrews, C. N., Holzhausen, M., Chapman, K., Cottrell, G., Andrade-Gordon, P., et al. (2007). Role for Protease Activity in Visceral Pain in Irritable Bowel Syndrome. *J. Clin. Investig.* 117, 636–647. doi:10.1172/JCI29255.636

Cenac, N., Bautzova, T., Le Faouder, P., Veldhuis, N. A., Poole, D. P., Rolland, C., et al. (2015). Quantification and Potential Functions of Endogenous Agonists of Transient Receptor Potential Channels in Patients with Irritable Bowel Syndrome. *Gastroenterology* 149, 433–444. e7. doi:10.1053/j.gastro.2015.04.011

Cenac, N. (2013). Protease-Activated Receptors as Therapeutic Targets in Visceral Pain. *Cn* 11, 598–605. doi:10.2174/1570159X113119990039

Ceuleers, H., Hanning, N., Heirbaut, J., Van Remoortel, S., Joossens, J., Van Der Veken, P., et al. (2018). Newly Developed Serine Protease Inhibitors Decrease Visceral Hypersensitivity in a Post-Inflammatory Rat Model for Irritable Bowel Syndrome. *Br. J. Pharmacol.* 175, 3516–3533. doi:10.1111/bph.14396

Coutinho, S. V., Plotsky, P. M., Sablad, M., Miller, J. C., Zhou, H., Bayati, A. I., et al. (2002). Neonatal Maternal Separation Alters Stress-Induced Responses to Viscerosomatic Nociceptive Stimuli in Rat. *Am. J. Physiology-Gastrointestinal Liver Physiology* 282, G307–G316. doi:10.1152/ajpgi.00240.2001

Dai, Y., Moriyama, T., Higashi, T., Togashi, K., Kobayashi, K., Yamanaka, H., et al. (2004). Proteinase-Activated Receptor 2-Mediated Potentiation of Transient Receptor Potential Vanilloid Subfamily 1 Activity Reveals a Mechanism for Proteinase-Induced Inflammatory Pain. *J. Neurosci.* 24, 4293–4299. doi:10.1523/JNEUROSCI.0454-04.2004

De Bruyn, M., Ceuleers, H., Hanning, N., Berg, M., De Man, J. G., Hulpiau, P., et al. (2021). Proteolytic Cleavage of Bioactive Peptides and Protease-Activated

Receptors in Acute and Post-Colitis. *Ijms* 22, 10711. doi:10.3390/ijms221910711

Denadai-Souza, A., Bonnart, C., Tapias, N. S., Marcellin, M., Gilmore, B., Alric, L., et al. (2018). Functional Proteomic Profiling of Secreted Serine Proteases in Health and Inflammatory Bowel Disease. *Sci. Rep.* 8, 1–9. doi:10.1038/s41598-018-26282-y

Desormeaux, C., Bautzova, T., Garcia-Caraballo, S., Rolland, C., Barbaro, M. R., Brierley, S. M., et al. (2018a). Protease-Activated Receptor 1 Is Implicated in Irritable Bowel Syndrome Mediators-Induced Signaling to Thoracic Human Sensory Neurons. *Pain* 159, 1257–1267. doi:10.1097/j.pain.0000000000001208

Drag, M., and Salvesen, G. S. (2010). Emerging Principles in Protease-Based Drug Discovery. *Nat. Rev. Drug Discov.* 9, 690–701. doi:10.1038/nrd3053

Drossman, D. A., Chang, L., Schneck, S., Blackman, C., Norton, W. F., and Norton, N. J. (2009). A Focus Group Assessment of Patient Perspectives on Irritable Bowel Syndrome and Illness Severity. *Dig. Dis. Sci.* 54, 1532–1541. doi:10.1007/s10620-009-0792-6

Drossman, D. A. (2016). Functional Gastrointestinal Disorders: History, Pathophysiology, Clinical Features, and Rome IV. *Gastroenterology* 150, 1262–1279. doi:10.1053/J.GASTRO.2016.02.032

Edogawa, S., Edwinson, A. L., Peters, S. A., Chikkamenahalli, L. L., Sundt, W., Graves, S., et al. (2020). Serine Proteases as Luminal Mediators of Intestinal Barrier Dysfunction and Symptom Severity in IBS. *Gut* 69, 62–73. doi:10.1136/gutjnl-2018-317416

Eutamene, H., Bradesi, S., Larauche, M., Theodorou, V., Beaufrand, C., Ohning, G., et al. (2010). Guanylate Cyclase C-Mediated Antinociceptive Effects of Linaclotide in Rodent Models of Visceral Pain. *Neurogastroenterol. Motil.* 22, 312–e84. doi:10.1111/j.1365-2982.2009.01385.x

Fabisiak, A., Sobocińska, M., Kamysz, E., Fichna, J., and Zielińska, M. (2018). Antinociceptive Potency of Enkephalins and Enkephalinase Inhibitors in the Mouse Model of Colorectal Distension-Proof-Of-Concept. *Chem. Biol. Drug Des.* 92, 1387–1392. doi:10.1111/cbdd.13186

Farzaei, M. H., Bahramsoltani, R., Abdollahi, M., and Rahimi, R. (2016). The Role of Visceral Hypersensitivity in Irritable Bowel Syndrome: Pharmacological Targets and Novel Treatments. *J. Neurogastroenterol. Motil.* 22, 558–574. doi:10.5056/jnm16001

Flacco, M. E., Manzoli, L., De Giorgio, R., Gasbarrini, A., Cicchetti, A., Bravi, F., et al. (2019). Costs of Irritable Bowel Syndrome in European Countries with Universal Healthcare Coverage: A Meta-Analysis. *Eur. Rev. Med. Pharmacol. Sci.* 23, 2986–3000. doi:10.26355/eurrev_201904_17580

Giardina, S. F., Werner, D. S., Pingle, M., Bergstrom, D. E., Arnold, L. D., and Barany, F. (2018). A Novel, Nonpeptidic, Orally Active Bivalent Inhibitor of Human β-Tryptase. *Pharmacology* 102, 233–243. doi:10.1159/000492078

Gottesman-Katz, L., Latorre, R., Vanner, S., Schmidt, B. L., and Bunnett, N. W. (2021). Targeting G Protein-Coupled Receptors for the Treatment of Chronic Pain in the Digestive System. *Gut* 70, 970–981. doi:10.1136/gutjnl-2020-321193

Grant, A. D., Cottrell, G. S., Amadesi, S., Trevisani, M., Nicoletti, P., Materazzi, S., et al. (2007). Protease-Activated Receptor 2 Sensitizes the Transient Receptor Potential Vanilloid 4 Ion Channel to Cause Mechanical Hyperalgesia in Mice. *J. Physiol.* 578, 715–733. doi:10.1113/jphysiol.2006.121111

Gschossmann, J. M., Liebregts, T., Adam, B., Buenger, L., Ruwe, M., Gerken, G., et al. (2004). Long-Term Effects of Transient Chemically Induced Colitis on the Visceromotor Response to Mechanical Colorectal Distension. *Dig. Dis. Sci.* 49, 96–101. doi:10.1023/B:DDAS.0000011609.68882.3a

Hanning, N., De bruyn, M., Ceuleers, H., Boogaerts, T., Berg, M., Smet, A., et al. (2021). Local Colonic Administration of a Serine Protease Inhibitor Improves Post-Inflammatory Visceral Hypersensitivity in Rats. *Pharmaceutics* 13, 811. doi:10.3390/pharmaceutics13060811

Hughes, P. A., Brierley, S. M., Martin, C. M., Brookes, S. J. H., Linden, D. R., and Blackshaw, L. A. (2009). Post-Inflammatory Colonic Afferent Sensitisation: Different Subtypes, Different Pathways and Different Time Courses. *Gut* 58, 1333–1341. doi:10.1136/gut.2008.170811

Joossens, J., Ali, O. M., El-Sayed, I., Surpateanu, G., Van der Veken, P., Lambeir, A.-M., et al. (2007). Small, Potent, and Selective Diaryl Phosphonate Inhibitors for Urokinase-Type Plasminogen Activator with *In Vivo* Antimetastatic Properties. *J. Med. Chem.* 50, 6638–6646. doi:10.1021/jm700962j

Kasperkiewicz, P., Poreba, M., Snipas, S. J., Parker, H., Winterbourn, C. C., Salvesen, G. S., et al. (2014). Design of Ultrasensitive Probes for Human Neutrophil Elastase through Hybrid Combinatorial Substrate Library Profiling. *Proc. Natl. Acad. Sci. U.S.A.* 111, 2518–2523. doi:10.1073/pnas.1318548111

Kawao, N., Ikeda, H., Kitano, T., Kuroda, R., Sekiguchi, F., Kataoka, K., et al. (2004). Modulation of Capsaicin-Evoked Visceral Pain and Referred Hyperalgesia by Protease-Activated Receptors 1 and 2. *J. Pharmacol. Sci.* 94, 277–285. doi:10.1254/jphs.94.277

Kehoe, J. W., and Kay, B. K. (2005). Filamentous Phage Display in the New Millennium. *Chem. Rev.* 105, 4056–4072. doi:10.1021/cr000261r

Kugler, E. M., Mazzuoli, G., Demir, I. E., Ceyhan, G. O., Zeller, F., and Schemann, M. (2012). Activity of Protease-Activated Receptors in Primary Cultured Human Myenteric Neurons. *Front. Neurosci.* 6, 1–8. doi:10.3389/fnins.2012.00133

Lapek, J. D., Jiang, Z., Wozniak, J. M., Arutyunova, E., Wang, S. C., Lemieux, M. J., et al. (2019). Quantitative Multiplex Substrate Profiling of Peptidases by Mass Spectrometry, *Mol. Cell. Proteomics*, 18. ZIP, 968–981. doi:10.1074/MCP.TIR118.001099/ATTACHMENT/FC3E83B2-FE0F-46D3-8599-4AC07943FBAC/MMC1

Liang, W.-J., Zhang, G., Luo, H.-S., Liang, L.-X., Huang, D., and Zhang, F.-C. (2016). Tryptase and Protease-Activated Receptor 2 Expression Levels in Irritable Bowel Syndrome. *Gut Liver* 10, 382–390. doi:10.5009/gnl14319

Lichtenstein, G. R., Deren, J. J., Katz, S., Lewis, J. D., Kennedy, A. R., and Ware, J. H. (2008). Bowman-Birk Inhibitor Concentrate: A Novel Therapeutic Agent for Patients with Active Ulcerative Colitis. *Dig. Dis. Sci.* 53, 175–180. doi:10.1007/s10620-007-9840-2

Lomax, A. E., Pradhananga, S., Sessenwein, J. L., and O'Malley, D. (2019). Bacterial Modulation of Visceral Sensation: Mediators and Mechanisms. *Am. J. Physiology-Gastrointestinal Liver Physiology* 317, G363–G372. doi:10.1152/ajpgi.00052.2019

Martin, L., Augé, C., Boué, J., Buresi, M. C., Chapman, K., Asfaha, S., et al. (2009). Thrombin Receptor: An Endogenous Inhibitor of Inflammatory Pain, Activating Opioid Pathways. *Pain* 146, 121–129. doi:10.1016/j.pain.2009.07.016

Mayers, M. D., Moon, C., Stupp, G. S., Su, A. I., and Wolan, D. W. (2017). Quantitative Metaproteomics and Activity-Based Probe Enrichment Reveals Significant Alterations in Protein Expression from a Mouse Model of Inflammatory Bowel Disease. *J. Proteome Res.* 16, 1014–1026. doi:10.1021/acs.jproteome.6b00938

Meleine, M., Boudieu, L., Gelot, A., Muller, E., Lashermes, A., Matricon, J., et al. (2016). Comparative Effects of α2δ-1 Ligands in Mouse Models of Colonic Hypersensitivity. *Wjg* 22, 7111–7123. doi:10.3748/wjg.v22.i31.7111

Mizumura, K., Sugiura, T., Katanosaka, K., Banik, R. K., and Kozaki, Y. (2009). Excitation and Sensitization of Nociceptors by Bradykinin: What Do We Know? *Exp. Brain Res.* 196, 53–65. doi:10.1007/s00221-009-1814-5

Moayyedi, P., Andrews, C. N., MacQueen, G., Korownyk, C., Marsiglio, M., Graff, L., et al. (2019). Canadian Association of Gastroenterology Clinical Practice Guideline for the Management of Irritable Bowel Syndrome (IBS). *J. Can. Assoc. Gastroenterol.* 2, 6–29. doi:10.1093/jcag/gwy071

Mosinska, P., Zielinska, M., and Fichna, J. (2016). Expression and Physiology of Opioid Receptors in the Gastrointestinal Tract. *Curr. Opin. Endocrinol. Diabetes Obes.* 23:(1):3-10. doi:10.1097/MED.0000000000000219

Moussa, L., Bézirard, V., Salvador-Cartier, C., Bacquié, V., Houdeau, E., and Théodorou, V. (2013). A New Soy Germ Fermented Ingredient Displays Estrogenic and Protease Inhibitor Activities Able to Prevent Irritable Bowel Syndrome-Like Symptoms in Stressed Female Rats. *Clin. Nutr.* 32, 51–58. doi:10.1016/j.clnu.2012.05.021

Mueller, K., Michel, K., Krueger, D., Demir, I. E., Ceyhan, G. O., Zeller, F., et al. (2011). Activity of Protease-Activated Receptors in the Human Submucous Plexus. *Gastroenterology* 141, 2088–2097. doi:10.1053/j.gastro.2011.08.034

Myers, B., and Greenwood-Van Meerveld, B. (2012). Differential Involvement of Amygdala Corticosteroid Receptors in Visceral Hyperalgesia Following Acute or Repeated Stress. *Am. J. Physiology-Gastrointestinal Liver Physiology* 302, G260–G266. doi:10.1152/ajpgi.00353.2011

Noble, F., Soleilhac, J. M., Soroca-Lucas, E., Turcaud, S., Fournie-Zaluski, M. C., and Roques, B. P. (1992a). Inhibition of the Enkephalin-Metabolizing Enzymes by the First Systemically Active Mixed Inhibitor Prodrug RB 101 Induces Potent Analgesic Responses in Mice and Rats. *J. Pharmacol. Exp. Ther.* 261, 181–190.

Noble, F., Turcaud, S., Fournié-Zaluski, M.-C., and Roques, B. P. (1992b). Repeated Systemic Administration of the Mixed Inhibitor of Enkephalin-Degrading Enzymes, RB101, Does Not Induce Either Antinociceptive Tolerance or Cross-Tolerance with Morphine. *Eur. J. Pharmacol.* 223, 83–89. doi:10.1016/0014-2999(92)90821-k

Nozu, T., Kumei, S., Takakusaki, K., and Okumura, T. (2014). Water-Avoidance Stress Enhances Gastric Contractions in Freely Moving Conscious Rats: Role of Peripheral CRF Receptors. *J. Gastroenterol.* 49, 799–805. doi:10.1007/s00535-013-0828-8

O' Mahony, S. M., Coelho, A.-M., Fitzgerald, P., Lee, K., Winchester, W., Dinan, T. G., et al. (2011). The Effects of Gabapentin in Two Animal Models of Co-Morbid Anxiety and Visceral Hypersensitivity. *Eur. J. Pharmacol.* 667, 169–174. doi:10.1016/j.ejphar.2011.05.055

O'Donoghue, A. J., Eroy-Reveles, A. A., Knudsen, G. M., Ingram, J., Zhou, M., Statnekov, J. B., et al. (2012). Global Identification of Peptidase Specificity by Multiplex Substrate Profiling. *Nat. Methods* 9, 1095–1100. doi:10.1038/nmeth.2182

Ovaere, P., Lippens, S., Vandenabeele, P., and Declercq, W. (2009). The Emerging Roles of Serine Protease Cascades in the Epidermis. *Trends Biochem. Sci.* 34, 453–463. doi:10.1016/J.TIBS.2009.08.001

Owczarek, D., Cibor, D., Mach, T., Cieśla, A., Pierzchała-Koziec, K., Sałapa, K., et al. (2011). Met-Enkephalins in Patients with Inflammatory Bowel Diseases. *Adv. Med. Sci.* 56, 158–164. doi:10.2478/v10039-011-0051-x

Poreba, M., Rut, W., Vizovisek, M., Groborz, K., Kasperkiewicz, P., Finlay, D., et al. (2018). Selective Imaging of Cathepsin L in Breast Cancer by Fluorescent Activity-Based Probes. *Chem. Sci.* 9, 2113–2129. doi:10.1039/C7SC04303A

Puente, X. S., Sánchez, L. M., Overall, C. M., and López-Otín, C. (2003). Human and Mouse Proteases: A Comparative Genomic Approach. *Nat. Rev. Genet.* 4, 544–558. doi:10.1038/nrg1111

Quinn, T. M., Gaughan, E. E., Bruce, A., Antonelli, J., O'Connor, R., Li, F., et al. (2022). Randomised Controlled Trial of Intravenous Nafamostat Mesylate in COVID Pneumonitis: Phase 1b/2a Experimental Study to Investigate Safety, Pharmacokinetics and Pharmacodynamics. *eBioMedicine* 76, 103856. doi:10.1016/j.ebiom.2022.103856

Rolland-Fourcade, C., Denadai-Souza, A., Cirillo, C., Lopez, C., Jaramillo, J. O., Desormeaux, C., et al. (2017). Epithelial Expression and Function of Trypsin-3 in Irritable Bowel Syndrome. *Gut* 66, 1767–1778. doi:10.1136/gutjnl-2016-312094

Ryan, B., Musazzi, L., Mallei, A., Tardito, D., Gruber, S. H. M., El Khoury, A., et al. (2009). Remodelling by Early-Life Stress of NMDA Receptor-Dependent Synaptic Plasticity in a Gene-Environment Rat Model of Depression. *Int. J. Neuropsychopharm.* 12, 553–559. doi:10.1017/S1461145708009607

Sawada, K., Ohdo, M., Ino, T., Nakamura, T., Numata, T., Shibata, H., et al. (2016). Safety and Tolerability of Nafamostat Mesilate and Heparin as Anticoagulants in Leukocytapheresis for Ulcerative Colitis: Post Hoc Analysis of a Large-Scale, Prospective, Observational Study. *Ther. Apher. Dial.* 20, 197–204. doi:10.1111/1744-9987.12357

Solà-Tapias, N., Vergnolle, N., Denadai-Souza, A., and Barreau, F. (2020). The Interplay Between Genetic Risk Factors and Proteolytic Dysregulation in the Pathophysiology of Inflammatory Bowel Disease. *J. Crohns. Colitis* 14, 1149–1161. doi:10.1093/ecco-jcc/jjaa033

Sostegni, S., Diakov, A., McIntyre, P., Bunnett, N., Korbmacher, C., and Haerteis, S. (2015). Sensitisation of TRPV4 by PAR2 Is Independent of Intracellular Calcium Signalling and Can Be Mediated by the Biased Agonist Neutrophil Elastase. *Pflugers Arch. - Eur. J. Physiol.* 467, 687–701. doi:10.1007/s00424-014-1539-6

Sperber, A. D., Bangdiwala, S. I., Drossman, D. A., Ghoshal, U. C., Simren, M., Tack, J., et al. (2021). Worldwide Prevalence and Burden of Functional Gastrointestinal Disorders, Results of Rome Foundation Global Study. *Gastroenterology* 160, 99–114. e3. doi:10.1053/J.GASTRO.2020.04.014

Stadnicki, A. (2011). Intestinal Tissue Kallikrein-Kinin System in Inflammatory Bowel Disease. *Inflamm. Bowel Dis.* 17, 645–654. doi:10.1002/ibd.21337

Steck, N., Mueller, K., Schemann, M., and Haller, D. (2012). Bacterial Proteases in IBD and IBS. *Gut* 61, 1610–1618. doi:10.1136/gutjnl-2011-300775

Tominaga, K., Fujikawa, Y., Tanaka, F., Kamata, N., Yamagami, H., Tanigawa, T., et al. (2016). Structural Changes in Gastric Glial Cells and Delayed Gastric Emptying as Responses to Early Life Stress and Acute Adulthood Stress in Rats. *Life Sci.* 148, 254–259. doi:10.1016/j.lfs.2016.02.025

Tooth, D., Garsed, K., Singh, G., Marciani, L., Lam, C., Fordham, I., et al. (2014). Characterisation of Faecal Protease Activity in Irritable Bowel Syndrome with Diarrhoea: Origin and Effect of Gut Transit. *Gut* 63, 753–760. doi:10.1136/gutjnl-2012-304042

Tremaine, W. J., Brzezinski, A., Katz, J. A., Wolf, D. C., Fleming, T. J., Mordenti, J., et al. (2002). Treatment of Mildly to Moderately Active Ulcerative Colitis with a Tryptase Inhibitor (APC 2059): An Open-Label Pilot Study. *Aliment. Pharmacol. Ther.* 16, 407–413. doi:10.1046/j.1365-2036.2002.01194.x

Turk, B. (2006). Targeting Proteases: Successes, Failures and Future Prospects. *Nat. Rev. Drug Discov.* 5, 785–799. doi:10.1038/nrd2092

van den Wijngaard, R. M., Stanisor, O. I., van Diest, S. A., Welting, O., Wouters, M. M., de Jonge, W. J., et al. (2012). Peripheral α-helical CRF (9-41) Does Not Reverse Stress-Induced Mast Cell Dependent Visceral Hypersensitivity in Maternally Separated Rats. *Neurogastroenterol. Motil. Off. J. Eur. Gastrointest. Motil. Soc.* 24, 274–e111. doi:10.1111/j.1365-2982.2011.01840.x

Van Spaendonk, H., Ceuleers, H., Witters, L., Patteet, E., Joossens, J., Augustyns, K., et al. (2017). Regulation of Intestinal Permeability: The Role of Proteases. *Wjg* 23, 2106–2123. doi:10.3748/wjg.v23.i12.2106

Vergnolle, N. (2005). Clinical Relevance of Proteinase Activated Receptors (Pars) in the Gut. *Gut* 54, 867–874. doi:10.1136/gut.2004.048876

Vergnolle, N. (2016). Protease Inhibition as New Therapeutic Strategy for GI Diseases. *Gut* 65, 1215–1224. doi:10.1136/gutjnl-2015-309147

Vermeulen, W., De Man, J. G., Pelckmans, P. A., and De Winter, B. Y. (2014). Neuroanatomy of Lower Gastrointestinal Pain Disorders. *World J. Gastroenterol.* 20, http://www.wjgnet.com/20, 1005–1020. doi:10.3748/WJG.V20.I4.1005

Winston, J. H., and Sarna, S. K. (2013). Developmental Origins of Functional Dyspepsia-Like Gastric Hypersensitivity in Rats. *Gastroenterology* 144, 570–579. doi:10.1053/J.GASTRO.2012.11.001

Wood, S. E., Sinsinbar, G., Gudlur, S., Nallani, M., Huang, C.-F., Liedberg, B., et al. (2017). A Bottom-Up Proteomic Approach to Identify Substrate Specificity of Outer-Membrane Protease OmpT. *Angew. Chem. Int. Ed.* 56, 16531–16535. doi:10.1002/anie.201707535

Wouters, M. M., Balemans, D., Van Wanrooy, S., Dooley, J., Cibert-Goton, V., Alpizar, Y. A., et al. (2016). Histamine Receptor H1-Mediated Sensitization of TRPV1 Mediates Visceral Hypersensitivity and Symptoms in Patients with Irritable Bowel Syndrome. *Gastroenterology* 150, 875–887. doi:10.1053/j.gastro.2015.12.034

Zhao, J.-h., Dong, L., Shi, H.-t., Wang, Z.-y., Shi, H.-y., and Ding, H. (2012). The Expression of Protease-Activated Receptor 2 and 4 in the Colon of Irritable Bowel Syndrome Patients. *Dig. Dis. Sci.* 57, 58–64. doi:10.1007/s10620-011-1827-3

Zhao, J., Wang, J., Dong, L., Shi, H., Wang, Z., Ding, H., et al. (2011). A Protease Inhibitor Against Acute Stress-Induced Visceral Hypersensitivity and Paracellular Permeability in Rats. *Eur. J. Pharmacol.* 654, 289–294. doi:10.1016/j.ejphar.2010.12.032

Zhao, P., Lieu, T., Barlow, N., Metcalf, M., Veldhuis, N. A., Jensen, D. D., et al. (2014a). Cathepsin S Causes Inflammatory Pain via Biased Agonism of PAR2 and TRPV4. *J. Biol. Chem.* 289, 27215–27234. doi:10.1074/jbc.M114.599712

Zhao, P., Lieu, T., Barlow, N., Sostegni, S., Haerteis, S., Korbmacher, C., et al. (2015). Neutrophil Elastase Activates Protease-Activated Receptor-2 (PAR2) and Transient Receptor Potential Vanilloid 4 (TRPV4) to Cause Inflammation and Pain. *J. Biol. Chem.* 290, 13875–13887. doi:10.1074/jbc.M115.642736

Zhao, P., Metcalf, M., and Bunnett, N. W. (2014b). Biased Signaling of Protease-Activated Receptors. *Front. Endocrinol.* 5, 1–16. doi:10.3389/fendo.2014.00067

Zielińska, M., Chen, C., Mokrowiecka, A., Cygankiewicz, A. I., Zakrzewski, P. K., Sałaga, M., et al. (2015). Orally Administered Novel Cyclic Pentapeptide P-317 Alleviates Symptoms of Diarrhoea-Predominant Irritable Bowel Syndrome. *J. Pharm. Pharmacol.* 67, 244–254. doi:10.1111/jphp.12335

Conflict of Interest: The authors declare that the research was conducted in the absence of any commercial or financial relationships that could be construed as a potential conflict of interest.

Publisher's Note: All claims expressed in this article are solely those of the authors and do not necessarily represent those of their affiliated organizations, or those of the publisher, the editors and the reviewers. Any product that may be evaluated in this article, or claim that may be made by its manufacturer, is not guaranteed or endorsed by the publisher.

Copyright © 2022 Decraecker, Boeckxstaens and Denadai-Souza. This is an open-access article distributed under the terms of the Creative Commons Attribution License (CC BY). The use, distribution or reproduction in other forums is permitted, provided the original author(s) and the copyright owner(s) are credited and that the original publication in this journal is cited, in accordance with accepted academic practice. No use, distribution or reproduction is permitted which does not comply with these terms.

frontiers | Frontiers in Pharmacology

REVIEW
published: 20 June 2022
doi: 10.3389/fphar.2022.914630

Anti-Inflammatory Effects of Natural Products on Cerebral Ischemia

Yuanhong Shang, Zhe Zhang, Jinfeng Tian and Xiaokai Li*

College of Biological and Chemical Engineering, Panzhihua University, Panzhihua, China

Cerebral ischemia with high mortality and morbidity still requires the effectiveness of medical treatments. A growing number of investigations have shown strong links between inflammation and cerebral ischemia. Natural medicine's treatment methods of cerebral ischemic illness have amassed a wealth of treatment experience and theoretical knowledge. This review summarized recent progress on the disease inflammatory pathways as well as 26 representative natural products that have been routinely utilized to treat cerebral ischemic injury. These natural products have exerted anti-inflammatory effects in cerebral ischemia based on their inflammatory mechanisms, including their inflammatory gene expression patterns and their related different cell types, and the roles of inflammatory mediators in ischemic injury. Overall, the combination of the potential therapeutic interventions of natural products with the inflammatory mechanisms will make them be applicable for cerebral ischemic patients in the future.

Keywords: anti-inflammatory effect, inflammatory mechanism, compound, cerebral ischemia, inflammation, natural product

OPEN ACCESS

Edited by:
Jack Arbiser,
Emory University, United States

Reviewed by:
Sivareddy Challa,
University of Illinois, United States
Emiliano Barreto,
Federal University of Alagoas, Brazil

****Correspondence:***
Jinfeng Tian
tjfasyh@163.com

Specialty section:
This article was submitted to Inflammation Pharmacology, a section of the journal Frontiers in Pharmacology

Received: *07 April 2022*
Accepted: *30 May 2022*
Published: *20 June 2022*

Citation:
Shang Y, Zhang Z, Tian J and Li X (2022) Anti-Inflammatory Effects of Natural Products on Cerebral Ischemia. Front. Pharmacol. 13:914630. doi: 10.3389/fphar.2022.914630

INTRODUCTION

Stroke is a brain disease that causes numerous deaths and disabilities (Yuan et al., 2021), and it is the 3rd in disease mortality rate worldwide (Lo et al., 2003). Stroke is subdivided into ischemia and hemorrhage. Ischemic strokes account for approximately 87% of all deaths and were the focus of major drug trials (Rosenzweig et al., 2007). While ischemia is a pathologic condition in which blood flow is reduced to the point where normal cellular activity is disrupted (Adams et al., 2005; Sacco et al., 2006; Shang et al., 2013). The complex pathophysiology of cerebral ischemia primarily includes inflammatory pathways except ionic imbalances, neuroprotection, apoptosis, oxidative damage and angiogenesis (Deb et al., 2010; Dodd et al., 2021). There is growing evidences that some inflammatory mechanisms play a key role during the setting or acute phase of cerebral ischemia owing to subarachnoid hemorrhage, brain injury or cardiac arrest.

Inflammation, a dynamic tissue response mechanism to resist the invasion of pathogens, evolves over the course of evolution (Headland and Norling, 2015). The role of inflammatory mechanisms is crucial in stroke-related brain injury and tissue damage after ischemia (Przykaza, 2021). The understanding inflammatory of response mechanisms will help workers to choose appropriate intervention measures of blocking the cerebral ischemic injury cascade, and reducing neuronal death, and more efficiently preventing cerebral ischemia and treat disease in the theoretical and clinical applications. As a requirement of novel drug development for cerebral ischemia, there is a focus on the anti-inflammatory mechanisms and effects of natural products. Therefore, understanding and treatments of cerebral ischemic disease will be esential for scientists and clinicians to chooose the suitable anti-inflammatory measures and agents. Some specific natural products discovered from

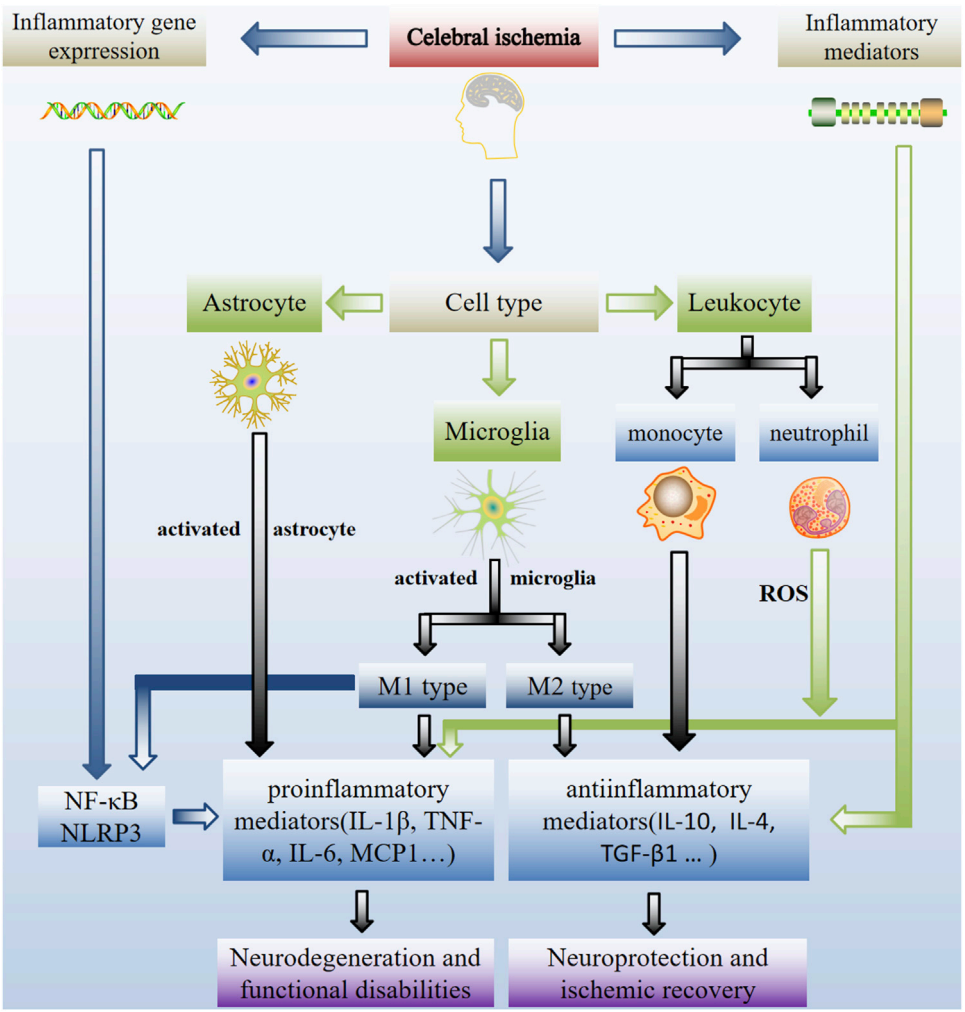

FIGURE 1 | Schematic representation of inflammatory mechanisms in cerebral ischemia. Inflammation is crucial to the pathogenesis of ischemic stroke. Critical inflammatory and anti-inflammatory events involved in inflammatory gene expression, different cell types and inflammatory mediators contribute to ischemic injury. Inflammation inhibition is a possible treatment option for ischemic stroke-related neuro-inflammatory damage. Activation of local microglia and infiltrating macrophages from the compromised BBB occurs during cerebral ischemia. Microglia activation has two-way role (a double-edged sword). Stimulation the activity of microglia migrate to injured neurons and then switche to the M1 or M2 phenotype, which is implicated in nerve injury and repair. As a result, after an ischemic stroke, controlling the M1/m2 phenotype of microglia is critical for brain healing.

natural medical resources with the potentials in possessing anti-inflammatory effects on cerebral ischemia will increase the opportunity in laboratory and clinical trials.

METHODOLOGY

Using exhaustive searches in the PubMed, China National Knowledge Internet (CNKI), Springer and Elsevier SDOL database, the present review gathered data of the research and trials from 2002 until February 2022 for 2 decades by adopting the following keywords and MeSH (medical subject heading) terms according to the Preferred Reporting Items for Systematic Reviews (Bayat et al., 2021). This review mainly summarized the inflammatory mechanisms and some representative natural products that have been commonly used in experimental research for the treatment of cerebral ischemia according to the inflammatory mechanism of ischemia.

INFLAMMATORY MECHANISMS OF ISCHAEMIA

Inflammation acts as a critical role in the pathological progression of cerebral ischemia. Inflammation progresses in response to various stimuli are produced after ischemia. These progresses require activation and undergoes the rapid upregulation of multifarious genes, invasion of leukocyte (monocytes and neutrophils), and stimulation the activity of microglia, astrocytes, and endothelial cells following ischemia with the

duration from hours to days (Huang et al., 2006; Zaleska et al., 2009), including many different inflammatory mediators and extracellular receptors. To avoid the evolution of acute resolving into persistent chronic inflammatory symptoms and further tissue damages, the inflammatory reaction should be actively resolved. Taken all together, the following discussions provided insights into the contributions of key inflammatory gene expression, different cell types, and inflammatory mediators to ischemic injury (**Figure 1**).

Inflammatory Gene Expression

Ischemic injury in the brain parenchyma sets off an inflammatory cascade that exacerbates tissue damage. Each of these events may be affected by heredity, which makes it difficult to prove the classical pattern of heredity. Within minutes of occlusion, pro-inflammatory genes (heat shock proteins, transcription factors, adhesion molecules, chemokines and cytokines) that produce mediators of inflammation are upregulated (Raghay et al., 2020). Among these transcription factors, NF-κB (nuclear factor) regulated the expression of TNF-α (tumor necrosis factor α), NOS (nitric oxide synthase), IL-1β (interleukin-1β), IL-6 (interleukin-6), COX-2 (cyclooxygenase-2) and MCP1 (monocyte chemoattractant protein 1) *in vitro* (Deb et al., 2010). This has been demonstrated by reduced ischemic damage in mutant mice that targeted disruption of these genes (Adibhatla and Hatcher, 2008; Tănăsescu et al., 2008). Intercellular adhesion molecule-1 (ICAM-1) was found to appear in the postischemic no-reflow regions during cerebral ischemia. And it was also a mediator of leukocyte-endothelial cell adhesion (Sun et al., 2019). Matrix metalloproteinase (MMP) levels, especially MMP-9, have been found that associated with infarct growth, bleeding, transformation events, and neurological dysfunction (Montaner et al., 2003; Deb et al., 2010).

Cell Types in Inflammation

The aggregation of inflammatory cells and mediators during cerebral ischemia is a characteristic of inflammation. After vascular occlusion, ischemic injury causes inflammatory cascade and further aggravates tissue injury (Amantea et al., 2014; Soliman et al., 2021). Reactive microglia, leukocytes (inflammatory cells) and macrophages have found to be recruited into the ischemic brain, and then resulting in inflammatory injury and the generation of inflammatory mediators by these cells, neurons and astrocytes.

Microglia

Microglia play critical roles in brain inflammation following stroke, especially in the penumbral region of damage (Subedi and Gaire, 2021). Promoting the polarization of microglia and macrophages from the pro-inflammatory M1 to the anti-inflammatory M2 phenotype has been demonstrated to be a possible treatment for ischemic stroke (Li et al., 2021). M1 is generally considered to be neurotoxic, while M2 exhibits neuroprotective effects. Microglia are in a resting phase. And they account for 5–20% of glial cells (Deb et al., 2010). During ischemia, these cells get the significantly morphological and metabolic changes, as well as rapid and extensive genetic upregulations. These cells are the principal central nervous system (CNS) source of cytokines including transforming growth factor-β (TGF-β), TNF-α and IL-1β (Zarruk et al., 2018). Microglial cells have been indicated that can also produce pro-inflammatory cytokines and neuroprotective factors, such as TGF-β1, metallothionein-2 and erythropoietin. Because of the mixed nature of destructive and protective factors from microglial and astrocytes, the overall role of glia may differ at different time points following stroke insult, with protective or regenerative activities occurring days to weeks after the onset of ischemia. Several studies imply that activated microglia induce to injury (Wang et al., 2007). However, whether microglia cause damage following cerebral ischemia is not clear, and their anti-inflammatory potential is considered to be an significant neuroprotective factor after ischemic injury (Jin et al., 2017; Fukumoto et al., 2019; Gaire, 2021).

Leukocytes

With increasing evidences, leukocytes are related to the pathogenesis of ischemic stroke. An increase in peripheral leukocyte counts are involved in the earliest inflammatory reactions in stroke. Neutrophils are the first leukocytes to respond, and their level is related to the infarct volume. From minutes to hours after reperfusion, neutrophil adhesion and migration have been observed in cerebral venules. After ischemia, the recruited cell population were switched from polymorphonuclear cells to mononuclear leukocytes and lymphocytes, and leukocyte recruitment continued days to weeks (Yilmaz et al., 2006; Gavins et al., 2007). Leukocyte-endothelial cell adhesion was prevented using adhesion molecule antibodies against stroke (Ishikawa et al., 2004). Therefore, leukocytes accumulate in the tissue after ischemia before tissue injury, and specific targeting of leukocytes provides substantive protection for ischemic injury.

Astrocytes

In the human CNS, astrocytes are the main glial cell type and generally exceed the number of neurons. Astrocyte response is one of the earliest and the most significant changes in the CNS after ischemic injury. Astrocytes express different inflammatory mediators in inflammatory responses that may influence the outcome of ischemic injury (Falsig et al., 2006; Denes et al., 2008; Sofroniew, 2020).

Inflammatory Mediators

Inflammatory mediators of cell adhesion to cerebral ischemia are primarily divided into cytokines and chemokines. Cytokines are a flock of small glycoproteins (~25kd) from different sources. As a kind of cytokines, chemokines have chemotactic properties, which can stimulate cells to migrate to the source of chemokines. Chemokines polypeptides have been found to play the role in inflammation, immunological activation, cell differentiation, and cell death.

Cytokines

Cytokines associated with inflammation in stroke, such as IL-1, TNF-α, IL-6, TGF-β and IL-10, are released and serve as

intercellular messengers. Messengers mediate inflammatory and immunological responses. IL-6, IL-10 and TGF-β may have neuroprotective effect. IL-1 and TNF-α aggravate brain injury.

IL-1: IL-1 has two isoforms (IL-1α and IL-1β) and an endogenous inhibitor, IL-1 receptor antagonist (IL-1ra). Its pro-inflammatory properties were neutralized by IL-1ra administration (Emsley et al., 2005), and ischemic injury in IL-1ra deficient mice increased significantly (Pinteaux et al., 2006).

IL-10: an anti-inflammatory cytokine. Lower IL-10 levels are related to one of increased risks in stroke. Guizhi Fuling Capsule significantly upregulate the level of IL-10 mRNA and protein expression and its receptor in rats with focal cerebral ischemia and reperfusion (I/R) (Sun et al., 2015).

IL-6: a pro-inflammatory cytokine with unclear function in stroke. The clinical focus of IL-6 has revealed that IL-6 serum concentrations was an excellent independent predictor value for in-hospital mortality. (Rallidis et al., 2006).

TNF-α: TNF-α is a cellular signal protein involved in systemic inflammation and one of the cytokines involved in acute phase response. Activated macrophages primarily produce TNF-α. Its expression occurs peri-infarct areas in the ischemic core, adjacent distal areas in brain.

TGF-β: TGF-β may helpful for the rehabilitation therapy of ischemic stroke. Microglia secrete TGF-β1 that is reported to protect cultured neurons from ischemia-like injury (Lu et al., 2005). Its expression suggests a neuroprotective function in the penumbra during the recovery phase of cerebral injury.

Chemokines

Chemokines play roles in cellular communication and inflammatory cell recruitment in host defense. Cytokines stimulate the production and release of chemokines C, CC, CXC, and CX3C [location based on the cysteine residues (C)] and MCP-1 (monocyte chemoattractant protein-1) in cerebral ischemia.

CX3C: CX3C expression was limited to surviving neurons around infarction and some endothelial cells during ischemia, and the CX3CR1 expression (CX3C receptor) was found only on microglia. Those suggest that fractalkine is involved in neuron-microglia signal transduction (Tarozzo et al., 2002).

MCP-1: MCP-1 overexpression significantly exacerbated the ischemic injury. This phenomenon is related to the activation of inflammatory cells. MCP-1 increased the cell permeability *in vitro*, and it generated changes in tight junction proteins, which suggest that it helps to 'open' the blood-brain barrier (BBB) (Stamatovic et al., 2005).

THE ANTI-INFLAMMATORY EFFECTS OF NATURAL PRODUCTS

Historically, as folk medicines, natural products have been revealed the vast potentials for drug discoveries and the managements of various human diseases (Mu et al., 2020; Newman and Cragg, 2020; Atanasov et al., 2021). To date, the natural products used for anti-inflammation have been widely investigated and reported (Azab et al., 2016). These natural products with anti-inflammation effects are extensively distributed in different classes, e.g., flavonoids, terpenoids, saponins, phenylpropanoidss, anthraquinones, alkaloids, and phenols, etc., (Wang and Zeng, 2019) (**Figure 2**). These natural products exert significant anti-inflammatory effects *via* acting on different drug targets and cell signaling pathways.

Anti-Inflammatory Effects of Flavonoids in Cerebral Ischemia

Flavonoids are low molecular weight phenolic compounds including A-, B- and C- rings. Most flavonoids that discovered so far have displayed a remarkable array of biochemical and pharmacological actions including anti-inflammatory effects (Romano et al., 2013). Several mechanisms have been proposed to explain the anti-inflammatory effects of flavonoids *in vivo*, including reducing the production of pro-inflammatory molecules and regulating the function of inflammatory cells (Serafini et al., 2010). The natural accuring flavonoids, such as apigenin, baicalin, biochanin A, icariin, mangiferin, and puerarin the flavonoid examples have exhibited anti-inflammatory effects of flavonoids (**Table 1**).

Anti-Inflammatory Effects of Alkaloids in Cerebral Ischemia

Alkaloids are nitrogen-containing organic compounds with an alkali like properties. They that are widely distributed in plants with diverse anti-inflammatory activities provide various potentials for the design and discovery of new anti-inflammatory drugs (Bai et al., 2021). Some alkaloids have strong anti-inflammatory activities and play important roles in the treatment of vascular disease (Alasvand et al., 2019). Anti-inflammatory alkaloids can be mainly divided into the following categories: isoquinoline alkaloids, indole alkaloids, pyridine alkaloids, terpenoid alkaloids, organic amine alkaloids, etc (Li S. et al., 2020). Several studies support the significance of the anti-inflammatory activity as an underlying mechanism for most of the pharmacological activities of the alkaloid (Tian et al., 2019; Geetha and Ramachandran, 2021). Alkaloids, such as berberine, cepharanthine, hydroxysafflor yellow A, sinomenine, tetramethylpyrazine, and vinpocetine, with anti-inflammatory effects in cerebral ischemia treatment, were summaried in **Table 1**.

Anti-Inflammatory Effects of Saponins in Cerebral Ischemia

Saponins are glycosides that release sugar(s) and an aglycone (sapogenin) after acid hydrolysis. The aglycone of saponins can be triterpenoid or steroidal in nature. Steroidal saponins and saponins have been found to have diverse activities of inflammatory cytokines on a variety of inflammatory models (Passos et al., 2022). Studies support the anti-inflammatory activity as an underlying mechanism of the saponin in cerebral ischemia treatment (Sun et al., 2020; Yang F. et al.,

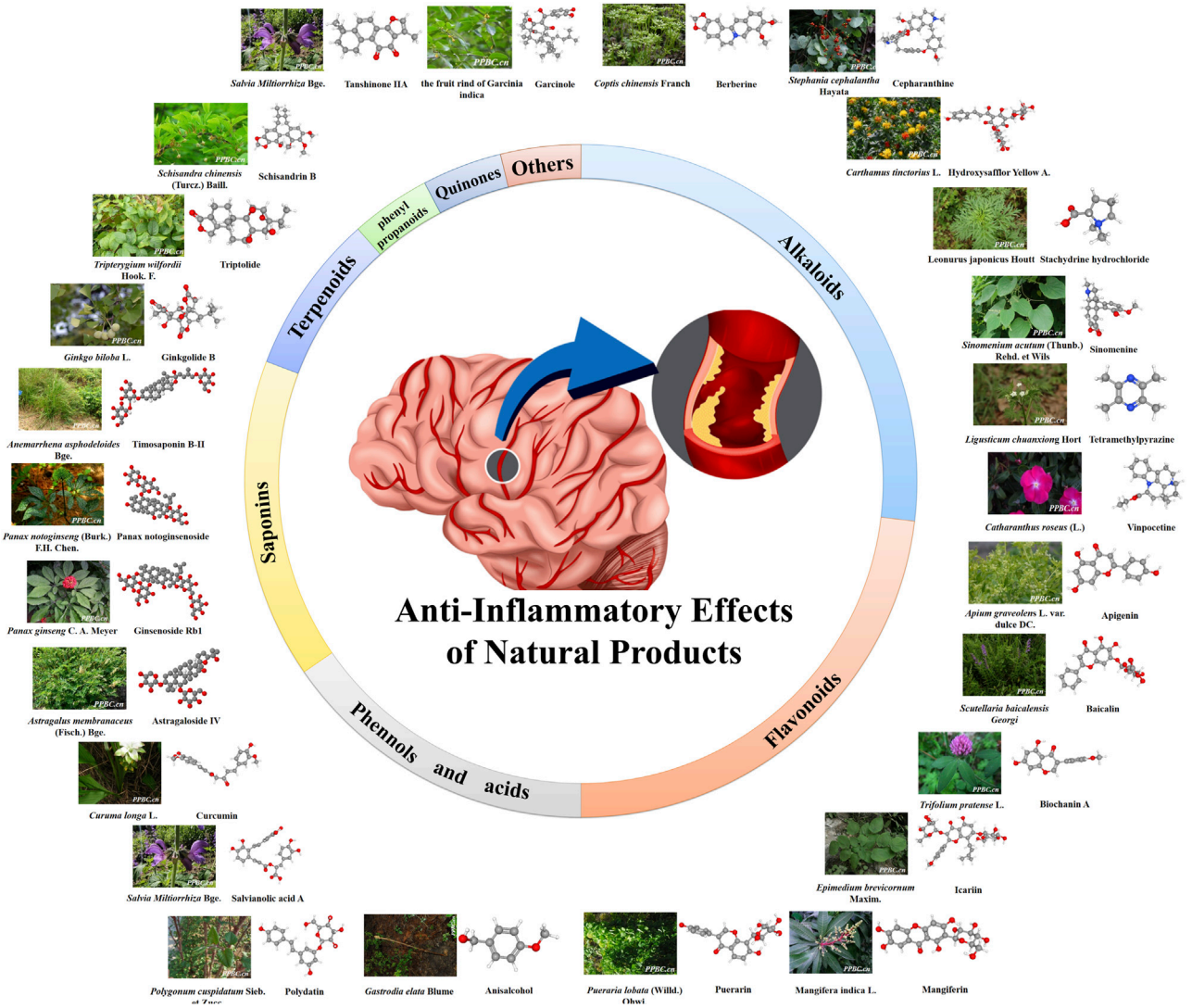

FIGURE 2 | Anti-inflammatory effect of natural products. The color figures of medicine are viewed in www.iplant.cn. The club model comes from PubChem and Guidechem.

2020; Xue et al., 2021). The anti-inflammatory sapnins, such as astragaloside IV, Ginsenoside Rb1, notoginsenoside R1, and Timosaponin B-II were summaried in **Table 1**.

Anti-Inflammatory Effects of Terpenoids in Cerebral Ischemia

Terpenoids are secondary metabolites widely distributed in nature with diverse structures, and they represent a promising chemical group with potential beneficial effects in neurological diseases in view of the pleiotropic effects on cell death and survival, which consolidate their therapeutic value (Gonzalez-Cofrade et al., 2019; Proshkina et al., 2020). Several studies support the therapeutic potential compounds known to be effective among various inflammatory diseases (Downer, 2020; Khoshnazar et al., 2020; Kim et al., 2020). Terpenoids, combined with the studied mechanism and commonly used drugs, may be new strategy for further anti-inflammatory treatment. The anti-inflammatory effects of terpenoids including ginkgolide B and triptolide are reviewed in cerebral ischemic treatment (**Table 1**).

Anti-Inflammatory Effects of Phenols and Acids in Cerebral Ischemia

(Poly) Phenols are natural substances with variable phenolic structures, and they are generally known to possess potent anti-inflammatory properties. It has been found that phenols can affect the polarization of M1/M2 *via* TLR-4/NF-κB pathway and exert anti-inflammatory properties to treat ischemic stroke (Li et al., 2022). The anti-inflammatory effects of phenols and acids including anisalcohol, curcumin, polydatin and salvianolic acid A are reviewed in cerebral ischemic treatment (**Table 1**).

TABLE 1 | Twenty-six active compounds from natural medicine with anti-inflammatory effects in cerebral ischemia.

Compound	Representative Sources	Cell Lines/Mode	Dose	Effects/Results	Safety evaluation (IC_{50}/ID_{50}/Others)	Reference
Anisalcohol	*Gastrodia elata* Blume	LPS-stimulated BV-2 cells	0.01–1 μM	TNF-α↓, JNK↓, IL-10↑, TGF-β↑	—	Xiang et al. (2018)
Apigenin	*Apium graveolens* L. var. dulce DC.	LPS-stimulated BV-2 cells	1, 5 and 10 μM	JNK↓, PGE_2↓	12.5 μg/ml (MNTC)	Ha et al. (2008); Zhou et al. (2021)
Astragaloside IV	*Astragalus membranaceus* (Fisch.) Bge	(male ICR mice) bilateral common carotid artery occlusion/reperfusion (bCCAO/R)	10, 20 mg/kg	TNF-α↓, IL-1β↓, TLR4 ↓, NLRP3↑	1,000 μg/ml (MNTC, 90% vero cells)	Li M. et al. (2017); Indu et al. (2021)
Baicalin	*Scutellaria baicalensis Georgi*	(male SD rat) tMCAO LPS-induced RAW 264.7 cells	100 mg/kg 50, 100 and 200 μM	TNF-α↓, IL-6↓, p65↓, IL-10↑ IL-6↓, TNF-α↓, MCP1 (CCL2) ↓,IL-13↑, IL-1a↑	125 μg/ml (MNTC)	Xu et al. (2022); Zhou et al. (2021)
Berberine	*Coptis chinensis* Franch.(rhizomes of *Coptis chinensis*)	(male mice) tMCAO	25, 50 mg/kg	HMGB1↓, NF-κB↓, TLR4↓	IC_{50} values of berberine for U87 cells at 24, 48, and 72 h were 113.2, 62.15, and 33.07 mg/L, respectively	Zhu et al. (2018); Liu et al. (2020)
Biochanin A	*Trifolium pratense* L	(male SD rat) MCAO/R	10, 20 and 40 mg/kg	TNF-α↓, IL-1β↓, p38↑	IC_{50} value of 6.77 ± 0.83 μM in MGC-803 cells	Wang et al. (2015); Wang L. et al. (2020)
Cepharanthine	*Stephania cephalantha* Hayata	(male C57/BL6 mice) tMCAO OGD/R-treated BV-2 cells	10, 20 mg/kg 0.25–2.5 μM	NLRP3↓, IL-1β↓, IL-18↓	10 μg/ml (MNTC)	Zhao et al. (2020); Zhou et al. (2021)
Curcumin	*Curuma longa* L	(male Swiss albino mice) bCCAO/R	100 mg/kg	IL-6↓, NF-κB↓, MCP-1↓	IC_{50} values of curcumin for A431 cells were 19.2 μM for 24 h and 14.3 μM for 48 h	Hussein et al. (2020); Babaei et al. (2012)
Garcinol	fruit rind of Garcinia indica	(male SD rat) MCAO/R OGD/R-treated PC12 cells	5, 10 and 20 mg/kg 2.5, 5 and 10 μM	TNF-α↓, IL-1β↓ IL-6↓, TLR4↓, NF-κB ↓	The 40% garcinol (2000 mg/kg, ig) did not show any adverse effect at rats' acute safety study	Kang et al. (2020); Majeed et al. (2018)
Ginkgolide B	*Ginkgo biloba* L	(male ICR mice) tMCAO/R	10, 20 and 40 mg/kg	TNF-α↓, IL-1b↓	—	Gu et al. (2012)
Ginsenoside Rb1	*Panax ginseng* C. A. Mey	(male SD rat)MCAO/R	12.5 mg/kg	TNF-α↓, IL-6↓, NF-κB ↓	—	Zhu et al. (2012)
Hydroxysafflor Yellow A	*Carthamus tinctorius* L	(male Wistar rats) MCAO/R	2, 4 and 8 mg/kg	NF-κB↓, ICAM-1↓	In the safe and well-tolerated of phase III, it (75 mg/d) might be the optimal dose	Sun et al. (2010); Hu et al. (2020)
Icariin	*Epimedium brevicornum* Maxim	(male SD rat) MCAO/R	10, 30 mg/kg	IL-1β↓, NF-κB↓, TGF-$β_1$↓, PPARα↑, PPARγ↑	3.0 ± 1.3 μM of IC_{50} in HEK293 cells	Xiong et al. (2016); Li et al. (2014)
Mangiferin	mango and papaya	(male Wistar rats) MCAO/R	25, 50 and 100 mg/kg	IL-10↑, L-1β↓, TNF-α↓	About 9 mM of IC_{50} in 3T3L1 cells	Zhang et al. (2016); Kumar et al. (2013)
Notoginsenoside R1	*Panax notoginseng* (Burk.) F.H.Chen	(male SD rat)the aorta clamped and rperfusion	30 mg/kg	IL-1β↓, IL-10↑, TNF-α↓	—	Ning et al. (2012)
Polydatin	*Polygonum Cuspidatum* Sieb. et Zucc	(male SD rat) pMCAO	50 mg/kg	NF-κB↓	IC_{50} at 24 and 48 h were 90 and 50 μmol/L in THP-1 cells	Ji et al. (2012); Wang et al. (2016)
Puerarin	*Pueraria lobata* (Willd.) Ohwi	(male Wistar rat) MCAO/R	18 mg/kg	NF-κB↓, ICAM-1↓	LD_{50} of oral puerarin is 2,000 mg/kg/d in rats	Lou et al. (2007); Chung et al. (2009)
Salvianolic acid A	*Salvia Miltiorrhiza* Bge	(male SD rat) MCAO/R	5, 10, and 20 mg/kg	NF-κB↓	48.4 ± 1.4 μM of IC_{50} on MMP-2 in Raw264.7 cells	Zhang et al. (2018); Zhang et al. (2014)
Schisandrin B	*Schisandra chinensis* (Turcz.) Baill	(male SD rat) MCAO/R	10, 30 mg/kg	TNF-α↓, IL-1β↓	—	Lee et al. (2012)
Stachydrine hydrochloride	*Leonurus japonicas* Houtt	(male KM mice) CCAO/R	15, 30 and 60 mg/kg	TNF-α↓, ICAM-1↓	—	Miao et al. (2017)
Sinomenine	*Sinomenium acutum* (Thunb.) Rehd. et Wils	(C57BL/6 mice) MCAO	10, 20 mg/kg	IL-1β↓, IL-6↓, IL-18↓, TNF-α↓	—	Qiu et al. (2016)

(Continued on following page)

TABLE 1 | (*Continued*) Twenty-six active compounds from natural medicine with anti-inflammatory effects in cerebral ischemia.

Compound	Representative Sources	Cell Lines/Mode	Dose	Effects/Results	Safety evaluation (IC_{50}/ID_{50}/Others)	Reference
Tanshinone IIA	*Salvia Miltiorrhiza* Bge	OGD/R-treated BV-2 cells	0.5, 1 and 2 μM	NLRP3↓, IL-1β↓, IL-18↓	—	Cai et al. (2016)
Tetramethylpyrazine	*Ligusticum chuanxiong* Hort	(male SD rat) MCAO/R	20 mg/kg	PGE2↓	It (1,800 mg) is well tolerated in healthy volunteers of phase I	Liao et al. (2004); Zhao et al. (2021)
Timosaponin B-II	*Anemarrhena asphodeloides* Bge	(male SD rat) MCAO/R	100, 200 mg/kg	IL-10↑, IL-10R↑	No-observed-adverse-effect level is proposed to be 180 mg/kg (ig, rats)	Li et al. (2007); Lin et al. (2017)
Triptolide	*Tripterygium wilfordii* Hook. F	(male SD rat) intrahippocampal injection of LPS LPS-stimulated A172 cells	10–50 mg/kg 0.2–5 μM	COX-2↓, NF-$_k$B↓	206.1 nM of IC_{50} in H295R cells	Dai et al. (2006); Xu et al. (2019)
Vinpocetine	*Catharanthus roseus* (L.)G. Don	(male Wistar rat) MCAO/R	10 mg/kg	NF-$_k$B↓, TNF-α↓	—	Wang et al. (2014)

Note: "-" indicates that information on the potential toxicity and/or safety of the compound is not available or not in the literature that published in the last 20 years. MNTC, is a maximal non-toxic concentration of a compound that enables at least 80% of cells to survive.

Anti-Inflammatory Effects of Quinones, Phenylpropanoids and Others in Cerebral Ischemia

In addition to the types of compounds mentioned above, phenylpropanoids, quinones and others are a large group of organic compounds in the nature (**Table 1**). Anti-inflammatory effects of them are found and reported (Gui et al., 2020; Yang et al., 2021).

MAJOR ANTI-INFLAMMATORY NATURAL PRODUCTS FROM NATURAL MEDICINES

Natural products have been long used as folk drugs all over the world although the resources and applications vary among different regions. In China, many natural medicines have been accustomed to treat stroke for years. The direct experience gained from human subjects provides a huge resource for new drug candidates and treatment methods for stroke. Therefore, this review primarily discussed several representative natural products (compounds) with anti-inflammatory effects in cerebral ischemia treatment.

Anisalcohol is a phenolic compound that was originally isolated from *Gastrodia elata* Blume (Chen H. L. et al., 2020). Anisalcohol has ability to significantly decrease TNF-α and increase IL-10 and TGF-β in lipopolysaccharide (LPS)-stimulated BV-2 cells (a murine microglial cell line). Anisalcohol has also found to inhibit c-Jun N-terminal kinase (JNK) phosphorylation and suppress NF-κB activation. Therefore, anisalcohol reduces the generation of inflammatory mediators and cytokines by suppressing NF-κB and mitogen-activated protein kinase (MAPK) activation (Xiang et al., 2018).

Apigenin is one of the active ingredients in the leaves of *Apium graveolens* L. var. dulce DC. Apigenin decreased prostaglandin E_2 (PGE_2) levels by inhibiting COX-2 expression and mediating inflammation in LPS-stimulated BV-2 cells. They found that LPS induced p38 MAPK and apigenin inhibited the phosphorylation of JNK in BV-2 microglia, suggesting that it played an anti-inflammatory role through p38 MAPK and JNK. However, apigenin had no significant effect on extracellular signal-regulated kinase activation (Ha et al., 2008).

Astragaloside IV is an ingredient isolated from the dried roots of *Astragalus membranaceus* (Fisch.) Bge (Zhang et al., 2020). As shown by Morris water maze test, bilateral common carotid artery occlusion in mice can lead to serious memory impairment. Oral administration of astragaloside IV (10 and 20 mg/kg, once daily, beginning 7 days before surgery and continued for 7 days after surgery) could reduce Toll-like receptor-4 (TLR4) expression and its downstream adaptor proteins, including tumor necrosis factor receptor associated factor-6 (TRAF6), so NF-κB phosphorylation was inhibited as a result (Li M. et al., 2017). These findings show that astragaloside IV protects against transient cerebral I/R by suppressing the TLR4 signaling pathway, in part through its anti-inflammatory properties.

Baicalin is an important flavonoid that is extracted from the root of *Scutellaria baicalens*is Georgi (Chen H. et al., 2020; Li Y. et al., 2020). The report was found that baicalin inhibited the secretion of NO, IL-6, TNF-α, and CCL22 (C-C motif chemokine ligand 22) in macrophages, promoted the secretion of IL-13, IFNG (interferon gamma), and IL-1a *in vitro* (Xu et al., 2022). It inhibited CCL2 expression, reduced the phosphorylation levels of p65 and IκBα protein, and downregulated the level of CCR2 *in vivo*. Meanwhile, it discovered that baicalin had a neuroprotective effect, most likely via blocking NF-κB p65 activation, which improved neurological functioning and reduced the extent of cerebral infarction (Xue et al., 2010). The anti-inflammatory and anti-apoptotic benefits of baicalin were validated by Tu et al. (Tu et al., 2009), and the molecular mechanism may be related to the downregulated levels of iNOS, COX-2, and cleaved caspase-3 protein, as well as the enhanced enzymatic activity of myeloperoxidase (MPO). Current studies indicate that baicalin protects from ischemic injury by inhibiting of NF-κB–mediated inflammation.

Berberine is a non-basic and quaternary benzylisoquinoline alkaloid in berberine-containing plants (the berberidaceae family) worldwide, and it is an active ingredient isolated from the dried roots of *Coptidis rhizoma* (rhizomes of *Coptis chinensis*) in China (Neag et al., 2018). In I/R injury, berberine dramatically lowered the levels of pro-inflammatory cytokines, which was prevented by a SIRT1 inhibitor (Yu et al., 2016). It found that pretreatment with berberine dose-dependently inhibited high-mobility group box 1 (HMGB1) and NF-κB translocation from the nucleus to the cytoplasm in cerebral I/R injury and decreased Toll-like receptor 4 (TLR4) expression in ischemic cortical tissue (Zhu et al., 2018). According to new findings, berberine's anti-inflammatory benefits against the injury are aided by reducing the activation of the HMGB1/TLR4/NF-κB signaling pathway. In clinical studies, berberine administration lowered serum levels of IL-6 and macrophage migration inhibitory factor, as well as plasma levels of C-reactive protein, TNF-α, and IL-6 (Li et al., 2016; Liu et al., 2019). Berberine appears to reduce I/R injury by reducing excessive inflammatory responses in patients according to recent research. Berberine could be employed as an alternate therapeutic technique for I/R injury management.

Biochanin A is an O-methylated natural isoflavonoid isolated from *Trifolium pratense* L. (red clover). In a rat model, the anti-inflammatory properties of biochanin A against I/R damage were examined. TNF-α and IL-1β expression, as well as p38 phosphorylation, were assessed using RT-PCR or WB. As a result, TNF-α and IL-1β levels were markedly elevated following I/R injury, and biochanin A therapy significantly reduced these inflammatory processes. Meawhile, the increase in p-p38 levels in I/R brain tissue was reduced by biochanin A (Wang et al., 2015). These results suggest that biochanin A protects against focal cerebral I/R in rats via inhibition of p38-mediated inflammatory responses.

Cepharanthine is a bibenzylisoquinoline alkaloid isolated from *Stephania cephalantha* Hayata (Huang H. et al., 2014). Cepharanthine reduced microglia activation in transient middle cerebral artery occlusion (tMCAO) mouse models and in hypoxia, glucose deprivation/reoxygenation microglia models (OGD/R). Cepharanthine reduced microglial activation. Following tMCAO, cepharanthine reduced elevation of NLR family pyrin domain containing 3 (NLRP3) immunoreactivity in Ibal-labeled microglia as well as total Iba1 and NLRP3 expression in the brain, according to immunofluorescence labeling. Cepharanthine reduced the overproduction of the M1 microglia-regulated pro-inflammatory cytokines IL-1 and IL-18 generated by tMCAO and OGD/R (Zhao et al., 2020). Cepharanthine reduced cerebral I/R injury by reducing microglial activation and inflammation generated by the NLRP3 inflammasome.

Curcumin is an effective ingredient from the dried roots of *Curuma longa* L. Curcumin (100 mg/kg) decreased the degree of neutrophilic granulocyte infiltration in cerebral tissues and inhibited TNF-α expression in a cerebral I/R injury model (Lei et al., 2010). Treatment with curcumin (IP) decreased IL-6, NF-κB and MCP-1 levels after I/R injury (Hussein et al., 2020). These findings suggest that curcumin has a neuroprotective role by inhibiting the inflammatory reaction.

Garcinol is a benzophenone compound isolated from the fruit rind of Garcinia indica (Balasubramanyam et al., 2004). In MCAO/R-induced animals and OGD/R-treated cells of models, garcinol reduced model-induced inflammation, including inhibiting the production of IL-6, IL-1β, and TNF-α, and it also inhibited TLR4 and NF-κB (p65) expression. The data indicate that garcinol protects against cerebral I/R injury. And garcinol attenuates inflammation by suppression of the TLR4/NF-κB signaling pathway (Kang et al., 2020).

Ginkgolide B is a compound extracted from the dried leaves of *Ginkgo biloba* L. The tMCAO model of mice was made by an intraluminal filament technique. Ginkgolide B (10, 20 and 40 mg/kg in 2 h after MCAO, iv) inhibited I/R-induced NF-κB, microglial activation and the production of pro-inflammatory cytokines (Gu et al., 2012). Taken together, the information indicates that ginkgolide B has an anti-inflammatory function by inhibition of NF-κB pathway.

Ginsenoside Rb1 (Rb1) is one of the primary active compounds of *Panax ginseng* C. A. Mey. Male Sprague-Dawley (SD) rats were given Rb1 (12.5 mg/kg/d) intranasally for 7 days before being subjected to transient blockage of the right middle cerebral artery and reperfusion. The rats were slaughtered 6 hours, 12 hours, 24 hours, and 72 hours following reperfusion, and brain tissues were taken for testing. Key inflammatory aspects of CNS, such as inflammatory cells, pro-inflammatory cytokines, and transcription factors, were used to assess Rb1's neuroprotection. Rb1 inhibited microglia activity in the penumbra from 24 to 72 h after reperfusion, as well as microglia conversion to phagocytic microglia. In the Rb1 group, the mRNA and protein level of TNF-α was lower 12 h after reperfusion. From 6 to 72 h, Rb1 partially reduced NF-κB pathway activation (Zhu et al., 2012). These findings suggest that local inflammation suppression during cerebral ischemia may be one mechanism contributing to Rb1's neuroprotective benefits.

Hydroxysafflor Yellow A is a component of flavonoids extracted from the flower of the safflower plant *Carthamus tinctorius* L. Hydroxysafflor Yellow A (2, 4, 8 mg/kg, respectively, iv) prevented brain injury in a focal cerebral I/R model by inhibiting thrombin generation. Hydroxysafflor yellow A treatment suppressed NF-κB p65 nuclear translation and p65 binding activity, as well as ICAM-1 mRNA and protein levels and neutrophil infiltration. Hydroxysafflor yellow A enhanced the number of CA1 pyramidal cells in the hippocampus CA1 and lowered plasma angiotensin II levels, all of which improved neurological deficit scores (Sun et al., 2010). Another study revealed the neuroprotective effect of hydroxysafflor yellow A on GSK-3β/NF-κB-mediated inflammatory pathways (Yang X. et al., 2020). These findings demonstrated that hydroxysafflor yellow A had an anti-inflammatory effect by reducing angiotensin II content or regulating NF-κB.

Icariin is a natural compound of flavonoids extracted from *Epimedium brevicornum* Maxim. Pretreatment with icariin (10, 30 mg/kg) decreased NF-κB activation, IL-1β and TGF-β_1 protein levels in the cerebral I/R model of rats. Icarin also increased the levels of peroxisome proliferator-activated receptor (PPARα and PPARγ) protein in this study. These results suggest that icariin protects rats from ischemic stroke by inhibiting inflammatory

responses mediated by NF-κB, PPARα and PPARγ (Xiong et al., 2016).

Mangiferin is a natural compund found in papaya and mango (the Anacardiaceae and Gentianaceae families). Mangiferin (25, 50, 100 mg/kg, respectively, iv) increased IL-10 levels and reduced IL-1β and TNF-α levels in the rat brain tissues with cerebral I/R injury. These results demonstrate that mangiferin has a significant protective ability that may be its effect to inhibit the overproduction of inflammatory cytokines (Zhang et al., 2016).

Notoginsenoside R1 is an active component extracted from the dried roots of *Panax notoginseng* (Burk.) F.H. Chen. After administration notoginsenoside R1 for 3 days, bilateral CCA were occluded with artery clip for 20 min followed by reperfusion for 24 h in C57BL/6 mice, notoginsenoside R1 reduced both TNF-α and ICAM-1 mRNA (Huang et al., 2015). Panax notoginsenoside (30 mg/kg, including notoginsenoside R1) was injected intraperitoneally approximately 30 min before aortic clamping and reperfusion, and it decreased the expression of IL-1β, IL-10, and TNF-α levels in this acute spinal cord I/R injury model, as shown by immunohistochemistry and Western blotting (Ning et al., 2012). These results indicated that panax notoginsenoside effectively decreased inflammation in damaged spinal cord tissues, but it did not completely ameliorate the symptoms.

Polydatin is a stilbene chemical isolated from *Polygonum cuspidatum* Sieb. et Zuccdried.'s roots (Ji et al., 2012; Tang and Tan, 2019). Polydatin (50 mg/kg) decreased the number of cells positive for NF-κB in an SD rat model of permanent MCAO (pMCAO) compared to the blank control group 24 and 72 h after pMCAO (Ji et al., 2012). These findings indicate that polydatin inhibits the inflammation in response to exert its neuroprotective effects after pMCAO.

Puerarin is one of the main active ingredients from the dried roots of *Pueraria lobata* (Willd.) Ohwi. (Wei et al., 2014). A cerebral I/R injury model was created using MCAO in rats. Puerarin (18 mg/kg) was administered just before occlusion and immediately after reperfusion, and it decreased ICAM-1 protein level and the nuclear translocation of the NF-κB p65 subunit (Lou et al., 2007). These effects may be due to its inhibition of the neutrophil-mediated inflammatory response.

Salvianolic acid A is one of the main active components isolated from *Salvia Miltiorrhiza* Bge. MCAO operation was used to create a focal cerebral I/R model for 1.5 h of ischemia, followed by reperfusion after 24 h. Salvianolic acid A (5, 10, and 20 mg/kg, respectively, i. v.) administration kept off cerebral NF-κB p65 activation and released the inflammatory response (Chien et al., 2016; Zhang et al., 2018; Yang et al., 2022). These findings suggest that salvianolic acid A attenuates I/R-induced rat brain injury by protecting the BBB via anti-inflammation.

Schisandrin B is a compound isolated from the dried fruits of *Schisandra chinensis* (Turcz.) Baill. Schisandrin B (10, 30 mg/kg, i. p.) was administered twice 30 min before the onset of ischemia and 2 h after reperfusion. Schisandrin B therapy suppressed the TNF-α and IL-1β protein expression in ischemic hemispheres (Lee et al., 2012). These findings show that schisandrin B therapy protects rats from neurodegeneration by suppressing inflammation.

Stachydrine hydrochloride is an alkaloid isolated from *Leonurus japonicus* Houtt. Stachydrine hydrochloride (15, 30 and 60 mg/kg) was administered in a repetitive cerebral ischemia reperfusion mouse model, and it reduced the levels of TNF-α, ICAM-1, and MPO. These results suggest that stachydrine hydrochloride inhibits inflammatory reactions after ischemia (Miao et al., 2017).

Sinomenine is an isoquinoline-type alkaloid originally extracted from the *Sinomenium acutum* (Thunb.) Rehd. et Wils and *S. acutum* (Thunb.) Rehd. et Wils var. *cinereum* Rehd. et Wils. (Zhao et al., 2015). Sinomenine inhibited pro-inflammatory factors including IL-1β, TNF-α, IL-6 and IL-18 to protect BBB integrity and improve neurological functions (Qiu et al., 2016). It reduced the activation of microglia and astrocytes, and it also decreased inflammasome-related molecules (NLRP3, ASC, and caspase-1) and proinflammatory cytokines in ischemic brains *in vivo* and cultured microglia *in vitro* (Yang et al., 2016). Therefore, sinomenine inhibits inflammatory reactions in ischemic stroke treatment.

Tanshinone IIA is an active ingredients isolated from *Salvia Miltiorrhiza* Bge. (Subedi and Gaire, 2021). Tanshinone IIA has an anti-inflammatory impact in N2a cells, where it increases cell viability and reduces inflammation via the PI3K/Akt/mTOR signaling pathway (Wang J. et al., 2020). Another study in OGD/R-exposed microglia found that Salvia Miltiorrhiza extract containing tanshinone IIA significantly reduced inflammatory responses, as shown by lower expression of NLRP3, caspase-1, IL-1, and IL-18 (Cai et al., 2016). Tanshinone IIA also had anti-inflammatory effects in OGD/R-activated astrocytes by reducing proliferation, GFAP staining, HIF-1 expression, and SDF-1, ERK, and Akt signaling (Huang X. et al., 2014). It enhanced cell viability while lowering NO production and NF-κB signaling (Dong et al., 2009). These studies suggest that tanshinone IIA prevents inflammatory responses after ischemia.

Tetramethylpyrazine is an active compound from *Ligusticum chuanxiong* Hort . The MCAO model was produced in rats by occluding the right middle cerebral artery for 90 min and then reperfusing for 3 days, using tetramethylpyrazine (20 mg/kg) administered intraperitoneally 60 min before the occlusion. Tetramethylpyrazine significantly reduced inflammatory cell activation and pro-inflammatory mediator synthesis in the brain after ischemia and reperfusion. In cultured glial cells, it reduced inflammation generated by lipopolysaccharide and interferon, as well as the formation of prostaglandin E2 (PGE2) (Liao et al., 2004). These findings show that one of tetramethylpyrazine's neuroprotective properties to prevent brain injury is its anti-inflammatory capability.

Timosaponin B-II is an active ingredient isolated from the dried roots of *Anemarrhena asphodeloides* Bge. Timosaponin B-II treatment significantly increased IL-10 and IL-10R mRNA expression in an SD rat model of focal cerebral I/R produced by transient MCAO (2 h) (Li et al., 2007). The results demonstrated that the anti-dementia effect of timosaponin B-II is at least partially due to its anti-inflammatory properties.

Triptolide is a biologically active natural chemical derived from the *Tripterygium wilfordii* Hook plant. F. Triptolide

(0.2–5 mg/L) suppressed the astroglial response and NF-κB/DNA binding activity *in vitro*, while triptolide (10–50 mg/kg) lowered LPS-induced COX-2 expression *in vivo* and *in vitro* (Dai et al., 2006). These findings imply that triptolide protects against neuroinflammation by suppressing COX-2 production, at least in part through suppression of the NF-κB signaling pathway.

Vinpocetine is one of the major active ingredients in *Catharanthus* roseus (L.) Don. Vinpocetine (10 mg/kg) was intraperitoneally injected in a murine model of transient MCAO (2 h) and then reperfusion. Vinpocetine decreased the expression of NF-κB and TNF-α at 24 h and 3 days and inhibited the inflammatory response after cerebral I/R (Jeon et al., 2010; Wang et al., 2014).

STRCTURE-ACTIVITY RELATIONSHIP BETWEEN INFLAMMATION AND NATURAL PRODUCTS

Structure activity relationship (SAR) has been demonstrated as a useful tool for investigating the bioactivities of various classes of compounds (Li X. et al., 2017). The SAR of biological activity is mainly related to the type (or basic parent nucleus) of compounds and the position of main functional groups (Xie et al., 2021; Zhou et al., 2021). Flavonoids are based on 2-phenylchromone as the skeleton. The position of C-5 and 7 on the ring A of flavonoids that coupled with hydroxyl groups has found to affect the cell secretion process, mitosis and cell interactions with strong anti-inflammatory effects (Xie et al., 2021). Forthermore, C_5-OH, C_7-OH, $C_2 = C_3$ and $C_4 = O$ functional groups that present in the flavonoids has also been indicated to performa greater anti-inflammatory effect. C_3-OH or glycosylation group at the ring A has greatly effection in the decrease the anti-inflammatory (Zhang et al., 2019). For alkaloids and other types of natural compounds mentioned above, due to the number or complex structure of compounds, this review did not draw a suitable SAR.

CONCLUSION

Even though cerebral ischemia as a serious issue with global health concern, the lack of effective drug options still limit its treatment (Gaire, 2021). The present study provides a wealth of information to elucidate the important role of inflammation in ischemic brain injury. Natural medicines with anti-inflammatory effects in cerebral ischemia have great potential for treatment based on the above mentioned 26 active ingredients in experimental studies (**Table 1**). This review fully demonstrated that compounds of natural medicine have protective effects against cerebral ischemia *via* anti-inflammatory mechanisms.

Inflammation is a critical mediator of cerebral ischemic injury, and it is increasingly regarded as the important factor to the pathological processes in cerebral ischemia. Experimental anti-inflammatory strategies to diminish cerebral ischemic injury have certainly been useful. In-depth study of the inflammatory response of cerebral ischemic injury offers a novel method for the prevention and treatment. However, whether inflammation is harmful or useful may depend on the severity of the ischemia and the stage of ischemia in which inflammatory responses contribute, and detailed mechanisms of inflammation-induced injury or recovery are far from complete. In the laboratory, a lot of time and money has gone into studying the mechanisms, but it hasn't translated into effective treatments in the clinic. Compound preparation is difficult to prepare for the international market because internationality only admits the curative effect of monomers, which is worthy of attention in the future.

The use of natural medicine compounds to study the anti-inflammatory effect of cerebral ischemia should strengthen the recent research achievements of physiology, pathology, immunology, molecular biology, neurobiology, neuroscience and omics methods. Using the research method of Western-style drugs and recognizing each step of the inflammatory response leads to the possibility of developing a new compound from natural medicines that interferes with a specific inflammatory mechanism of ischemic injury and creating a new situation that prevents and treats cerebral ischemic injury using compounds of natural medicines for anti-inflammatory effects. Review of the inflammatory mechanism and anti-inflammatory effect of the above mentioned 26 compounds revealed great new progress and breakthroughs in the future, thanks to a strong scientific research capability to protect cerebral ischemia with natural products based on the inflammatory theory.

AUTHOR CONTRIBUTIONS

YS and JT designed and revised this review article. YS wrote the manuscript. ZZ, XL and JT amended the text.

FUNDING

This work was supported by the Department of Science and Technology of Sichuan Province (2021YFN0101).

REFERENCES

Adams, H., Adams, R., Del Zoppo, G., and Goldstein, L. B. (2005). Guidelines for the Early Management of Patients with Ischemic Stroke: 2005 Guidelines Update a Scientific Statement from the Stroke Council of the American Heart Association/American Stroke Association. *Stroke* 36, 916–923. doi:10.1161/01.STR.0000163257.66207.2d

Adibhatla, R. M., and Hatcher, J. F. (2008). Tissue Plasminogen Activator (tPA) and Matrix Metalloproteinases in the Pathogenesis of Stroke: Therapeutic Strategies. *CNS Neurol. Disord. Drug Targets* 7, 243–253. doi:10.2174/187152708784936608

Alasvand, M., Assadollahi, V., Ambra, R., Hedayati, E., Kooti, W., and Peluso, I. (2019). Antiangiogenic Effect of Alkaloids. *Oxid. Med. Cell Longev.* 2019, 9475908. doi:10.1155/2019/9475908

Amantea, D., Tassorelli, C., Petrelli, F., Certo, M., Bezzi, P., Micieli, G., et al. (2014). Understanding the Multifaceted Role of Inflammatory Mediators in Ischemic

Stroke. *Curr. Med. Chem.* 21, 2098–2117. doi:10.2174/0929867321666131227162634

Atanasov, A. G., Zotchev, S. B., Dirsch, V. M., International Natural Product Sciences Taskforceand Supuran, C. T. (2021). Natural Products in Drug Discovery: Advances and Opportunities. *Nat. Rev. Drug Discov.* 20, 200–216. doi:10.1038/s41573-020-00114-z

Azab, A., Nassar, A., and Azab, A. N. (2016). Anti-Inflammatory Activity of Natural Products. *Molecules* 21 (10), 1321. doi:10.3390/molecules21101321

Babaei, E., Sadeghizadeh, M., Hassan, Z. M., Feizi, M. A., Najafi, F., and Hashemi, S. M. (2012). Dendrosomal Curcumin Significantly Suppresses Cancer Cell Proliferation *In Vitro* and *In Vivo*. *Int. Immunopharmacol.* 12, 226–234. doi:10.1016/j.intimp.2011.11.015

Bai, R., Yao, C., Zhong, Z., Ge, J., Bai, Z., Ye, X., et al. (2021). Discovery of Natural Anti-inflammatory Alkaloids: Potential Leads for the Drug Discovery for the Treatment of Inflammation. *Eur. J. Med. Chem.* 213, 113165. doi:10.1016/j.ejmech.2021.113165

Balasubramanyam, K., Altaf, M., Varier, R. A., Swaminathan, V., Ravindran, A., Sadhale, P. P., et al. (2004). Polyisoprenylated Benzophenone, Garcinol, a Natural Histone Acetyltransferase Inhibitor, Represses Chromatin Transcription and Alters Global Gene Expression. *J. Biol. Chem.* 279, 33716–33726. doi:10.1074/jbc.M402839200

Bayat, P., Farshchi, M., Yousefian, M., Mahmoudi, M., and Yazdian-Robati, R. (2021). Flavonoids, the Compounds with Anti-Inflammatory and Immunomodulatory Properties, as Promising Tools in Multiple Sclerosis (MS) Therapy: A Systematic Review of Preclinical Evidence. *Int. Immunopharmacol.* 95, 107562. doi:10.1016/j.intimp.2021.107562

Cai, L., Yi, X. B., Yuan, L. B., and Gong, G. (2016). The Protective Effect of Tanshinone IIA on Oxygen-Glucose Deprivation and Reperfusion Injury of MicrogliaThrough the NLRP3 Inflammatory Signaling Pathway. *J. Sichuan Univ. Med. Sci. Ed.* 47, 660–664. doi:10.13464/j.scuxbyxb.2016.05.006

Chen, H., He, Y., Chen, S., Qi, S., and Shen, J. (2020a). Therapeutic Targets of Oxidative/Nitrosative Stress and Neuroinflammation in Ischemic Stroke: Applications for Natural Product Efficacy with Omics and Systemic Biology. *Pharmacol. Res.* 158, 104877. doi:10.1016/j.phrs.2020.104877

Chen, H. L., Jia, W. J., Li, H. E., Han, H., Li, F., Zhang, X. L., et al. (2020b). Scutellarin Exerts Anti-Inflammatory Effects in Activated Microglia/Brain Macrophage in Cerebral Ischemia and in Activated BV-2 Microglia through Regulation of MAPKs Signaling Pathway. *Neuromolecular Med.* 22, 264–277. doi:10.1007/s12017-019-08582-2

Chien, M. Y., Chuang, C. H., Chern, C. M., Liou, K. T., Liu, D. Z., Hou, Y. C., et al. (2016). Salvianolic Acid A Alleviates Ischemic Brain Injury through the Inhibition of Inflammation and Apoptosis and the Promotion of Neurogenesis in Mice. *Free Radic. Biol. Med.* 99, 508–519. doi:10.1016/j.freeradbiomed.2016.09.006

Chung, H. J., Chung, M. J., Houng, S.-J., Jeun, J., Kweon, D.-K., Choi, C. H., et al. (2009). Toxicological Evaluation of the Isoflavone Puerarin and its Glycosides. *Eur. Food Res. Technol.* 230, 145–153. doi:10.1007/s00217-009-1156-3

Dai, Y. Q., Jin, D. Z., Zhu, X. Z., and Lei, D. L. (2006). Triptolide Inhibits COX-2 Expression via NF-kB Pathway in Astrocytes. *Neurosci. Res.* 55, 154–160. doi:10.1016/j.neures.2006.02.013

Deb, P., Sharma, S., and Hassan, K. M. (2010). Pathophysiologic Mechanisms of Acute Ischemic Stroke: An Overview with Emphasis on Therapeutic Significance beyond Thrombolysis. *Pathophysiology* 17, 197–218. doi:10.1016/j.pathophys.2009.12.001

Dénes, A., Ferenczi, S., Halász, J., Környei, Z., and Kovács, K. J. (2008). Role of CX3CR1 (Fractalkine Receptor) in Brain Damage and Inflammation Induced by Focal Cerebral Ischemia in Mouse. *J. Cereb. Blood Flow. Metab.* 28, 1707–1721. doi:10.1038/jcbfm.2008.64

Dodd, W. S., Laurent, D., Dumont, A. S., Hasan, D. M., Jabbour, P. M., Starke, R. M., et al. (2021). Pathophysiology of Delayed Cerebral Ischemia after Subarachnoid Hemorrhage: A Review. *J. Am. Heart Assoc.* 10, e021845. doi:10.1161/JAHA.121.021845

Dong, K., Xu, W., Yang, J., Qiao, H., and Wu, L. (2009). Neuroprotective Effects of Tanshinone IIA on Permanent Focal Cerebral Ischemia in Mice. *Phytother. Res.* 23, 608–613. doi:10.1002/ptr.2615

Downer, E. J. (2020). Anti-Inflammatory Potential of Terpenes Present in Cannabis Sativa L. *ACS Chem. Neurosci.* 11, 659–662. doi:10.1021/acschemneuro.0c00075

Emsley, H. C., Smith, C. J., Georgiou, R. F., Vail, A., Hopkins, S. J., Rothwell, N. J., et al. (2005). A Randomised Phase II Study of Interleukin-1 Receptor Antagonist in Acute Stroke Patients. *J. Neurol. Neurosurg. Psychiatry* 76, 1366–1372. doi:10.1136/jnnp.2004.054882

Falsig, J., Pörzgen, P., Lund, S., Schrattenholz, A., and Leist, M. (2006). The Inflammatory Transcriptome of Reactive Murine Astrocytes and Implications for Their Innate Immune Function. *J. Neurochem.* 96, 893–907. doi:10.1111/j.1471-4159.2005.03622.x

Fukumoto, Y., Tanaka, K. F., Parajuli, B., Shibata, K., Yoshioka, H., Kanemaru, K., et al. (2019). Neuroprotective Effects of Microglial P2Y1 Receptors against Ischemic Neuronal Injury. *J. Cereb. Blood Flow. Metab.* 39, 2144–2156. doi:10.1177/0271678X18805317

Gaire, B. P. (2021). Microglia as the Critical Regulators of Neuroprotection and Functional Recovery in Cerebral Ischemia. *Cell Mol. Neurobiol.* doi:10.1007/s10571-021-01145-9 https://link.springer.com/article/10.1007/s10571-021-01145-9

Gavins, F., Yilmaz, G., and Granger, D. N. (2007). The Evolving Paradigm for Blood Cell-Endothelial Cell Interactions in the Cerebral Microcirculation. *Microcirculation* 14, 667–681. doi:10.1080/10739680701404903

Geetha, R. G., and Ramachandran, S. (2021). Recent Advances in the Anti-Inflammatory Activity of Plant-Derived Alkaloid Rhynchophylline in Neurological and Cardiovascular Diseases. *Pharmaceutics* 13 (8), 1170. doi:10.3390/pharmaceutics13081170

González-Cofrade, L., de Las Heras, B., Apaza Ticona, L., and Palomino, O. M. (2019). Molecular Targets Involved in the Neuroprotection Mediated by Terpenoids. *Planta Med.* 85, 1304–1315. doi:10.1055/a-0953-6738

Gu, J. H., Ge, J. B., Li, M., Wu, F., Zhang, W., and Qin, Z. H. (2012). Inhibition of NF-κB Activation is Associated with Anti-inflammatory and Anti-Apoptotic Effects of Ginkgolide B in a Mouse Model of Cerebral Ischemia/Reperfusion Injury. *Eur. J. Pharm. Sci.* 47, 652–660. doi:10.1016/j.ejps.2012.07.016

Gui, Y. H., Liu, L., Wu, W., Zhang, Y., Jia, Z. L., Shi, Y. P., et al. (2020). Discovery of Nitrogenous Sesquiterpene Quinone Derivatives from Sponge Dysidea Septosa with Anti-Inflammatory Activity *In Vivo* Zebrafish Model. *Bioorg Chem.* 94, 103435. doi:10.1016/j.bioorg.2019.103435

Ha, S. K., Lee, P., Park, J. A., Oh, H. R., Lee, S. Y., Park, J. H., et al. (2008). Apigenin Inhibits the Production of NO and PGE2 in Microglia and Inhibits Neuronal Cell Death in a Middle Cerebral Artery Occlusion-Induced Focal Ischemia Mice Model. *Neurochem. Int.* 52, 878–886. doi:10.1016/j.neuint.2007.10.005

Headland, S. E., and Norling, L. V. (2015). The Resolution of Inflammation: Principles and Challenges. *Semin. Immunol.* 27, 149–160. doi:10.1016/j.smim.2015.03.014

Hu, M. Z., Zhou, Z. Y., Zhou, Z. Y., Lu, H., Gao, M., Liu, L. M., et al. (2020). Effect and Safety of Hydroxysafflor Yellow A for Injection in Patients with Acute Ischemic Stroke of Blood Stasis Syndrome: A Phase II, Multicenter, Randomized, Double-Blind, Multiple-Dose, Active-Controlled Clinical Trial. *Chin. J. Integr. Med.* 26, 420–427. doi:10.1007/s11655-020-3094-7

Huang, H., Hu, G., Wang, C., Xu, H., Chen, X., and Qian, A. (2014a). Cepharanthine, an Alkaloid from Stephania Cepharantha Hayata, Inhibits the Inflammatory Response in the RAW264.7 Cell and Mouse Models. *Inflammation* 37, 235–246. doi:10.1007/s10753-013-9734-8

Huang, J., Upadhyay, U. M., and Tamargo, R. J. (2006). Inflammation in Stroke and Focal Cerebral Ischemia. *Surg. Neurol.* 66, 232–245. doi:10.1016/j.surneu.2005.12.028

Huang, X., Li, Y., Li, J., Feng, Y., and Xu, X. (2014b). Tanshinone IIA Dampens the Cell Proliferation Induced by Ischemic Insult in Rat Astrocytes via Blocking the Activation of HIF-1α/SDF-1 Signaling. *Life Sci.* 112, 59–67. doi:10.1016/j.lfs.2014.07.020

Huang, X. P., Ding, H., Lu, J. D., Tang, Y. H., Deng, B. X., and Deng, C. Q. (2015). Effects of the Combination of the Main Active Components of Astragalus and Panax Notoginseng on Inflammation and Apoptosis of Nerve Cell after Cerebral Ischemia-Reperfusion. *Am. J. Chin. Med.* 43, 1419–1438. doi:10.1142/S0192415X15500809

Hussein, Y. A., Al-sarraf, A. M., and Alfalluji, W. L. (2020). Modulation of Oxidative Stress, Inflammatory and Apoptotic Response by Curcumin against Cerebral Ischemia Reperfusion Injury in a Mouse Model. *Interdiscip. Neurosurg.* 21, 100741. doi:10.1016/j.inat.2020.100741

Indu, P., Arunagirinathan, N., Rameshkumar, M. R., Sangeetha, K., Divyadarshini, A., and Rajarajan, S. (2021). Antiviral Activity of Astragaloside II, Astragaloside III and Astragaloside IV Compounds against Dengue Virus: Computational Docking and *In Vitro* Studies. *Microb. Pathog.* 152, 104563. doi:10.1016/j.micpath.2020.104563

Ishikawa, M., Zhang, J. H., Nanda, A., and Granger, D. N. (2004). Inflammatory Responses to Ischemia and Reperfusion in the Cerebral Microcirculation. *Front. Biosci.* 9, 1339–1347. doi:10.2741/1330

Jeon, K. I., Xu, X., Aizawa, T., Lim, J. H., Jono, H., Kwon, D. S., et al. (2010). Vinpocetine Inhibits NF-kappaB-Dependent Inflammation via an IKK-dependent but PDE-independent Mechanism. *Proc. Natl. Acad. Sci. U. S. A.* 107, 9795–9800. doi:10.1073/pnas.0914414107

Ji, H., Zhang, X., Du, Y., Liu, H., Li, S., and Li, L. (2012). Polydatin Modulates Inflammation by Decreasing NF-κB Activation and Oxidative Stress by Increasing Gli1, Ptch1, SOD1 Expression and Ameliorates Blood-Brain Barrier Permeability for its Neuroprotective Effect in pMCAO Rat Brain. *Brain Res. Bull.* 87, 50–59. doi:10.1016/j.brainresbull.2011.09.021

Jin, W. N., Shi, S. X., Li, Z., Li, M., Wood, K., Gonzales, R. J., et al. (2017). Depletion of Microglia Exacerbates Postischemic Inflammation and Brain Injury. *J. Cereb. Blood Flow. Metab.* 37, 2224–2236. doi:10.1177/0271678X17694185

Kang, Y., Sun, Y., Li, T., and Ren, Z. (2020). Garcinol Protects against Cerebral Ischemia-Reperfusion Injury *In Vivo* and *In Vitro* by Inhibiting Inflammation and Oxidative Stress. *Mol. Cell Probes* 54, 101672. doi:10.1016/j.mcp.2020.101672

Khoshnazar, M., Parvardeh, S., and Bigdeli, M. R. (2020). Alpha-Pinene Exerts Neuroprotective Effects via Anti-Inflammatory and Anti-Apoptotic Mechanisms in a Rat Model of Focal Cerebral Ischemia-Reperfusion. *J. Stroke Cerebrovasc. Dis.* 29, 104977. doi:10.1016/j.jstrokecerebrovasdis.2020.104977

Kim, T., Song, B., Cho, K. S., and Lee, I. S. (2020). Therapeutic Potential of Volatile Terpenes and Terpenoids from Forests for Inflammatory Diseases. *Int. J. Mol. Sci.* 21 (6), 2187. doi:10.3390/ijms21062187

Kumar, B. D., Krishnakumar, K., Jaganathan, S. K., and Mandal, M. (2013). Effect of Mangiferin and Mahanimbine on Glucose Utilization in 3T3-L1 Cells. *Pharmacogn. Mag.* 9, 72–75. doi:10.4103/0973-1296.108145

Lee, T. H., Jung, C. H., and Lee, D. H. (2012). Neuroprotective Effects of Schisandrin B against Transient Focal Cerebral Ischemia in Sprague-Dawley Rats. *Food Chem. Toxicol.* 50, 4239–4245. doi:10.1016/j.fct.2012.08.047

Lei, J. R., Jun, Q., Zhang, J., Huang, K. M., Fu, R., and Zhou, Z. M. (2010). Effects of Curcumin on Inflammatory Reaction and Blood-Brain Barrierpermeability in Rats Following Cerebral Ischemic Injury. *Chin. Pharmacol. Bull.* 26, 120–123.

Li, L., Gan, H., Jin, H., Fang, Y., Yang, Y., Zhang, J., et al. (2021). Astragaloside IV Promotes Microglia/Macrophages M2 Polarization and Enhances Neurogenesis and Angiogenesis through PPARγ Pathway after Cerebral Ischemia/reperfusion Injury in Rats. *Int. Immunopharmacol.* 92, 107335. doi:10.1016/j.intimp.2020.107335

Li, M., Li, H., Fang, F., Deng, X., and Ma, S. (2017a). Astragaloside IV Attenuates Cognitive Impairments Induced by Transient Cerebral Ischemia and Reperfusion in Mice via Anti-Inflammatory Mechanisms. *Neurosci. Lett.* 639, 114–119. doi:10.1016/j.neulet.2016.12.046

Li, R., Zhou, Y., Zhang, S., Li, J., Zheng, Y., and Fan, X. (2022). The Natural (Poly) phenols as Modulators of Microglia Polarization via TLR4/NF-κB Pathway Exert Anti-Inflammatory Activity in Ischemic Stroke. *Eur. J. Pharmacol.* 914, 174660. doi:10.1016/j.ejphar.2021.174660

Li, S., Liu, X., Chen, X., and Bi, L. (2020a). Research Progress on Anti-Inflammatory Effects and Mechanisms of Alkaloids from Chinese Medical Herbs. *Evid. Based Complement. Altern. Med.* 2020, 1303524. doi:10.1155/2020/1303524

Li, T. J., Qiu, Y., Yang, P. Y., Rui, Y. C., and Chen, W. S. (2007). Timosaponin B-II Improves Memory and Learning Dysfunction Induced by Cerebral Ischemia in Rats. *Neurosci. Lett.* 421, 147–151. doi:10.1016/j.neulet.2007.04.082

Li, X., Li, N., Sui, Z., Bi, K., and Li, Z. (2017b). An Investigation on the Quantitative Structure-Activity Relationships of the Anti-Inflammatory Activity of Diterpenoid Alkaloids. *Molecules* 22 (3), 363. doi:10.3390/molecules22030363

Li, Y., Song, K., Zhang, H., Yuan, M., An, N., Wei, Y., et al. (2020b). Anti-Inflammatory and Immunomodulatory Effects of Baicalin in Cerebrovascular and Neurological Disorders. *Brain Res. Bull.* 164, 314–324. doi:10.1016/j.brainresbull.2020.08.016

Li, Y., Wang, P., Chai, M. J., Yang, F., Li, H. S., Zhao, J., et al. (2016). Effects of Berberine on Serum Inflammatory Factors and Carotid Atherosclerotic Plaques in Patients with Acute Cerebral Ischemic Stroke. *China J. Chin. Materia Medica* 41, 4066–4071. doi:10.4268/cjcmm20162128

Li, Z., Cheung, F. S., Zheng, J., Chan, T., Zhu, L., and Zhou, F. (2014). Interaction of the Bioactive Flavonol, Icariin, with the Essential Human Solute Carrier Transporters. *J. Biochem. Mol. Toxicol.* 28, 91–97. doi:10.1002/jbt.21540

Liao, S. L., Kao, T. K., Chen, W. Y., Lin, Y. S., Chen, S. Y., Raung, S. L., et al. (2004). Tetramethylpyrazine Reduces Ischemic Brain Injury in Rats. *Neurosci. Lett.* 372, 40–45. doi:10.1016/j.neulet.2004.09.013

Lin, N., Liu, B., Zhang, J., Long, Y., Dong, G., Jin, H., et al. (2017). Acute Toxicity, 28-day Repeated-Dose Toxicity and Toxicokinetic Study of Timosaponin BII in Rats. *Regul. Toxicol. Pharmacol.* 90, 244–257. doi:10.1016/j.yrtph.2017.09.021

Liu, D. Q., Chen, S. P., Sun, J., Wang, X. M., Chen, N., Zhou, Y. Q., et al. (2019). Berberine Protects against Ischemia-Reperfusion Injury: A Review of Evidence from Animal Models and Clinical Studies. *Pharmacol. Res.* 148, 104385. doi:10.1016/j.phrs.2019.104385

Liu, Z., Chen, Y., Gao, H., Xu, W., Zhang, C., Lai, J., et al. (2020). Berberine Inhibits Cell Proliferation by Interfering with Wild-Type and Mutant P53 in Human Glioma Cells. *Onco Targets Ther.* 13, 12151–12162. doi:10.2147/OTT.S279002

Lo, E. H., Dalkara, T., and Moskowitz, M. A. (2003). Mechanisms, Challenges and Opportunities in Stroke. *Nat. Rev. Neurosci.* 4, 399–415. doi:10.1038/nrn1106

Lou, H. Y., Wei, X. b., Wang, R. X., and Zhang, X. M. (2007). Inhibitory Effects of Puerarin on Inflammation Following Focal Brain Ischemia-Reperfusion Injury in Rats. *Chin. J. Pathophysiol.* 23, 366–369.

Lu, Y. Z., Lin, C. H., Cheng, F. C., and Hsueh, C. M. (2005). Molecular Mechanisms Responsible for Microglia-Derived Protection of Sprague-Dawley Rat Brain Cells during *In Vitro* Ischemia. *Neurosci. Lett.* 373, 159–164. doi:10.1016/j.neulet.2004.10.004

Majeed, M., Bani, S., Bhat, B., Pandey, A., Mundkur, L., and Neupane, P. (2018). Safety Profile of 40% Garcinol from garcinia Indica in Experimental Rodents. *Toxicol. Rep.* 5, 750–758. doi:10.1016/j.toxrep.2018.06.009

Miao, M., Wang, T., Lou, X., MingBai, M., Xi, P., Liu, B., et al. (2017). The Influence of Stachydrine Hydrochloride on the Reperfusion Model of Mice with Repetitive Cerebral Ischemia. *Saudi J. Biol. Sci.* 24, 658–663. doi:10.1016/j.sjbs.2017.01.039

Montaner, J., Molina, C. A., Monasterio, J., Abilleira, S., Arenillas, J. F., Ribó, M., et al. (2003). Matrix Metalloproteinase-9 Pretreatment Level Predicts Intracranial Hemorrhagic Complications after Thrombolysis in Human Stroke. *Circulation* 107, 598–603. doi:10.1161/01.cir.0000046451.38849.90

Mu, J. K., Li, Y. Q., Shi, T. T., Yu, L. P., Yang, Y. Q., Gu, W., et al. (2020). Remedying the Mitochondria to Cure Human Diseases by Natural Products. *Oxid. Med. Cell Longev.* 2020, 5232614. doi:10.1155/2020/5232614

Neag, M. A., Mocan, A., Echeverría, J., Pop, R. M., Bocsan, C. I., Crişan, G., et al. (2018). Berberine: Botanical Occurrence, Traditional Uses, Extraction Methods, and Relevance in Cardiovascular, Metabolic, Hepatic, and Renal Disorders. *Front. Pharmacol.* 9, 557. doi:10.3389/fphar.2018.00557

Newman, D. J., and Cragg, G. M. (2020). Natural Products as Sources of New Drugs over the Nearly Four Decades from 01/1981 to 09/2019. *J. Nat. Prod.* 83, 770–803. doi:10.1021/acs.jnatprod.9b01285

Ning, N., Dang, X., Bai, C., Zhang, C., and Wang, K. (2012). Panax Notoginsenoside Produces Neuroprotective Effects in Rat Model of Acute Spinal Cord Ischemia-Reperfusion Injury. *J. Ethnopharmacol.* 139, 504–512. doi:10.1016/j.jep.2011.11.040

Passos, F. R. S., Araújo-Filho, H. G., Monteiro, B. S., Shanmugam, S., Araújo, A. A. D. S., Almeida, J. R. G. D. S., et al. (2022). Anti-Inflammatory and Modulatory Effects of Steroidal Saponins and Sapogenins on Cytokines: A Review of Pre-clinical Research. *Phytomedicine* 96, 153842. doi:10.1016/j.phymed.2021.153842

Pinteaux, E., Rothwell, N. J., and Boutin, H. (2006). Neuroprotective Actions of Endogenous Interleukin-1 Receptor Antagonist (IL-1ra) Are Mediated by Glia. *Glia* 53, 551–556. doi:10.1002/glia.20308

Proshkina, E., Plyusnin, S., Babak, T., Lashmanova, E., Maganova, F., Koval, L., et al. (2020). Terpenoids as Potential Geroprotectors. *Antioxidants (Basel)* 9, 529. doi:10.3390/antiox9060529

Przykaza, Ł. (2021). Understanding the Connection between Common Stroke Comorbidities, Their Associated Inflammation, and the Course of the Cerebral Ischemia/Reperfusion Cascade. *Front. Immunol.* 12, 782569. doi:10.3389/fimmu.2021.782569

Qiu, J., Yan, Z., Tao, K., Li, Y., Li, Y., Li, J., et al. (2016). Sinomenine Activates Astrocytic Dopamine D2 Receptors and Alleviates Neuroinflammatory Injury via the CRYAB/STAT3 Pathway after Ischemic Stroke in Mice. *J. Neuroinflammation* 13, 263–276. doi:10.1186/s12974-016-0739-8

Raghay, K., Akki, R., Bensaid, D., and Errami, M. (2020). Ghrelin as an Anti-inflammatory and Protective Agent in Ischemia/Reperfusion Injury. *Peptides* 124, 170226. doi:10.1016/j.peptides.2019.170226

Rallidis, L. S., Vikelis, M., Panagiotakos, D. B., Rizos, I., Zolindaki, M. G., Kaliva, K., et al. (2006). Inflammatory Markers and In-Hospital Mortality in Acute Ischaemic Stroke. *Atherosclerosis* 189, 193–197. doi:10.1016/j.atherosclerosis.2005.11.032

Romano, B., Pagano, E., Montanaro, V., Fortunato, A. L., Milic, N., and Borrelli, F. (2013). Novel Insights into the Pharmacology of Flavonoids. *Phytother. Res.* 27, 1588–1596. doi:10.1002/ptr.5023

Rosenzweig, H. L., Minami, M., Lessov, N. S., Coste, S. C., Stevens, S. L., Henshall, D. C., et al. (2007). Endotoxin Preconditioning Protects against the Cytotoxic Effects of TNFalpha after Stroke: A Novel Role for TNFalpha in LPS-Ischemic Tolerance. *J. Cereb. Blood Flow. Metab.* 27, 1663–1674. doi:10.1038/sj.jcbfm.9600464

Sacco, R. L., Adams, R., Albers, G., Alberts, M. J., Benavente, O., Furie, K., et al. (2006). Guidelines for Prevention of Stroke in Patients with Ischemic Stroke or Transient Ischemic Attack: A Statement for Healthcare Professionals from the American Heart Association/American Stroke Association Council on Stroke: Co-Sponsored by the Council on Cardiovascular Radiology and Intervention: The American Academy of Neurology Affirms the Value of This Guideline. *Stroke* 37, 577–617. doi:10.1161/01.STR.0000199147.30016.74

Serafini, M., Peluso, I., and Raguzzini, A. (2010). Flavonoids as Anti-Inflammatory Agents. *Proc. Nutr. Soc.* 69, 273–278. doi:10.1017/S002966511000162X

Shang, Y. H., Tian, J. F., Hou, M., and Xu, X. Y. (2013). Progress on the Protective Effect of Compounds from Natural Medicines on Cerebral Ischemia. *Chin. J. Nat. Med.* 11, 588–595. doi:10.1016/S1875-5364(13)60068-0

Sofroniew, M. V. (2020). Astrocyte Reactivity: Subtypes, States, and Functions in CNS Innate Immunity. *Trends Immunol.* 41, 758–770. doi:10.1016/j.it.2020.07.004

Soliman, A. M., Das, S., and Mahakkanukrauh, P. (2021). Inflammatory Molecular Mediators and Pathways Involved in Vascular Aging and Stroke: A Comprehensive Review. *Curr. Med. Chem.* 28, 1–21. doi:10.2174/0929867328666210901122359

Stamatovic, S. M., Shakui, P., Keep, R. F., Moore, B. B., Kunkel, S. L., Van Rooijen, N., et al. (2005). Monocyte Chemoattractant Protein-1 Regulation of Blood-Brain Barrier Permeability. *J. Cereb. Blood Flow. Metab.* 25, 593–606. doi:10.1038/sj.jcbfm.9600055

Subedi, L., and Gaire, B. P. (2021). Tanshinone IIA: A Phytochemical as a Promising Drug Candidate for Neurodegenerative Diseases. *Pharmacol. Res.* 169, 105661. doi:10.1016/j.phrs.2021.105661

Sun, K., Fan, J., and Han, J. (2015). Ameliorating Effects of Traditional Chinese Medicine Preparation, Chinese Materia Medica and Active Compounds on Ischemia/Reperfusion-Induced Cerebral Microcirculatory Disturbances and Neuron Damage. *Acta Pharm. Sin. B* 5, 8–24. doi:10.1016/j.apsb.2014.11.002

Sun, P., Bu, F., Min, J. W., Munshi, Y., Howe, M. D., Liu, L., et al. (2019). Inhibition of Calcium/Calmodulin-Dependent Protein Kinase Kinase (CaMKK) Exacerbates Impairment of Endothelial Cell and Blood-Brain Barrier after Stroke. *Eur. J. Neurosci.* 49, 27–39. doi:10.1111/ejn.14223

Sun, T., Wang, P., Deng, T., Tao, X., Li, B., and Xu, Y. (2020). Effect of Panax Notoginseng Saponins on Focal Cerebral Ischemia-Reperfusion in Rat Models: A Meta-Analysis. *Front. Pharmacol.* 11, 572304. doi:10.3389/fphar.2020.572304

Sun, X., Wei, X., Qu, S., Zhao, Y., and Zhang, X. (2010). Hydroxysafflor Yellow A Suppresses Thrombin Generation and Inflammatory Responses Following Focal Cerebral Ischemia-Reperfusion in Rats. *Bioorg Med. Chem. Lett.* 20, 4120–4124. doi:10.1016/j.bmcl.2010.05.076

Tănăsescu, R., Nicolau, A., Ticmeanu, M., Luca, D., Caraiola, S., Cojocaru, I. M., et al. (2008). An Immunological Approach to Cerebral Ischemia (I). Immune Cells and Adhesion Molecules. *Rom. J. Intern Med.* 46, 3–8. doi:10.1890/03-0369

Tang, K. S., and Tan, J. S. (2019). The Protective Mechanisms of Polydatin in Cerebral Ischemia. *Eur. J. Pharmacol.* 842, 133–138. doi:10.1016/j.ejphar.2018.10.039

Tarozzo, G., Campanella, M., Ghiani, M., Bulfone, A., and Beltramo, M. (2002). Expression of Fractalkine and its Receptor, CX3CR1, in Response to Ischaemia-Reperfusion Brain Injury in the Rat. *Eur. J. Neurosci.* 15, 1663–1668. doi:10.1046/j.1460-9568.2002.02007.x

Tian, K. M., Li, J. J., and Xu, S. W. (2019). Rutaecarpine: A Promising Cardiovascular Protective Alkaloid from Evodia Rutaecarpa (Wu Zhu Yu). *Pharmacol. Res.* 141, 541–550. doi:10.1016/j.phrs.2018.12.019

Tu, X. K., Yang, W. Z., Shi, S. S., Wang, C. H., and Chen, C. M. (2009). Neuroprotective Effect of Baicalin in a Rat Model of Permanent Focal Cerebral Ischemia. *Neurochem. Res.* 34, 1626–1634. doi:10.1007/s11064-009-9953-4

Wang, C., Luo, Y., Lu, J., Wang, Y., and Sheng, G. (2016). Polydatin Induces Apoptosis and Inhibits Growth of Acute Monocytic Leukemia Cells. *J. Biochem. Mol. Toxicol.* 30, 200–205. doi:10.1002/jbt.21779

Wang, H., Zhang, K., Zhao, L., Tang, J., Gao, L., and Wei, Z. (2014). Anti-Inflammatory Effects of Vinpocetine on the Functional Expression of Nuclear Factor-Kappa B and Tumor Necrosis Factor-Alpha in a Rat Model of Cerebral Ischemia-Reperfusion Injury. *Neurosci. Lett.* 566, 247–251. doi:10.1016/j.neulet.2014.02.045

Wang, J., Tong, H., Wang, X., Wang, X., and Wang, Y. (2020a). Tanshinone IIA Alleviates the Damage of Neurocytes by Targeting GLUT1 in Ischaemia Reperfusion Model (*In Vivo* and *In Vitro* Experiments). *Folia Neuropathol.* 58, 176–193. doi:10.5114/fn.2020.96983

Wang, L., Li, L., Han, Q., Wang, X., Zhao, D., and Liu, J. (2020b). Identification and Biological Evaluation of Natural Product Biochanin A. *Bioorg Chem.* 97, 103674. doi:10.1016/j.bioorg.2020.103674

Wang, Q., Tang, X. N., and Yenari, M. A. (2007). The Inflammatory Response in Stroke. *J. Neuroimmunol.* 184, 53–68. doi:10.1016/j.jneuroim.2006.11.014

Wang, W., Tang, L., Li, Y., and Wang, Y. (2015). Biochanin A Protects against Focal Cerebral Ischemia/Reperfusion in Rats via Inhibition of P38-Mediated Inflammatory Responses. *J. Neurol. Sci.* 348, 121–125. doi:10.1016/j.jns.2014.11.018

Wang, Y. H., and Zeng, K. W. (2019). Natural Products as a Crucial Source of Antiinflammatorydrugs Recent Trends and Advancements. *Tradit. Med. Res.* 4, 257–268. doi:10.53388/tmr20190831133

Wei, S. Y., Chen, Y., and Xu, X. Y. (2014). Progress on the Pharmacological Research of Puerarin: A Review. *Chin. J. Nat. Med.* 12, 407–414. doi:10.1016/s1875-5364(14)60064-9

Xiang, B., Xiao, C., Shen, T., and Li, X. (2018). Anti-Inflammatory Effects of Anisalcohol on Lipopolysaccharide-Stimulated BV2 Microglia via Selective Modulation of Microglia Polarization and Down-Regulation of NF-κB P65 and JNK Activation. *Mol. Immunol.* 95, 39–46. doi:10.1016/j.molimm.2018.01.011

Xie, Q., Li, H., Lu, D., Yuan, J., Ma, R., Li, J., et al. (2021). Neuroprotective Effect for Cerebral Ischemia by Natural Products: A Review. *Front. Pharmacol.* 12, 607412. doi:10.3389/fphar.2021.607412

Xiong, D., Deng, Y., Huang, B., Yin, C., Liu, B., Shi, J., et al. (2016). Icariin Attenuates Cerebral Ischemia-Reperfusion Injury through Inhibition of Inflammatory Response Mediated by NF-κB, PPARα and PPARγ in Rats. *Int. Immunopharmacol.* 30, 157–162. doi:10.1016/j.intimp.2015.11.035

Xu, L. Y., Wu, W., Cheng, R., Sun, L. X., Jiang, Z. Z., Zhang, L. Y., et al. (2019). Toxic Effects of Triptolide on Adrenal Steroidogenesis in H295R Cells and Female Rats. *J. Biochem. Mol. Toxicol.* 33, e22394. doi:10.1002/jbt.22394

Xu, T., Wang, X., Ma, C., Ji, J., Xu, W., Shao, Q., et al. (2022). Identification of Potential Regulating Effect of Baicalin on NFκB/CCL2/CCR2 Signaling Pathway in Rats with Cerebral Ischemia by Antibody-Based Array and Bioinformatics Analysis. *J. Ethnopharmacol.* 284, 114773. doi:10.1016/j.jep.2021.114773

Xue, X., Qu, X. J., Yang, Y., Sheng, X. H., Cheng, F., Jiang, E. N., et al. (2010). Baicalin Attenuates Focal Cerebral Ischemic Reperfusion Injury through Inhibition of Nuclear Factor κB P65 Activation. *Biochem. Biophys. Res. Commun.* 403, 398–404. doi:10.1016/j.bbrc.2010.11.042

Xue, Z., Cao, Z., Jin, M., Zhang, X., Wang, X., Dou, J., et al. (2021). New Steroid Saponins from Dioscorea Zingiberensis Yam and Their Medicinal Use Against

I/R via Anti-Inflammatory Effect. *Food Funct.* 12, 8314–8325. doi:10.1039/d1fo01301g

Yang, F., Ma, Q., Matsabisa, M. G., Chabalala, H., Braga, F. C., and Tang, M. (2020a). Panax Notoginseng for Cerebral Ischemia: A Systematic Review. *Am. J. Chin. Med.* 48, 1331–1351. doi:10.1142/S0192415X20500652

Yang, L., Liu, R., Fang, Y., and He, J. (2021). Anti-Inflammatory Effect of Phenylpropanoids from Dendropanax Dentiger in TNF-α-Induced MH7A Cells via Inhibition of NF-κB, Akt and JNK Signaling Pathways. *Int. Immunopharmacol.* 94, 107463. doi:10.1016/j.intimp.2021.107463

Yang, S., Ning, F., Li, J., Guo, D., Zhang, L., Cui, R., et al. (2016). Therapeutic Effect Analysis of Sinomenine on Rat Cerebral Ischemia-Reperfusion Injury. *J. Stroke Cerebrovasc. Dis.* 25, 1263–1269. doi:10.1016/j.jstrokecerebrovasdis.2016.02.023

Yang, X., Chen, L., Li, Y., Gao, F., Yan, Z., Zhang, P., et al. (2020b). Protective Effect of Hydroxysafflor Yellow A on Cerebral Ischemia Reperfusion-Injury by Regulating GSK3β-Mediated Pathways. *Neurosci. Lett.* 736, 135258. doi:10.1016/j.neulet.2020.135258

Yang, Y., Song, J., Liu, N., Wei, G., Liu, S., Zhang, S., et al. (2022). Salvianolic Acid A Relieves Cognitive Disorder after Chronic Cerebral Ischemia: Involvement of Drd2/Cryab/NF-κB Pathway. *Pharmacol. Res.* 175, 105989. doi:10.1016/j.phrs.2021.105989

Yilmaz, G., Arumugam, T. V., Stokes, K. Y., and Granger, D. N. (2006). Role of T Lymphocytes and Interferon-Gamma in Ischemic Stroke. *Circulation* 113, 2105–2112. doi:10.1161/CIRCULATIONAHA.105.593046

Yu, L., Li, Q., Yu, B., Yang, Y., Jin, Z., Duan, W., et al. (2016). Berberine Attenuates Myocardial Ischemia/Reperfusion Injury by Reducing Oxidative Stress and Inflammation Response: Role of Silent Information Regulator 1. *Oxid. Med. Cell Longev.* 2016, 1689602. doi:10.1155/2016/1689602

Yuan, Q., Yuan, Y., Zheng, Y., Sheng, R., Liu, L., Xie, F., et al. (2021). Anti-Cerebral Ischemia Reperfusion Injury of Polysaccharides: A Review of the Mechanisms. *Biomed. Pharmacother.* 137, 111303. doi:10.1016/j.biopha.2021.111303

Zaleska, M. M., Mercado, M. L., Chavez, J., Feuerstein, G. Z., Pangalos, M. N., and Wood, A. (2009). The Development of Stroke Therapeutics: Promising Mechanisms and Translational Challenges. *Neuropharmacology* 56, 329–341. doi:10.1016/j.neuropharm.2008.10.006

Zarruk, J. G., Greenhalgh, A. D., and David, S. (2018). Microglia and Macrophages Differ in Their Inflammatory Profile after Permanent Brain Ischemia. *Exp. Neurol.* 301, 120–132. doi:10.1016/j.expneurol.2017.08.011

Zhang, P., Mak, J. C., Man, R. Y., and Leung, S. W. (2019). Flavonoids Reduces Lipopolysaccharide-Induced Release of Inflammatory Mediators in Human Bronchial Epithelial Cells: Structure-Activity Relationship. *Eur. J. Pharmacol.* 865, 172731. doi:10.1016/j.ejphar.2019.172731

Zhang, T., Xu, J., Li, D., Chen, J., Shen, X., Xu, F., et al. (2014). Salvianolic Acid A, a Matrix Metalloproteinase-9 Inhibitor of Salvia Miltiorrhiza, Attenuates Aortic Aneurysm Formation in Apolipoprotein E-Deficient Mice. *Phytomedicine* 21, 1137–1145. doi:10.1016/j.phymed.2014.05.003

Zhang, W., Song, J. K., Zhang, X., Zhou, Q. M., He, G. R., Xu, X. N., et al. (2018). Salvianolic Acid A Attenuates Ischemia Reperfusion Induced Rat Brain Damage by Protecting the Blood Brain Barrier through MMP-9 Inhibition and Anti-inflammation. *Chin. J. Nat. Med.* 16, 184–193. doi:10.1016/s1875-5364(18)30046-3

Zhang, Y., Tao, C., Xuan, C., Jiang, J., and Cao, W. (2020). Transcriptomic Analysis Reveals the Protection of Astragaloside IV against Diabetic Nephropathy by Modulating Inflammation. *Oxid. Med. Cell Longev.* 2020, 9542165. doi:10.1155/2020/9542165

Zhang, Y., Chen, W. A., Huang, S. S., and Wang, H. M. (2016). Protective Effects of Mangiferin on Cerebral Ischemia-Reperfusion Injury and its Mechanisms. *Eur. J. Pharmacol.* 771, 145–151. doi:10.1016/j.ejphar.2015.12.003

Zhao, C., Lv, Y., Cui, H., Zhu, Y., Wei, M., Xia, Y., et al. (2021). Phase I Safety, Tolerability, and Pharmacokinetic Studies of Tetramethylpyrazine Nitrone in Healthy Chinese Volunteers. *Drug Dev. Res.* 82, 97–107. doi:10.1002/ddr.21733

Zhao, J., Piao, X., Wu, Y., Liang, S., Han, F., Liang, Q., et al. (2020). Cepharanthine Attenuates Cerebral Ischemia/Reperfusion Injury by Reducing NLRP3 Inflammasome-Induced Inflammation and Oxidative Stress via Inhibiting 12/15-LOX Signaling. *Biomed. Pharmacother.* 127, 110151. doi:10.1016/j.biopha.2020.110151

Zhao, Z., Xiao, J., Wang, J., Dong, W., Peng, Z., and An, D. (2015). Anti-Inflammatory Effects of Novel Sinomenine Derivatives. *Int. Immunopharmacol.* 29, 354–360. doi:10.1016/j.intimp.2015.10.030

Zhou, J., Wen, B., Xie, H., Zhang, C., Bai, Y., Cao, H., et al. (2021). Advances in the Preparation and Assessment of the Biological Activities of Chitosan Oligosaccharides with Different Structural Characteristics. *Food Funct.* 12, 926–951. doi:10.1039/d0fo02768e

Zhu, J., Jiang, Y., Wu, L., Lu, T., Xu, G., and Liu, X. (2012). Suppression of Local Inflammation Contributes to the Neuroprotective Effect of Ginsenoside Rb1 in Rats with Cerebral Ischemia. *Neuroscience* 202, 342–351. doi:10.1016/j.neuroscience.2011.11.070

Zhu, J. R., Lu, H. D., Guo, C., Fang, W. R., Zhao, H. D., Zhou, J. S., et al. (2018). Berberine Attenuates Ischemia-Reperfusion Injury through Inhibiting HMGB1 Release and NF-κB Nuclear Translocation. *Acta Pharmacol. Sin.* 39, 1706–1715. doi:10.1038/s41401-018-0160-1

Conflict of Interest: The authors declare that the research was conducted in the absence of any commercial or financial relationships that could be construed as a potential conflict of interest.

Publisher's Note: All claims expressed in this article are solely those of the authors and do not necessarily represent those of their affiliated organizations, or those of the publisher, the editors and the reviewers. Any product that may be evaluated in this article, or claim that may be made by its manufacturer, is not guaranteed or endorsed by the publisher.

Copyright © 2022 Shang, Zhang, Tian and Li. This is an open-access article distributed under the terms of the Creative Commons Attribution License (CC BY). The use, distribution or reproduction in other forums is permitted, provided the original author(s) and the copyright owner(s) are credited and that the original publication in this journal is cited, in accordance with accepted academic practice. No use, distribution or reproduction is permitted which does not comply with these terms.

frontiers | Frontiers in Physiology

TYPE Brief Research Report
PUBLISHED 27 June 2023
DOI 10.3389/fphys.2023.1055706

Check for updates

OPEN ACCESS

EDITED BY
Zsuzsanna Helyes,
University of Pécs, Hungary

REVIEWED BY
Attila Oláh,
University of Debrecen, Hungary
Rolland Péter Gyulai,
University of Pécs, Hungary
Zsofia Hajna,
University of Pécs, Hungary

*CORRESPONDENCE
Soraia K. P. Costa,
skcosta@usp.br

RECEIVED 28 September 2022
ACCEPTED 12 June 2023
PUBLISHED 27 June 2023

CITATION
Cerqueira ARA, Rodrigues L, Coavoy-Sánchez SA, Teixeira SA, Feitosa KB, Taniguchi EY, Lopes LR, Cassola AC, Muscará MN, Sá-Nunes A and Costa SKP (2023), *Aedes aegypti* salivary gland extract alleviates acute itching by blocking TRPA1 channels. *Front. Physiol.* 14:1055706. doi: 10.3389/fphys.2023.1055706

COPYRIGHT
© 2023 Cerqueira, Rodrigues, Coavoy-Sánchez, Teixeira, Feitosa, Taniguchi, Lopes, Cassola, Muscará, Sá-Nunes and Costa. This is an open-access article distributed under the terms of the Creative Commons Attribution License (CC BY). The use, distribution or reproduction in other forums is permitted, provided the original author(s) and the copyright owner(s) are credited and that the original publication in this journal is cited, in accordance with accepted academic practice. No use, distribution or reproduction is permitted which does not comply with these terms.

Aedes aegypti salivary gland extract alleviates acute itching by blocking TRPA1 channels

Anderson R. A. Cerqueira[1], Leandro Rodrigues[1], Silvia Abigail Coavoy-Sánchez[1], Simone A. Teixeira[1], Karla B. Feitosa[1], Erika Y. Taniguchi[2], Lucia R. Lopes[1], Antônio C. Cassola[2], Marcelo N. Muscará[1], Anderson Sá-Nunes[3,4] and Soraia K. P. Costa[1]*

[1]Departamento de Farmacologia, Instituto de Ciências Biomédicas, Universidade de São Paulo, São Paulo, Brazil, [2]Departamento de Fisiologia e Biofísica, Instituto de Ciências Biomédicas, Universidade de São Paulo, São Paulo, Brazil, [3]Departamento de Imunologia, Instituto de Ciências Biomédicas, Universidade de São Paulo, São Paulo, Brazil, [4]Instituto Nacional de Ciência e Tecnologia em Entomologia Molecular, Conselho Nacional de Desenvolvimento Científico e Tecnológico (INCT-EM/CNPq), Rio de Janeiro, Brazil

Aedes aegypti (*Ae. aegypti*) saliva induces a variety of anti-inflammatory and immunomodulatory activities. Interestingly, although it is known that mosquito bites cause allergic reactions in sensitised hosts, the primary exposure of humans to *Ae. aegypti* does not evoke significant itching. Whether active components in the saliva of *Ae. aegypti* can counteract the normal itch reaction to injury produced by a histaminergic or non-histaminergic pathway in vertebrate hosts is unknown. This study investigated the effects of *Ae. aegypti* mosquito salivary gland extract (SGE) on sensitive reactions such as itching and associated skin inflammation. Acute pruritus and plasma extravasation were induced in mice by the intradermal injection of either compound 48/80 (C48/80), the Mas-related G protein-coupled receptor (Mrgpr) agonist chloroquine (CQ), or the transient receptor potential ankyrin 1 (TRPA1) agonist allyl isothiocyanate (AITC). The i.d. co-injection of *Ae. aegypti* SGE inhibited itching, plasma extravasation, and neutrophil influx evoked by C48/80, but it did not significantly affect mast cell degranulation *in situ* or *in vitro*. Additionally, SGE partially reduced CQ- and AITC-induced pruritus *in vivo*, suggesting that SGE affects pruriceptive nerve firing independently of the histaminergic pathway. Activation of TRPA1 significantly increased intracellular Ca^{2+} in TRPA-1-transfected HEK293t lineage, which was attenuated by SGE addition. We showed for the first time that *Ae. aegypti* SGE exerts anti-pruriceptive effects, which are partially regulated by the histamine-independent itch TRPA1 pathway. Thus, SGE may possess bioactive molecules with therapeutic potential for treating nonhistaminergic itch.

KEYWORDS

nonhistaminergic, skin, itch, sensory neurons, TRPA1, salivary gland, *Aedes* (Ae) *aegypti*, MrgprA3

1 Introduction

The itch-scratch reflex is modulated by small-diameter sensory neurons in the dorsal root ganglia (DRG) and it is usually associated with inflammatory responses (Bartsch et al., 2019). This reaction is a protective sensory modality that triggers specific neural histaminergic and non-histaminergic pathways with a complex interplay between keratinocytes, immune cells, and cutaneous neurons (Koch et al., 2018; Moore et al.,

2018). Whereas acute itch evoked by insect bites is relieved by scratching or antihistamine therapy and is mainly associated with biogenic amines released from mast cells, persistent (chronic) itching is commonly associated with chronic skin diseases, such as atopic dermatitis and, thus, difficult to control (Berger et al., 2013; Pereira et al., 2019; van Laarhoven et al., 2019). In this sense, patients with these conditions could benefit from additive antipruritic therapies.

The transient receptor potential (TRP) proteins are a superfamily of structurally related non-selective cation channels. One of its members, the transient receptor potential ankyrin 1 (TRPA1), mediates temperature sensing (Story et al., 2003; Moparthi et al., 2014) and is highly expressed in the terminal ends of sensory neurons throughout the body. It also functions as a chemosensor for pain-producing compounds and histamine-independent itch-signalling pathways (Lee et al., 2008; Liu et al., 2009; Wilson et al., 2011; Kemény et al., 2018; Liu et al., 2021). TRPA1 knockout mice exhibited a marked reduction of itching in response to selective agonists of Mas-related G protein-coupled receptor (Mrgpr) subtypes, such as chloroquine (CQ; MrgprA3) or BAM8-22 (MrgprC11). These receptors are expressed on C-fiber-sensitive neurons, thus reinforcing the role of TRPA1 receptor signalling in histamine-independent itch pathways (Wilson et al., 2011). Notably, the widely used secretagogue C48/80 can trigger Mas-related G protein-coupled receptor X2 (MRGPRX2), the mouse ortholog of MrgprB2, expressed in skin-resident mast cells, thus inducing pseudoallergies due to IgE-independent mast cell degranulation, the release of histamine and proteases, and thereby evoking inflammation and pruritus (Bradford, 1976; McNeil et al., 2015; Rodrigues et al., 2017; Dondalska et al., 2020; Yang et al., 2021). It was previously reported that murine MrgprA3 and human MrgprX1 are the predominant CQ receptors (Li et al., 2022).

Aedes aegypti (*Ae. aegypti*) saliva is a complex mixture of bioactive components with anti-hemostatic and immunomodulatory properties (Bissonnette et al., 1993; Ribeiro, 1995; Bizzarro et al., 2013; Barros et al., 2019). Together, these components contribute to female mosquitoes' blood acquisition and facilitate the transmission of several arboviruses (Jin et al., 2018; Sun et al., 2020). Due to these properties, *Ae. aegypti* saliva and its constituents have been prospected for compounds that can prevent or treat clinical conditions using experimental disease models (Sales-Campos et al., 2015; de Souza Gomes et al., 2018; Assis et al., 2021; Lara et al., 2021).

In addition to the various biological activities characterised in the *Ae. aegypti* saliva, there may still exist many others not yet to be identified and assessed. Knowing the expression profile of TRPA1 and its role as a pain chemosensor, we were interested in assessing the effect of SGE on TRPA1 by measuring TRPA1-mediated Ca^{2+} influx in hTRPA1-HEK293t cells and the *in vivo* effect of SGE on TRPA1 Allyl isothiocyanate (AITC) or MrgprA3 (CQ) receptor agonist-induced pruritus. Thus, the present study evaluated the effects of *Ae. aegypti* SGE on histaminergic and non-histaminergic itch induced in mice. We also evaluated if *Ae. aegypti* SGE acts on TRPA1 receptors using TRPA1-transfected HEK293t cells.

2 Methods

2.1 Animals

Male BALB/c mice and male Wistar rats, 7-10-week-old, were obtained from the institutional animal care facilities and housed in groups of five animals per cage under standard controlled conditions (22°C; 12/12 light/dark cycle) in ventilated racks (Alesco, Monte Mor, SP, Brazil) with free access to food and water. Experiments were approved by the Institutional Animal Care and Use Committee (CEUA-ICB/USP; protocol no. 33, page 85, book no. 02/2010), according to the guidelines of the Brazilian Council for Control of Animal Experimentation (CONCEA) and the Directive 2010/63/EU, combined with the Animal Welfare Act.

2.2 *Aedes aegypti* salivary gland extract

Mosquitoes were bred and maintained in an insectary at 26°C, 80% humidity, 12/12 light/dark cycle, and fed a 10% sucrose solution *ad libitum* (Maciel et al., 2014). Female mosquitos (5–7 days old) were anesthetised under low temperatures (4°C), sterilised in 70% alcohol, and immersed in 200 µL of phosphate-buffered saline (PBS). The mosquito heads were removed, and the salivary glands were dissected from the thorax under a microscope and transferred to a microtube containing 50 µL of cold PBS. The samples were sonicated and centrifuged (4 °C, 14,000 × *g*, 10 min) to remove particulate material (Bizzarro et al., 2013; Maciel et al., 2014). The supernatant was sterilised through a 0.22 µm nitrocellulose membrane filter (Millipore, Billerica, MA, United States). Protein concentration was measured using a NanoDrop 2000 (A_{280}; Thermo Fisher Scientific, Wilmington, DE, United States). Aliquots of 2 mg/mL SGE were prepared and stored at −80°C until use.

2.3 Materials

3,3′-Dimethoxybenzidine dihydrochloride, urethane, HTAB (hexadecyltrimethylammonium bromide), Trypan blue, Toluidine blue, CQ (N-dimethyl-1,4-pentane diamine diphosphate), compound 48/80 (C48/80 N-methyl-p-methoxy phenethylamine), phthalaldehyde, AITC (Allyl isothiocyanate), 2-(1,3-Dimethyl-2,6-dioxo-1,2,3,6-tetrahydro-7H-purin-7-yl)-N-(4-isopropylphenyl)acetamide (HC030031), pyrilamine and Fura-2-AM were purchased from Sigma Chemical Co. (St Louis, MO, United States). Percoll was purchased from GE Healthcare (Uppsala, Sweden). Isoflurane (1-chloro-2,2,2-trifluoroethyl difluoromethyl ether) and sodium heparin were purchased from Cristália (Itapira, São Paulo, Brazil). Hydrogen peroxide (H_2O_2) and formaldehyde (CH_2O) were purchased from Labsynth® (Diadema, SP, Brazil).

2.4 Drug-induced scratching

Itch behaviour was evaluated as described (Costa et al., 2006; Rodrigues et al., 2017). C48/80 (10 µg/site), CQ (25 or 100 µg/site),

AITC (20 mM reagent = 1 μmol/50 μL per site), or the corresponding vehicle (Tyrode solution) was intradermally (i.d.) injected, in a volume of 50 μL, alone or in combination with either *Ae. aegypti* SGE (1–10 μg/site) or the TRPA1 antagonist HC030031 (20 μg/site) or both. Mice were individually confined into an acrylic transparent box (12 × 20 × 17 cm) in a room fitted with a video recorder. The animals were acclimatised for 40 min for 2 days before the experiments. For animals showing a repeated number of scratching behaviour and a series of these movements, one bout of scratching was counted, and the number was expressed as absolute or percentage values determined in 30 min. In all experiments, the scratching behaviour was quantified in a blinded fashion.

2.5 Absorbance spectrum analysis of combined SGE and HC030031 solution

In order to evaluate the potential chemical interference between SGE and HC030031 (100, 200 and 400 μg/mL), the absorbance spectrum of increasing concentrations of SGE (50, 100 and 200 μg/mL) with and without increasing concentrations of HC030031 in 96-well microplates was measured on SpectraMax Plus 384 (Molecular Devices Corp, Sunnyvale, CA, United States) within the interval of 200–260 nm.

2.6 Assessment of plasma extravasation and myeloperoxidase activity

Shaved mice were anesthetised with urethane (2.5 g/kg; i.p.), and a volume of 100 μL of ^{125}I–bovine serum albumin (^{125}I-BSA, 0.037 MBq/mouse) was intravenously injected via the tail vein. Either C48/80 (10 μg/site) or vehicle (Tyrode) were i.d. injected alone or co-injected with SGE (1–10 μg/site) throughout six randomised skin sites (Rodrigues et al., 2017). Thirty minutes later, a blood sample was collected, and plasma was separated by centrifugation (10,000 × *g*, 10 min, 4°C). The skin injection sites were removed, and radioactivity present in these specimens was measured in a γ-counter (Packard Bioscience, Meriden, CT, USA). The plasma volume extravasated in the injected skin sites was calculated and expressed as μL of plasma per g of tissue or as a percentage of the control values (obtained with C48/80) alone.

In a separate set of experiment, mice were anaesthetised and i.d. injected with C48/80 (10 μg/site) or Tyrode in the presence or absence of SGE (1–10 μg/site). After 4 hours (4 h), animals were euthanised, and the injected sites were removed. Tissue MPO activity was measured as a marker of neutrophil infiltration into the skin tissue, as previously described (Rodrigues et al., 2017).

2.7 Immunohistochemistry for intercellular adhesion molecule-1 (ICAM-1) and vascular cell adhesion molecule-1 (VCAM-1) expression

Skin specimens i.d. injected with Tyrode, C48/80 (10 μg/site) alone or plus SGE (10 μg/site) were obtained and fixed in glass slides were heated (98 °C) for antigen retrieval in sodium citrate buffer (0.05% Tween-80, pH 6.0) and washed with PBS (pH 7.2). Following 30 min of incubation with 3% H_2O_2 in PBS (pH 7.2), the specimens were treated with 10% rabbit serum in PBS/10% BSA solution (1:1) for 1 h. The sections were overnight incubated with polyclonal antibodies anti-ICAM-1 (0.5 μg/mL); #AF796; R&D Systems, Minneapolis, MN, United States) or anti-VCAM-1 (2 μg/mL#AF643; R&D Systems) diluted in PBS/Tween 20 (0.3%). Following incubation with rabbit anti-goat IgG secondary antibody for 1 h (1 μg/mL]; at 21°C; Rockland Immunochemicals Inc., Limerick, PA, United States), vectastin ABC-kit (Vector Laboratories, Burlingame, CA, United States) was applied for 1 h for signal amplification and 3,3-diaminobenzidine, diluted in PBS containing 0.03% H_2O_2 (v/v), was utilised as the chromogen, yielding the overall brown colour. Images of three (ICAM-1) or six (VCAM-1) regions from both epidermis and dermis were randomly selected, and the stained area were acquired by optical microscopy (×200 magnification, LeicaDM 2500) and quantified using the Image-Pro Plus 4.5 software (Media Cybernetics, MD, United States). The images were calibrated using an image of a stage micrometer scale with the same optical set up and pre-established colour filter applied to quantify the positive areas. The ratio between the labelled (VCAM-1 or ICAM-1 immunoreactivity) area per total area analysed was given as stained area fraction in μm^2. For each image a tissue area was defined and used to calculate the percentage (%) of positive area, based on the equation: (positive area/total tissue area) x 100.

2.8 Mast cell degranulation *in situ*

Mice were anaesthetised with isoflurane in oxygen, followed by i.d. injection with C48/80 (10 μg/site), Tyrode alone or in the presence of SGE (1 μg/site). After 30 min, the animals were submitted for euthanasia, and the i.d. injected skin sites were removed and soaked in 4% buffered formalin solution pH 7.4 for 24 h before being fixed in paraffin. Five micrometer-thick sections were mounted on glass microscope slides and stained with 1% toluidine blue working solution for 1–2 min at room temperature (22°C). The number of toluidine blue positive mast cells was quantified based on their morphological characteristics of intact or activated/degranulated cells by an investigator blinded to the treatment in randomly areas of ≅ 100 μm^2 (Lidegran et al., 1996; Santos et al., 2014), using ten random fields of each 5 μm skin section, under optical microscopy (Leica DM2500; Basel, Switzerland), with a high-power objective lens (×40 and 100×). The number or corresponding percentage of degranulated mast cells was subsequently calculated. Complete cells were considered those with a well-defined contour and that are not in the process of changing shape and releasing the granule contents in the cytoplasm, whilst the activated/degranulated mast cells exhibited irregular contours and dispersed (metachromatic) granules.

2.9 Mast cell degranulation *in vitro*

A total number of 15 male rats were used in three independent experiments. Animals were exsanguinated under deep anaesthesia

with inhaled isoflurane in oxygen. Mast cells were isolated from the peritoneal cavity and purified (95%) using a Percoll gradient. In a volume of 0.5 mL mast cell aliquots (4×10^5 cells/mL), SGE was added in various concentrations (1–100 μg/mL) followed by C48/80 (1 μg/mL). After 15 min at 37 °C, samples were centrifuged (300×g, 4°C, 10 min) to determine the histamine released in the supernatant and residual histamine in the cell pellet. Samples were incubated with 300 μL of 1M NaOH and 1% phthalaldehyde (in methanol) for 4 min, followed by adding 15 μL of 3M HCl with vigorous agitation. Fluorescence was measured in a microplate reader (Synergy HT; Biotek, Winooski, VT, USA) at 360/450 nm (excitation/emission). Histamine concentrations were calculated from a histamine standard curve (prepared in 1M NaOH, range: 0.005–1.5 μg/mL). Results were expressed as % of histamine released [$\text{Histamine}_{\text{released}}$/($\text{Histamine}_{\text{released}}$ + $\text{Histamine}_{\text{cell lysate}}$) × 100].

2.10 HEK293t cell culture, TRPA1 transfection and western blot analysis

The human embryonic kidney cells (HEK 293), donated by Dr. Nancy Rebouças (ICB, University of São Paulo), were grown in Dulbecco's Modified Eagle Medium (DMEM) supplemented with 10% fetal bovin serum, penicillin and streptomycin sulfate (1%; 37 °C, 5% CO2) and maintained in six-well culture plates until 80% confluence. The medium was removed, and the cells were incubated with Opti-MEM (#31985070, Invitrogen, Carlsbad, CA, United States) containing 5 μg of the hTRPA1 vector and 5 μg of pCMVSB100X in the presence of Lipofectamine 2000 for 8 h (37 °C, 5% CO_2). After incubation, the medium was removed, and DMEM containing 10% SFB and G418 (500 μg/mL was added.

We expressed hTRPA1 in a TRPA1-negative cell line (HEK293t) to evaluate the inhibitory effect of SGE on TRPA1 receptor agonist AITC-induced increased intracellular Ca^{2+}. For this, mammalian expression plasmid vectors hTRPA1 (# 100016279; Life Technologies, Carlsbad, CA, United States) and pCMVSB100X, a pT2/BH sleeping beauty transposon derived with ampicillin and neomycin resistance (# 26556; Addgene, Watertown, MA, United States), was provided by Dr Zoltan Sandor (Department of Pharmacology and Pharmacotherapy, University of Pecs, Hungary) and transfected into HEK293t cells using Lipofectamine 2000 (Pozsgai et al., 2017). A fluorescence assay was performed 4 h and 24 h after transfection.

Protein concentration was determined (Bradford, 1976), and TRPA1 expression was analysed using 20 μg of total protein by sodium dodecyl sulphate-polyacrylamide SDS-PAGE gel electrophoresis via Western blot device using specific electrophoresis buffer, accordingly (Laemmli, 1970). TRPA1-negative or TRPA1-positive cell line HEK293t (5x 10^6 cell/mL) were centrifuged (10.000 rpm, 5 min at 4°C), and the resulting pellet resuspended in TRIS buffer (50 mM pH 7.4, Triton X-100 1%, sodium dodecyl sulfate 0.1%, phenylmethylsulfonyl fluoride 1 mM and protease inhibitor mixture 0.1%; Sigma, St. Louis, MO, United States) and assayed for TRPA1 expression. Both the primary antibody rabbit polyclonal anti-TRPA1 (1:1500; Novus Biologicals, CO, United States) and the corresponding HRP-conjugated secondary antibody (goat anti-rabbit; Bio-Rad Laboratoris, Inc, CA, United States) were used. The immunoreactive bands were detected by chemiluminescence in a ChemiDoc™ MP images system (Bio-Rad Laboratories, Inc, CA, United States). The molecular weights of the immunoreactive bands were determined using the ImageLab™ software by comparison of the electrophoretic mobilities with those of known molecular weight standard anti-β-Actin antibody (1:2000; Thermo Fisher Scientific, IL, United States).

2.11 Intracellular Ca^{2+}

Transfected cells were incubated with Fura-2-AM at 37 °C. After 30 min, the cells were moved to a microscope, where they remained under a constant flow of Tyrode throughout the experiment. Tyrode buffer containing AITC (100 μM) or SGE (1 μg/mL) was alternated to evaluate fluorescence variations. During the experiments, the temperature was carefully controlled at 37°C (de Carvalho et al., 2014). The images were obtained using a Leica AF6000 inverted fluorescence microscope. For images with Fura-2-AM, a rotating excitation filter system of 340 and 380 nm was used. The emission was observed with a high-pass filter for wavelengths above 510 nm (2 Hz). The data presented as the 340/380 nm fluorescence ratio.

2.12 Data analysis and statistics

Data are expressed as the mean ± SD or median (interquartile range [IQR]) of n animals unless otherwise stated. A normality Shapiro–Wilk test was performed for each set of results. ANOVA, Sidak's post-test, or Kruskal-Wallis, Dunn's post-test were used to compare means between groups when the variable was in a normal or non-normal distribution, respectively. Values of $p < 0.05$ were considered significant. When required, Student's t-test (two-tailed paired) were calculated. Data were analysed using GraphPad Prism Co. (Version 9.5.1, San Diego, CA, USA).

3 Results

3.1 Pruritus and skin inflammation

Figure 1A shows that itch behaviour was effectively triggered in the animals by i.d. injection of C48/80 in the dorsal skin. The co-injection of SGE significantly reduced this response at the lowest and intermediate doses (1 and 3 μg/site). The histamine receptor antagonist pyrilamine (10 μg/site) reduced C48/80-induced pruritus, and the presence of co-injected SGE could not further inhibit the pruritus response (Figure 1B).

SGE, at 10 μg/site, but not at 1 and 3 μg/site, significantly prevented C48/80-induced plasma extravasation by ~50% (Figure 1C). SGE alone did not evoke any plasma extravasation compared to Tyrode (Figure 1C).

C48/80 (10 μg/site) promoted a significant increase in tissue MPO compared to vehicle, and co-injection with SGE at the highest

10.3389/fphys.2023.1055706

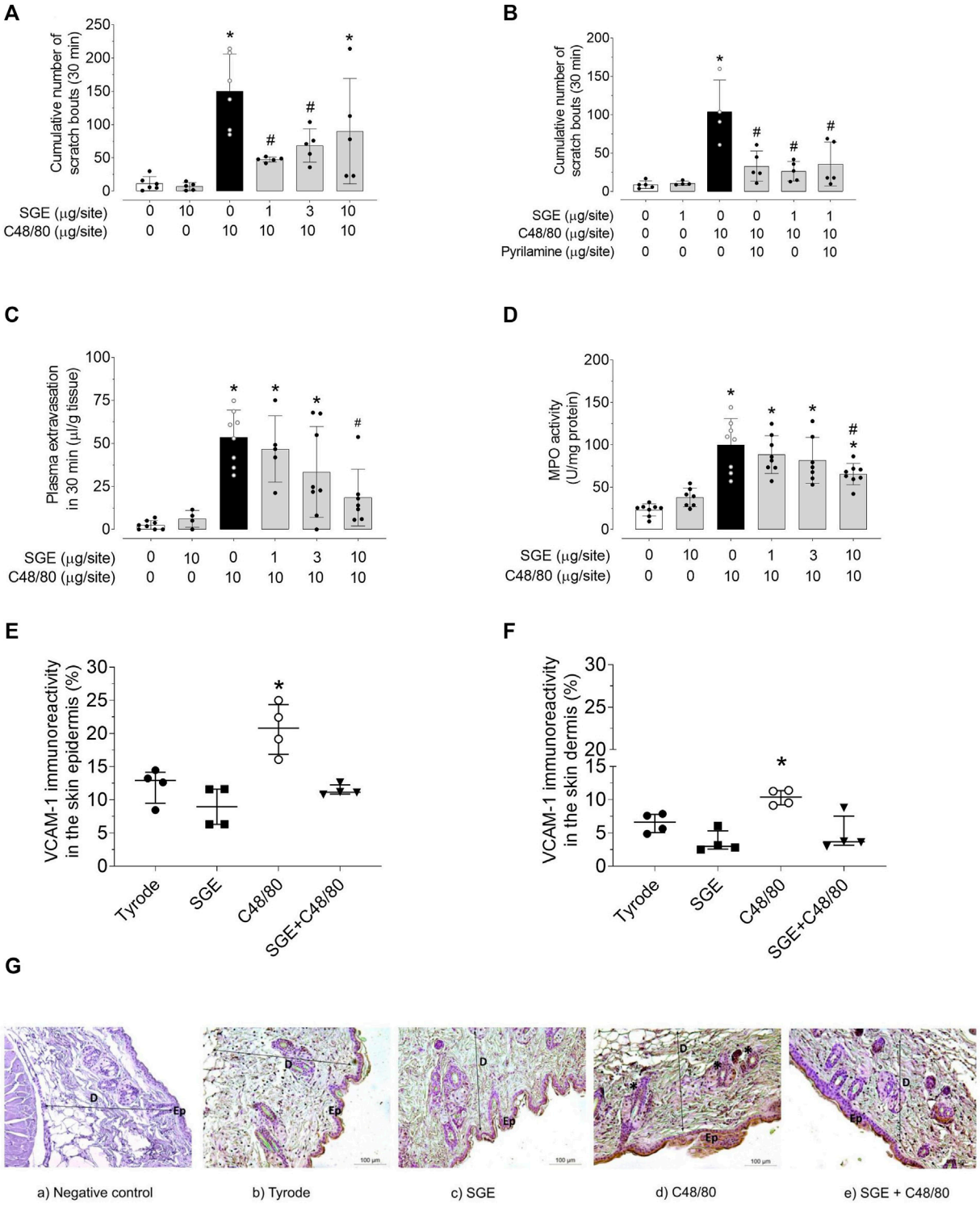

FIGURE 1
Aedes aegypti SGE downmodulates histaminergic responses triggered by compound 48/80. Bar scatter dot plot graphs showing itch evoked by C48/80 in the presence of different doses of SGE **(A)**, or in the presence of 1 µg/site dose of SGE alone and co-injected with the antihistamine pyrilamine **(B)**, effects of *Ae. aegypti* SGE on C48/80-induced plasma extravasation **(C)**, and C48/80-induced increased neutrophil influx measured by MPO activity **(D)**. Values are expressed as mean ± SD. **p* < 0.05 *vs.* "Vehicle or *Ae. aegypti* SGE group"; #*p* < 0.05 vs. "C48/80" group (*n* = 4–8). Quantitative immunoreactivity staining analysis showing the % of VCAM-1 positive epidermal and dermal area of C48/80 (10 µg/site)-injected skin treated and untreated with SGE (10 µg/site) represented by the column scatter dot plot graphs **(E)** and **(F)**, respectively. Data are expressed as median with interquartile range (*n* = 4 mice/group). **p* < 0.05 vs *Ae. aegypti* SGE group. Panel G shows representative images of VCAM-1 immunohistochemical staining differences (* asterisks show DAB-positive signal) in the epidermis and dermis of mouse dorsal skin i.d. injected with Tyrode **(B)**, SGE **(C)**, C48/80, **(D)** and C48/80 + SGE **(E)**. Panel **(Ga)** shows the negative control specimen (skin without primary antibody). Double ended arrows indicate dermal-epidermal junction, Ep = epidermis, D = dermis. DAB, hematoxylin counterstain, ×100 magnification.

10.3389/fphys.2023.1055706

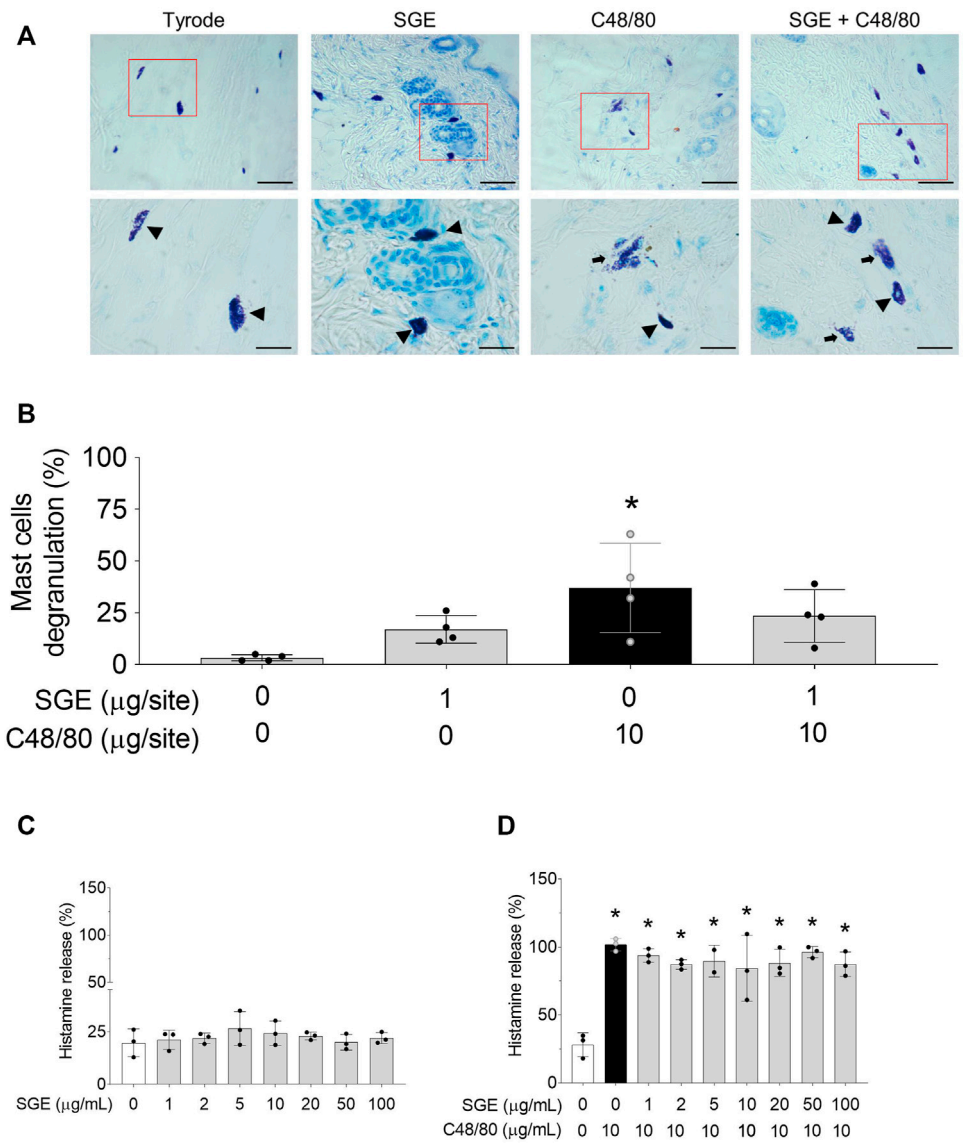

FIGURE 2
Effects of *Aedes aegypti* SGE on mast cell degranulation induced by C48/80. Panel **(A)** illustrates representative images of intact (arrowhead) and degranulated mast cells (arrow) in mice´s skin *in situ* (by the colouration of toluidine blue) following 30 min i.d. injection of Tyrode, SGE, C48/80 and C48/80 + SGE, respectively, on the magnification of ×400 (top images) and 1000x (bottom images), Bar = 50 µm. Panel **(B)** shows the corresponding percentage of degranulated mast cells counted in random fields of the observed mice skin tissue *in situ*. Data are expressed as mean ± SD for n = 4 mice/group. *$p < 0.05$ vs. "Vehicle" group. Panels **(C, D)** show the effect of increasing concentrations of SGE on the percentage of histamine released *in vitro* from rat peritoneal mast cell following 15 min incubation with vehicle or C48/80, respectively. Data presented as scatter plot expressed as mean ± SD are representative of three independent experiments for a total n = 15 rats. *$p < 0.05$ vs. "Vehicle" group. One-way ANOVA (Sidak's multiple comparisons test).

dose (10 µg/site) significantly decreased MPO activity (Figure 1D). SGE alone did not induce increased MPO activity compared to Tyrode (Figure 1D).

Immunohistochemistry analyses revealed that VCAM-1 (Figures 1E,F and G), but not ICAM-1 (Supplementary Figure S1A, B; Supplementary Table S1) expression was significantly upregulated in the epidermis and dermis of mice dorsal skin by the i.d. injection of C48/80 (10 µg/site) 4 h later. When co-injected with SGE, C48/80-induced VCAM-1 expression did not significantly differ from SGE- or Tyrode-induced response (Figures 1E,F and G; Supplementary Figure S1A, B; Supplementary Table S1).

3.2 Mast cell stabilisation *in situ and in vitro*

Mast cell staining with toluidine blue was not triggered by the i.d. injection of vehicle or Ae. aegypti SGE in the mouse dorsal skin; however, an i.d. injection of C48/80 promoted significative *in situ* mast cell degranulation compared to the

10.3389/fphys.2023.1055706

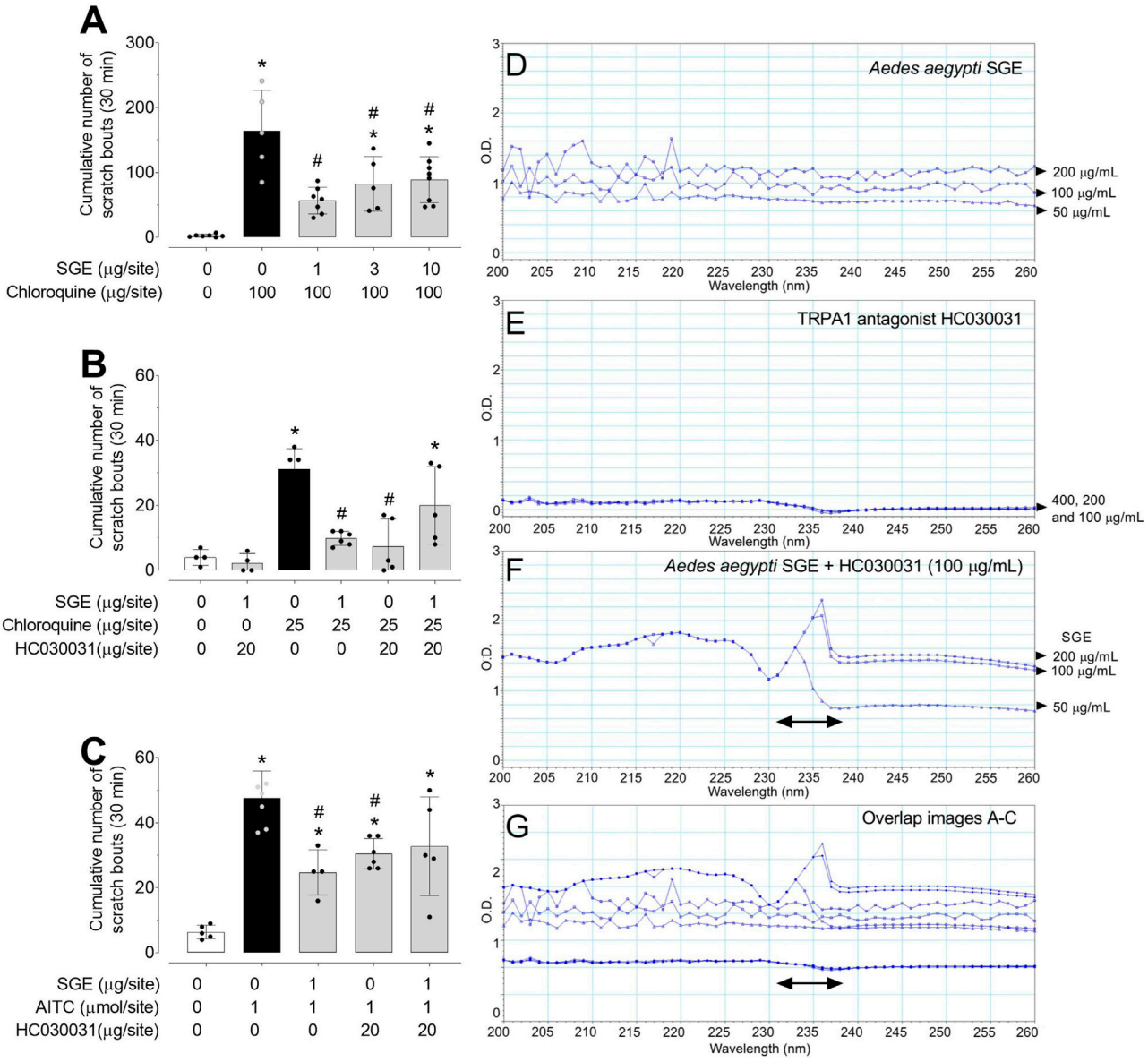

FIGURE 3
Aedes aegypti SGE downmodulates non-histaminergic itch caused by TRPA1 interaction evaluated during 30 min. Itch evoked by chloroquine in the presence of increasing doses of SGE **(A)**. Effect of SGE and/or TRPA1 antagonist HC030031 in chloroquine-induced itch **(B)**. Effect of SGE and/or TRPA1 antagonist HC030031 in AITC-induced itch **(C)**. Data are expressed as mean ± SD. *$p < 0.05$ vs. "Vehicle" group; #$p < 0.05$ vs. "chloroquine" or "AITC" group (n = four to eight mice). Panels **(D, E)** show the absorbance spectrum of three different concentrations of SGE (50, 100 and 200 µg/mL) or HC03003 (100, 200 and 400 µg/mL), respectively measured in the 200–260 nm range. Panel **(F)** shows the spectra of three individually concentrations of SGE (50, 100 and 200 µg/mL) co-incubated with HC030031 (100 µg/mL), in which an important change in the absorbance spectrum was observed in the 230–237 nm interval compared with either compound alone. Panel **(G)** shows overlap images for all testing substances. One-way ANOVA (Sidak's multiple comparisons test).

vehicle or SGE alone (Figures 2A, B; Supplementary Table S2). Co-injection of C48/80 with SGE did not significantly reduce the amount of degranulated mast cells (Figures 2A, B; Supplementary Table S2). The *in vitro* incubation of mast cells obtained from the rat peritoneal cavity with increasing concentrations of SGE did not significantly promote histamine release from these cells compared with the control (Figure 2C). C48/80 significantly induced mast cell histamine release compared to the control group, which was not affected by pre-treating the cells with different SGE concentrations (Figure 2D).

3.3 TRPA1 signalling mediates the anti-pruriceptive properties of SGE

CQ-induced intense pruritus was significantly decreased when SGE was co-injected at all the tested doses (Figure 3A). CQ (25 µg/

10.3389/fphys.2023.1055706

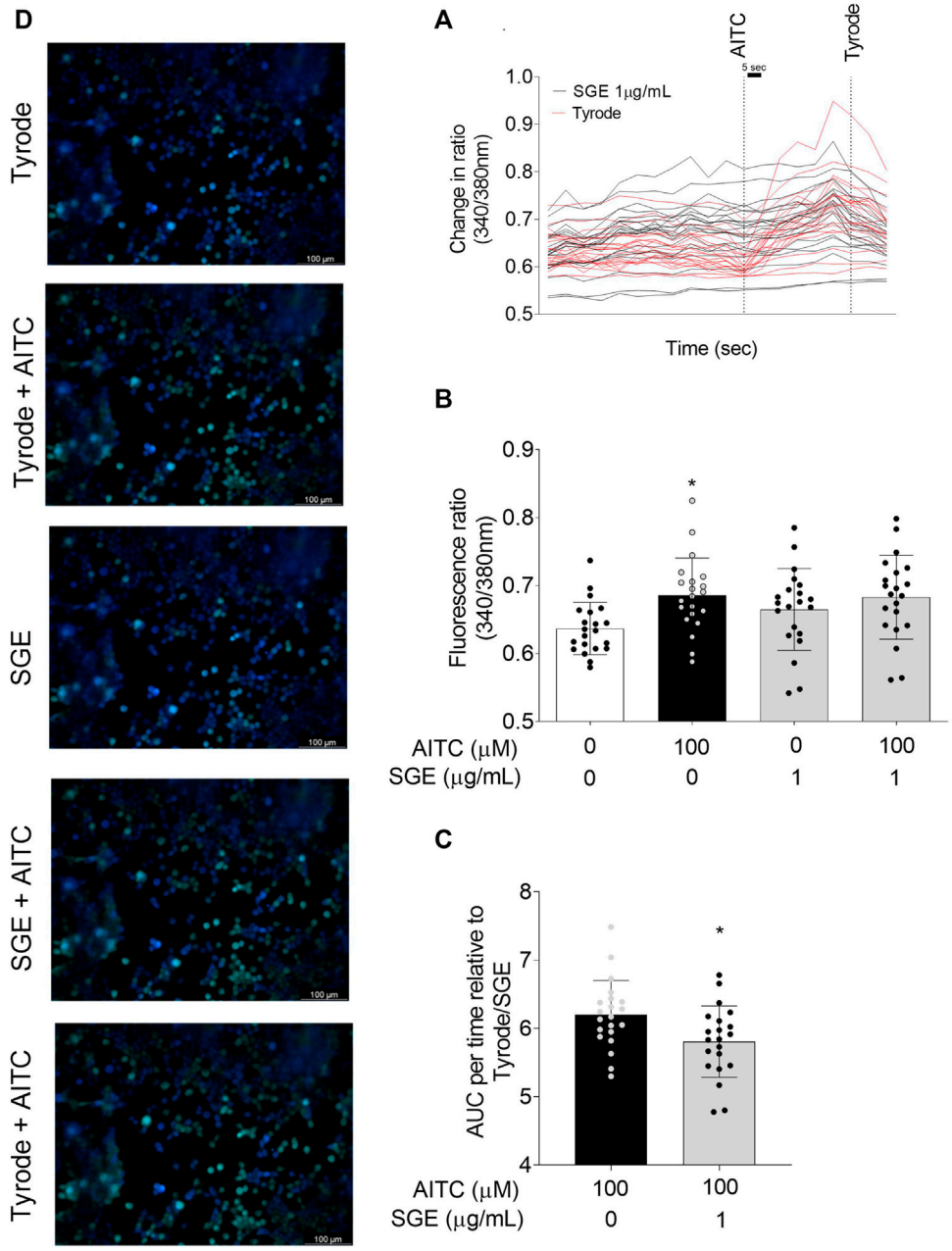

FIGURE 4
Aedes aegypti SGE attenuates TRPA1 receptor agonist AITC-induced Ca^{2+} mobilization in hTRPA1-HEK293t cells. Panel **(A)** shows representative scan lines displayed horizontally of continuously Ca^{2+} changes in relation to the time (sec) in responses to SGE (1 µg/mL), SGE +100 µM AITC, and Tyrode +100 µM AITC in TRPA1-HEK293t cells loaded with Fura-2-AM. Panel **(B)** shows corresponding fluorescence ratio (calcium changes) as mean ± SD from 3 independent experiments in responses to SGE (1 µg/mL), SGE +100 µM AITC, and Tyrode +100 µM AITC in TRPA1-HEK293t cells loaded with Fura-2-AM (n = 21 cells). *$p < 0.05$ vs. "Control" group. Fura-2 fluorescence signals are presented as the 340/380 nm ratio. Panel **(C)** demonstrates values as mean ± SD of the area under the curve (AUC) per time relative to Tyrode/SGE of calcium responses evoked by AITC (100 µM) in hTRPA1-HEK293t cells. *$p < 0.05$ vs. "Vehicle" group. One-way ANOVA (Sidak's multiple comparisons test; panel **(A)** or Student's t-test was used (panel **(B)**). The left **(D)** panel containing five images demonstrates the fractional fluorescence recorded from hTRPA1-HEK293t cells loaded with Fura-2-AM and scanned at a rate of ≅ 3 s per image in response to different stimuli. Transient events were recorded before (top image; basal fluorescence of the cells treated with vehicle Tyrode). The second from the top image illustrates the dynamic changes in intracellular Ca^{2+} measured by changes in the intensity of Fura-2-AM fluorescence (green colour) following the addition of AITC (peak time≅ 300 s). After washing out the cells with Tyrode, the third and fourth images illustrate reduced changes in fluorescence intensity after the addition of SGE alone (time ≅ 480 s) and together with AITC (time≅ 510 s), respectively. The bottom image illustrates intracellular Ca^{2+} increases in response to the new addition of AITC (time≅ 780 s) following a new washing session of the cells to assess viability. Non-responsive cells are observed in blue.

site)-induced moderate pruritus was also inhibited by the TRPA1 antagonist HC030031 (20 µg/site; Figure 3B), showing the involvement of TRPA1 channels in the CQ response. Likewise, the AITC-evoked scratching behaviour was effectively antagonised by HC030031 (20 µg/site) and the *Ae. aegypti* SGE co-injection (1 µg/site; Figure 3C, respectively). In the presence of

SGE and HC030031, the itching behaviour induced by either agonist was not markedly affected. Of note, the combination of SGE and HC030031 did not promote itch (Figure 3B).

The spectra measured in the 200–260 nm range of SGE and HC030031, individually or co-incubated, showed that combined SGE and HC030031 changed the absorbance spectrum in the 230–237 nm interval compared with either compound alone (Figures 3D–G).

The WB analysis revealed immunoreactive bands in TRPA1-positive cells but not in negative hTRPA1-HEK293 cells, consistent with TRPA1 (≅ 105 kDa) and β-actin MW (≅ 33 kDa; Supplementary Figure S2). Given the requirement for TRPA1 mediating calcium response *in vitro*, we showed that hTRPA1-HEK293t cells stimulated with AITC exhibited significant calcium increment (mean fluorescence ratio 340/380 nm), when compared to hTRPA1-HEK293t cells stimulated with Tyrode (Figures 4A, B, D; Supplementary Figure S3A, B); but not with SGE (Figures 4A–D). Fluorescence changes in Ca^{2+} were taken continuously on the same cell population (Supplementary Figure S3; Supplementary Table S3). When analysed as the area under the curve (AUC) in relation to the vehicle, the treatment with SGE significantly attenuated AITC-induced calcium increase in hTRPA1-HEK293t cells (Figures 4C,D).

4 Discussion and concluding remarks

Pruritus is the most frequent symptom in dermatologic clinics and is among the 50 most prevalent conditions worldwide (Roh et al., 2021). The incidence of chronic pruritus varies among different studies, but it seems especially common among the elderly (Yalçin et al., 2006). The local itching sensation is intimately associated with touch, pain, and insect bites. However, at least for *Ae. aegypti* bites, pruritus is instead associated with hypersensitivity reactions since non-sensitive individuals did not report an itch sensation within 5 minutes of mosquito exposure (Conway, 2021). As opposed to the excessive inflammatory skin reaction observed in sensitised mice (Henrique et al., 2019), *Ae. aegypti* saliva and salivary preparations are associated with anti-inflammatory responses in various experimental conditions (Bissonnette et al., 1993; Surasombatpattana et al., 2012; Barros et al., 2019; Assis et al., 2021; Lara et al., 2021). This result suggests that *Ae. aegypti* saliva *per se* has no components capable of inducing acute pruritus, and the pruritus symptom may occur later in the bite site due to an allergic reaction triggered by immunoglobulin E (IgE) antibodies resulting from the host's previous sensitisation (Barros et al., 2016).

Several groups, including our own, showed that histamine or C48/80 injected in rodent skin promotes pruritus, and this effect is abolished by histamine receptor antagonists and mast cell stabilisers (Rodrigues et al., 2017; Thangam et al., 2018). We showed that co-injection of SGE with C48/80 reduced C48/80-induced pruritus but not in a dose-dependent manner. Of note, in the absence of stimulation, the injection of *Ae. aegypti* SGE promoted a similar response to that evoked with Tyrode (control). *Ae. aegypti* saliva comprises a complex mixture of bioactive components with anti-hemostatic and immunomodulatory properties, with therapeutic potential both *in vivo* and *in vitro* studies. Among these molecules, those from the D7 family can bind a variety of vasoactive components, such as biogenic amines, including histamine and serotonin (Calvo et al., 2006; Martin-Martin et al., 2020; Martin-Martin et al., 2021).

Mast cell degranulation induced by C48/80 includes the interaction of the molecule with Gi_2 and Gi_3 proteins present in the cell membrane, stimulating phospholipase C-dependent signalling, promoting the synthesis of second messengers and increased intracellular Ca^{2+}, and favouring the granule breakdown and the release of histamine release and other cell contents (de Vasconcelos et al., 2011; Yang et al., 2016). Accordingly, C48/80-induced plasma extravasation and increased MPO activity, which is an indirect marker for neutrophil presence in the mouse dorsal skin. The co-injection with SGE resulted in a trend to dose-dependently decrease C48/80-induced plasma extravasation, but only the highest dose of SGE reduced the skin plasma extravasation significantly.

SGE, at the highest dose, also reduced C48/80-increased MPO activity in the tissue. Our hypothesis is that bioactive component(s) present in the *Ae. aegypti* SGE could prevent neutrophil recruitment by acting on mast cells (i.e., stabilising the mast cell membrane–preventing its degranulation – and/or interfering with the H1 receptor-dependent responses). This hypothesis was examined histologically *in situ* by staining tissue sections with toluidine blue, which binds to the glycosaminoglycans in the mast cell granules (Sridharan & Shankar, 2012), and by *in vitro* histamine determinations. SGE did not significantly change the integrity of mast cells *in situ* in the mouse dorsal skin i.d. injected with the C48/80 or the histamine content *in vitro* in the presence or absence of C48/80. Our data corroborate previous findings, showing that *Ae. aegypti* SGE could not change antigen-dependent mast cell degranulation, although it decreased the TNF-α production by these cells (Bissonnette et al., 1993).

Because *Ae. aegypti* SGE did not change mast cell phenotype or histamine release, we next evaluated whether the decreased MPO activity could be related to the modulation of adhesion molecules in the tissue. In this sense, ICAM-1 and VCAM-1 are actively involved in cell adhesion to the endothelium and transmigration to the tissues. The immunohistochemical analysis of skin showed no changes in ICAM-1 expression, but a significant increase in (%) VCAM-1 expression was detected in both the dermis and epidermis of mice receiving C48/80 alone, while its co-injection with SGE did not significantly differ from control levels. Mast cell-dependent ICAM-1 expression has been shown in chronic cutaneous conditions, such as psoriasis and atopic dermatitis (Ackermann & Harvima, 1998), but it was never reported at earlier time points. Regarding VCAM-1 expression, no study has evaluated its expression following C48/80 injection in the skin *in situ*. We hypothesised that 4 h after C48/80 injection (as assessed by our study) is not enough time to observe marked changes in the expression of these molecules. In agreement, an increase of ICAM-1 and VCAM-1 was observed *in vitro* in endothelial cells cultured with intact mast cells or C48/80-degranulated mast cells, but only after 16 h of co-incubation (van Haaster et al., 1997). Although discrete, the VCAM-1 results reinforce the findings observed for MPO activity since VCAM-1 is dependent on NF-κB activation (Nourshargh, 1993). Thus, our results indicate that *Ae. aegypti* SGE may affect

endothelial cells, in line with a previous study (Schmid et al., 2016).

Sensory neurons expressing Mrgprs also regulate histamine-independent pruritus (Wilson et al., 2011). Due to the critical role of various proteases, TRPs, and Mrgprs in skin homeostasis and the pathophysiology of pruritus (Rajka, 1967; Steinhoff et al., 2003; Reddy et al., 2015; Coavoy-Sánchez et al., 2016), the co-participation of these receptors in the anti-pruriceptive effects of SGE was assessed. CQ is commonly used to prevent or treat malaria, but, as a side effect, produces intense itching in humans (Sowunmi et al., 1989; Sowunmi et al., 2001) or in mice when i.d. injected (Liu et al., 2009; Haddadi et al., 2020). This symptom cannot be alleviated by antihistamine drugs, reinforcing the role of a histamine-independent pathway (Li et al., 2022). Accordingly, co-injection of *Ae. aegypti* SGE significantly inhibited in a non-dose-dependent manner, the intense pruritus evoked by a high CQ dose. Curiously, the simultaneous i.d. injection with the TRPA1 antagonist HC030031 did not further enhance *Ae. aegypti* SGE anti-pruriceptive effect on CQ-induced pruritus and instead, it reversed the anti-pruritus effect of *Ae. aegypti* SGE against CQ-induced mild pruritus.

With this in mind, we hypothesise that TRPA1 is somehow essential to the signalling pathways that regulate the *Ae. aegypti* SGE anti-pruriceptive effect against CQ-induced pruritus. In agreement, in cultured DRG neurons, MAS-related GPCRs, MrgprA3 and MrgprC11, modulate the function of TRPA1 (Wilson et al., 2011; Lieu et al., 2014), which is activated by its agonist AITC. Moreover, at 1 µmol, AITC promoted scratching behaviour when i.d. injected in the mouse dorsal skin (Coavoy-Sánchez et al., 2016) or into the mouse nape (Liu et al., 2021), while in the cheek model, doses of 1–4 µmol evoked both wiping and scratching behaviour (Esancy et al., 2018; Han et al., 2018; Liu et al., 2021). Therefore, pruritus and nocifensive behaviour vary according to the dose and the site of TRPA1 agonist injection. Indeed, differences in TRPA1 expression can be found in the origins and extent of afferent fibers whose cell bodies reside in the DRG and trigeminal ganglion in the cutaneous area (Dong and Dong, 2018; Tobori et al., 2021).

Herein, the i.d. injection of TRPA1 agonist AITC in the mouse dorsal skin promoted itching behavior, which was significantly attenuated by the co-injection with *Ae. aegypti* SGE. However, the simultaneous injection with HC030031 neutralized SGE anti-pruriceptive effect against AITC-induced pruritus, thus suggesting that SGE (or some of its components) might typically act as partial agonist for TRPA1 receptors or perhaps, giving the biochemical complexity of SGE, an optimum range of action is reached for each situation due to the presence of molecules with additive, synergic or even opposite effects that might sometimes occlude each other, which may be the case here. It should also be noted that *Ae. aegypti* saliva contains kratagonists, scavenger molecules that interact with physiological effectors (Andersen & Ribeiro, 2017).

In fact, the absorption measurement of SGE and HC030031 combined solutions revealed notable changes in the 230–237 nm interval compared with either agent alone, indicating a potential antagonistic interaction between SGE and HC030031, which might explain the loss of efficacy on CQ- or AITC-induced pruritus. Furthermore, the presence of protease inhibitors has been revealed by transcriptome and proteome in *Ae. aegypti* salivary glands (Almeras et al., 2010; Ribeiro et al., 2016). These inhibitors may disrupt the cleavage of the amino-terminal region of the receptors and the activation of TRPA1 required for signal transduction (Coavoy-Sánchez et al., 2016; Derouiche et al., 2021). As suggested for other arthropod vectors (Sá-Nunes & Oliveira, 2021), the potential immunobiological properties of *Ae. aegypti* saliva have been successfully evaluated in several inflammatory models (Sales-Campos et al., 2015; de Souza Gomes et al., 2018; Assis et al., 2021). In some cases, the salivary molecules responsible for such activities have been elucidated. For example, one protein of the D7 family (scavengers of biogenic amines) was able to inhibit dengue virus infection (Conway et al., 2016); the peptide AeMOPE-1 displays many activities in macrophages and ameliorates experimental colitis (Lara et al., 2021); and many salivary proteins can interact with human receptors involved in immune responses (Gavor et al., 2022).

Corroborating the findings *in vivo*, we showed that increased TRPA1-mediated calcium influx (measured by the Fura-2-AM) assay in TRPA1-hHEK293t cells is significantly reduced by the treatment with *Ae aegypti* SGE, thus supporting the suggestion that bioactive components present in *Ae. aegypti* SGE can act, at least partially, on non-histaminergic (TRPA1) pathways of pruritus.

Our findings show the potential of salivary components of *Ae. aegypti* as a prospective source of bioactive molecules that may serve as templates for developing new compounds to prevent or treat skin conditions involving the histamine-independent itch TRPA1 pathway.

Data availability statement

The raw data supporting the conclusion of this article will be made available by the authors, without undue reservation.

Ethics statement

The animal study was reviewed and approved by the Institutional Animal Care and Use Committee (CEUA-ICB/USP; protocol no. 33, page 85, book no. 02/2010), by the guidelines from the Brazilian Council for Control of Animal Experimentation (CONCEA), and the Directive 2010/63/EU, combined with the Animal Welfare Act.

Author contributions

SKPC, ARAC, and AS-N: Conceptualization, SKPC, MNM, and AS-N: Supervision, LR, SAC-S, and SAT: Methodology *in vivo* and *in vitro* and histopathology, ARAC, LRL, EYT, KBF, AS-N, and ACC: Data curation on calcium images and cell transfection, ARAC, SKPC, and SAT: Writing—Original draft preparation and Data analysis and curation, ARAC, LR, SKPC, KBF, and ASN: Investigation, ARAC, MNM, KBF, ASN, and SKPC: Writing—Reviewing, Editing—Resources. All authors contributed to the article and approved the submitted version.

Funding

AC received the Conselho Nacional de Desenvolvimento Científico e Tecnológico scholarship -CNPq (142029/2020-3). LL, MM, AS-N, and SC received a scientific productivity scholarship from the Conselho Nacional de Desenvolvimento Científico e Tecnológico-CNPq (313492/2020-4, 306294/2019-2, 312674/2021-0, and 312514/2019-0, respectively). Partial financial support was received from the Coordenação de Aperfeiçoamento de Pessoal e Nível Superior-Brazil (CAPES) (Finance code 001). SC received a Royal Society 2016/R1 Newton Grant-eGAP SZ50730. LL is a member of CEPID Redoxoma FAPESP (2013/07937-8).

Acknowledgments

We thank Prof. Zoltan Sandor (University of Pécs, Hungary) for kindly donating the hTRPA1 vector and Mr Sidney Verissimo Filho for his top technical support. We thank Robert Ryan Geyer (R2G English Editing Services) for proofreading the manuscript.

Conflict of interest

The authors declare that the research was conducted in the absence of any commercial or financial relationships that could be construed as a potential conflict of interest.

Publisher's note

All claims expressed in this article are solely those of the authors and do not necessarily represent those of their affiliated organizations, or those of the publisher, the editors and the reviewers. Any product that may be evaluated in this article, or claim that may be made by its manufacturer, is not guaranteed or endorsed by the publisher.

Supplementary material

The Supplementary Material for this article can be found online at: https://www.frontiersin.org/articles/10.3389/fphys.2023.1055706/full#supplementary-material

SUPPLEMENTARY FIGURE S1
Quantitative immunoreactivity staining analysis showing the percentage of ICAM-1 positive dermal area in the mouse dorsal skin i.d. injected with C48/80 (10 mg/site) in the absence and presence of SGE. Data are represented by the column scatter dot plot graphs **(A)**, and expressed as median with interquartile range (n = 4 mice/group). Panel **B** shows representative images containing scarce ICAM-1 expression in the dermis of mouse dorsal skin i.d. injected with Tyrode **(B)**, SGE **(C)**, C48/80, **(D)** and C48/80 + SGE **(E)**. Panel **G(a)** shows the negative control specimen (skin without primary antibody). Arrows show hair follicles, Ep = epidermis, D = dermis. DAB, hematoxylin counterstain, 100× magnification.

SUPPLEMENTARY FIGURE S2
Representative Western Blot of TRPA1 expression in both hTRPA1-positve (transfected) and hTRPA1-negative (non-transfected) HEK293t (5×10^6) cells. Immunoreactive bands are correspondent to approximately 42 kDa and 127 kDa for β-actin and TRPA1, respectively. hTRPA1-negative cells (non-transfected) or cells exposed to empty plasmid did not exhibit TRPA1 expression.

SUPPLEMENTARY FIGURE S3
Ae aegypti SGE reduced hTRPA1-mediated receptor mobilization of intracellular calcium in TRPA1-HEK293t cells in response to TRPA1 agonist AITC. Representative individual traces showing intracellular calcium changes in responses to SGE (1 µg/mL), SGE + 100 µM AITC, and Tyrode + 100 µM AITC in TRPA1-HEK293t cells loaded with Fura-2-AM (panel **A**). Panel **B** shows corresponding scan line displayed of continuously calcium changes (mean ± SD) from 5 independent experiments in responses to SGE (1 µg/mL), SGE + 100 µM AITC, and Tyrode + 100 µM AITC in TRPA1-HEK293t cells (n = 21) loaded with Fura-2-AM. Fura-2 fluorescence signals are presented as the 340/380 nm ratio.

References

Ackermann, L., and Harvima, T. (1998). Mast cells of psoriatic and atopic dermatitis skin are positive for TNF-alpha and their degranulation is associated with expression of ICAM-1 in the epidermis. *Arch. Dermatol Res.* 290 (7), 353–359. doi:10.1007/s004030050317

Almeras, L., Fontaine, A., Belghazi, M., Bourdon, S., Boucomont-Chapeaublanc, E., Orlandi-Pradines, E., et al. (2010). Salivary gland protein repertoire from *Aedes aegypti* mosquitoes. *Vector Borne Zoonotic Dis.* 10 (4), 391–402. doi:10.1089/vbz.2009.0042

Andersen, J. F., and Ribeiro, J. M. C. (2017). "Salivary kratagonists: Scavengers of host physiological effectors during blood feeding," in *Arthropod vector: Controller of disease transmission*. Editors S. K. Wikel, S. Aksoy, and G. Dimopoulos (Cambridge: Academic Press), 51–63.

Assis, J. B., Cogliati, B., Esteves, E., Capurro, M. L., Fonseca, D. M., and Sá-Nunes, A. (2021). *Aedes aegypti* mosquito saliva ameliorates acetaminophen-induced liver injury in mice. *PLoS One* 16 (2), e0245788. doi:10.1371/journal.pone.0245788

Barros, M. S., Gomes, E., Gueroni, D. I., Ramos, A. D., Mirotti, L., Florsheim, E., et al. (2016). Exposure to *Aedes aegypti* bites induces a mixed-type allergic response following salivary antigens challenge in mice. *PLoS One* 11 (5), e0155454. PMID: 27203689. doi:10.1371/journal.pone.0155454

Barros, M. S., Lara, P. G., Fonseca, M. T., Moretti, E. H., Filgueiras, L. R., Martins, J. O., et al. (2019). *Aedes aegypti* saliva impairs M1-associated proinflammatory phenotype without promoting or affecting M2 polarization of murine macrophages. *Parasit. Vectors* 12 (1), 239. doi:10.1186/s13071-019-3487-7

Bartsch, V. B., Niehaus, J. K., Taylor-Blake, B., and Zylka, M. J. (2019). Enhanced histamine-induced itch in diacylglycerol kinase iota knockout mice. *PLoS One* 14 (6), e0217819. doi:10.1371/journal.pone.0217819

Berger, T. G., Shive, M., and Harper, G. M. (2013). Pruritus in the older patient: A clinical review. *JAMA* 310 (22), 2443–2450. doi:10.1001/jama.2013.282023

Bissonnette, E. Y., Rossignol, P. A., and Befus, A. D. (1993). Extracts of mosquito salivary gland inhibit tumour necrosis factor alpha release from mast cells. *Parasite Immunol.* 15 (1), 27–33. doi:10.1111/j.1365-3024.1993.tb00569.x

Bizzarro, B., Barros, M. S., Maciel, C., Gueroni, D. I., Lino, C. N., Campopiano, J., et al. (2013). Effects of *Aedes aegypti* salivary components on dendritic cell and lymphocyte biology. *Parasit. Vectors* 6, 329. doi:10.1186/1756-3305-6-329

Bradford, M. M. (1976). A rapid and sensitive method for the quantification of microgram quantities of protein utilizing the principle of protein-dye binding. *Analytical Biochemistry* 72, 248–254. doi:10.1016/0003-2697(76)90527-3

Calvo, E., Mans, B. J., Andersen, J. F., and Ribeiro, J. M. (2006). Function and evolution of a mosquito salivary protein family. *J. Biol. Chem.* 281 (4), 1935–1942. doi:10.1074/jbc.M510359200

Coavoy-Sánchez, S. A., Rodrigues, L., Teixeira, S. A., Soares, A. G., Torregrossa, R., Wood, M. E., et al. (2016). Hydrogen sulfide donors alleviate itch secondary to the activation of type-2 protease-activated receptors (PAR-2) in mice. *Pharmacol. Res.* 113, 686–694. doi:10.1016/j.phrs.2016.09.030

Conway, M. J., Londono-Renteria, B., Troupin, A., Watson, A. M., Klimstra, W. B., Fikrig, E., et al. (2016). *Aedes aegypti* D7 saliva protein inhibits dengue virus infection. *PLoS Negl. Trop. Dis.* 10 (9), e0004941. doi:10.1371/journal.pntd.0004941

Conway, M. J. (2021). Type I hypersensitivity promotes *Aedes aegypti* blood feeding. *Sci. Rep.* 11 (1), 14891. doi:10.1038/s41598-021-94416-w

Costa, S. K., Starr, A., Hyslop, S., Gilmore, D., and Brain, S. D. (2006). How important are NK1 receptors for influencing microvascular inflammation and itch in the skin?

Studies using *Phoneutria nigriventer* venom. *Vasc. Pharmacol.* 45 (4), 209–214. doi:10.1016/j.vph.2005.08.025

de Carvalho, N. D., Garcia, R. C. T., Ferreira, A. K., Batista, D. R., Cassola, A. C., Maria, D., et al. (2014). Neurotoxicity of coral snake phospholipases A2 in cultured rat hippocampal neurons. *Brain Res.* 1552, 1–16. doi:10.1016/j.brainres.2014.01.008

de Souza Gomes, R., Navegantes-Lima, K. C., Monteiro, V. V. S., de Brito Oliveira, A. L., Rodrigues, D. V. S., Reis, J. F., et al. (2018). Salivary gland extract from *Aedes aegypti* improves survival in murine polymicrobial sepsis through oxidative mechanisms. *Cells* 7 (11), 182. doi:10.3390/cells7110182

de Vasconcelos, D. I., Leite, J. A., Carneiro, L. T., Piuvezam, M. R., de Lima, M. R., de Morais, L. C., et al. (2011). Anti-inflammatory and antinociceptive activity of ouabain in mice. *Mediat. Inflamm.* 2011, 912925. doi:10.1155/2011/912925

Derouiche, S., Li, T., Sakai, Y., Uta, D., Aoyagi, S., and Tominaga, M. (2021). Inhibition of transient receptor potential vanilloid 1 and transient receptor potential ankyrin 1 by mosquito and mouse saliva. *Pain* 163, 299–307. doi:10.1097/j.pain.0000000000002337

Dondalska, A., Rönnberg, E., Ma, H., Axberg Pålsson, S., Magnusdottir, E., Gao, T., et al. (2020). Amelioration of compound 48/80-mediated itch and LL-37-induced inflammation by a single-stranded oligonucleotide. *Front. Immunol.* 11, 559589. doi:10.3389/fimmu.2020.559589

Dong, X., and Dong, X. (2018). Peripheral and central mechanisms of itch. *Neuron* 98 (3), 482–494. doi:10.1016/j.neuron.2018.03.023

Esancy, K., Condon, L., Feng, J., Kimball, C., Curtright, A., and Dhaka, A. (2018). A zebrafish and mouse model for selective pruritus via direct activation of TRPA1. *Elife* 7, e32036. doi:10.7554/eLife.32036

Gavor, E., Choong, Y. K., Liu, Y., Pompon, J., Ooi, E. E., Mok, Y. K., et al. (2022). Identification of *Aedes aegypti* salivary gland proteins interacting with human immune receptor proteins. *PLoS Negl. Trop. Dis.* 16 (9), e0010743. doi:10.1371/journal.pntd.0010743

Haddadi, N. S., Shakiba, S., Afshari, K., Haj-Mirzaian, A., Vesaghati, S., Gharagozlou, S., et al. (2020). Possible involvement of nitric oxide in the antipruritic effect of metformin on chloroquine-induced scratching in mice. *Dermatology* 236 (2), 151–159. doi:10.1159/000501583

Han, Q., Liu, D., Convertino, M., Wang, Z., Jiang, C., Kim, Y. H., et al. (2018). miRNA-711 binds and activates TRPA1 extracellularly to evoke acute and chronic pruritus. *Neuron* 99 (3), 449–463. Epub 2018 Jul 19. doi:10.1016/j.neuron.2018.06.039

Henrique, M. O., Neto, L. S., Assis, J. B., Barros, M. S., Capurro, M. L., Lepique, A. P., et al. (2019). Evaluation of inflammatory skin infiltrate following *Aedes aegypti* bites in sensitized and non-sensitized mice reveals saliva-dependent and immune-dependent phenotypes. *Immunology* 158 (1), 47–59. doi:10.1111/imm.13096

Jin, L., Guo, X., Shen, C., Hao, X., Sun, P., Li, P., et al. (2018). Salivary factor LTRIN from *Aedes aegypti* facilitates the transmission of Zika virus by interfering with the lymphotoxin-β receptor. *Nat. Immunol.* 19 (4), 342–353. Epub 2018 Mar 5. doi:10.1038/s41590-018-0063-9

Kemény, Á., Kodji, X., Horváth, S., Komlódi, R., Szőke, É., Sándor, Z., et al. (2018). TRPA1 acts in a protective manner in imiquimod-induced psoriasiform dermatitis in mice. *J. Invest. Dermatol* 138 (8), 1774–1784. doi:10.1016/j.jid.2018.02.040

Koch, S. C., Acton, D., and Goulding, M. (2018). Spinal circuits for touch, pain, and itch. *Annu. Rev. Physiol.* 80, 189–217. doi:10.1146/annurev-physiol-022516-034303

Laemmli, U. K. (1970). Cleavage of structural proteins during the assembly of the head of bacteriophage T4. *Nature* 227, 680–685. doi:10.1038/227680a0

Lara, P. G., Esteves, E., Sales-Campos, H., Assis, J. B., Henrique, M. O., Barros, M. S., et al. (2021). AeMOPE-1, a novel salivary peptide from *Aedes aegypti*, selectively modulates activation of murine macrophages and ameliorates experimental colitis. *Front. Immunol.* 12, 681671. doi:10.3389/fimmu.2021.681671

Lee, M. G., Dong, X., Liu, Q., Patel, K. N., Choi, O. H., Vonakis, B., et al. (2008). Agonists of the MAS-related gene (Mrgs) orphan receptors as novel mediators of mast cell-sensory nerve interactions. *J. Immunol.* 180, 2251–2255. doi:10.4049/jimmunol.180.4.2251

Li, F., Wang, C., Hu, D., Zhang, X., Shen, R., Zhou, Y., et al. (2022). mMrgprA3/mMrgprC11/hMrgprX1: Potential therapeutic targets for allergic contact dermatitis-induced pruritus in mice and humans. *Contact Dermat.* 86 (4), 286–294. doi:10.1111/cod.14051

Lidegran, M., Domeij, S., Forsgren, S., and Dahlqvist, A. (1996). Mast cells in the laryngeal mucosa of the rat: Effect of compound 48/80 and dexamethasone: A quantitative and immunohistochemical study at the light- and electron-microscopic levels. *Acta Anat.* 157 (2), 135–143. doi:10.1159/000147874

Lieu, T., Jayaweera, G., and Bunnett, N. W. (2014). Gpba: A GPCR for bile acids and an emerging therapeutic target for disorders of digestion and sensation. *Br. J. Pharmacol.* 171 (5), 1156–1166. doi:10.1111/bph.12426

Liu, Q., Tang, Z., Surdenikova, L., Kim, S., Patel, K. N., Kim, A., et al. (2009). Sensory neuron-specific GPCR Mrgprs are itch receptors mediating chloroquine-induced pruritus. *Cell* 139, 1353–1365. doi:10.1016/j.cell.2009.11.034

Liu, X., Zhang, J. T., Hu, Y., Shan, W. Q., Wang, Z. H., Fu, Q. Y., et al. (2021). Formalin itch test: Low-dose formalin induces histamine-independent, TRPA1-mediated itch in mice. *Front. Med. (Lausanne)* 8, 627725. doi:10.3389/fmed.2021.627725

Maciel, C., Fujita, A., Gueroni, D. I., Ramos, A. D., Capurro, M. L., and Sá-Nunes, A. (2014). Evans blue as a simple method to discriminate mosquitoes' feeding choice on small laboratory animals. *PLoS One* 9 (10), e110551. doi:10.1371/journal.pone.0110551

Martin-Martin, I., Kern, O., Brooks, S., Smith, L. B., Valenzuela-Leon, P. C., Bonilla, B., et al. (2021). Biochemical characterization of AeD7L2 and its physiological relevance in blood-feeding in the dengue mosquito vector, *Aedes aegypti*. *FEBS J.* 288 (6), 2014–2029. doi:10.1111/febs.15524

Martin-Martin, I., Smith, L. B., Chagas, A. C., Sá-Nunes, A., Shrivastava, G., Valenzuela-Leon, P. C., et al. (2020). *Aedes albopictus* D7 salivary protein prevents host hemostasis and inflammation. *Biomolecules* 10 (10), 1372. doi:10.3390/biom10101372

McNeil, B., Pundir, P., Meeker, S., Han, L., Undem, B. J., Kulka, M., et al. (2015). Identification of a mast-cell-specific receptor crucial for pseudo-allergic drug reactions. *Nature* 519, 237–241. doi:10.1038/nature14022

Moore, C., Gupta, R., Jordt, S. E., Chen, Y., and Liedtke, W. B. (2018). Regulation of pain and itch by TRP channels. *Neurosci. Bull.* 34 (1), 120–142. doi:10.1007/s12264-017-0200-8

Moparthi, L., Survery, S., Kreir, M., Simonsen, C., Kjellbom, P., Högestätt, E. D., et al. (2014). Human TRPA1 is intrinsically cold- and chemosensitive with and without its N-terminal ankyrin repeat domain. *Proc. Natl. Acad. Sci. U. S. A.* 111 (47), 16901–16906. doi:10.1073/pnas.1412689111

Nourshargh, S. (1993). Mechanisms of neutrophil and eosinophil accumulation *in vivo*. *Am. Rev. Respir. Dis.* 148 (6), S60–S64. doi:10.1164/ajrccm/148.6_Pt_2.S60

Pereira, M. P., Mittal, A., and Ständer, S. (2019). Current treatment strategies in refractory chronic pruritus. *Curr. Opin. Pharmacol.* 46, 1–6. doi:10.1016/j.coph.2018.11.007

Pozsgai, G., Payrits, M., Sághy, E., Sebestyén-Bátai, R., Steen, E., Szőke, É., et al. (2017). Analgesic effect of dimethyl trisulfide in mice is mediated by TRPA1 and sst4 receptors. *Nitric Oxide* 65, 10–21. doi:10.1016/j.niox.2017.01.012

Rajka, G. (1967). Itch duration in the involved skin of atopic dermatitis (prurigo Besnier). *Acta Derm. Venereol.* 47, 154–157.

Reddy, V. B., Sun, S., Azimi, E., Elmariah, S. B., Dong, X., and Lerner, E. A. (2015). Redefining the concept of protease-activated receptors: cathepsin S evokes itch via activation of Mrgprs. *Nat. Commun.* 6, 7864. doi:10.1038/ncomms8864

Ribeiro, J. M., Martin-Martin, I., Arcà, B., and Calvo, E. (2016). A deep insight into the sialome of male and female *Aedes aegypti* mosquitoes. *PLoS One* 11 (3), e0151400. doi:10.1371/journal.pone.0151400

Ribeiro, J. M. C. (1995). Blood-feeding arthropods: Live syringes or invertebrate pharmacologists? *Infect. Agents Dis.* 4, 143–152.

Rodrigues, L., Ekundi-Valentim, E., Florenzano, J., Cerqueira, A. R., Soares, A. G., Schmidt, T. P., et al. (2017). Protective effects of exogenous and endogenous hydrogen sulfide in mast cell-mediated pruritus and cutaneous acute inflammation in mice. *Pharmacol. Res.* 115, 255–266. doi:10.1016/j.phrs.2016.11.006

Roh, Y. S., Choi, J., Sutaria, N., and Kwatra, S. G. (2021). Itch: Epidemiology, clinical presentation, and diagnostic workup. *J. Am. Acad. Dermatol* 86, 1–14. doi:10.1016/j.jaad.2021.07.076

Sá-Nunes, A., and Oliveira, C. J. F. (2021). Dendritic cells as a disputed fortress on the tick-host battlefield. *Trends Parasitol.* 37 (4), 340–354. doi:10.1016/j.pt.2020.11.004

Sales-Campos, H., de Souza, P. R., Basso, P. J., Ramos, A. D., Nardini, V., Chica, J. E., et al. (2015). *Aedes aegypti* salivary gland extract ameliorates experimental inflammatory bowel disease. *Int. Immunopharmacol.* 26 (1), 13–22. doi:10.1016/j.intimp.2015.03.002

Santos, K. T., Florenzano, J., Rodrigues, L., Favaro, R. R., Ventura, F. F., Ribeiro, M. G., et al. (2014). Early postnatal, but not late, exposure to chemical ambient pollutant 1,2-naphthoquinone increases susceptibility to pulmonary allergic inflammation at adulthood. *Arch. Toxicol.* 88, 1589–1605. doi:10.1007/s00204-014-1212-z

Schmid, M. A., Glasner, D. R., Shah, S., Michlmayr, D., Kramer, L. D., and Harris, E. (2016). Mosquito saliva increases endothelial permeability in the skin, immune cell migration, and dengue pathogenesis during antibody-dependent enhancement. *PLoS Pathog.* 12 (6), e1005676. doi:10.1371/journal.ppat.1005676

Sowunmi, A., Falade, A. G., Adedeji, A. A., and Falade, C. O. (2001). Comparative clinical characteristics and responses to oral 4-aminoquinoline therapy of malarious children who did and did not develop 4-aminoquinoline-induced pruritus. *Ann. Trop. Med. Parasitol.* 95 (7), 645–653. doi:10.1080/00034980120103216

Sowunmi, A., Walker, O., and Salako, L. (1989). Pruritus and antimalarial drugs in Africans. *Lancet* 2 (8656), 213. doi:10.1016/s0140-6736(89)90391-7

Sridharan, G., and Shankar, A. A. (2012). Toluidine blue: A review of its chemistry and clinical utility. *J. Oral Maxillofac. Pathol.* 16 (2), 251–255. doi:10.4103/0973-029X.99081

Steinhoff, M., Neisius, U., Ikoma, A., Fartasch, M., Heyer, G., Skov, P. S., et al. (2003). Proteinase-activated receptor-2 mediates itch: A novel pathway for pruritus in human skin. *J. Neurosci.* 23 (15), 6176–6180. doi:10.1523/JNEUROSCI.23-15-06176.2003

Story, G. M., Peier, A. M., Reeve, A. J., Eid, S. R., Mosbacher, J., Hricik, T. R., et al. (2003). ANKTM1, a TRP-like channel expressed in nociceptive neurons, is activated by cold temperatures. *Cell* 112 (6), 819–829. doi:10.1016/s0092-8674(03)00158-2

Sun, P., Nie, K., Zhu, Y., Liu, Y., Wu, P., Liu, Z., et al. (2020). A mosquito salivary protein promotes flavivirus transmission by activation of autophagy. *Nat. Commun.* 11 (1), 260. doi:10.1038/s41467-019-14115-z

Surasombatpattana, P., Patramool, S., Luplertlop, N., Yssel, H., and Missé, D. (2012). Aedes aegypti saliva enhances dengue virus infection of human keratinocytes by suppressing innate immune responses. *J Invest Dermatol* 132 (8), 2103–5. doi:10.1038/jid.2012.76

Thangam, E. B., Jemima, E. A., Singh, H., Baig, M. S., Khan, M., Mathias, C. B., et al. (2018). The role of histamine and histamine receptors in mast cell-mediated allergy and inflammation: The hunt for new therapeutic targets. *Front. Immunol.* 9, 1873. doi:10.3389/fimmu.2018.01873

Tobori, S., Hiyama, H., Miyake, T., Yano, Y., Nagayasu, K., Shirakawa, H., et al. (2021). MrgprB4 in trigeminal neurons expressing TRPA1 modulates unpleasant sensations. *J. Pharmacol. Sci.* 146 (4), 200–205. doi:10.1016/j.jphs.2021.04.006

van Haaster, C., Derhaag, J., and Engels, W. (1997). Mast cell-mediated induction of ICAM-1, VCAM-1 and E-selectin in endothelial cells *in vitro*: constitutive release of inducing mediators but no effect of degranulation. *Pflügers Arch* 435, 137–144. doi:10.1007/s004240050493

van Laarhoven, A. I. M., Marker, J. B., Elberling, J., Yosipovitch, G., Arendt-Nielsen, L., and Andersen, H. H. (2019). Itch sensitization? A systematic review of studies using quantitative sensory testing in patients with chronic itch. *Pain* 160 (12), 2661–2678. doi:10.1097/j.pain.0000000000001678

Wilson, S. R., Gerhold, K. A., Bifolck-Fisher, A., Liu, Q., Patel, K. N., Dong, X., et al. (2011). TRPA1 is required for histamine-independent, Mas-related G protein-coupled receptor-mediated itch. *Nat. Neurosci.* 14 (5), 595–602. doi:10.1038/nn.2789

Yalçin, B., Tamer, E., Toy, G. G., Oztaş, P., Hayran, M., and Alli, N. (2006). The prevalence of skin diseases in the elderly: Analysis of 4099 geriatric patients. *Int. J. Dermatol* 45 (6), 672–676. doi:10.1111/j.1365-4632.2005.02607.x

Yang, F., Guo, L., Li, Y., Wang, G., Wang, J., Zhang, C., et al. (2021). Structure, function and pharmacology of human itch receptor complexes. *Nature* 600, 164–169. doi:10.1038/s41586-021-04077-y

Yang, N. N., Shi, H., Yu, G., Wang, C. M., Zhu, C., Yang, Y., et al. (2016). Osthole inhibits histamine-dependent itch via modulating TRPV1 activity. *Sci. Rep.* 6, 25657. doi:10.1038/srep25657

Frontiers in Pharmacology

Explores the interactions between chemicals and living beings

The most cited journal in its field, which advances access to pharmacological discoveries to prevent and treat human disease.

Discover the latest Research Topics

See more →

Frontiers

Avenue du Tribunal-Fédéral 34
1005 Lausanne, Switzerland
frontiersin.org

Contact us

+41 (0)21 510 17 00
frontiersin.org/about/contact